



Cyclodextrin nanoparticles for targeted ocular drug delivery of kinase inhibitors

Pitsiree Praphanwittaya

Thesis for the degree of Philosophiae Doctor

Supervisor:

Prof. Þorsteinn Loftsson

Doctoral committee:

Prof. Einar Stefánsson

Dr. Phatsawee Jansook

Dr. Gauti Jóhannesson

Prof. Hákon Hrafn Sigurðsson

November 2020



UNIVERSITY OF ICELAND

SCHOOL OF HEALTH SCIENCES

FACULTY OF PHARMACEUTICAL SCIENCES

Sýklóðextrín nanóagnir fyrir markbundna lyfjagjöf í augu

Pitsiree Praphanwittaya

Ritgerð til doktorsgráðu

Leiðbeinandi

Prof. Þorsteinn Loftsson

Doktorsnefnd:

Prof. Einar Stefánsson

Dr. Phatsawee Jansook

Dr. Gauti Jóhannesson

Prof. Hákon Hrafn Sigurðsson

Nóvember 2020



UNIVERSITY OF ICELAND
SCHOOL OF HEALTH SCIENCES

FACULTY OF PHARMACEUTICAL SCIENCES

Thesis for a doctoral degree at the University of Iceland. All right reserved.
No part of this publication may be reproduced in any form without the prior
permission of the copyright holder.

© Pitsiree Praphanwittaya 2020

ISBN 978-9935-9445-4-2

ORCID 0000-0003-2900-4294

Printing by Háskólaprent EHF.

Reykjavik, Iceland 2020

Ágrip

Bakgrunnur: Aldursbundin augnbotnahrörnun (AMD) veldur sjónskerðingu hjá öldruðum vegna nýmyndunar æða. Fyrsti meðferðarkostur er inndæling lyfja í glerhlaup augans en þessi framkvæmd veldur sársauka og ýmsum aukaverkunum. Lyfjagjöf um munn hefur aftur á móti miðlægar aukaverkanir (systemic side effects) í för með sér. Sýklódextrín (CD) geta hópað sig saman og myndað nanóagnir sem geta ferjað lyfjasameindir til bakhluta augans. Þess vegna geta augndropa með sýklódextrínum verið góður kostur til meðhöndlunar á AMD.

Inngangur: Fjölkínasahemlar (KI) bæla vöxt nýrra æða hjá sjúklingum með augnbotnahrörnun með því að hemja virkni ensímans týrósín-kínasa og VEGF-viðtaka. Vandinn við gjöf fjölkínasahemla er torleysni þeirra í vatni. Í þessari rannsókn var γ -sýklódextrín valið til að auka vatnleysanleika fjölkínasahemla. Þrátt fyrir aukna leysni í vatni þá var virkinn samt ófullnægjandi. Þar að auki höfðu kínasasöltin tilhneigingu til að brotna niður við hækkað hitastig við framleiðslu á fjölkínasahemla/ γ -sýklódextrín fléttum. Þess vegna var markmið þessarar rannsóknar að auka leysni fjölkínasahemla með tæknilausnum eins og að bæta við vatnleysanlegum fjölliðum eða mótjónum, í augndropna og þróa þar með hitastigsstöðuga augndropa sem geta komið völdum fjölkínasahemlum á tilætlaðan stað í auganu.

AÐFERÐ: Í aðalatriðum voru viðhafðar tvær aðferðir til undirbúnings á efnasamsetningunni og ördreifunni. Í leysnitilraunum voru flétturnar undirbúnar við lág hitastig (hljóðbað við 30°C í 30 mínútur) vegna óstöðugleika fjölkínasahemlanna við hærri hitastig. Við sýnaundirbúning var notast við gufusæfi (120°C í 20 mínútur) ásamt því sem hann var notaður til dauðhrensunar við þróun á lyfjaformanna. Eðlisefnafræðilegir eiginleikar augndropna voru einnig metnir.

Niðurstöður: Í fasa-leysnitilraunum voru sex fjölkínasahemlar skoðaðir og reyndust þeir allir mynda leysanleikaferla af B_s-gerð. Dovitininb var með besta leysanleikan vegna mikillar sækni í γ -sýklódextrín ($K_{1:1}$ gildi 684 M⁻¹, CE: 0.011) og þar á eftir kom motesanib. Fjölkínasahemlar voru leysanlegri við lágt sýrustig þar sem þeir voru á prótóneruðu formi. Vatnssæknu fjölliðurnar sem voru rannsakaðar höfðu áhrif á leysni fjölkínasahemla í sýklódextrinlausnum. Að auki var hægt að auka leysni fjölkínasahemla-y-

sýklódeþrínfléttunnar, með saltmyndun á milli EDTA og lyfsins. Hexadímetrínbrómíð (HDMBr) jók almennt leysni lyfjasameindanna og γ -sýklódeþrína með samverkandi áhrifum.

Dovitinib var valið til frekari rannsókna. Tilvist HDMBr í formúleringunni stuðlaði að því að B_s-skilgreining viðheldist, ásamt því að það jók bæði γ -sýklódeþrín leysanleika og CE gildi úr 0,0110 í 0,0391. Myndun dovitinib/ γ -sýklódeþrína/HDMBr fléttunnar var staðfest með rafeindasmásjá (TEM) ásamt öðrum greiningum á föstu formi efnisins, þ.m.t. röntgengeislunardreifingu (XRPD), varmamælingu (DSC) og innroðagreining með Fourier-vörpun (FTIR). γ -Sýklódeþrín gat aukið stöðugleika á yfirmettaða dovitinb lausn og aukið losunarhraða, en losunarhraðinn lækkaði aftur við myndun HDMBr matrixu. Í lyfjaformuleríngunum bar á saltmyndun lyfja-sýklódeþrín fléttunnar og því var bætt við súrum mótjónum til að auka leysni fléttunnar sem er veikur basi. Sítrónusýra var sú mótjón sem náði fram mestri virkni sýklódeþrína vegna saltmyndunar og/eða víxlverkanna. Losun lyfs í gegnum hálf-gegndræpa himnu jókst ekki í *in vitro* tilraunum þrátt fyrir aukna leysni lyfsins af völdum sýklódeþrína. Saltform Fjölkinasahemlanna voru notuð við þróun lyfjaformanna vegna þess að leysni lyfsins var betri á því formi. Óvænt vandamál kom upp varðandi dovitinib saltið, hins vegar sýndi cediranib maleat (CM) einnig áhugaverðar niðurstöður vegna mikillar leysni þess og því var það endanlega valið í augndropana í stað dovitinib. Notkun ríbóflavíns dugði til að halda stöðugleika á lyfinu leystu upp í 15% (w / v) γ -sýklódeþrín lausn í a.m.k. eina hringrás í gufusæfi. Sú flétta var staðfest með NMR greiningu. Leysileiki, gegndræpi og form nanóagnir hélst óbreytt í viðurvist ríbóflavíns. Samsetning ríbóflavíns og annarra hjálparefna (þ.e. fjölliða og annara leysa) drógu úr varmaniðurbrotinu í ördreifunni. Augndroparnir skilufu lyfinu aftan í augað. Þessa vöru á að geyma við 25 °C til að viðhalda réttu sýrustigi, agnastærð og lögun. Aðeins óveruleg rýrnun á lyfjaefninu greindist eftir 6 mánaða geymslu.

Ályktanir: Leysni á γ -sýklódeþrínunum í fléttni með fjökinasahemlum var aukin með viðbótaraðferðum, þar með talið vatnssæknar fjölliður og mótjónir. Viðeigandi sveiflufjafnari gæti verndað fjölkínasahemlasaltið í lyfjaformúleringu frá varmaniðurbroti. Lyfjagjöf til aftari hluta augans tókst og var geymslufolið að minnsta kosti 6 mánuðir.

Lykilorð:

γ -Sýklódeþrín, vatnssæknar fjölliður, mótjónir, stöðugleiki, ördreifun

Abstract

Background: Age-related macular degeneration (AMD) causes vision loss in elderly people due to neovascularization. The first line treatments are intravitreal injections but this route of administration induces severe pain. Oral administration still produces side effects. Cyclodextrins (CDs) can self-assemble into aggregates or larger nanoparticle platform that can deliver drugs to the back of eye. Thus, CD-based eye drops can be a more favorable formulation for AMD.

Introduction: Tyrosine kinase inhibitors (KIs) suppress the growth of new blood vessels in AMD by inhibiting the activity of tyrosine kinase and VEGF receptors. The obstacle of delivery of small molecule KIs is their very low aqueous solubility. Here γ CD was used as a solubilizing complexing agent due to its toxicological profile. Despite improved solubility, the efficiency remained inadequate. In addition, the KI salt tended to degrade at elevated temperatures during preparation of KI/ γ CD complexes. Hence, the aim of this research was to enhance the γ CD solubilization of KIs by additional techniques such as by including hydrophilic polymers or counter ions, and to develop the thermally stable eye drops with suitable stabilizers for delivery of a KI candidate to the targeted site.

Method: Two main methods were applied to prepare the complexes and the ophthalmic eye-drop micro-suspensions. In solubility studies, the complexes were prepared by mild heat (i.e. ultrasonication at 30°C for 30 min.) due to the heat sensitivity of some KIs. The moist heat (i.e. autoclaving at 121°C for 20 min) was utilized for the complex preparation as well as sterilization throughout formulation development. All complex characterizations used samples from the complex supernatants. The physicochemical properties of the aqueous eye drop micro-suspensions were also evaluated.

Results: In phase-solubility studies all six KIs studied displayed B_s-type profiles. Dovitinib had the best solubility performance due to the high affinity for γ CD ($K_{1:1}$ 684 M⁻¹, CE 0.011), followed by motesanib. KIs were more soluble at low pH where they were in their protonated form. The tested hydrophilic polymers affected the KI solubility in complexation media. Besides that, the formulation vehicle could also solubilize KI/ γ CD complexes, mainly influenced by salt formation between EDTA and the drug. Hexadimethrine bromide (HDMBr) generally enhanced the γ CD solubilization through a

synergist effect. Dovitinib was therefore the appropriate candidate for further investigations. The presence of HDMBr still provided a B_s-type profile and increased both γ CD solubilization and the CE from 0.0110 to 0.0391. The formation of dovitinib/ γ CD/HDMBr complex was confirmed by transmission electron microscopy (TEM) imaging as well as solid state characterizations including X-ray powder diffraction (XRPD), differential scanning calorimetry (DSC), and Fourier transform infrared spectroscopy (FT-IR). The γ CD could stabilize the supersaturated dovitinib solution and increase the release rate, yet this rate was decreased by the formation of HDMBr matrix.

Salt formation was observed in formulation vehicle systems and, thus, several acidic counter ions were introduced to enhance the solubility of the weakly basic drug/CD complex. Citrate was the most powerful counter ion that reinforced CD efficiency by salt formation and/or charge-charge interactions. *In vitro* drug permeation did not increase as result of increased CD solubilization.

KI salt was used in formulation studies because salt formation had a greater capacity to solubilize the drug. An unexpected problem occurred regarding the dovitinib salt. However, cediranib maleate (CM) also yielded noteworthy performance due to its high intrinsic solubility. Thus, it was selected for eye drops instead. Riboflavin could thermally stabilize CM dissolved in 15% (w/v) γ CD solution during at least one autoclaving cycle. The partial inclusion complex was observed by NMR analysis. The phase solubility, permeation, and morphology of nanoparticles remained unchanged in the presence of this stabilizer. The combination of riboflavin and other excipients (i.e. polymer and co-solvent) actually reduced the thermal degradation in micro-suspensions. The optimized eye drops did deliver the drug into the back of eye. This product should be stored at 25°C to maintain pH, particle size and shape. Only negligible drug loss was found after a six-month storage period.

Conclusion: The γ CD solubilization and complexation of KIs was increased by additional techniques including the addition of hydrophilic polymers or counter ions. An appropriate stabilizer could protect the KI salt from thermal degradation in a concentrated complexation media. The thermally stable eye drops achieved ocular delivery and had a shelf life of at least six months.

Keywords:

γ -Cyclodextrin, Hydrophilic polymers, Counter ions, Thermal stabilizer, Suspension formulation

Acknowledgements

This study was carried out during the period of 2016-2020 at the Faculty of Pharmaceutical Sciences, University of Iceland. The project was funded by the Icelandic Center for Research (RANNIS) (Grant no. 173841-051), the University of Iceland Research Fund, and Bergþóra and Þorsteinn Scheving Thorsteinsson Fund. After an intensive period of several months, I would like to reflect on all those people who made this Ph.D. dissertation possible and a precious experience for me.

First of all, it is an honor for me to express my absolute privilege to my supervisor, Professor Þorsteinn Loftsson for offering me the invaluable opportunity to join his team as Ph.D. candidate. His guidance, advice, encouragement and patience throughout my doctoral program have been deeply appreciated. He helped me overcome many crisis situations and finally succeeded this project.

My grateful gratitude goes to Prof. Einar Stefánsson, Dr. Phatsawee Jansook, Dr. Gauti Jóhannesson, and Prof. Hákon Hrafn Sigurðsson for serving as members of my Ph.D. committee and the insightful guidance.

In particular, I appreciatively acknowledge Faculty of Pharmaceutical Sciences, University of Iceland, for the laboratory equipment and other facilities to proceed my research and publications.

Most of the journeys described in this thesis would not have been achieved without a good collaboration. I owe a great deal of appreciation to lecturers, administrative and technical staff members of the school who have been kind enough to advise and help in their respective roles.

In my daily work I have been blessed with a friendly and cheerful group of fellow students and particularly Thai seniors. Many thanks to them for their gorgeous care and helpful suggestions during experiments. I am indebted to Mr. Maonian Xu who generously shared his time and valuable knowledge, especially LC-MS information. Thank you.

Finally, I must express my very profound gratitude to my family for understanding and love during the past few years. Their unfailing motivation and continuous encouragement though the process of coursework and research were the end of this accomplishment.

Contents

| | |
|---|--------------|
| Ágrip | iii |
| Abstract | v |
| Acknowledgements | vii |
| Contents | ix |
| List of abbreviations | xii |
| List of figures | xiv |
| List of tables | xix |
| List of original papers | xxi |
| List of original papers not a part of Ph.D. thesis | xxii |
| Declaration of contribution | xxiii |
| 1 Introduction | 1 |
| 1.1 Age-related macular degeneration (AMD) | 1 |
| 1.1.1 Pathophysiology of AMD | 1 |
| 1.1.2 Drug treatment for wet AMD | 3 |
| 1.2 Tyrosine kinase inhibitors | 6 |
| 1.2.1 Mechanism of action | 6 |
| 1.2.2 Physicochemical properties | 6 |
| 1.2.3 KI eye drops in literature and patent..... | 8 |
| 1.3 Cyclodextrins..... | 11 |
| 1.3.1 Structure and physicochemical properties..... | 11 |
| 1.3.2 Toxicological consideration..... | 13 |
| 1.3.3 Complex formation and drug solubility | 13 |
| 1.3.4 Enhancing the CE | 15 |
| 1.3.5 CD application for topical drug delivery to the posterior segment of eye | 20 |
| 1.4 Thermal Stabilizer | 21 |
| 1.4.1 Thermal stability in pharmaceuticals | 21 |
| 1.4.2 Mode of action | 21 |
| 1.4.3 Oxidation inhibitors | 22 |
| 1.4.4 Conformational-change inducers..... | 22 |
| 1.4.5 Chaotropic agents..... | 23 |
| 1.4.6 Other excipients | 24 |
| 2 Aims | 25 |
| 3 Materials and methods | 27 |
| 3.1 Materials..... | 27 |
| 3.2 Quantitative analysis | 28 |
| 3.2.1 Quantitative analysis of drugs..... | 28 |

| | | |
|----------|---|-----------|
| 3.2.2 | Quantitative analysis of γ CD..... | 29 |
| 3.3 | Research design and methods | 29 |
| 3.4 | Solution-state experiments..... | 32 |
| 3.4.1 | Complex preparation methods..... | 32 |
| 3.4.2 | pH profiles..... | 32 |
| 3.4.3 | Thermal stability studies | 33 |
| 3.4.4 | Degradation studies | 34 |
| 3.4.5 | Phase-solubility studies | 34 |
| 3.4.6 | Solubility enhancement studies | 36 |
| 3.4.7 | Physicochemical properties in solution-state..... | 37 |
| 3.4.8 | Spectroscopic studies | 38 |
| 3.4.9 | Morphological analysis | 39 |
| 3.4.10 | <i>In vitro</i> permeation studies | 39 |
| 3.5 | Solid-state experiments..... | 40 |
| 3.5.1 | Preparation of solid complex | 40 |
| 3.5.2 | X-ray Powder Diffraction (XRPD) studies | 40 |
| 3.5.3 | Differential Scanning Calorimetric (DSC) studies | 40 |
| 3.5.4 | Fourier Transform Infrared (FT-IR) studies | 41 |
| 3.5.5 | <i>In vitro</i> dissolution studies..... | 41 |
| 3.6 | Experiments in formulation stage..... | 41 |
| 3.6.1 | Preparation of cediranib maleate eye drops | 41 |
| 3.6.2 | Solid-drug fraction determinations | 41 |
| 3.6.3 | Physicochemical characterizations of formulation | 42 |
| 3.6.4 | Stability testing of formulation | 42 |
| 3.6.5 | Morphological analysis | 42 |
| 3.6.6 | <i>In vivo</i> permeation study | 43 |
| 4 | Results and discussions | 45 |
| 4.1 | The effect of hydrophilic polymers on KI/ γ CD solubilization and complexation | 45 |
| 4.1.1 | Phase-solubility studies (KI/ γ CD complex)..... | 45 |
| 4.1.2 | pH solubility profiles (KI/CD complex) | 48 |
| 4.1.3 | Effect of hydrophilic polymer on drug solubility | 49 |
| 4.1.4 | Effect of formulation vehicle on drug solubility | 54 |
| 4.1.5 | Characterization of KI/ γ CD/polymer complex aggregates in solution state | 55 |
| 4.1.6 | Phase-solubility studies due to hydrophilic polymer | 58 |
| 4.1.7 | ¹ H-NMR Spectroscopic studies (dovitinib/ γ CD and dovitinib/ γ CD/HDMBr complexes) | 59 |
| 4.1.8 | Physicochemical characteristics of solid dovitinib/ γ CD and dovitinib/ γ CD/HDMBr complex | 64 |

| | | |
|----------|---|------------|
| 4.1.9 | <i>In vitro</i> dissolution studies (dovitinib/ γ CD and dovitinib/ γ CD/HDMBr complexes)..... | 69 |
| 4.2 | Effect of acidic counter ion on the dovitinib/ γ CD solubilization and complexation | 70 |
| 4.2.1 | pH-solubility studies (pure dovitinib and dovitinib/ γ CD complexes) | 70 |
| 4.2.2 | Phase-solubility studies (dovitinib/ γ CD complex) | 71 |
| 4.2.3 | Effect of acidic counter ion on drug solubility | 73 |
| 4.2.4 | Effect of acidic counter ion on phase-solubility profile..... | 76 |
| 4.2.5 | Physicochemical properties of dovitinib/CD and dovitinib/CD/counter ion complex aggregates..... | 78 |
| 4.2.6 | ¹ H-NMR Spectroscopic studies (dovitinib/CD and dovitinib/CD/counter ion complexes)..... | 81 |
| 4.2.7 | <i>In vitro</i> permeation studies (dovitinib/CD and dovitinib/CD/counter ion complex aggregates) | 84 |
| 4.3 | Development of thermally stable formulation of cediranib maleate based γ CD for ophthalmic drug delivery | 86 |
| 4.3.1 | Effect of stabilizer on thermal stability of CM/CD complex aggregates in solution-state..... | 86 |
| 4.3.2 | Development and characterization of ophthalmic formulation | 103 |
| 5 | Summary and conclusions..... | 115 |
| | References | 119 |
| | Paper I..... | 141 |
| | Paper II..... | 155 |
| | Paper III..... | 167 |
| | Paper IV | 181 |
| | Paper V | 195 |

List of abbreviations

| | |
|---------------------|--|
| AMD | Age-related macular degeneration disease |
| AREDS | Age related eye disease study |
| ATR | Attenuated total reflection |
| BAC | Benzalkonium chloride |
| BSC | Biopharmaceutics classification system |
| CD | Cyclodextrin |
| CE | Complexation efficiency |
| CM | Cediranib maleate |
| CMC | Carboxymethylcellulose sodium salt |
| CNV | Choroidal neovascularization |
| D ₂ O | Deuterium oxide |
| DSC | Differential Scanning Calorimetry |
| DLS | Dynamic Light Scattering |
| DMSO-d ₆ | Dimethyl sulfoxide-d ₆ |
| ΔpK_a | pK_a different |
| ϵ | Dielectric constant |
| E_a | Activation energy |
| EDTA | Ethylenediaminetetraacetic acid disodium salt |
| ESI | Electrospray ionization |
| FT-IR | Fourier transform infrared spectroscopy |
| GA | Geographic atropy |
| γ CD | γ -Cyclodextrin |
| HDMBBr | Hexadimethrine bromide |
| HP γ CD | 2-Hydroxypropyl- γ -cyclodextrin |
| HPLC | Reverse-phase high performance liquid chromatography |
| HPMC | Hydroxypropylmethylcellulose |
| IVT | Intravitreal |
| J | Flux of drug |
| $K_{1:1}$ | Complex stability constant |
| kDA | Kilodaltons |

| | |
|-----------------|--|
| KI | Kinase inhibitor |
| MWCO | Molecular weight cut-off |
| NMR | Nuclear Magnetic Resonance Spectroscopy |
| P_{app} | Apparent permeability coefficient |
| PBS | Phosphate buffer saline |
| PDFT | Platelet-derived growth factor |
| PEG400 | Polyethylene glycol 400 |
| Poloxamer 407 | poly(ethylene glycol)- <i>block</i> -poly(propylene glycol)- <i>block</i> -poly(ethylene glycol) |
| PVP | Polyvinyl pyrrolidone |
| PVA | Polyvinyl alcohol |
| RAF | Rapidly accelerated fibrosarcoma |
| RF | Riboflavin |
| RPE | Retinal pigment epithelium |
| SBE γ CD | Sulfobutyl ether γ -cyclodextrin sodium salt |
| SD | Standard deviation |
| TEM | Transmission electron microscopy |
| UHPLC | Ultra-high performance liquid chromatography |
| UV/VIS | Visible and Ultraviolet Spectroscopy |
| VEGF | Vascular endothelial growth factor |
| VEGFR | Vascular endothelial growth factor receptor |
| XRPD | X-ray Powder Diffraction |
| ZP | Zeta potential |

List of figures

| | |
|--|----|
| Figure 1. Anatomy of total eye (left), and the healthy and pathological conditions of the retinal and choroid regions (right). | 2 |
| Figure 2. Fundus photographs of A) healthy eye, and eyes with B) dry AMD, and C) wet AMD..... | 2 |
| Figure 3. Drug mechanisms to inhibit VEGF and PDGF pathways..... | 3 |
| Figure 4. Intravitreal (IVT) injection photograph (left) and schematic diagram (right). | 4 |
| Figure 5. Schematic representation of α CD, β CD and γ CD structure..... | 11 |
| Figure 6. Formation of 1:1 drug/CD complex. | 14 |
| Figure 7. Phase-solubility profiles and classification of complexes according to Higuchi and Connors. | 15 |
| Figure 8. The phase-solubility profiles of the KIs in an unbuffered aqueous γ CD media (pH 6.3 to 6.8) at ambient temperature (mean \pm standard deviation; n = 3). | 46 |
| Figure 9. The pH-solubility profiles of the KIs in pure aqueous 5% (w/v) γ CD and 5% (w/v) HP γ CD solutions at room temperature (mean \pm standard deviation; n = 3)..... | 49 |
| Figure 10. Aqueous solubility of the KIs in unbuffered pure aqueous γ CD, (pH 6.3 to 6.8), with and without 1% (w/v) hydrophilic polymer solution at room temperature (mean \pm standard deviation; n=3). The concentration of γ CD is shown below each figure. | 52 |
| Figure 11. Aqueous solubility of the KIs in an EDTA solution with 0% or 8% (w/v) pure aqueous γ CD solution at room temperature (mean \pm standard deviation; n=3)..... | 54 |
| Figure 12. Aqueous solubility of the KIs in a benzalkonium chloride solution with 0% or 8% (w/v) pure unbuffered aqueous γ CD solution (pH 6.3-6.8) at room temperature (mean \pm standard deviation; n=3). | 55 |
| Figure 13. Transmission electron microscopic images of dovitinib with 5% or 8% (w/v) γ CD at magnitude of 50k; (A) | |

| | |
|---|----|
| dovitinib/ γ CD5% system, (B) dovitinib/ γ CD8% system, and (C) dovitinib/ γ CD8%/HDMBr system. | 58 |
| Figure 14. Phase-solubility profiles of dovitinib complexes without and with HDMBr (mean \pm standard deviation; n=3). The media was pure water. | 59 |
| Figure 15. Structure of (A) γ CD, (B) dovitinib, (C) HDMBr and their protons probed in the NMR experiment. | 61 |
| Figure 16. Representative NMR spectrum of (A) γ CD, (B) dovitinib, (C) HDMBr and their protons. | 63 |
| Figure 17. Proposed complex formation of dovitinib /HDMBr/ γ -CD ternary system. | 64 |
| Figure 18. XRPD spectra of (A) γ CD, (B) pure dovitinib, (C) HDMBr, (D) Dovitinib/ γ CD physical mixture, (E) Dovitinib/ γ CD/HDMBr physical mixture, (F) Dovitinib/ γ CD complex, (G) Dovitinib/ γ CD/HDMBr complex. | 65 |
| Figure 19. DSC of (A) γ CD, (B) pure dovitinib, (C) HDMBr, (D) dovitinib/ γ CD physical mixture, (E) dovitinib/ γ CD/HDMBr physical mixture, (F) dovitinib/ γ CD complex, (G) dovitinib/ γ CD/HDMBr complex. | 66 |
| Figure 20. DSC of (A) γ CD, (B) pure axitinib, (C) HDMBr, (D) axitinib/ γ CD physical mixture, (E) axitinib/ γ CD/HDMBr physical mixture, (F) axitinib/ γ CD complex, (G) axitinib/ γ CD/HDMBr complex. | 66 |
| Figure 21. DSC of (A) γ CD, (B) pure motesanib, (C) HDMBr, (D) motesanib/ γ CD physical mixture, (E) motesanib/ γ CD/HDMBr physical mixture, (F) motesanib/ γ CD complex, (G) motesanib/ γ CD/HDMBr complex. | 67 |
| Figure 22. FT-IR spectra of 8(A) γ CD, (B) pure dovitinib, (C) HDMBr, (D) Dovitinib/ γ CD physical mixture, (E) Dovitinib/ γ CD/HDMBr physical mixture, (F) Dovitinib/ γ CD complex, (G) Dovitinib/ γ CD/HDMBr complex. | 68 |
| Figure 23. <i>In vitro</i> dissolution of dovitinib in solid complexes with γ CD at a concentration of 5% or 8% (w/v) (mean \pm standard deviation; n=3). | 69 |

| | |
|--|----|
| Figure 24. pH-solubility profiles of dovitinib in pure water and in 5% (w/v) aqueous γ CD solutions (mean \pm standard deviation; n=3). | 70 |
| Figure 25. Ionization of dovitinib assuming the nitrogen in position 4 of the 4-methyl-1-piperaziny moiety is the most basic one. | 71 |
| Figure 26. Phase-solubility profiles of dovitinib complexes in pure water (pH about 6.86) and in aqueous hydrochloric acid solution, at pH 6 (mean \pm standard deviation; n=3). | 71 |
| Figure 27. Aqueous solubility of the dovitinib in buffered aqueous 1% (w/v) acidic counter ion solution at pH 6.0 with and without 8% (w/v) γ CD at room temperature (mean \pm standard deviation; n=3). | 74 |
| Figure 28. Characteristics of pure dovitinib and dovitinib complexes (A) particle size, (B) zeta potential, (C) electrical conductivity, and (D) osmolality (mean \pm standard deviation; n=3). | 80 |
| Figure 29. Proposed complex formation of dovitinib/CD/citric acid ternary system. | 84 |
| Figure 30. Permeation parameters a) solubility, b) flux through a MWCO 12-14k semi-permeable membrane, c) apparent permeation (P_{app}), and d) fraction of aggregate complex (f_A) calculated from dovitinib ternary complexes with citric acid (mean \pm standard deviation; n=3). | 85 |
| Figure 31. The pH profile of CM in pure water (mean \pm standard deviation; n=3). | 87 |
| Figure 32. Thermal stability of CM in aqueous γ CD solutions at concentration of 0%, 5%, and 15% (w/v) under autoclaving (mean \pm standard deviation; n=3). | 88 |
| Figure 33. Thermal stabilizer of CM in 15% (w/v) γ CD aqueous solution in presence of 0.1% (w/v) stabilizer (mean \pm standard deviation; n=3). | 90 |
| Figure 34. Thermal stability of CM after 3 cycles of autoclaving in aqueous γ CD solutions and 0.1 % (w/v) stabilizer (mean \pm standard deviation; n=3). | 91 |
| Figure 35. LC/UV chromatogram of CM in pure water at pH 1; A) Drug peak, B) Degradation peak. | 92 |

| | |
|--|-----|
| Figure 36. LC/PDA/MS spectra of CM in pure water at pH 1; A) UV chromatogram, B) UV absorbance, C) mass spectra. | 93 |
| Figure 37. Possible degradation products of CM after storage in strong acid or exposure to autoclaving. | 94 |
| Figure 38. Phase solubility profile of CM containing 0.1% (w/v) riboflavin in aqueous γ CD solution (mean \pm standard deviation; n=3). | 95 |
| Figure 39. Amount of dissolved γ CD from CM/ γ CD/Riboflavin complexes in pure water (mean \pm standard deviation; n=3). | 96 |
| Figure 40. $^1\text{H-NMR}$ spectra and proton assignments of a) γ CD, b) CM, and c) riboflavin prepared under room temperature. | 98 |
| Figure 41. $^1\text{H-NMR}$ spectra and proton assignments of CM prepared under a) room temperature, and b) autoclaving. | 99 |
| Figure 42. NOESY spectra of ternary CM/ γ CD/riboflavin (RF) complex prepared under autoclaving. | 101 |
| Figure 43. Permeation parameters of CM/ γ CD and CM/ γ CD/Riboflavin complexes a) flux, b) apparent permeation coefficient, and c) fraction of aggregate complex (mean \pm standard deviation; n=3). | 102 |
| Figure 44. TEM images at magnitude of 10,000 a) 15% (w/v) γ CD, b) 0.1% (w/v) riboflavin, c) CM, d) CM/ γ CD15, e) CM/ γ CD15/riboflavin. | 103 |
| Figure 45. Thermal stability of CM/ γ CD complex in presence of 0.1% (w/v) stabilizer after 1-cycle autoclaving (mean \pm standard deviation; n=3). | 106 |
| Figure 46. Thermal stability of CM/ γ CD complex in different pH after 1-cycle autoclaving (mean \pm standard deviation; n=3). | 107 |
| Figure 47. pH of CM-F6 in 3 months (mean \pm standard deviation; n=2). | 112 |
| Figure 48. Mean particle diameter (nm) of CM-F6 in 3 months (mean \pm standard deviation; n=2). | 112 |
| Figure 49. Light microscope images of a) undiluted micro-suspension, b) diluted micro-suspension (dilution of 1/20), and c) supernatant at 400X magnitude. | 113 |
| Figure 50. TEM image at magnitude 25,000x of CM-F6 a) undiluted micro-suspension, b) diluted micro-suspension (dilution of 1/20), c) supernatant. | 114 |

Figure 51. TEM images at magnitude 25,000x of 3-month CM-F6 at
a) 5°C, b) 25°C, and c) 40°C. 114

List of tables

| | |
|--|----|
| Table 1. The structure, physicochemical properties, and bioavailability of the KIs. | 7 |
| Table 2. KI eye drops in literature. | 8 |
| Table 3. Patent of KI eye drops. | 10 |
| Table 4. Characteristics of the natural α CD, β CD and γ CD. | 12 |
| Table 5. The structure and physicochemical properties of CDs (i.e. the complexing agent) used. | 12 |
| Table 6. The structure and physicochemical properties of the polymers (co-complexing agents) used. | 17 |
| Table 7. The structure and physicochemical properties of the acidic counter ion. | 19 |
| Table 8. The structure and physicochemical properties of the stabilizer. | 23 |
| Table 9. The chromatographic conditions. | 28 |
| Table 10. The excipient combinations tested during solubilization and stabilization testing of drug substances. | 30 |
| Table 11. Solubilization efficacy of six KIs in pure water (pH between 6.3 and 6.8). | 47 |
| Table 12. An increase of KI solubility by comparison of the drug alone and the drug/ γ CD complex (pH between 6.3 and 6.8). | 53 |
| Table 13. The pH, Osmolality, DLS data of pure KI and KI complex aggregates (mean \pm standard deviation; n=3). | 57 |
| Table 14. Solubilization efficacy of dovitinib complexes without and with HDMBr in pure water. | 59 |
| Table 15. ^1H NMR chemical shift difference ($\Delta\delta$, ppm) of free γ CD and in the binary (i.e. dovitinib/ γ CD and HDMBr/ γ CD) and ternary dovitinib/ γ CD/HDMBr complexes. | 62 |
| Table 16. ^1H NMR chemical shift difference ($\Delta\delta$, ppm) of dovitinib (D) in free-state and in the complexes. | 62 |
| Table 17. ^1H NMR chemical shift difference ($\Delta\delta$, ppm) of HDMBr in free-state and in complex. | 63 |
| Table 18. Solubilization efficacy of dovitinib in different CD solution. | 72 |

| | |
|--|-----|
| Table 19. Solubilizing ratio of ionized dovitinib at pH 6 in comparison of control, and the ratio between presence and absence of γ CD. | 75 |
| Table 20. Solubilization efficacy of dovitinib in different CD solution..... | 77 |
| Table 21. ^1H NMR chemical shift difference ($\Delta\delta$, ppm) of free γ CD and in the binary (i.e. dovitinib/ γ CD and citric acid/ γ CD) and ternary dovitinib/ γ CD/citric acid complexes. | 82 |
| Table 22. ^1H NMR chemical shift difference ($\Delta\delta$, ppm) of free HP γ CD and in the binary (i.e. dovitinib/HP γ CD and citric acid/HP γ CD) and ternary dovitinib/HP γ CD/citric acid complexes. | 83 |
| Table 23. ^1H NMR chemical shift difference ($\Delta\delta$, ppm) of free SBE γ CD and in the binary (i.e. dovitinib/SBE γ CD and citric acid/SBE γ CD) and ternary dovitinib/SBE γ CD/citric acid complexes. | 83 |
| Table 24. Peak characteristics of CM determined by LC/PDA/MS..... | 94 |
| Table 25. Estimated phase-solubility parameters of CM/ γ CD complex and CM/ γ CD/riboflavin complex in pure water. | 96 |
| Table 26. ^1H NMR chemical shift of γ CD containing riboflavin in free-state and in complex by preparing under a) room temperature, and b) autoclave. | 100 |
| Table 27. CM eye drop formula containing 15% (w/v) γ CD..... | 109 |
| Table 28. Physicochemical data of CM-F6 suspension (n =3). | 110 |
| Table 29. Drug assay of CM-F6 in 6 months (mean \pm standard deviation; n=2). | 111 |

List of original papers

This thesis is based on the following original publications:

- I. Aqueous solubility of kinase inhibitors: I the effect of hydrophilic polymers on their γ -cyclodextrin solubilization, **Pitsiree Praphanwittaya**, Phennapha Saokham, Phatsawee Jansook, Thorsteinn Loftsson. *Journal of Drug Delivery Science and Technology*. 55, 101462 (2020).
- II. Aqueous solubility of kinase inhibitors: II the effect of hexadimethrine bromide on the dovitinib/ γ -cyclodextrin complexation. **Pitsiree Praphanwittaya**, Phennapha Saokham, Phatsawee Jansook, Thorsteinn Loftsson. *Journal of Drug Delivery Science and Technology*. 55, 101463 (2020).
- III. Aqueous solubility of kinase inhibitors: III The effect of acidic counter ion on the dovitinib/ γ -cyclodextrin complexation. **Pitsiree Praphanwittaya**, Phatsawee Jansook, Thorsteinn Loftsson. "Accepted for publication".

Some unpublished data are presented:

- IV. Effect of stabilizer on thermal stability of cediranib maleate/cyclodextrin complexes in solution state. **Pitsiree Praphanwittaya**, Phennapha Saokham, Phatsawee Jansook, Thorsteinn Loftsson. "Manuscript".
- V. Development of thermally stable formulation of cediranib maleate based cyclodextrin for ophthalmic drug delivery. **Pitsiree Praphanwittaya**, Phennapha Saokham, Phatsawee Jansook, Thorsteinn Loftsson. "Manuscript".

In addition, other scientific publications as a co-author:

- VI. Solubilization and *in vitro* permeation of dovitinib/cyclodextrin complexes and their aggregates. Phatsawee Jansook, **Pitsiree Praphanwittaya**, Suppakan Sripetch, Thorsteinn Loftsson. *Journal of Inclusion Phenomena and Macrocyclic Chemistry*. <https://doi.org/10.1007/s10847-020-00995-y>. (2020).

All papers are reprinted by kind permission of the publishers.

List of original papers not a part of Ph.D. thesis

- I. Characterization and evaluation of ternary complexes of ascorbic acid with γ -cyclodextrin and poly(vinyl alcohol). Phennapa Saokham, Kanokporn Burapapadh, **Pitsiree Praphanwittaya**, Thorsteinn Loftsson. "Submitted for publication".

Declaration of contribution

The doctoral student, Pitsiree Praphanwittaya, and her supervisor, Prof. Þorsteinn Loftsson, worked together on planning the research described in this thesis. The doctoral student performed the experiments, applied for the appropriate ethical and research approvals, drafted the manuscripts and wrote this thesis with the sound guidance of her supervisor, the doctoral committee, and worked in close co-operation with the co-authors of each study. Specifically, the contributions of other co-authors are as follows:

Phennapha Saokham supervised the physical pharmacy labs in the beginning of the project. She designed some of the experiments, especially in Papers I and II, and her analytical methods were applied in Papers I, II, IV, and V.

Phatsawee Jansook provided the relevant study in parallel of Papers I and II. His preliminary study inspired the directions of experiments described in Papers IV and V. He contributed valuable revisions to those manuscripts.

All authors contributed to and approved the final versions of all the manuscripts.

1 Introduction

1.1 Age-related macular degeneration (AMD)

1.1.1 Pathophysiology of AMD

Age-related macular degeneration (AMD) is the principle cause of irreversible blindness in elderly populations (aged ≥ 55) worldwide (Klein, 2007). AMD is a late onset neurodegenerative disease in the posterior segment of the eye. Age Related Eye Disease Study (AREDS) classifies AMD into early, intermediate, and advance stages ("The Age-Related Eye Disease Study (AREDS): design implications. AREDS report no. 1," 1999; Ferris et al., 2013). AMD is divided into two major forms; Dry AMD (90% of cases), and Wet AMD (10% of cases) (Bressler, Bressler, & Fine, 1988). The dry form of AMD, also known as non-neovascular, non-exudative, or atrophic AMD, is a chronic condition associated with the build-up yellow protein deposits called "drusen" in macular during early stage, leading to a disruption of the retinal pigment epithelium (RPE), and eventually geographic atrophy (GA). Advance stages, a subset of patients with dry form will progress to wet AMD due to irregular production of vascular endothelial growth factor (VEGF) by the RPE cell. This VEGF can bind tyrosine kinase receptors (VEGFR) on the cell surface (Liu et al., 2007). The imbalanced VEGF signals induce ES (CNV) and malfunctioning of the photoreceptors. This CNV, or angiogenesis, causes the new growth of blood vessels, specifically in choroid region, that leads leakage of exudates and hemorrhage into the retina (Bhutto & Lutty, 2012). In other words, wet AMD can be recognized as neovascular AMD and exudative AMD. Without management, these severe retinal damages lead to blurred vision and, eventually central visual loss (Hanout et al., 2013). The healthy and pathological conditions of the eye are shown in Figs. 1 and 2. To prevent blindness, several treatments including thermal laser photo coagulation, photodynamic therapy with verteporfin, and drug targeted at VEGF have been introduced for wet AMD (Hanout et al., 2013). This Ph.D. project focuses on pharmacologic therapy only.

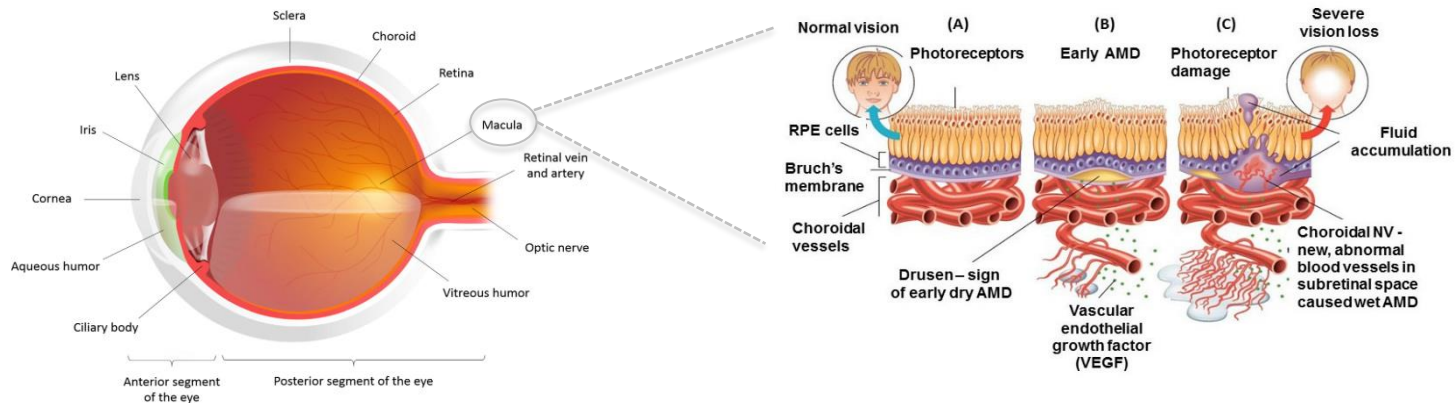


Figure 1. Anatomy of total eye (left), and the healthy and pathological conditions of the retinal and choroid regions (right) (Delplace, Payne, & Shoichet, 2015; Salimiaghdam, Riazi-Esfahani, Fukuhara, Schneider, & Kenney, 2019).

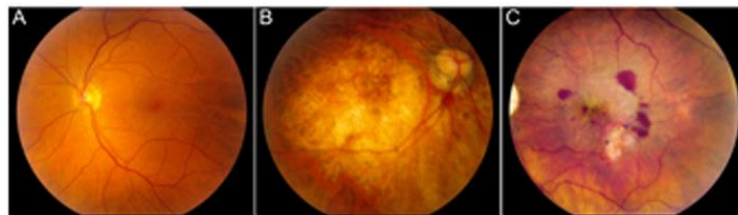


Figure 2. Fundus photographs of A) healthy eye, and eyes with B) dry AMD, and C) wet AMD (Ambati & Fowler, 2012).

1.1.2 Drug treatment for wet AMD

The main goal for the treatment of Wet AMD is improving or maintaining visual activity. Specific pharmacotherapeutic agents are required to prevent CNV and reduce the fluid leakage. VEGF is a major mediator of CNV. In most cases, inhibitors of VEGF signal merely halts or slows vision loss, rather than curing or treating the underlying condition (Khan, Agarwal, Loutfi, & Kamal, 2014). Besides that, platelet-derived growth factor (PDGF) also plays a role in the formation of new blood vessels (Hannink & Donoghue, 1989). Currently, various types of drugs with different mechanisms against VEGF and PDFT signaling have been investigated to prevent the progression of Wet AMD as illustrated in Fig. 3.

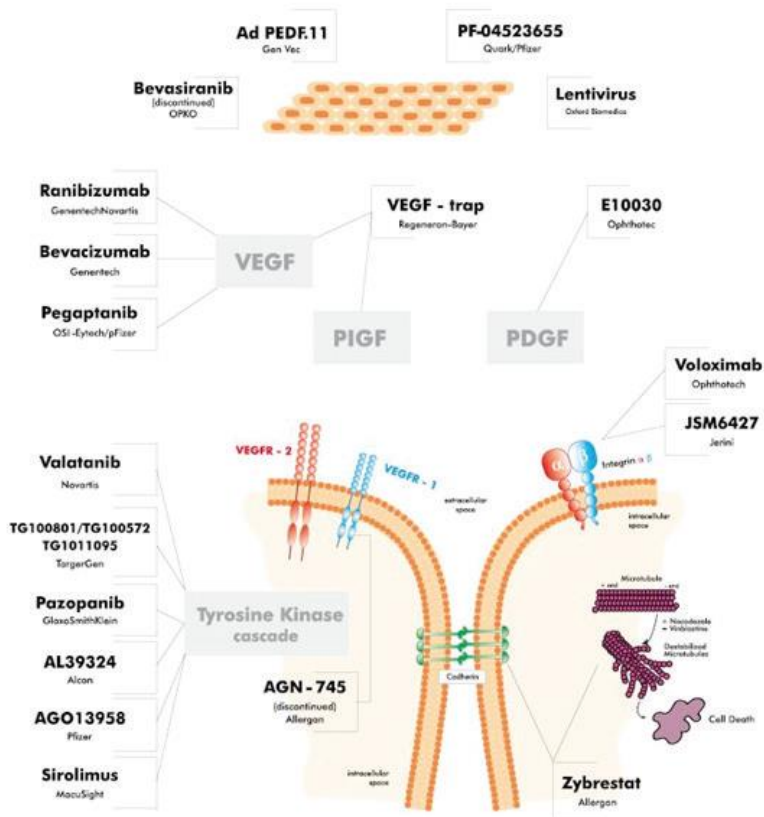


Figure 3. Drug mechanisms to inhibit VEGF and PDGF pathways. **Source:** www.amdbook.org.

The current FDA-approved therapy consists of monthly intravitreal (IVT) injections (Fig. 4) of anti-VEGF agents, including pegaptanib sodium (2004), ranizumab (2006), aflibercept (2011) and brolucizumab (2019), respectively (Gragoudas et al., 2004; Nguyen et al., 2020; Rosenfeld et al., 2006; Traynor, 2012).

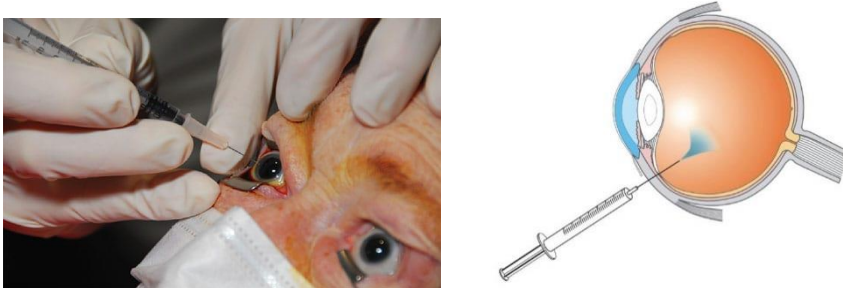


Figure 4. Intravitreal (IVT) injection photograph (left) and schematic diagram (right).
Source: Steve Charles, MD, <https://www.eyeworld.org/>. (Honda et al., 2013).

Pegaptanib sodium (Macugen, Eyetech/Pfizer) is the first anti-VEGF drug which received FDA approval for the treatment of CNV in 2004. This antagonist is a 28-nucleotide PEGylated RNA aptamer that binds to specific VEGF₁₆₅. The clinical dose for IVT injection is recommended at 0.3 mg once every six weeks (Gragoudas et al., 2004).

The second agent, ranizumab (Lucentis®, Genentech), received FDA approval for AMD therapy in 2006. Ranizumab is a monoclonal antibody fragment which specifically binds all active isoforms of VEGF. The approved evidence suggests that ranizumab should be used as an IVT injection of 0.5 mg every four-week interval regimen (Moutray & Chakravarthy, 2011; Rosenfeld et al., 2006).

Bevacizumab (Avastin®, Genentech) is a humanized monoclonal antibody with a similar mechanism of action and efficacy to ranibizumab. It had been widely used in neovascular AMD due to its lower cost compared to ranibizumab, approximately 30 times cheaper dose (Martin et al., 2012). Practically, patients are treated with 1.25 mg of drug, and review every four to six weeks (Foss et al., 2015). However, since the long-term trials demonstrating its safety are still limited, bevacizumab is currently prescribed as off-label use only (Khan et al., 2014).

The US FDA approved aflibercept, also known as VEGF-Trap (Eylea®, Regeneron), for Wet AMD treatment in 2011 (Heier et al., 2012). Aflibercept is an antibody fusion protein consisting of ligand-binding elements from

extracellular domains which specifically bind to all isoforms of VEGF-A, and form an inert 1:1 complex (Stewart, Grippon, & Kirkpatrick, 2012). This antagonist was developed to reduce the dosing schedule from every four weeks, as approved for ranibizumab, to an eight-week interval regimen with 2.0 mg due to higher efficacy (Holash et al., 2002; Stewart et al., 2012).

Most recently, the anti-VEGF brolocizumab (Beovu[®], Novartis) has been approved by the US FDA for patient with neovascular AMD since 2019 (Nguyen et al., 2020). It is a humanized single-chain antibody fragment with a high affinity for multiple isoforms of VEGF-A. The binding capacity of this biologic is up to 22 times greater than those previous antagonists. Thus, the brolocizumab IVT administration is allowed 6 mg of effective dose every three months (Holz et al., 2016; Tietz et al., 2015).

Overall, the adverse events of frequent IVT injections may include substantial burdens at the local site such as retinal detachment, endophthalmitis, traumatic cataract, and systemic side effects like stroke (Falavarjani & Nguyen, 2013; Meyer et al., 2010). Although the frequency of the newest IVT therapy with brolocizumab is relatively less due to the prolonged effectiveness of q12-week intervals, it can still result in ocular inflammations, such as occlusive retinal vasculitis (Nguyen et al., 2020). The repeated use of anti-VEGF drugs may reduce the bio-efficacy of current anti-VEGF agents; a condition known as tachyphylaxis (Doguizi, Ozdek, & Yuksel, 2015; Kuno & Fujii, 2012). However, oral administrations have demonstrated severe adverse systemic effects, especially thromboembolic events (Falavarjani & Nguyen, 2013).

A possible remedy for such adverse events could be the use of alternative therapeutic agents with different modes of action such as tyrosine kinase inhibitors (TKIs) (Barak, Heroman, & Tezel, 2012). Non-invasive administration, such as topical eye drops, may eliminate many of the risks associated with IVT injections and increase patient compliance. Generally, biologics cannot penetrate through the corneal epithelium, thus the topical delivery of these large molecules is not feasible (Kim, Schlesinger, & Desai, 2015; Subrizi et al., 2019). However, several *in vivo* studies in rodent models have claimed success in topically delivering small molecules to back of the eye (Rodrigues et al., 2018). Here tyrosine KI is considered as the favorable candidate for eye drops formulations to treat retinal disease.

1.2 Tyrosine kinase inhibitors

1.2.1 Mechanism of action

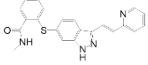
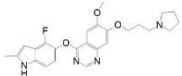
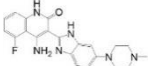
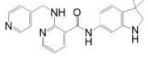
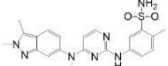
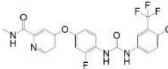
Tyrosine kinase inhibitors (KIs) are an alternative strategy to inhibit the biological effects of VEGF through disrupting the downstream tyrosine kinase cascade when VEGF attaches its receptors as present in Fig. 3 (Barak et al., 2012; Chappelow & Kaiser, 2008). Three major VEGF receptors of kinase enzyme include VEGFR-1, VEGFR-2, and VEGFR-3. Some studies have demonstrated that the inhibition of VEGF signaling by multiple receptors is more potent to suppress CNV (Bergers, Song, Meyer-Morse, Bergsland, & Hanahan, 2003; Kwak, Okamoto, Wood, & Campochiaro, 2000). The efficacy of multiple-tyrosine KIs i.e. axitinib, cediranib, dovitinib (TG100801), motesanib, pazopanib, and reforafenib was confirmed in preclinical studies with models of pathologic ocular neovascularization (Doukas et al., 2008; Giddabasappa et al., 2016; Kang et al., 2013; Klar et al., 2015; Rho et al., 2015; Takahashi et al., 2009). These small-molecule kinase inhibitors contain the suffix, “nib”, which is a verbal short form for “inhibit”. However, the generic name of drugs can be more specific by indicating receptor type, or pharmacological function. For example, “tinib” is used for tyrosine kinase inhibitors, “anib” for angiogenesis inhibitors, and “rafenib” for rapidly accelerated fibrosarcoma (RAF) kinase inhibitors (Arora & Scholar, 2005).

1.2.2 Physicochemical properties

The majority of tyrosine KIs are designed on a series of quinazoline derivatives (Zhou et al., 2020). The core structure of these molecules contains highly lipophilic moieties such as aromatic amines, substituted phenyls, aromatic heterocycles and biaryl constructs. In drug development studies, the aqueous solubility of the drug can be improved by the addition of hydrophilic groups to the backbone (Thomas, 2011). However, the replacement of essential hydrophobic residues by such hydrophilic structures may interfere with the binding areas of the inhibitors (Herbrink, Schellens, Beijnen, & Nuijen, 2016; Reddy & Aggarwal, 2012; Weisberg et al., 2010). Cyclodextrin is one of various excipients for enhancing aqueous solubility without causing structural modification of the drug candidate. Several studies have confirmed that CDs can solubilize KIs such as erlotinib, lapatinib, and gefitinib (Fahmy et al., 2019; Qiu, Li, & Liu, 2017; Gergő Tóth et al., 2016; Gergő Tóth et al., 2017). Based on structure, KIs are generally weak bases that are more soluble in acidic environments due to protonation (Herbrink, Nuijen, Schellens, & Beijnen, 2015). Vemurafenib and trametinib are exceptions herein with an almost pH-independent solubility because their

pKa values that are either above or below the physiological pH-range (Herbrink et al., 2016). The physicochemical properties of six KIs tested are shown in Table 1.

Table 1. The structure, physicochemical properties, and bioavailability of the KIs (ACS, 2019; Praphanwittaya, Saokham, Jansook, & Loftsson, 2020).

| Model drug | Chemical structure | MW | Melting point (°C) | Log P _{o/w} ^a | pK _a ^b | S ₀ (µg/mL) in water ^c | S ₀ (µg/mL) in water ^d | BA ^e (%) |
|-------------|---|--------|--------------------|-----------------------------------|------------------------------|--|--|---------------------|
| Axitinib |  | 386.47 | 184-282 | 2.4 | 4.3 | 40 | 0.37 | 58 |
| Cediranib |  | 450.51 | 158-257 | 0.8 | 10.1 | 190 | 1154.63 | ND ^f |
| Dovitinib |  | 392.43 | 285-310 | 0.48 | 7.7 | 350 | 6.34 | ND ^f |
| Motesanib |  | 373.45 | 140-151 | 3.9 | 5.2 | 12 | 13.98 | ND ^f |
| Pazopanib |  | 437.52 | 285-289 | 3.1 | 5.6 | 1.7 | 0.55 | 14-39% |
| Regorafenib |  | 482.82 | 141-206 | 4.2 | 2.3 | 0.13 | 0.12 | 69% |

^a Calculated octanol-water partition coefficient at pH 7 and 25°C.

^b Calculated value of the protonated base at 25°C.

^c Calculated solubility at pH 7 and 25°C.

^d Experimental solubility at approximately pH 6.5 and 22-23°C.

^e Mean absolute bioavailability in human after oral administration (Chen et al., 2013; Deng et al., 2013; Fong, 2016; Tang, McCormick, Li, & Masson, 2017).

^f Not determined clinically.

1.2.3 KI eye drops in literature and patent

Table 2. KI eye drops in literature.

| KI | Formulation | Composition | Type of study | Reference |
|-----------|----------------------|--|---------------|--|
| Dovitinib | N/A | N/A | Phase I | Clinical trial no. NCT00414999 (2006) |
| | N/A | N/A | Phase II | Clinical trial no. NCT00509548 (2007) |
| | Aqueous suspension | 0.6% Dovitinib 1% HEC, 0.2% tyloxapol, 3.4% dextrose, 0.006% BAC, 0.025% EDTA (280 mOsmol/kg, pH 5.4) | Murine model | (Doukas et al., 2008) |
| Motesanib | Non-aqueous solution | Motesanib 5 mg/mL DMSO: 0.5% sodium CMC =1:19 | Mouse model | (Rho et al., 2015) |
| Pazopanib | Aqueous suspension | Pazopanib 5 mg/mL 0.5% (w/v) sodium CMC, PBS (pH 7.4) | Rat model | (Thakur, Scheinman, Rao, & Kompella, 2011) |
| | N/A | Pazopanib 2 and 5 mg/mL | Phase II | (Danis et al., 2014) |

| Other excipients were not shown | | | | |
|---------------------------------|---|--|-----------|---------------------------|
| | Aqueous suspension | Pazopanib 4.9-5.0 mg/mL Captisol, sodium dihydrogen phosphate, and sodium chloride | Rat model | (Horita et al., 2019) |
| Regorafenib | Non-aqueous suspension | Regorafenib 20 and 30 mg/mL in light liquid paraffin | Phase I | (Zimmermann et al., 2018) |
| | 1.Non-aqueous suspension 2.Aqueous nanocrystal | 1. Regorafenib 17.1-24.1 mg/mL dispersed in liquid paraffin. 2. Regorafenib 1.7 and 2.1 mg/mL in HPC, Polysorbate 80, D-mannitol, glucose and BAC | Rat model | (Horita et al., 2019) |
| | Non-aqueous suspension | Regorafenib 20 and 30 mg/mL Light liquid paraffin | Phase II | (Joussen et al., 2019) |

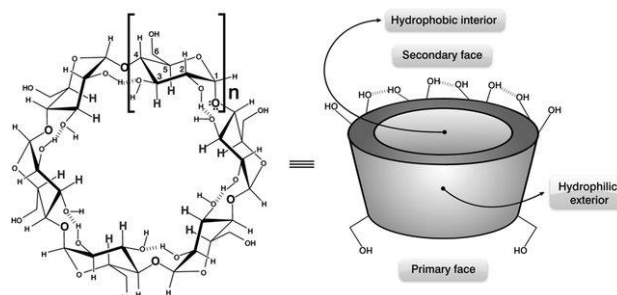
Table 3. Patent of KI eye drops.

| KI | Formulation | Composition | Year | Patent no. |
|-------------|------------------------|--|-------------|--------------------|
| Acrizaniib | Aqueous suspension | No specific formula | 2014 | US 2014/0364392 A1 |
| Axitinib | Non-aqueous suspension | Axitinib 20 mg/mL in liquid paraffin | 2013 | WO 2013/188273 A1 |
| | Aqueous suspension | No specific formula | 2016 | WO 2016/209555 A1 |
| Cediranib | Non-aqueous suspension | Cediranib 20 mg/mL in light liquid paraffin | 2013 | WO 2013/188279 A1 |
| | Non-aqueous suspension | Cediranib 20 mg/mL in light liquid paraffin | 2015 | US 2015/0165028 A1 |
| Pazopanib | Aqueous suspension | Pazopanib 5 mg/mL in buffered 7% (w/v) CD | 2013 | US 2013/0012531 A1 |
| | Aqueous suspension | No specific formula | 2016 | WO 2016/209555 A1 |
| Regorafenib | Non-aqueous suspension | Regorafenib 20 mg/mL in 100% (v/v) liquid paraffin, or hydrophobic colloidal silica in liquid paraffin, or 100% (v/v) PEG glycerides | 2013 | WO 2013/000917 A1 |

1.3 Cyclodextrins

1.3.1 Structure and physicochemical properties

Cyclodextrins (CDs) are cyclic oligosaccharides consisting of six α CD, seven β CD, and eight γ CD or more glucopyranose units linked by α -(1,4) bonds (Loftsson & Brewster, 2010). Due to the chair formation of their glucopyranose units, CD molecules have a toroid shape with secondary hydroxyl groups extending from the wider edge and the primary groups from the narrow edge (Fig. 5). This gives CD molecules a hydrophilic outer surface, whereas the central cavity is lipophilic (Loftsson, Saokham, & Sá Couto, 2019; Saokham & Loftsson, 2017).



When α CD: $n = 6$, β CD: $n = 7$, γ CD: $n = 8$

Figure 5. Schematic representation of α CD, β CD and γ CD structure (Giani, Linde, Laverde, Colauto, & Linde, 2011).

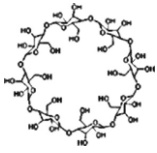
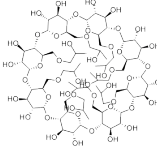
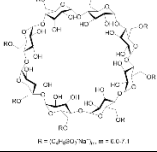
CD molecules are relatively large, with a number of hydrogen donors and acceptors and therefore they do not usually permeate lipophilic membranes (Tiwari, Tiwari, & Rai, 2010). The natural CDs, in particularly β CD, have limited aqueous solubility due to the strong intermolecular hydrogen bonding in the crystal state. This means complexes resulting from the interaction of lipophiles with these CD can be of limited solubility, resulting in precipitation of solid CD complexes from water and other aqueous systems (Loftsson, Jarho, Masson, & Jarvinen, 2005).

The suitability of different CDs for pharmaceutical applications varies in relation to the size of the guest molecule which the CD ring can accommodate. With its larger ring size, γ CD is better suited for larger molecules (i.e. KIs) than α CD or β CD (Meier, Bordignon-Luiz, Farmer, & Szpoganicz, 2001). The main properties of those CDs are given in Table 4. In addition, Table 5 shows the structure and the essential physicochemical properties of CDs for product development in this project.

Table 4. Characteristics of the natural α CD, β CD and γ CD (Saokham & Loftsson, 2017).

| Properties | α CD | β CD | γ CD |
|-------------------------------------|-------------|------------|-------------|
| Number of glucopyranose units | 6 | 7 | 8 |
| Molecular weight (g/mol) | 972.84 | 1134.98 | 1297.12 |
| Approximate dimensions (nm) | | | |
| height (H) | 0.78 | 0.78 | 0.78 |
| inner diameter (ID) | 0.50 | 0.62 | 0.80 |
| outer diameter (OD) | 1.46 | 1.54 | 1.75 |
| Solubility in water at 25°C (mg/mL) | 130 | 18 | 249 |
| Log P at 25°C | -12.9 | -14.0 | -17.3 |

Table 5. The structure and physicochemical properties of CDs (i.e. the complexing agent) used (ACS, 2019; NCBI, 2019; Rowe, Sheskey, Quinn, & Association, 2009).

| Compound | Chemical structure | Molecular weight | Melting point (°C) | Log P _{o/w} (25°C) | pK _a | S ₀ (mg/mL) in water |
|-----------------|--|------------------|--------------------|-----------------------------|-----------------|---------------------------------|
| γ CD |  | 1297.1 | ≥200 | -17.3 | - | 232 |
| HP γ CD |  | 1576 | 250 | - | - | >500 |
| SBE γ CD |  N = 3, 6, 9, 12, 15, 18, 21, 24, 27, 30 | 2072 | - | - | - | Very soluble |

1.3.2 Toxicological consideration

Safety and toxicity are the main concerns with utilizing CDs as pharmaceutical excipients. The route of CD administration can influence the degree of these parameters. Natural CDs are not absorbed through the gastrointestinal tract, thus their oral administration is practically non-toxic (Irie & Uekama, 1997). When parenterally administered, CDs disappear rapidly from systemic circulation. They can be distributed to liver, kidney, urinary bladder, and other body tissues, and finally excreted via the renal intact. Specifically, γ CD shows the enzymatic degradation in humans and animals where α -amylase is present such as saliva, bile fluid, and tears (Lumholdt, Holm, Jorgensen, & Larsen, 2012; Munro, Newberne, Young, & Bar, 2004). As per acute toxicity, the profile of γ CD displays no signs of toxicity after oral, subcutaneous, intravenous (low dose) intraperitoneal, or ophthalmic administration to mice and rats (Donaubauer, Fuchs, Langer, & Bär, 1998; Munro et al., 2004; Saokham & Loftsson, 2017). In terms of toxicity in the use of CDs as excipients, γ CD is generally recognized as safe by the US FDA, with the most favorable toxicological profiles (Saokham & Loftsson, 2017).

1.3.3 Complex formation and drug solubility

CDs can enhance the solubility of drugs through the formation of water-soluble complexes. These complexes can be formed by various techniques, such as physical mixing, kneading, precipitation, and lyophilization. Heating method is commonly used to prepare drug/CD complexes both on a laboratory scale and in industrial production. However, this method is applicable only for heat stable guests (Loftsson et al., 2005).

The thermodynamic interaction between the different components of the CD and the drug is complexation. The toroid configuration of the CD molecule creates a thermodynamic driving force, which is required to form a complex of the active drug with polar molecules and a functional group (Loftsson, Másson, & Brewster, 2004). During complex formation, drug molecules in the complex are in rapid equilibrium with free molecules in the solution, and Van der Waal forces, hydrophobic bonding, and hydrogen bonding may occur (Loftsson et al., 2005). Dissociation of the inclusion complex is a relatively rapid process, usually driven by a large increase in the number of water molecules in the surrounding environment. The most common type of interaction is CD inclusion complex formation of a 1:1 molar ratio where one drug molecule (D) forms a complex with one CD molecule. Fig. 6 is a schematic diagram that describes the complexation process

between CD and a drug, the term “stability constant” or “equilibrium constant” ($K_{1:1}$) indicates affinity of the drug molecules (D) within the host (CD) and its inverse, the dissociation constant (K_d) (see Eq. 1-3) (Loftsson, Magnusdottir, Masson, & Sigurjonsdottir, 2002). This parameter can be varied due to the physicochemical properties of a compound upon inclusion.

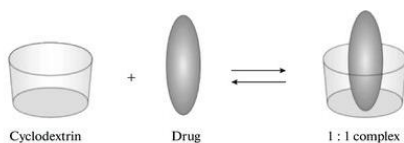


Figure 6. Formation of 1:1 drug/CD complex (Deygen, Skuredina, & Kudryashova, 2017).



$$K_{1:1} = \frac{[D/CD]}{[D][CD]} \quad (2)$$

$$K_d = \frac{1}{K_{1:1}} \quad (3)$$

One of the most widely used traditional approaches to determine the solubilizing effect of CDs on the apparent solubility of a drug through complex formation is phase-solubility analysis. Higuchi and Connor described the profiles by plotting the amount of dissolved drug against the CD concentration. Several types of complex behaviors can be identified in two main categories based on the shape of the phase-solubility relationships (Loftsson & Brewster, 2010). A-type curves represent soluble complexes, while the complexes with limited solubility in water form type-B behaviors. Type A diagrams can be subdivided into A_L (linear phase-solubility diagram, or first order with respect to the CD), A_N (negative direction from linearity), and A_P (positive direction from linearity). Type B diagrams describe two subclasses, including B_S and B_I . B_S -type is indicative of some limited soluble complexes, and B_I -type denotes insoluble complexes where the initial ascending component of the isotherm has not risen (Brewster & Loftsson, 2007; Higuchi & Connors, 1965). The different types of phase-solubility diagrams are shown in Fig. 7.

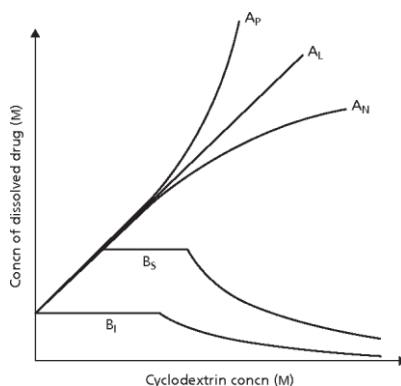


Figure 7. Phase-solubility profiles and classification of complexes according to Higuchi and Connors (Loftsson & Brewster, 2010).

A 1:1 inclusion complex will display an A_L -type phase-solubility diagram, with slope less than unity, and the stability constant ($K_{1:1}$) of the complex can be calculated from the slope and the intrinsic solubility (S_0) of the drug in the aqueous complexation media (i.e. drug solubility when no CD is present), see eq. 4.

$$K_{1:1} = \frac{\text{slope}}{S_0(1-\text{slope})} \quad (4)$$

The complexation efficiency (CE) can be determined from the slope of phase-solubility diagrams following Eq. 5

$$CE = \frac{[D/CD]}{[CD]} = S_0 \cdot K_{1:1} = \frac{\text{slope}}{(1-\text{slope})} \quad (5)$$

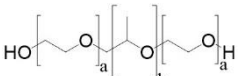
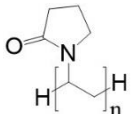
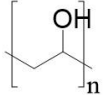
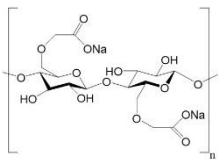
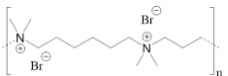
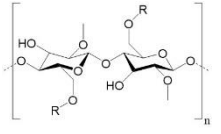
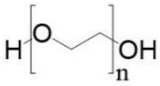
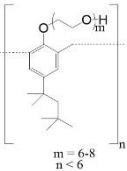
1.3.4 Enhancing the CE

Addition of hydrophilic polymer

Hydrophilic polymers can interact with drugs, CD molecules, or even drug/CD complexes. Both the polymers and CDs are known to form water-soluble complexes with poorly water-soluble drugs (Loftsson & Brewster, 2012; Loftsson et al., 2004). These complexes possibly have different solubility and physicochemical properties than those of CD molecule alone (Carrier, Miller, & Ahmed, 2007). The addition of a small amount of hydrophilic polymer, such as water-soluble cellulose derivatives, has been shown to improve the solubilizing efficiencies and complexation of CDs (Carrier et al., 2007; Loftsson & Brewster, 2012). These results are attributed to the synergistic effects of the polymer and CDs solubilization through

formation of a ternary complex or co-complex consisting of drug, CD and polymer (Hirlekar, Sonawane, & Kadam, 2009; Loftsson & Masson, 2004). In general, the observed CE is increased due to an increase in the $K_{1:1}$ value. These observations suggest that the polymers enhance the stability of the CD complex aggregates, and that perhaps the aggregates have the ability to solubilize lipophilic drugs through micelle-type solubilization (Messner, Kurkov, Jansook, & Loftsson, 2010). The list of tested polymers is presented in Table 6.

Table 6. The structure and physicochemical properties of the polymers (co-complexing agents) used (Praphanwittaya et al., 2020; Rowe et al., 2009).

| Polymer | Chemical structure | MW | Melting point | Solubility in water at RT (mg/mL) |
|--------------------------------|--|--------------|---------------|-----------------------------------|
| Poloxamer 407 |  <p style="text-align: center;">a = 101, b = 56</p> | 9,840-14,600 | 53-57 | Miscible >175 g/L |
| Poly(vinyl pyrrolidone) (PVP) |  | 10 k | 130-150 | Soluble >130 g/L |
| poly(vinyl alcohol) (PVA) |  | 30-70k | 180-190 | Soluble |
| Carboxymethyl cellulose (CMC) |  | 90 kDa | 300 | Soluble |
| Hexadimethrine bromide (HDMBr) |  | 374 kDa | - | Soluble 10%w/v |
| HPMC |  <p style="text-align: center;">R = -CH₂CHOHCH₃</p> | 17-20k | 190-200 | Varies with the molecular weight |
| PEG400 |  | 380-420 | 4-8 | 0.232 |
| Tyloxapol |  <p style="text-align: center;">m = 6-8 n < 6</p> | 298.4 | - | Miscible |

Drug ionization and salt formation

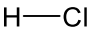
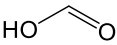
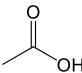
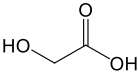
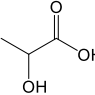
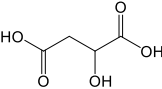
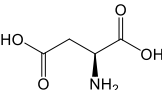
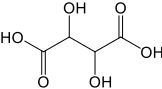
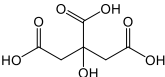
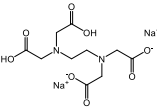
In general, the ionized form of a poorly water-soluble drug has a lesser affinity for hydrophobic CD cavity than the unionized form, hence, the ionized form has a lower $K_{1:1}$ value. Practically, ionization of a lipophilic drug will increase the apparent S_0 , which leads to an enhanced CE, where the increase in S_0 is greater than the decrease in $K_{1:1}$ (see Eq. 5). Although the ionization increases the S_0 value, it also decreases the $K_{1:1}$. However, the decrease in $K_{1:1}$ is not worth consideration when compared to the increase in S_0 (Loftsson & Brewster, 2012).

Salt formation improves the water solubility of compounds, either acidic or basic, because it allows the substances to dissociate in hydrated ions (Herbrink et al., 2015; Thomas, 2011). It is the most common method of increasing aqueous solubility during drug development (Serajuddin, 2007). The solubility of the salt is governed by the solubility product constant of the salt, the solubility of the unionized drug, and the pK_a value. The counter ion can originate from the drug salt or it can be adventitiously present in the aqueous solution as, for example, a buffer salt.

For a given drug substance, the choices of counter ions that are feasible for salt formation depends on the basicity or acidity of the ionizable groups in the compound. According to the pK_a rule, ideally, the pK_a of the counter ion should be two to three pH units lower than the pK_a of the basic drug to employ stable salt formation (Cerrea Vioglio, Chierotti, & Gobetto, 2017; Cruz-Cabeza, 2012; Tong & Whitesell, 1998).

Here the KI salts were formed using different (mono, di, tri, and tetra-) carboxylic derivatives with acceptable pK_a in comparison to a commercial salt, and inorganic acid i.e. hydrochloric acid (HCl). HCl has been the most frequently used for making salts of a wide range of basic drugs due to its very low pK_a (H. Lee, 2014). The essential information of acids tested is given in Table 7.

Table 7. The structure and physicochemical properties of the acidic counter ion (NCBI, 2019; Rowe et al., 2009).

| Acid | Chemical structure | Molecular weight | Melting point (°C) | Log P _{o/w} | pK _a | S _o (mg/mL) in water |
|-----------------|---|------------------|--------------------|----------------------|----------------------------|---------------------------------|
| HCl |  | 36.46 | -26 | 0.00 | -10 | 823 |
| Formic acid |  | 46.03 | 8.4 | -0.54 | 3.75 | 100 |
| Acetic acid |  | 60.05 | 16.6 | -0.22 | 4.75 | 10k-30k |
| Glycolic acid |  | 76.05 | 75 | -1 | 3.6 | 50 |
| D-lactic acid |  | 90.08 | 17 | -0.7 | 4.14 | 562 |
| DL-malic acid |  | 134.09 | 130 | -1.26 | 3.46, 5.10 | 558 |
| L-aspartic acid |  | 133.11 | 270 | -3.5 | 1.99, 3.90, 9.60 | 5 |
| Tartaric acid |  | 150.09 | 206 | -1.8 | 2.98, 4.34 | 1330 |
| Citric acid |  | 192.12 | 153-159 | -1.64 | 3.08, 4.74, 5.40 | 592 |
| EDTA.2Na |  | 336.21 | 252 | - | 2.0, 2.7, 6.2, 10.31 | 110 |

1.3.5 CD application for topical drug delivery to the posterior segment of eye

Drug/CD complexes, especially those of the natural CDs, are known to self-assemble to form nanosized aggregates in an aqueous medium. In aqueous γ CD solutions the size of the aggregates increases with increasing γ CD concentration until they precipitate to form micro- or nanoparticles (P. Jansook, Ogawa, & Loftsson, 2018; Loftsson & Duchêne, 2007).

CDs enhance drug permeability through biological membranes, such as eye cornea and skin by disrupting the membrane, either by permeating into the membrane or by extracting or complexing with lipophilic components such as cholesterol and phospholipids from the membrane (Másson, Loftsson, & Stefánsson, 1999). The formation of CD complexes with corticosteroids, chloramphenicol, diclofenac, cyclosporine, and sulfonamide carbonic anhydrase inhibitors demonstrate significant corneal penetration (Loftsson & Stefánsson, 2017; Loftsson & Järvinen, 1999; Sahoo, Dilhawaz, & Krishnakumar, 2008).

Sigurdsson and colleagues determined that CD complexes containing dexamethasone delivered topically to rabbit eyes were detected at significant levels in the retina and vitreous (Sigurdsson, Konráethsdóttir, Loftsson, & Stefánsson, 2007). The drug can permeate into the eye when high amount of dissolved dexamethasone is sustained in the aqueous tear fluid for longer duration of time. Additionally, the tear fluid saturated with drug practically maximizes ocular drug permeation. To achieve such condition, the drug could be formulated as a micro-suspension with the appropriate ratio of drug amount in each fraction. For example, the total dexamethasone concentration is 1.5% (w/v) in eye drops, and the concentration of dissolved fraction is 0.5% (w/v) which is higher than the solubility of the pure drug by about 50 times (Loftsson, Hreinsdóttir, & Stefánsson, 2007). In this case, the thermodynamic activity of the drug in tear fluid is closer to unity which then leads to the dissolved drug molecules having a higher tendency to diffuse through the membrane barriers (Loftsson & Stefánsson, 2017).

Dorzolamide is another candidate for eye drop micro-suspension. This formulation contained dorzolamide/ γ CD complex in an aqueous medium. The total dorzolamide concentration (i.e. both dissolved and solid) was 3.0% (w/v) where about one-third of dorzolamide was dissolved as free drug molecules, soluble drug/ γ CD complexes as well as nanoparticles, and about two-third of the drug was solid drug/ γ CD complexes in microparticles (Phatsawee Jansook et al., 2010). In aqueous eye drop medium and tear fluid,

dorzolamide/ γ CD complex was more soluble than the pure drug. Consequently, solid dorzolamide/ γ CD microparticles could be retained on the eye surface and it enhanced corneal penetration of drug into the back of eye (Jóhannesson et al., 2014). Thus, a topical CD approach may be useful in the treatment of vitreoretinal diseases requiring chronic drug delivery.

1.4 Thermal Stabilizer

1.4.1 Thermal stability in pharmaceuticals

The thermal stability of drug containing pharmaceutical preparation is important, and closely monitored to maintain the pharmaceutical potency of the formulation. Manufacturing and storing the drug under controlled conditions can challenge thermal stability (Niazi, 2016). The consequences of exposure to heat and thermal oxidation may result in not only the loss of potency but also in the formation of degradation products that can be harmful to the human body (Küpper et al., 2006). In general, drug degradation may be affected by the medium pH, buffer salts, and other excipients, air exposure, and use of stabilizers. In case the dosage form compositions are not appropriate, then modification of a formulation can be considered to improve the stability and shelf-life of the product (Lieberman & Murti Vemuri, 2015).

Autoclaving is a practical technique of producing sterile products such as parenteral dosage forms and eye drops. Here γ CD aggregates and nanoparticles were utilized for ocular drug delivery. Typically, CDs are used to protect compounds against degradation (Loftsson & Brewster, 1996). The γ CD at high concentration has tendency to form larger aggregates that can induce adversary effects. Thus, preparation of CD nanoparticle suspension by heating may require the use of thermal stabilizer for the chemical stabilization of the drug.

1.4.2 Mode of action

The stabilizer is added to the aqueous suspension to enhance the chemical stability of the drug against high temperature. Another main chemical reaction that affects drug stability is oxidation. The oxidation involves the addition of oxygen or the removal of electrons from a drug molecule. Such reaction can be initiated by heat, light, or certain trace metals (Hovorka & Schöneich, 2001; Waterman et al., 2002). A rational choice of stabilizers involves an empirical basis, since its protective effect is variable depending on the drug behavior in concentrated CD aggregates. For example, the stabilizer is

expected to yield a thermally stable system by inhibiting oxidation, changing conformation of drug/CD complexes, or even disrupting CD aggregates.

1.4.3 Oxidation inhibitors

Oxidation inhibitors are chemical additive that acts as preservatives to prevent oxygen from reacting with the active ingredient. The stabilization of pharmaceuticals against oxidative degradation can be improved by using inert gas for exclusion of oxygen (e.g., nitrogen gas), antioxidants (e.g., Mg ascorbate, and Na thiosulfate), and chelating agents (e.g., EDTA) (Waterman et al., 2002).

1.4.4 Conformational-change inducers

KIs have more aromatic carbon and nitrogen atoms on their complex heterocyclic structure than non-kinase compounds (Lackey, 2008). Thus, a change in conformation of KI/CD complex requires binding in a flat lipophilic pocket and making the essential hydrogen bonds. The idea to protect the drug from thermal degradation in complexation media was expanded to include combinations of such binary complexes with an inert molecule such as amino acids or nitrogenous compounds (e.g., caffeine, or riboflavin) which are capable of hydrogen bonding. These molecules are expected to shield some parts of the KI molecule which stand outside of the CD cavity from thermal destruction. The selection of amino acids is based on the binding site of KIs at the biological receptors, for example, lysine (LYS) and arginine (ARG) (Suebsuwong et al., 2018). Caffeine is a purine analogue which has been used as a complexing agent to stabilize drugs by stacking formation due to aromatic ring (Yoshioka & Stella, 2007). Similar stabilization by caffeine was reported for base-catalyzed degradation and photolysis of riboflavin (Ahmad, Ahmed, Sheraz, Aminuddin, & Vaid, 2009; Guttman, 1962). Riboflavin is generally stable to heat sterilization and oxidation. Its thermal stability increases as acidity increases at pH 2-5 (Al-Ani, 2006; Combs & McClung, 2017; Pinto & Zemleni, 2016). In aqueous condition, riboflavin can form complex with small molecules such as quinine sulfate via hydrogen bond and van de Waals force, and with salicylic acid in other mechanisms (i.e. charge transfer or stacking) interaction (Bhattar, Kolekar, & Patil, 2010; Patil, Bhattar, Kolekar, & Patil, 2011). Due to several binding abilities, chemicals such as amino acids, caffeine and riboflavin may change the drug/CD conformation and shield some parts of drug molecule during heating.

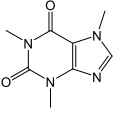
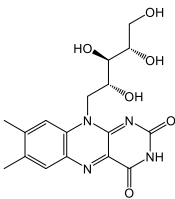
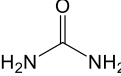
1.4.5 Chaotropic agents

Chaotropic agents (e.g., urea) can modify the structural order of water molecules (Szente, Szejtli, & Kis, 1998). Sá Couto and colleagues found that urea disrupted γ CD aggregates into smaller units through hindering the formation of H-bonds, which is applicable to pharmaceutical formulation (Sá Couto, Ryzhakov, & Loftsson, 2018). The stabilizers tested during this present study are listed in Table 8.

Table 8. The structure and physicochemical properties of the stabilizer (NCBI, 2019; Rowe et al., 2009).

| Stabilizer | Chemical structure | Molecular weight | Melting point (°C) | Log P _{o/w} | pK _a | S _o (mg/mL) in water at RT |
|----------------------------|--------------------------|------------------|--------------------|----------------------|---------------------|---------------------------------------|
| <u>Oxidation inhibitor</u> | | | | | | |
| Nitrogen gas | $\text{N}\equiv\text{N}$ | 28.014 | -210 | 0.67 | - | 18.1 mg/mL at 21°C |
| EDTA.2Na | | 336.21 | 252 | - | 2.0, 2.7, 6.2, 10.3 | 110 |
| Mg ascorbate | | 374.54 | 415-416 | -2.65 | - | >0.95 ^a |
| Sodium thiosulfate | | 158.11 | 48.5 | -4.35 | 11.35 | 209 at 20°C |
| <u>Amino acid</u> | | | | | | |
| L-lysine | | 146.19 | 224.5 | -3.05 | 3.12 | 1,000 |
| L-arginine | | 174.2 | 244 | -4.2 | 2.18, 9, 13.2 | 182 |

Nitrogenous compound

| | | | | | | |
|-------------------------|---|--------|-------|-------|-----------------|------|
| Caffeine |  | 194.19 | 238 | -0.07 | 14 | 21.6 |
| Riboflavin |  | 376.4 | 280 | 1.46 | 10.2 | 0.1 |
| <u>Chaotropic agent</u> | | | | | | |
| Urea |  | 60.056 | 132.7 | -2.11 | 0.21 at 21°C | 545 |

^a refers to (EFSA, 2009)

1.4.6 Other excipients

Although those stabilizers have the potential to suppress thermal degradation of drugs, excessively large amounts of these stabilizers are required, which is beyond the FDA criteria for eye products. In theory, the co-solvent could dissolve the excess guest molecules which are not incorporated into the CDs cavity. In addition, it would help in facilitating complex formation by dissolving the guest before entering the cavity (Viernstein, Weiss-Greiler, & Wolschann, 2003). Thus, the addition of a co-solvent may help resolve the thermal degradation. Moreover, polymeric compounds are also particularly promising in this regard, as many parameters such as functionality and shape. can be adjusted to meet the formulation requirements (Jones, 2004). Few researchers reported that the application of polymers induced the favorable thermal stability for pharmaceutical platforms. For example, poly-anionic polymers could stabilize microcapsule containing protein for at least about 60 minutes in retort processing at 121°C and 15 PSI or hot fill pasteurization at 104°C (P. K. Lee, 2009). The thermal stability of retinol (vitamin A) encapsulated nanoparticles is influenced by the types of polyester used for the nanoparticles (Cho, 2012). Poloxamers significantly enhanced the thermal stability of *in situ* hydrogels with high loading levels of modified nanocrystals or insulin (Li et al., 2017; Lin & Dufresne, 2013). Here co-solvents and polymers are included as supportive stabilizers to prevent KI from thermal degradation in complexation media.

2 Aims

The two major aims of this dissertation were to investigate the feasibility of γ CD as a complexing agent along with supportive techniques, such as hydrophilic polymers and/or counter ions, to increase KI solubility. Furthermore, the thermostable formulations containing KI/ γ CD nanosized aggregates and nanoparticles were prepared for ocular drug delivery.

This research was divided into three parts:

1. Investigation of the effects of various hydrophilic polymers on γ CD solubilization of KIs, and characterization of the ternary complexation containing KI, γ CD, and the optimal polymer in a solid state.
2. Improving γ CD and its derivatives solubilization of dovitinib through salt formation with acidic counter ions in the aqueous complexation media.
3. Enhancement of the thermal stability of selected KI/ γ CD complex aggregates and nanoparticles using stabilizer in aqueous condition, and the development of a thermally stable eye drop micro-suspension with suitable stabilizers for drug delivery to rabbit eyes.

3 Materials and methods

3.1 Materials

Model drugs: axitinib (A), cediranib (C), motesanib (M), pazopanib (P), and regorafenib (R) were purchased from Molekula (Newcastle, UK) whereas dovitinib (D) was purchased from Reagents Direct (Encinitas, CA, USA). Cediranib maleate (CM) was purchased from Shanghai Huirui Chemical Technology Co., Ltd (Shanghai, China).

γ -Cyclodextrin (γ CD) and (2-hydroxypropyl)- γ -cyclodextrin (HP γ CD) were purchased from Wacker (München, Germany). Sulfobutylether- γ -cyclodextrin (SBE γ CD) was kindly supplied by Ligand pharmaceuticals (Lawrence, KS, USA).

Solvents and excipients: hexadimethrine bromide molecular weight of 374 kDa (HDMBR), poly (vinyl pyrrolidone) molecular weight 10 kDa (PVP), low viscosity carboxymethyl cellulose (viscosity of a 4% solution in water at 25°C is 50-200 cps) (CMC), poloxamer 407, poly(vinyl alcohol) with molecular weight 30-70 kDa (PVA), hydroxypropyl methylcellulose (HPMC), viscosity of 2% aqueous solution at 25°C is approximately 50 cP, poly(ethylene glycol 400) (PEG400), tyloxapol, benzalkonium chloride (BAC), 0.1N hydrochloric acid, sodium hydroxide, sodium chloride, acetic acid, glycolic acid, DL-malic acid, L-aspartic acid, tartaric acid, citric acid, magnesium ascorbate, sodium thiosulfate, L-lysine, L-arginine, caffeine, riboflavin, and urea were purchased from Sigma-Aldrich (St. Louis, MO, USA). Formic acid was purchased from Chemicals GmbH (Hamburg, Germany). Lactic acid was purchased from Fluka Chemie GmbH (Barcelona, Spain). Disodium edetate dihydrate (EDTA) was purchased from Merck (Darmstadt, Germany). Nitrogen gas was purchased from AGA (Reykjavik, Iceland). Milli-Q water (Millipore, Billerica, MA) was used throughout the study.

Material for permeation studies: semi-permeable cellophane membrane with molecular weight cutoff (MWCO) 12,000–14,000 Da, was purchased from Biotech CE, Spectrum Europe (Breda, The Netherlands).

Reagents for quantitative analysis by high performance liquid chromatography (HPLC) were commercial products of analytical grade. Acetonitrile (ACN), methanol (MeOH), dimethyl sulfoxide (DMSO), ammonium acetate, ammonium formate were obtained from Sigma–Aldrich (St. Louis, Missouri, USA). Phosphoric acid was purchased from GmbH Chemicals GmbH (Hamburg, Germany).

Reagents for Nuclear Magnetic Resonance (NMR) studies: deuterium oxide (D₂O) and dimethyl sulfoxide-d₆ (DMSO-d₆) were purchased from Sigma–Aldrich (St. Louis, Missouri, USA).

3.2 Quantitative analysis

3.2.1 Quantitative analysis of drugs

A reverse-phase high performance liquid chromatography system (HPLC) from Dionex Softron GmbH (Germering, Germany) was used for quantitative determination of the KIs concentration. Ultimate 3000 series consisting of a P680 pump with a DG-1210 degasser, an ASI-100 autosampler, a VWD-3400 UV-VIS detector. Kinetex Core-shell technology C18 A100 150 x 4.6 mm, 5 µm column connected with guard column (Phenomenex, UK) was used. The temperature of column was kept at 30°C, the flow rate at 1 mL/min, and the injection volume was 20 µL. The isocratic mobile phases composed of organic solvents and aqueous solution as presented in Table 9. All HPLC conditions showed good selectivity.

Table 9. The chromatographic conditions.

| KI | Mobile phase | | | Wavelength (nm) | Injection volume (µL) |
|------------------------|----------------------------------|-----------------|--------------------|-----------------|-----------------------|
| | Non-aqueous:Aqueous ^a | pH ^b | Ratio ^c | | |
| Axitinib | ACN:0.1% AC | 3.45 | 40:60 | 337 | 20 |
| Cediranib ^d | ACN:0.05% PA | 2.8 | 35:65 | 234 | 20 |
| Dovitinib | ACN:MeOH:10mM AF buffer | 4.5 | 20:40:40 | 233 | 20 |
| Motesanib | ACN:10mM AA | 6.4 | 55:45 | 260 | 20 |
| Pazopanib | ACN:10mM AA | 6.4 | 60:40 | 270 | 20 |
| Regorafenib | ACN:MeOH:0.05% PA | 2.8 | 65:10:25 | 265 | 100 |

^a ACN: acetonitrile; MeOH: methanol; AC: acetic acid; PA: phosphoric acid; AF: ammonium formate; AA: ammonium acetate.

^b pH of the aqueous phase before mixing with the non-aqueous phase.

^c Volume ratio of the phases before mixing.

^d This analytical method was also applied for its salt form or cediranib maleate (CM).

3.2.2 Quantitative analysis of γ CD

Quantitative analysis of γ CD was performed in a reverse-phase high-performance liquid chromatography system (Dionex, Softron GmbH Ultimate 3000 series, Germany) consisting of a LPG-3400SD pump with a built-in degasser, a WPS-3000 autosampler, a TCC-3100 column compartment, and a Coronary® ultra RS CAD detector. The HPLC conditions were modified from the γ CD USP 35-NF 30 official monograph and previous investigators (Saokham & Loftsson, 2015). The mobile phase consisted of acetonitrile and water (volume ratio 7:93). The temperatures of the column and sampler compartments were set at 30°C. The flow rate was 1.0 mL/min. The injection volume was 10 μ L.

3.3 Research design and methods

The extensive experiments of this study included 6 model drugs, 3 types of CDs, 8 hydrophilic polymers, 10 counter ions, 9 stabilizers, and 2 preparation methods. The scope of the work is summarized in Table 10.

Table 10. The excipient combinations tested during solubilization and stabilization testing of drug substances.

| Part | Aim | Supportive technique | Model drug | Type of CDs | Complex preparation method | Experiment |
|----------------------|---|--|---|--|----------------------------|---|
| 1. Polymer study | Increase of <u>KI solubility</u> by CD along with supportive technique. | Addition of <u>1% (w/v) polymer</u> (poloxamer 407, PVP, PVA, CMC, HDMBR, HPMC, PEG400, Tyloxapol) | Axitinib Cediranib Dovitinib Motesanib Pazopanib Regorafenib | γ CD HP γ CD | Ultrasonication | <u>In solution-state</u> <ul style="list-style-type: none"> pH profiles Phase-solubility studies Solubility enhancement studies Physicochemical characterizations Morphological analysis Spectroscopic studies <u>In solid-state</u> <ul style="list-style-type: none"> Physicochemical characterizations <i>In vitro</i> dissolution |
| 2. Counter ion study | Increase of <u>KI solubility</u> by CD along with supportive technique. | Salt formation by the addition of <u>1% (w/v) acid as counter ion</u> (HCl, EDTA, formic acid, acetic acid, glycolic acid, malic | Dovitinib | γ CD HP γ CD SBE γ CD | Ultrasonication | <u>In solution-state</u> <ul style="list-style-type: none"> pH profiles Phase-solubility studies Solubility enhancement studies Physicochemical characterizations Spectroscopic studies |

| | | | | | | |
|---------------------|--|--|-------------------|-----|-------------|--|
| | | acid, aspartic acid, tartaric acid, citric acid, lactic acid) | | | | <ul style="list-style-type: none"> • <i>In vitro</i> permeation studies |
| 3. Stabilizer study | Enhancement of <u>thermal stability</u> of KI/γCD complex aggregates, and development of thermally stable eye drops. | Addition of <u>0.1% (w/v) stabilizer</u> (Nitrogen gas, EDTA, magnesium ascorbate, sodium thiosulfate, L-lysine, L-arginine, caffeine, riboflavin, urea) | Cediranib maleate | γCD | Autoclaving | <p><u>In solution-state</u></p> <ul style="list-style-type: none"> • pH profiles • Thermal stability studies • Degradation products • Phase-solubility studies • Spectroscopic studies • <i>In vitro</i> permeation • Morphological analysis <p><u>In formulation stage</u></p> <ul style="list-style-type: none"> • Selection of supportive thermal stabilizers • Formulation preparation • Physicochemical characterizations • Stability studies • Morphological analysis • <i>In vivo</i> permeation studies |

3.4 Solution-state experiments

3.4.1 Complex preparation methods

Two different heating methods were used in preparation of drug/CD complexes (Loftsson, Hreinsdóttir, & Másson, 2005). Mild heat in the form of ultrasonication at 30°C, was applied to thermolabile drugs while heat stable drugs were autoclaved at 121°C for 20 min.

3.4.1.1 Ultrasonication method

The labile drug/CD mixtures were placed in well-sealed vials, and heated in an ultrasonic bath (Branson Bransonic®, CPX3800H ultrasonic bath, USA) at 30°C for 30 min, followed by cooling to an ambient temperature of 22-23°C. Then, the samples were equilibrated in a shaker (KS 15 A Shaker, EB Edmund Bühler GmbH, Germany) at room temperature under constant agitation for one week. Upon equilibrium, the samples were centrifuged at 12,000 rpm for 15 min (Heraeus Pico 17 Centrifuge, Thermo Fisher Scientific, Germany). The supernatant was then collected for further evaluation.

3.4.1.2 Autoclaving method

The heat stable drug/CD mixtures were heated in an autoclave at 121°C for 20 min, then allowed to equilibrate at room temperature (22-23°C) under constant agitation for 7 days. Their centrifuged supernatant was then collected for further evaluation.

3.4.2 pH profiles

*** For polymer study**

The solubilities of KIs including axitinib (A), cediranib (C), dovitinib (D), motesanib (M), pazopanib (P), and regorafenib (R) were determined from pH 1 to 11. An excess amount of the drug was added to 5% (w/v) HP γ CD or 5% (w/v) γ CD solutions. The addition of CDs here was aimed to increase very limited drug solubility to enable HPLC detection. HP γ CD was included in this experiment due to its characteristic non-turbidity (i.e. forms clear solutions). The concentrated γ CD solution can have a turbid appearance which might interfere with the saturation point of the dissolved drug in different pH media. The desired pH range was adjusted by dropwise titration of concentrated aqueous sodium hydroxide (NaOH) or hydrochloric acid (HCl) solution. The triplicate suspensions (n=3) were heated following ultrasonication (see Section 3.4.1.1). The pH was constantly monitored (Thermo Orion 3 Star™

bench top pH meter, Thermo Fisher Scientific, USA) and, if necessary, corrected with a concentrated aqueous HCl or NaOH solution during the agitation. After equilibration, samples were centrifuged, and their supernatant was analyzed for amount of dissolved KIs by HPLC. The values reported are the mean values \pm the standard deviation (SD).

*** For counter ion and stabilizer studies**

Excess amount of dovitinib (D) or cediranib maleate (CM) was placed in pure water in triplicate (n=3). The concentrated NaOH or HCl solution was added by dropwise titration to adjust the pH from 1 to 11. Those samples were constantly agitated at ambient temperature (22-23°C) for 7 days, and the pH readjusted periodically until equilibrium was reached. The supernatant of each sample was harvested by centrifugation. The centrifuged samples were diluted with 50% MeOH prior to determining the amount of dissolved drug by HPLC. The results reported are the mean values \pm standard deviation (SD).

3.4.3 Thermal stability studies

3.4.3.1 Thermal stability test for drug/CD complexes

*** For polymer and stabilizer studies**

The thermal stability of the drugs was investigated in pure water containing 0%, 5%, and 15% γ CD (w/v). Excess amount of given KIs were dissolved in pure water, and constantly agitated at room temperature for 24 h. The centrifuged supernatant was divided into two sets. One set was ready for drug analysis while another set was further exposed to autoclaving as previously described (see Section 3.4.1.2). The drug concentration of each set was then determined by HPLC. The thermal stability of KIs was presented in % drug amount which was compared heated and non-heated samples.

3.4.3.2 Thermal stability enhancement studies

*** For stabilizer study**

The stabilizer at a concentration of 0.1 % (w/v) was included in KI/15% γ CD complex ternary system. The media were unbuffered and the pH was 5.0 ± 0.5 . The samples were prepared by the same process as the polymer study and counter ion set. The selected stabilizer was re-heated for up to 3 cycles. The drug concentration of heated and non-heated samples was analyzed by HPLC.

3.4.4 Degradation studies

** For stabilizer study*

The degradation products of non-heated CM, 3-cycle heated CM, and CM at pH1 solutions were characterized by UPLC/PDA/MS (Waters ACQUITY QDa detector 2.0, Massachusetts, USA). The ESI (Electrospray Ionization) source conditions were also optimized to obtain high sensitivity and a good signal. Different conditions, such as drying gas flow, nebulizing gas flow, capillary voltage and spray voltage were optimized to maximize the sensitivity at a low concentration to identify and characterize the degradation products. The chromatographic separation was performed on an Acquity UPLC BEH C18 column, (130°C, 1.7 μm , 3 mm x 50 mm). The mobile phase used was a mixture of 0.1% (v/v) formic acid and acetonitrile in a ratio of (70:30 v/v). The mobile phase was freshly prepared and filtered by vacuum filtration through a 0.45 μm filter and degassed by an ultrasound sonicator prior to use. The analysis was performed under isocratic condition at a flow rate of 0.3 mL min^{-1} at 30°C using a UV detector at 234 nm.

3.4.5 Phase-solubility studies

** For the polymer and counter ion studies*

Binary systems

The phase-solubility of KIs was determined under different conditions by a heating technique as previously described (Loftsson et al., 2005). Each experiment was performed in triplicate (n=3) and the values reported are the mean values \pm the standard deviation (SD). The preliminary test showed that KI degraded by up to 60% during autoclaving and, thus, mild heating was applied in this study. In brief, when excess KI was added to unbuffered aqueous γCD solutions; the pH was 6.5 ± 0.3 . The well-sealed samples were heated following ultrasonication (see Section 3.4.1.1). The amount of dissolved drug was analyzed by HPLC.

The determination of the phase-solubility diagrams was performed according to the Higuchi and Connors method (Higuchi & Connors, 1965). The stability constant ($K_{1:1}$) of the KI/ γCD 1:1 (molar ratio) complex and the complexation efficiency (CE) were derived from the slope of initial linear phase-solubility diagrams using the equations previously described in the introduction:

$$K_{1:1} = \frac{\text{slope}}{S_0 \cdot (1 - \text{slope})} \quad (6)$$

$$CE = S_0 \cdot K_{1:1} = \frac{\text{slope}}{(1 - \text{slope})} = \frac{[KI/\gamma CD \text{ complex}]}{[\gamma CD]} \quad (7)$$

where S_0 is the intrinsic solubility of the drug, $[KI/\gamma CD \text{ complex}]$ is the concentration of dissolved complex and $[\gamma CD]$ is the concentration of dissolved γCD (and not in a complex) in the aqueous complexation media.

Ternary systems

In presence of a polymer as the third component, the determination of phase-solubility was performed by a heating technique in triplicate ($n=3$) (Loftsson et al., 2005; Praphanwittaya, Saokham, Jansook, & Loftsson, 2020). Briefly, the excess amount of dovitinib was added to aqueous solutions containing 0 to 20% (w/v) γCD and 1% (w/v) HDMBr. The experiment was conducted under unbuffered conditions to avoid the influence of buffer salts on the measured solubility value. The pH of the aqueous media was within the acceptable range or between 6.11 and 6.86. The mixtures were heated in ultrasonication bath (see Section 3.4.1.1).

When a counter ion was used as the third component, the determination of drug solubility was performed by a heating technique, as described above. Briefly, an excess amount of dovitinib was separately added to aqueous 0 to 20% (w/v) γCD solutions and to a combination of aqueous 0 to 20% (w/v) γCD solutions and 1% (w/v) acidic counter ion at pH 6, which is the initial point of soluble ionized drug determined from pH profiles according to Section 3.4.2.

The counter ions that enabled a significant increase in drug solubility were selected to determine their effect on phase-solubility profiles in ternary complexes with γCD , $HP\gamma CD$, and $SBE\gamma CD$ at pH 6.

*** For stabilizer study**

Binary systems

The complexes were prepared by an autoclaving method in triplicate ($n=3$). An excess amount of cediranib maleate (CM) was added to unbuffered aqueous γCD solutions of different concentrations with a pH between 4.5 and 5.5. The calculated pKa of cediranib is 10.1 (ACS, 2019), thus the drug can

be fully ionized at such a pH range. The amount of dissolved drug was analyzed by HPLC.

Ternary systems

The stabilizer at 0.1% (w/v) that protected the drug from thermal degradation was selected to determine phase-solubility profiles in ternary complexes with γ CD following a method mentioned in binary complexes.

3.4.6 Solubility enhancement studies

**** For polymer study***

The neutral, positively charged, or negatively charged polymer at a concentration of 1% (w/v) was added to the binary KI/ γ CD complexes. The concentration of γ CD with the highest KI solubility was selected from phase-solubility studies. This given amount of γ CD was dissolved in the medium during the ternary complex preparation. The previous heating technique, ultrasonication, was used to determine the KI solubility (see Section 3.4.1.1). The change in drug solubility of ternary hydrophilic polymer complexes was compared to the controls that consisted of the drug solubility in pure water, binary drug/ γ CD complexes, and drug/ γ CD in formulation vehicle. The formulation vehicle consists of 0.1% EDTA, 0.02% benzalkonium chloride, and 0.05% sodium chloride (% w/v) in pure water. Here the binary drug/polymer complex was not included as a control. Many studies have shown that the combination of polymer (i.e. PEG, PVP, CMC, and HPMC) and CDs can solubilize the drug more effectively than either polymers or CDs when used alone (Fauci & Mura, 2001; Loftsson & Masson, 2004; Mura, Fauci, & Bettinetti, 2001).

The main compositions in the formulation vehicle are EDTA and benzalkonium chloride. These chemicals were selected to investigate their effect on drug solubility of outstanding KIs. EDTA or benzalkonium chloride were prepared at concentration from 0 to 1% (w/v) in pure water and the given amount of aqueous γ CD solution which resulted in the maximum solubility of the KI. Excess amount of solid drug was added to those aqueous systems. The complexes were formed by using ultrasonication, as previously mentioned in Section 3.4.1.1.

**** For counter ion study***

The calculated 1% (w/v) acidic counter ion was added to the aqueous media to form binary dovitinib/counter ion salts and ternary dovitinib/ γ CD/counter ion complexes. The acid suspensions were alkalized to pH 6 by dropwise

titration of concentrated NaOH. The concentration of γ CD was selected from the phase-solubility profiles which most enhanced drug solubility. Those multicomponent systems were prepared by ultrasonication as previously described in Section 3.4.1.1.

3.4.7 Physicochemical properties in solution-state

* *For polymer and counter ion studies*

3.4.7.1 *pH and osmolality*

The pH values of suspension were determined by the use of a Thermo Orion Star TM Series pH meter (Thermo Scientific, USA) at ambient temperature (22-23°C) and osmolality was measured with a Knauer K- 7000 Vapor Pressure Osmometer (Germany) operated at 25°C.

3.4.7.2 *Dynamic Light Scattering (DLS)*

The particle size of the ternary γ CD complex aggregates was determined by dynamic light scattering (DLS) using Nanotracc Wave Particle Size Analyzer (Microtrac Inc., York, PA). The diluted sample was illuminated by a laser beam at a wavelength of 780 nm and its intensity fluctuation in scattered lights from Brownian motion of particles was detected at a known scattering angle θ of 180° at 25±0.2°C. The size population of the complexes was interpreted via the following Eq. (8):

$$M_i = \frac{A_i/R_i^a}{\sum A_i/R_i^a} \times 100 \quad (8)$$

where M_i is the mass distribution percentage, A_i is the intensity area, R_i is the hydrodynamic radius of the size population i , and a is the shape parameter that equals 3, assuming spherical shaped particles (Bhattacharjee, 2016; Stetefeld, McKenna, & Patel, 2016).

The measurement of zeta potential was performed by a Zetasizer Nano Series (Nano-Z, Malvern Instruments, UK). The disposable folded capillary cell for loading diluted samples (20 folds) is DTS1070. The data from each sample were calculated by mean zeta potential from 3 measurements, with a duration 20 runs/measurement, and a delay of 60s between measurements.

3.4.8 Spectroscopic studies

3.4.8.1 ¹H-Nuclear Magnetic Resonance (¹H-NMR) studies

The ¹H-NMR spectra of complexes were recorded in combined NMR solvents at 400 MHz and 298 K using a Bruker AVANCE 400 MHz instrument (Bruker Biospin GmbH, Karlsruhe, Germany). Solid samples of γ CD, KIs such as dovitinib, inactive compound (i.e. polymer, or counter ion), KI/ γ CD binary complex, and KI/ γ CD/inactive compound ternary complex were dissolved separately in a mixture of deuterated dimethyl sulfoxide (DMSO-d₆) and deuterium dioxide (D₂O), with a volume ratio of 9:1. The magnitude of chemical shifts was recorded in ppm (δ). The resonance at 2.5000 ppm, due to residual solvent (DMSO-d₆), was used as an internal reference. ¹H-NMR chemical shift change ($\Delta\delta$) caused upon complexation was calculated according to Eq. (9):

$$\Delta\delta = \delta_{complex} - \delta_{free}$$

In case of cediranib maleate (CM), the thermal impact was studied. The sample preparation was separated into 2 groups which were treated with a non-heated technique and a heated technique. For the non-heated group, solid samples of γ CD, CM, stabilizer (i.e. riboflavin), CM/ γ CD binary complex, and CM/ γ CD/stabilizer ternary complex were dissolved separately in a mixture of deuterated dimethyl sulfoxide (DMSO-d₆) and deuterium dioxide (D₂O), at a volume ratio of 9:1. All samples from the heated group were dissolved in pure water, autoclaved at 121°C for 20 min, lyophilized those solutions into solid form, and finally dissolved them with NMR solvents as described previously.

3.4.8.2 Nuclear Overhauser Effect Spectroscopy (NOESY-NMR) studies

* For stabilizer study

2D-NMR or Nuclear Overhauser Effect Spectroscopy (NOESY) experiment was performed by using a Bruker AVANCE 400 MHz instrument (Bruker Biospin GmbH, Karlsruhe, Germany). This experiment focused on CM only. The samples were prepared following ¹H-NMR studies. The 2D-NMR spectra were recorded under the following conditions: pulse delay time, 1.929 s; mixing time, 300 ms; 16 scans; 1024 x 1024 data points. The data were process with TopSpin 4.0.7 software.

3.4.9 Morphological analysis

3.4.9.1 Transmittance Electron Microscopy (TEM) analysis

** For polymer and stabilizer studies*

The morphology of the KI/ γ CD aggregates in aqueous solutions and suspension was evaluated, using a Model JEM-1400 Transmission Electron Microscopy (JEOL, Tokyo, Japan). The negative staining technique was used. Firstly, a small amount of clear liquid (i.e. the aggregate solution) was dropped on a 200-mesh coated grid and dried at 37 to 40°C for one hour. Then a drop of centrifuged 4%w/w uranyl acetate was added to the loaded grid. After 6 minutes of straining, the sample was dried overnight at room temperature. Finally, the strained specimen was placed in a holder and inserted into the microscope.

3.4.10 *In vitro* permeation studies

** For counter ion and stabilizer studies*

The effect of γ CD and ternary components such as counter ion, or stabilizer on CM permeation was conducted using unjacketed Franz Diffusion Cells (SES GmbH-Analyze system, Germany). The donor chamber and the receptor chamber were separated with a single layer of semi-permeable cellophane membrane (MWCO 12,000–14,000 Da with a diffusion area of 1.77 cm²). The membrane was soaked overnight in the receptor phase, which consisted of aqueous solution containing phosphate buffer saline solution pH 7.4, and 2.0% or 2.5% (w/v) γ CD for counter ion study and stabilizer study, respectively. γ CD was added to the receptor phase to ensure a sink condition. The receptor phase (12 ml) was sonicated under vacuum to remove dissolved gas. The sample (1 ml) was added to the donor chamber after filtration through a 0.45 mm membrane filter. The study was carried out at ambient temperature (22–23°C) under continuous stirring of the receptor phase (12 ml) by a magnetic stirring bar rotating at 300 rpm. A 150 μ l sample of the receptor medium was withdrawn at 30, 60, 120, 180, 240, 300, and 360 min and replaced immediately with an equal volume of fresh receptor phase. The drug concentration was determined by HPLC.

The calculation of the steady state flux (J) of KI/ γ CD was obtained from the slope (dq/dt) of linear regression relationship between the amount of drug in the receptor chamber (q) and time (t) profiles, and the apparent permeability coefficient (P_{app}) was calculated from the flux (J) according to Eq. (10):

$$J = \frac{dq}{A \times dt} = P_{app} \times C_d \quad (10)$$

where A is the surface area of the mounted chamber (1.77 cm^2) and C_d is the initial concentration of KI in the donor phase. Each experiment was performed in triplicate ($n=3$) and the results reported as the mean values \pm standard deviation (SD).

3.5 Solid-state experiments

* *For polymer study*

3.5.1 Preparation of solid complex

The complex was prepared by complexing KI (i.e. dovitinib) with γ CD and HDMBr to give at a 1:1:1 ratio. The 0.15 mg of drug were added to 10 mL of aqueous solution containing 5% (w/v) γ CD and 1% (w/v) HDMBr. The complexes were actively formed under heating condition in an ultrasonic bath as previously described in Section 3.4.1.1. This suspension was separated by centrifuging. The clear supernatant was then placed in a freezer overnight and lyophilized at -52°C for 48 hours in a freeze dryer (Snijders Scientific 2040 Freeze Dryer, Tilburg, Netherlands) to form complex powder. The physical mixture was prepared by grinding those compositions at equivalent molar ratio in a mortar. Solid-state characterization was introduced to all relevant samples.

3.5.2 X-ray Powder Diffraction (XRPD) studies

The estimate of internal crystal structure between amorphous and crystalline materials can be distinguished by XRPD analysis. X-ray diffraction patterns were determined using a XRPD Bruker AXS D8 Focus (Ser. no. 202418, Germany) using wide angle $\text{CuK}\alpha$ radiation with the voltage and working current set at 45 kV and 40 mA, respectively. The scan speed was set at $2^\circ/\text{min}$, and all scans were performed over an interval of $5-40^\circ/2\theta$. The raw materials i.e. dovitinib, γ CD, and HDMBr, their physical mixtures, and lyophilized complexes were all tested.

3.5.3 Differential Scanning Calorimetric (DSC) studies

DSC curves of the different references (dovitinib, γ CD, and HDMBr), their physical mixtures, and lyophilized complexes were recorded on Netzsch DSC 214 *Polyma* calorimeter (GmbH, Germany). Their thermal behaviors were investigated by heating 3 ± 0.1 mg of samples in perforated aluminum pan and an identical empty one used as reference under constant nitrogen gas flow. Samples were heated up over the temperature range $30-400^\circ\text{C}$ at $10^\circ\text{C}/\text{min}$.

3.5.4 Fourier Transform Infrared (FT-IR) studies

FT-IR analysis was performed by using a Nicolet iZ10 FT-IR module coupled with an Attenuated Total Reflexion (ATR) accessory (Thermo Scientific, USA) from 4000 to 400 cm^{-1} with an average of 32 scans. The solid sample, the pure drug, γ CD, physical mixtures, or the lyophilized complex, was placed in direct contact with the crystal surface. A pressure clamp was pressed onto the sample area to allow chemical interaction between the material and the ATR probe. The sample was analyzed in transmission mode at room temperature.

3.5.5 *In vitro* dissolution studies

The dissolution method was modified from another study in our group (Jansook, Pichayakorn, Muankaew, & Loftsson, 2016; Muankaew, Jansook, Sigurdsson, & Loftsson, 2016). An equivalent 1 mg of pure drug, 0.15 and 0.5 mg of binary complex, and 2.5 mg of ternary complex were added into 5 mL of PBS buffer pH 7.4. The sample was shaken at 50 rpm at a constant temperature of 37°C, and 1 mL of aliquot was withdrawn at appropriate time intervals. The sampling solution was centrifuged at 12,000 rpm for 15 min. The accumulated drug amount from that supernatant was analyzed by using HPLC.

3.6 Experiments in formulation stage

* *For stabilizer study*

3.6.1 Preparation of cediranib maleate eye drops

Aqueous cediranib maleate (CM)/ γ CD micro-suspensions were formulated by including the selected stabilizer, other excipients, and then adjusting to a pH 5 with NaOH or HCl prior to heating in an autoclave. The autoclaved solution at 60°C was sonicated in an ice bath for 30 min. The suspension was further incubated at room temperature under constant agitation for 3 days. The pH of the formulation was monitored throughout this process.

3.6.2 Solid-drug fraction determinations

The tested formulation was centrifuged at 12,000 rpm for 15 min. The amount of dissolved drug in supernatant was determined by HPLC. The drug content in solid phase was calculated as:

$$\% \text{ solid drug fraction} = \left(\frac{\text{Total drug-dissolved drug}}{\text{Total drug content}} \right) \times 100 \quad (11)$$

3.6.3 Physicochemical characterizations of formulation

Measurement of pH, osmolality, and particle size by DLS was previously described in solution-state experiments (see Section 3.4.7).

3.6.3.1 Viscosity

A cone and plate viscometer (Brookfield model DV-II+, Brookfield Engineering Laboratories, Inc., Massachusetts, USA) was used to determine the apparent viscosity of CM suspension at 25°C and 37°C. The calibration check of the instrument was verified through use of mineral oil standard with cone spindle no. CPE-40 prior to running the sample. The appropriate sample volume required for the spindle is 0.5 mL.

3.6.3.2 Particle size measurement

Particle size distribution in suspension was determined by using Nanosight NS300 (Malvern Technologies, UK) embedded with a 488 nm laser and a CMOS camera. Samples were diluted in pure water to a final volume of 1 mL. An acceptable concentration was found to be a dilution of 20 folds which presented the ideal particle per frame value (20-100 particles/frame) according to the manufacturer's recommendations. For each measurement, five 1-min videos were captured under the default program at 25°C. After capture, the videos were analyzed by the in-built NanoSight Software NTA 3.4 with a detection threshold of 9.

3.6.4 Stability testing of formulation

The standard conditions for stability study were performed following ICH guidelines. The eye drop formulations were incubated at $5 \pm 3^\circ\text{C}$ (refrigerator), and at $25 \pm 2^\circ\text{C}$, $60 \pm 5\%RH$ (incubator) and $40 \pm 2^\circ\text{C}$, $75 \pm 5\%RH$ (incubator). Each sample was taken for six months (i.e., at 0, 1, 2, 3 and 6 months) to capture the photo on a Galaxy Note 5 camera, measure pH and particle size, and analyze the drug content by HPLC.

3.6.5 Morphological analysis

3.6.5.1 Transmission Electron Microscopy (TEM) analysis

The methodology for TEM was previously described in the section on solution-state (see Section 3.4).

3.6.5.2 *Optical light microscope*

The morphology of particles was determined using an optical light microscope (Model BHT, Olympus, Japan). One drop of each formulation was placed on a microscope slide and observed under 400-fold magnification. The results were interpreted according to the monograph for Eye Preparations in the European Pharmacopeia 8.0 (01/2008:1163).

3.6.6 *In vivo* permeation study

Albino rabbits were used as the animal model for the investigation of topical drug delivery to the back of eye. However, the method cannot be revealed due to confidentiality.

4 Results and discussions

4.1 The effect of hydrophilic polymers on KI/ γ CD solubilization and complexation

The concept in the first part of work was to find the suitable KI candidates that γ CD effectively solubilized, and to investigate if and how the γ CD solubilization of KIs could be increased when various hydrophilic polymers were added to the complexation medium. Ultrasonication with mild heat was used to prepare the complexes due to heat-labile drug such as regorafenib. The solubilizing power of these polymers will be applied during the formulation development.

4.1.1 Phase-solubility studies (KI/ γ CD complex)

The phase-solubility profiles of the binary KI/ γ CD complexes in Fig. 8 are classified as B_s-type, such that the drug has limited solubility in an aqueous medium. The slope of the initial linear section of the diagrams was determined, and both the complexation efficiency (CE) and the apparent stability constant ($K_{1:1}$) were calculated from the slope according to Eq. (7). The measurement of the slope was based on the molar drug solubility in pure water and in γ CD solution at the certain concentration which gave maximum drug solubility, i.e. 10% (w/v) γ CD for cediranib. The estimated slopes of all KIs in Table 11 are less than unity, thus, a one-to-one complex can be assumed. For drugs with an $S_0 < 1$ mg/mL, such as KIs, the solubilizing effect of various CDs is estimated accurately by CE as that parameter is independent of S_0 (Loftsson, Hreinsdóttir, & Másson, 2005). The greatest γ CD solubilization was observed in cediranib (CE 0.0578), followed by dovitinib (CE 0.0110), and motesanib (CE 0.0052) (Fig. 8 and Table 11). The binding constant or stability constant ($K_{1:1}$) can be used to compare the strength of an interaction between a drug and a CD (Jambhekar & Breen, 2016; Loftsson, Másson, & Brewster, 2004). The affinity of cediranib ($K_{1:1}$ 23 M⁻¹) for γ CD was much less than that of dovitinib ($K_{1:1}$ 684 M⁻¹) and motesanib ($K_{1:1}$ 138 M⁻¹) as shown in Table 11.

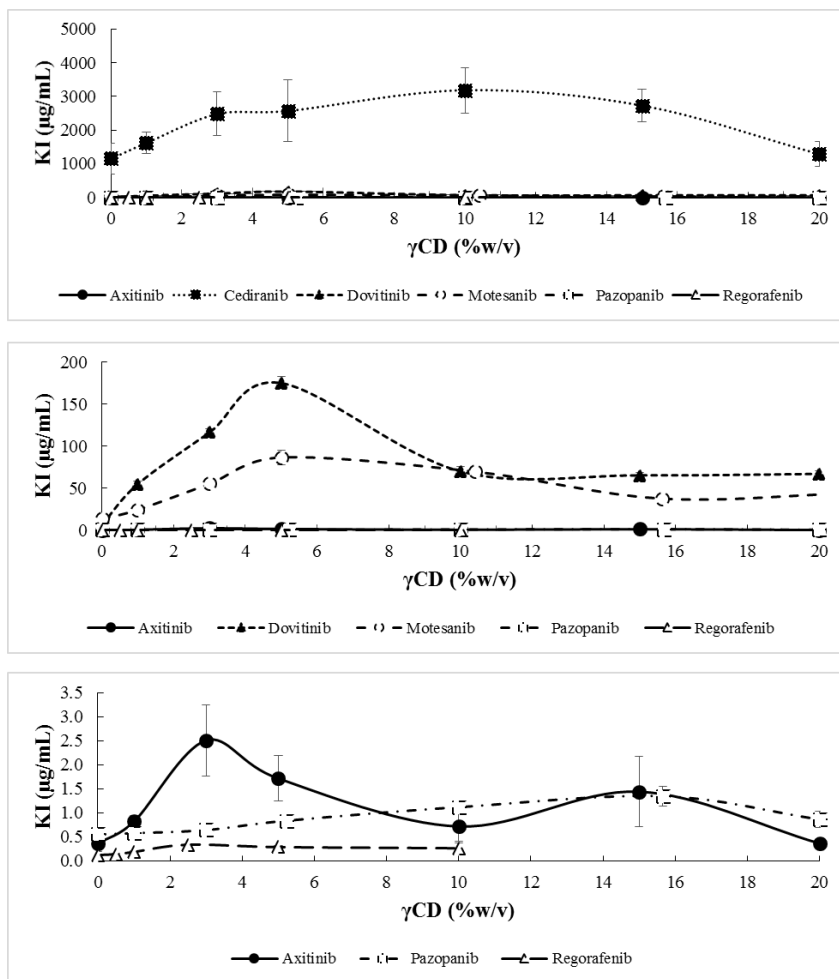


Figure 8. The phase-solubility profiles of the KIs in an unbuffered aqueous γ CD media (pH 6.3 to 6.8) at ambient temperature (mean \pm standard deviation; n = 3).

Table 11. Solubilization efficacy of six KIs in pure water (pH between 6.3 and 6.8).

| Drug | pH | PS ^a type | S ₀ (µg/mL) | Maximum solubility | | PS ^a parameter | | | |
|-------------|------|----------------------|------------------------|--------------------|--------------|---------------------------|----------------|-------------------------------------|----------|
| | | | | γCD (%w/v) | drug (µg/mL) | Slope | r ² | K _{1:1} (M ⁻¹) | CE |
| Axitinib | 6.42 | B _s | 0.37 | 3.0 | 2.51 | 0.0004 | 0.9831 | 260.67 | 0.0002 |
| Cediranib | 6.31 | B _s | 1154.63 | 10.0 | 3184.57 | 0.0546 | 0.8649 | 22.54 | 0.0578 |
| Dovitinib | 6.86 | B _s | 6.34 | 5.0 | 175.66 | 0.0109 | 0.9911 | 684.42 | 0.0110 |
| Motesanib | 6.51 | B _s | 13.98 | 5.0 | 86.73 | 0.0051 | 0.9971 | 137.70 | 0.0052 |
| Pazopanib | 6.57 | B _s | 0.55 | 15.7 | 1.35 | 0.000016 | 0.9873 | 12.65 | 0.000016 |
| Regorafenib | 6.65 | B _s | 0.12 | 2.5 | 0.33 | 0.000024 | 0.9812 | 94.45 | 0.000024 |

^a PS phase solubility.

4.1.2 pH solubility profiles (KI/CD complex)

The solubility of KIs in binary complex proved to be dependent on their pH, as shown in Fig. 9. The calculated pK_a values of protonated KIs were reported to be between 2.3 and 10.1 (Table 1). Thus, at pH below pK_a value KIs are partly unionized and partly in their cationic form, and therefore somewhat more soluble in water. For examples, the solubility of axitinib (pK_a 4.3) was increased at pH 3 while cediranib (pK_a 10.1) started being more soluble at pH 7. In brief, the drugs in the CD complexation media tended to be more soluble at low pH. The nitrogen groups on the KI structure, including nitrogen-based heterocyclic core and secondary amine moieties, can be ionized (Herbrink, Schellens, Beijnen, & Nuijen, 2016) and interact with a proton in an acidic environment (Budha et al., 2012; Zhang, Wu, Lee, Zhao, & Zhang, 2014). Besides that, some KIs such as cediranib, motesanib, and pazopanib had an acid-induced degradation at $pH \leq 3$ (Fig. 9) as observed in the HPLC chromatograms. These candidates obtained the highest solubility between pH 3 and 5.

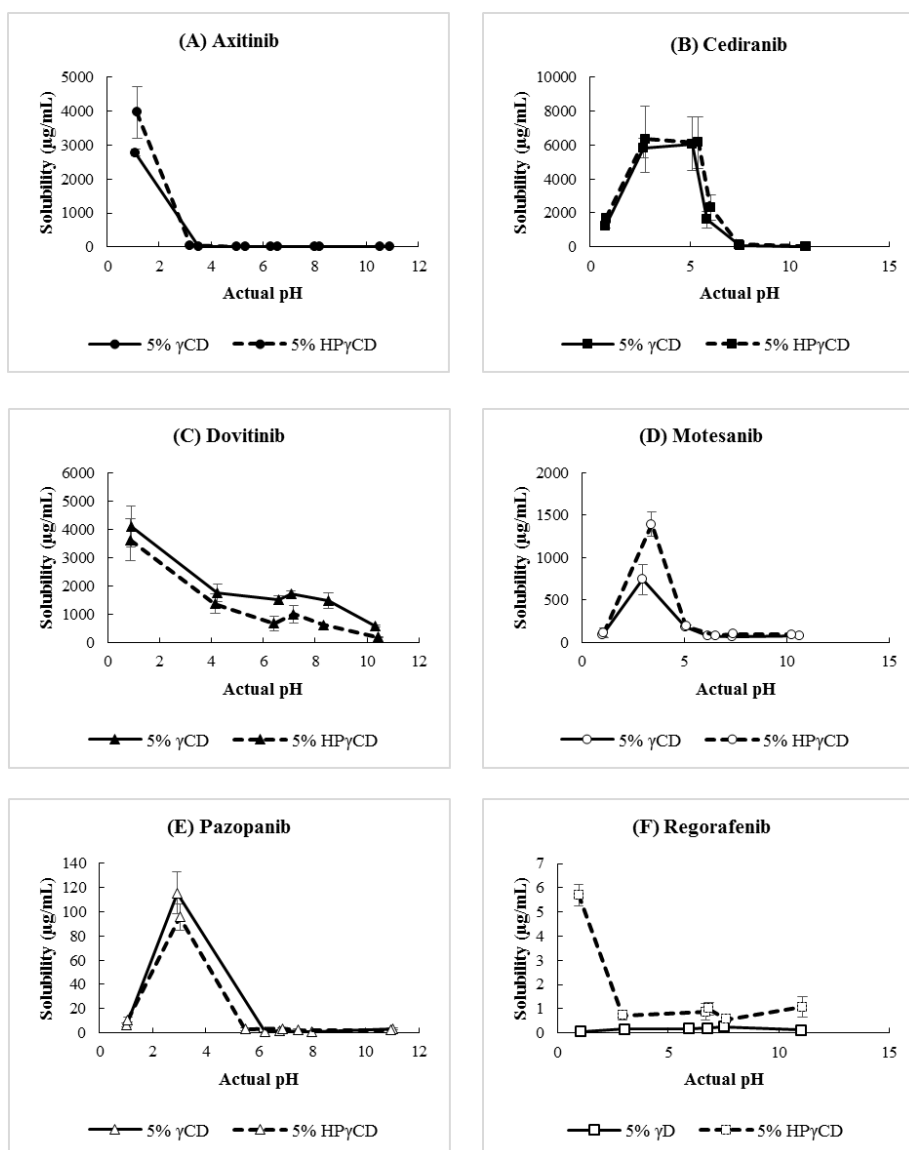


Figure 9. The pH-solubility profiles of the KIs in pure aqueous 5% (w/v) γ CD and 5% (w/v) HP γ CD solutions at room temperature (mean \pm standard deviation; $n = 3$).

4.1.3 Effect of hydrophilic polymer on drug solubility

Each solubility experiment was performed at a γ CD concentration slightly higher than maximum solubility determined from the phase solubility profile (see Fig. 8). For example, dovitinib and motesanib displayed maximum solubility at 5% (w/v) γ CD, thus 8% (w/v) γ CD was selected to form a ternary complex with the hydrophilic polymer. If the polymer resulted in an effective

solubilization, the improved drug solubility should not have been less than the maximum value observed for the binary complex in the phase solubility diagram.

The solubility of KIs was either decreased or increased upon ternary complex formation (Fig. 10 and Table 12). Hydrophilic polymers notably enhanced the aqueous solubility of KIs in the complexation media. However, some KIs, including axitinib, pazopanib, and regorafenib, were slightly more soluble due to the presence of polymers. For example, HPMC enhanced the solubility of pazopanib (52.67 $\mu\text{g/mL}$), tyloxapol could solubilize regorafenib to 5.29 $\mu\text{g/mL}$ and axitinib to 8.19 $\mu\text{g/mL}$, and the solubility of axitinib was also increased by HDMBr (17.28 $\mu\text{g/mL}$) in γCD complexation media. The cediranib base had higher solubility in pure water than the other KIs, and γCD complexation provided a rather small degree of solubility improvement. However, the cediranib/ γCD binary complex could be further solubilized by some polymers, particularly HDMBr, but the final solubility was still low. For the dovitinib/ γCD complex and motesanib/ γCD complex, the synergistic effect between γCD and hydrophilic polymers played an important role in the solubilization enhancement. HDMBr increased the solubility of motesanib to 339 $\mu\text{g/mL}$ and that of dovitinib to 798 $\mu\text{g/mL}$. In summary, HDMBr has the greatest potential to increase the solubility of KI/ γCD binary complex of dovitinib, motesanib, axitinib, and cediranib. In comparison to the pure drug, the dovitinib complex with γCD and HDMBr resulted in 160-fold solubility enhancement, as shown in Fig. 10 and Table 12. Other investigators have reported that HDMBr is capable of improving the γCD solubilization of dexamethason by 15% (Loftsson & Brewster, 2012; Moya-Ortega et al., 2011). The concentration of this cationic polymer can vary up to 3% (w/v) (Loftsson, Leeves, Sigurjonsdottir, Sigurdsson, & Masson, 2001; Sigurdsson et al., 2002).

It is thought that the HDMBr binding behaviors observed in the aqueous complexation media may relate to cation- π interaction and electrostatic forces. KIs are classified as nitrogen-containing heterocyclic compounds. In theory, the quaternary ammonium ions in HDMBr can form a non-covalent bond with the amines (i.e. KIs) and the phenyl groups as an electron withdrawer and as a result of the cation- π interaction, respectively (E Mohr, 2006; Mahadevi & Sastry, 2013; Reddy & Sastry, 2005). Besides that, some functional groups in KIs (i.e. sulfonamide: pazopanib, and 3-fluoromethylene: regorafenib) may hinder such a favorable cation- π effect. HDMBr can be dissolved in water up to 10% (w/v) which is high enough to lead to solvation between the drug and water molecules (Badrinarayan & Sastry, 2011, 2012;

Mahadevi & Sastry, 2013). In addition, this quaternary ammonium polymer may interact with the outer surface of the CD molecules, resulting in formation of aggregates through hydrogen bonding (Loftsson & Duchêne, 2007; L. S. Ribeiro, Ferreira, & Veiga, 2003), or it may reduce the movement of the CD, thus increasing the solubility of the KI/CD complex (F. Veiga, Pecorelli, & Ribeiro, 2006).

In aqueous γ CD solutions, poloxamer tends to decrease drug solubility, as presented in Table 12. Several studies have shown that poloxamer competes with the drug molecule for space inside the CD torus through formation of soluble polypseudorotaxanes (Nogueiras-Nieto, Alvarez-Lorenzo, Sandez-Macho, Concheiro, & Otero-Espinar, 2009; Nogueiras-Nieto, Sobarzo-Sanchez, Gomez-Amoza, & Otero-Espinar, 2012). These interactions between CD and poloxamer are able to hamper the drug solubilization of CD (Jansook, Pichayakorn, Muankaew, & Loftsson, 2016b). In this case the formation of KI/ γ CD complexes may be readily suppressed when poloxamer forms polypseudorotaxanes with γ CD.

The parameters under consideration, including CE, KI/ γ CD affinity or interaction strength (base on the $K_{1:1}$ value in Table 11), maximum solubility and solubilizing ratios, were used to select the optimal candidate in the screening study. Pazopanib and regorafenib have poor potential to form a complex with γ CD, and various polymers failed to enhance solubility of the KI/ γ CD complex. In aqueous γ CD solutions cediranib displays the highest solubility and high CE. Nonetheless, about 18 γ CD molecules are required to form complex with 1 drug molecule (Loftsson & Brewster, 2012). Many polymers do not actually solubilize the cediranib. HDMBR still increases the drug solubility with a relatively low solubilizing ratio. Axitinib has good interactions with γ CD, as well as dovitinib and motesanib, but it has the lowest CE. Although axitinib was more soluble in the presence of HDMBR, the overall improvement of drug solubility was still negligible. Here, HDMBR significantly solubilizes dovitinib and motesanib; therefore, their multicomponent complexes were further studied.

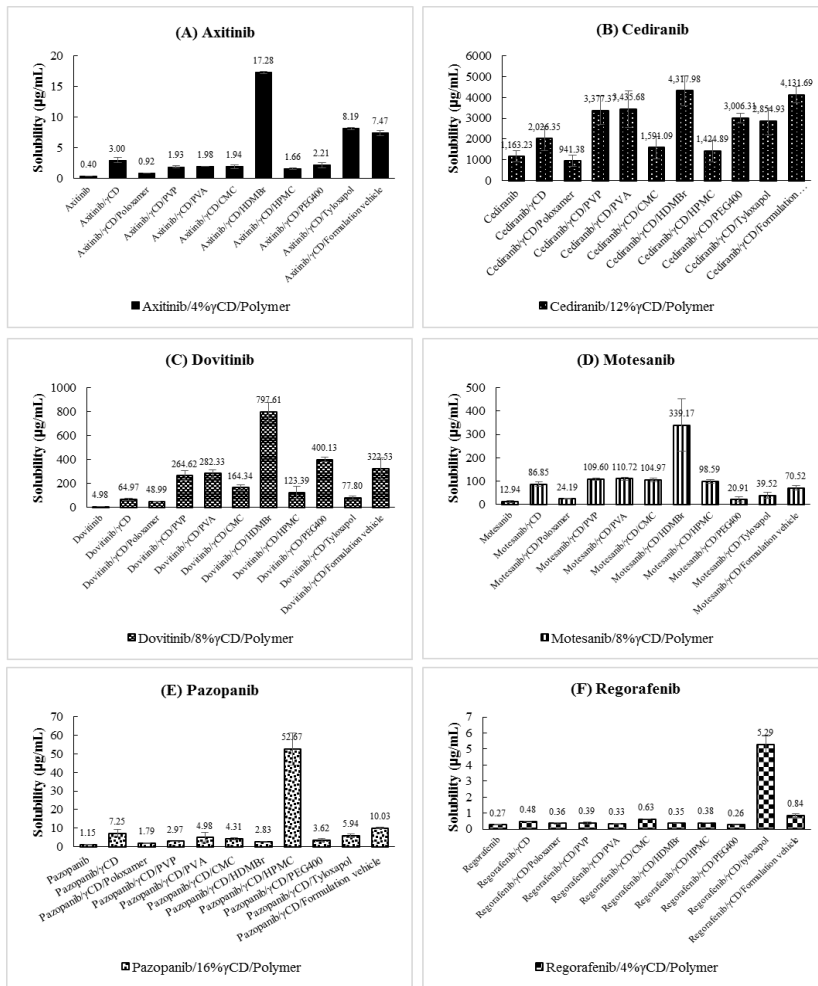


Figure 10. Aqueous solubility of the KIs in unbuffered pure aqueous γ CD, (pH 6.3 to 6.8), with and without 1% (w/v) hydrophilic polymer solution at room temperature (mean \pm standard deviation; n=3). The concentration of γ CD is shown below each figure.

Table 12. An increase of KI solubility by comparison of the drug alone and the drug/ γ CD complex (pH between 6.3 and 6.8).

| Sample | Solubilizing ratio | | | | | | | | | | | |
|-------------------------------------|--------------------|-----------------------------|-------------------|-----------------------------|---------------------|-----------------------------|--------------------|-----------------------------|--------------------|-----------------------------|--------------------|-----------------------------|
| | Axitinib (A) | | Cediranib (C) | | Dovitinib (D) | | Motesanib (M) | | Pazopanib (P) | | Regorafenib (R) | |
| | A ^a | A/ γ CD ^b | C ^a | C/ γ CD ^b | D ^a | D/ γ CD ^b | M ^a | M/ γ CD ^b | P ^a | P/ γ CD ^b | R ^a | R/ γ CD ^b |
| KI | 1.00 | - | 1.00 | - | 1.00 | - | 1.00 | - | 1.00 | - | 1.00 | - |
| KI/ γ CD | 7.50 | 1.00 | 1.74 | 1.00 | 13.04 | 1.00 | 6.71 | 1.00 | 6.31 | 1.00 | 1.78 | 1.00 |
| KI/ γ CD/Poloxamer | 2.30 | 0.31 | 0.81 | 0.46 | 9.83 | 0.75 | 1.87 | 0.28 | 1.56 | 0.25 | 1.33 | 0.74 |
| KI/ γ CD/PVP | 4.84 | 0.65 | 2.90 | 1.67 | 53.10 | 4.07 | 8.47 | 1.26 | 2.59 | 0.41 | 1.45 | 0.81 |
| KI/ γ CD/PVA | 4.95 | 0.66 | 2.95 | 1.70 | 56.65 | 4.35 | 8.56 | 1.27 | 4.33 | 0.69 | 1.21 | 0.68 |
| KI/ γ CD/CMC | 4.85 | 0.65 | 1.37 | 0.79 | 32.98 | 2.53 | 8.11 | 1.21 | 3.75 | 0.60 | 2.32 | 1.30 |
| KI/ γ CD/HDMBr | 43.20 ^c | 5.76 ^c | 3.71 ^c | 2.13 ^c | 160.05 ^c | 12.28 ^c | 26.21 ^c | 3.91 ^c | 2.46 | 0.39 | 1.31 | 0.74 |
| KI/ γ CD/HMPC | 4.15 | 0.55 | 1.22 | 0.70 | 24.76 | 1.90 | 7.62 | 1.14 | 45.84 ^c | 7.27 ^c | 1.42 | 0.80 |
| KI/ γ CD/PEG400 | 5.53 | 0.74 | 2.58 | 1.48 | 80.29 | 6.16 | 1.62 | 0.24 | 3.15 | 0.50 | 0.97 | 0.55 |
| KI/ γ CD/Tyloxapol | 20.49 | 2.73 | 2.45 | 1.41 | 15.61 | 1.20 | 3.05 | 0.45 | 5.17 | 0.82 | 19.62 ^c | 11.00 ^c |
| KI/ γ CD/Formulation vehicle | 18.67 | 2.49 | 3.55 | 2.04 | 64.72 | 4.96 | 5.45 | 0.81 | 8.73 | 1.38 | 3.11 | 1.75 |

^a refers to solubilizing ratio = $\frac{\text{drug solubility of sample}}{\text{drug solubility of drug alone}}$

^b refers to solubilizing ratio = $\frac{\text{drug solubility of sample}}{\text{drug solubility of drug and } \gamma\text{CD complex}}$

^c refers to maximum solubilizing ratio.

4.1.4 Effect of formulation vehicle on drug solubility

Previous studies confirmed the influence of hydrophilic polymers on drug solubility, particularly motesanib and dovitinib. Other major compositions of the medium, beside γ CD and polymer, are EDTA and benzalkonium chloride (BAC). Therefore, their effect on drug solubility was further investigated.

Without γ CD, EDTA and BAC enhanced the aqueous solubility of pure KIs (i.e. dovitinib, and motesanib). The solubility of the drugs tended to increase with increasing BAC concentration. The pattern of drug solubility was different when the γ CD was added. BAC decreased the γ CD solubilization while EDTA increased it (Fig. 11-12). BAC is a cationic surface-active agent that has been used as a preservative in pharmaceutical formulations. It can form micelles in saturated condition (Georgiev et al., 2011). At a higher concentration, BAC might interfere with the solubilizing effect of γ CD, possibly due to the competition between drug and BAC for forming a complex with γ CD (Loftsson, Matthíasson, & Másson, 2003). EDTA is an anionic chelating agent, thereby able to form a salt with positively charged KIs and increases the γ CD solubilization of KIs through hydrogen bonding and electrostatic forces.

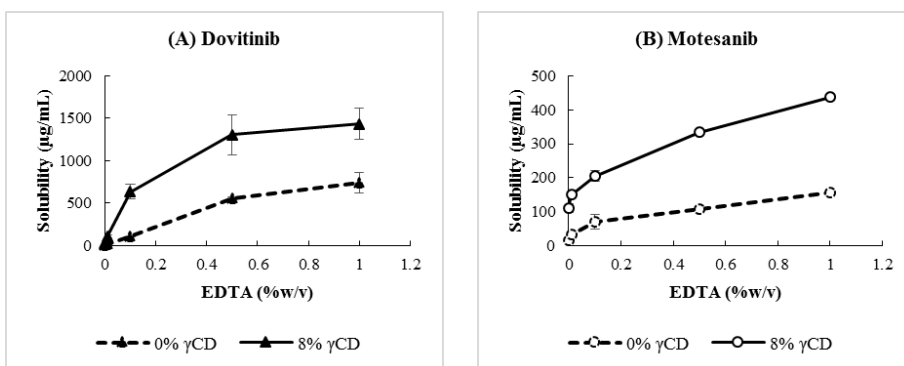


Figure 11. Aqueous solubility of the KIs in an EDTA solution with 0% or 8% (w/v) pure aqueous γ CD solution at room temperature (mean \pm standard deviation; n=3).

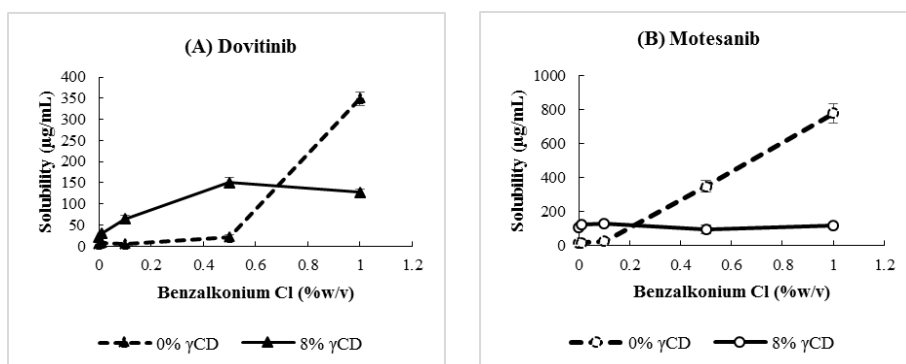


Figure 12. Aqueous solubility of the KIs in a benzalkonium chloride solution with 0% or 8% (w/v) pure unbuffered aqueous γ CD solution (pH 6.3-6.8) at room temperature (mean \pm standard deviation; $n=3$).

4.1.5 Characterization of KI/ γ CD/polymer complex aggregates in solution state

4.1.5.1 pH

In humans, the normal pH of internal tissues lies in a tight range of mildly alkaline pH from 7.35 to 7.45 (Waugh & Grant, 2007), while the surface skin pH is normally acidic, ranging between 4 and 6 (Raphael et al., 2016; Zlotogorski, 1987). Adjusting pH in the pharmaceutical formulation to physiological levels is an important parameter for avoiding irritation (Y.-C. Lee, Zocharski, & Samas, 2003; Surber, Abels, & Maibach, 2018). The observed pH of pure KIs and their complexes in the aqueous condition was mainly within the acidic to neutral range of 5.5-7 except that of the motesanib/ γ CD/HDMBr complex (Table 13). The addition of HDMBr to an unbuffered system such as motesanib provides $\text{pH} \leq 4$ which would be too acidic for ophthalmic formulation and irritating to use. However, this hydrophilic polymer did not lower the pH of dovitinib (Table 13) and pazopanib (data not shown) in such systems. Although dovitinib resulted in higher pH value when HDMBr was present, it was more soluble than motesanib. In addition to pH-solubility profiles (Fig. 9), the solubility of dovitinib was higher than that of motesanib at the pH value corresponding to their ternary complex in Table 13.

4.1.5.2 Osmolality

Osmolality is an estimation of how many particles or solutes are dissolved in water (Sweeney & Beuchat, 1993). The preferable formulations should have an osmolality close to physiological range, especially when developing the injectable dosage forms (Desai & Lee, 2007). The human reference range of osmolality in plasma is reported from 275 to 306 mOsmol/L (E Mohr, 2006; Faria, Mendes, & Sumita, 2017). None of the tested samples obtained osmolality above the ceiling of physiological criteria (Table 13). In the other words, they are classified as hypotonic which can be adjusted by tonicity agents including dextrose, glycerin, mannitol, potassium chloride and sodium chloride (Avis, Lachman, & Lieberman, 1986; Rowe, Sheskey, Quinn, & Association, 2009).

4.1.5.3 Particle size

The particle size of the measured particles is expressed by the mean particle diameter derived from the major intensity peak area (% A). A multimodal size distribution was commonly found in all KIs systems (data not shown). Briefly, they formed the complexes and self-assembled aggregates of various sizes. The size intervals varied from small (~1 nm), medium (100-500 nm), and large (1-2 μm) size aggregates, based on the studies of Gonzales-Gaitano et al. (González-Gaitano et al., 2002; C. Muankaew, Jansook, Stefansson, & Loftsson, 2014a). As previously stated, dovitinib and motesanib were the effective candidates in this study. The diameter of aggregates found in formulations containing these drugs generally ranged from 200 to 400 nm (Table 13). The reported size distribution of similar CD containing systems vary from 20 nm to merely a few μm (González-Gaitano et al., 2002; Ryzhakov et al., 2016; Szente, Szejtli, & Kis, 1998). Other KIs and their multicomponent systems also had the particle sizes within this range. The presence of CMC or HPMC tended to increase the particle size (diameter > 1 μm), especially in the systems containing axitinib or dovitinib (data not shown). Both CMC and HPMC are long chain water-soluble polymers with numerous hydroxyl groups which can adsorb more water into their molecular structure (Barba, d'Amore, Chirico, Lamberti, & Titomanlio, 2009; E Mohr, 2006). Because of their swelling ability, the thick wide layer of cellulose chain possibly interacts with other molecules such as drug molecules, CD molecules, and drug/CD complexes via hydrogen bonds, thus increasing the particle size compared to the other polymers (Dong, Ng, Shen, Kim, & Tan, 2009; M. Gupta, Chauhan, Sharma, & Chauhan, 2019). The natural CDs, such as γCD , are more prone to self-assembly to form aggregates than their

more water-soluble derivatives (González-Gaitano et al., 2002; Messner, Kurkov, Jansook, & Loftsson, 2010), and they can be stabilized by hydrophilic polymers (Brackman & Engberts, 1993; Xiao-ming, 2011).

Table 13. The pH, Osmolality, DLS data of pure KI and KI complex aggregates (mean \pm standard deviation; n=3).

| Sample | pH | | | Osmolality (mOsmol/kg) | | | Particle size (nm) | | |
|----------------------|------|-------|------|------------------------|-------|-----|--------------------|-------|------|
| | mean | \pm | SD | mean | \pm | SD | mean | \pm | SD |
| D | 6.81 | \pm | 0.01 | 1 | \pm | 0.1 | 283.4 | \pm | 12.6 |
| D/ γ CD | 7.04 | \pm | 0.04 | 63 | \pm | 2 | 114.7 | \pm | 16.9 |
| D/ γ CD/HDMBr | 6.22 | \pm | 0.36 | 94 | \pm | 1 | 406.7 | \pm | 90.7 |
| M | 5.54 | \pm | 0.63 | 7 | \pm | 1 | 355.7 | \pm | 62.7 |
| M/ γ CD | 5.48 | \pm | 0.09 | 68 | \pm | 1 | 417.3 | \pm | 51.5 |
| M/ γ CD/HDMBr | 3.71 | \pm | 0.45 | 103 | \pm | 2 | 273.8 | \pm | 30.3 |

4.1.5.4 Transmission Electron Microscopy (TEM) images of dovitinib/ γ CD and dovitinib/ γ CD/HDMBr complex aggregates

Dovitinib was the most promising candidate among the tested KIs. HDMBr provided the remarkable performance to improve drug solubility in ternary complexes. Therefore, the binary system and HDMBr ternary system of dovitinib were both investigated visually (Fig. 13). The diameter of all complex aggregates was smaller than 100 nm. The addition of HDMBr resulted in the formation of slightly larger aggregates. Number of aggregates that appeared in TEM images corresponded to the results of the solubility experiments. Firstly, at 5% (w/v) γ CD in a binary system resulted in the highest drug solubility, this concentration also provided larger amounts of aggregates than at 8% (w/v) γ CD. Secondly, the ternary system containing HDMBr resulted in the highest particle population and the highest dovitinib solubilization. However, the particle diameter from TEM measurement was smaller than those determined by DLS, as normally observed (Bhattacharjee, 2016). This inconsistency is due to the different principle of the techniques. TEM is a number-based technique that presents the projected surface area depended on how many incident electrons transmit through a dry sample under an ultrahigh vacuum (Kim, Xing, Zuo, Zhang, & Wang, 2015; Zhou & Yang, 2004). While DLS measurements, on the other hand, engage the intensity of the hydrodynamic radius of dispersed particles in aqueous solutions (X. Zhao, Zhu, Song, Zhang, & Yang, 2015). Therefore, it is to be

expected that the mean values from DLS would be higher than TEM due to the interference of the dispersant into the hydrodynamic diameter.

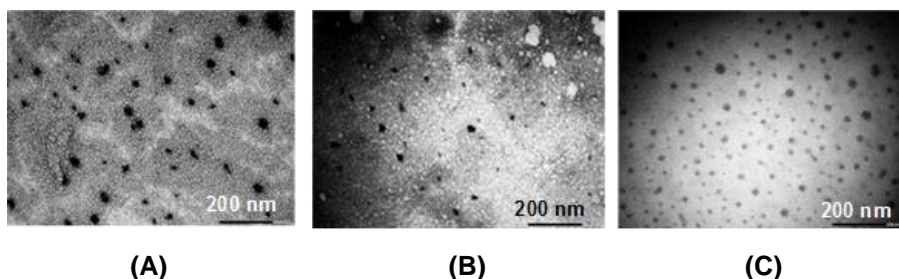


Figure 13. Transmission electron microscopic images of dovitinib with 5% or 8% (w/v) γ CD at magnitude of 50k; (A) dovitinib/ γ CD5% system, (B) dovitinib/ γ CD8% system, and (C) dovitinib/ γ CD8%/HDMBR system.

4.1.6 Phase-solubility studies due to hydrophilic polymer

The binary and ternary complexes in unbuffered media at pH between 6.11 and 6.86 show the phase-solubility profiles of B_s -type where the drug solubility is limited (Fig. 14). When 1% (w/v) HDMBR was present in the aqueous media, an increase of the apparent intrinsic solubility (S_0) was observed increased from 6.3 $\mu\text{g/ml}$ to 150 $\mu\text{g/ml}$, and of the total drug solubility at 5% (w/v) γ CD from 175 $\mu\text{g/ml}$ to 780 $\mu\text{g/ml}$ (Table 14). The calculated phase-solubility parameters show the contrast between the values of the complex constant ($K_{1:1}$) and the complexation efficiency (CE). The determined values were 680 M^{-1} and 0.01, respectively, for binary complex while ternary complex containing HDMBR gave $K_{1:1}$ 100 M^{-1} and CE 0.04 (Table 14). According to the Higuchi-Connors equation (See Eq.5), CE is the product of S_0 and $K_{1:1}$, thus, CE can be increased by increasing one or both of parameters. Here the enhancement of CE due to hydrophilic polymer is associated with apparent increase in the S_0 value only, but additional effect could be due to the stabilization of complex aggregates. In addition, the enhanced CE shows that the solubilizing effect of γ CD was improved upon ternary complex formation.

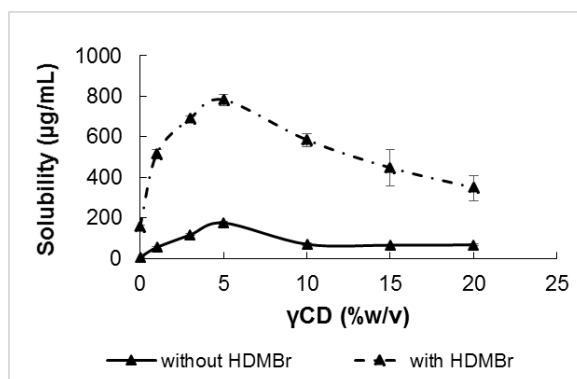


Figure 14. Phase-solubility profiles of dovitinib complexes without and with HDMBr (mean \pm standard deviation; $n=3$). The media was pure water.

Table 14. Solubilization efficacy of dovitinib complexes without and with HDMBr in pure water.

| Sample | pH | PS ^a type | S ₀ ($\mu\text{g/mL}$) | Maximum solubility | | PS ^a parameter | | | |
|-------------------------------------|------|-------------------------|--|-----------------------------|------------------------------|---------------------------|----------------|--|------|
| | | | | γCD (%w/v) | drug ($\mu\text{g/mL}$) | Slope | r ² | K _{1:1} (M ⁻¹) | CE |
| Dovitinib/ γCD | 6.86 | B _s | 6.34 | 5.0 | 175.66 | 0.01 | 0.99 | 684.42 | 0.01 |
| Dovitinib/ γCD /HDMBr | 6.11 | B _s | 152.88 | 5.0 | 781.34 | 0.04 | 0.83 | 100.35 | 0.04 |

4.1.7 ¹H-NMR Spectroscopic studies (dovitinib/ γCD and dovitinib/ γCD /HDMBr complexes)

The chemical structures of tested molecules and their proton assignment are depicted in Fig. 15, and the representative NMR spectra are presented in Fig. 16. The chemical shift variations of multicomponent complexes were determined in term of free γCD , dovitinib, and HDMBr.

Table 15 shows the chemical shifts of γCD in free-state and in complexes. The assigned protons in hydrophobic pocket of the γCD molecule include H-3 and H-5, whereas H-1, H-2, H-4, and H-6 all reside on the outer surface (Bekiroglu, Kenne, & Sandstrom, 2003; Pessine, Calderini, & Alexandrino, 2012). For the entire situation, the variation in proton assignments were observed upon complex formation with guest molecules such as dovitinib and HDMBr. The upfield shifts ($\delta < 0$) of γCD protons are H-3, H-5, H-6, and H-4 when dovitinib forms a complex with γCD . This is due to the shielding effects of guest molecule from π electron-rich groups such as oxygen atom or benzene ring of dovitinib, or the conformational change upon complexation (L. Ribeiro, Carvalho, Ferreira, & Veiga, 2005; R. Zhao, Tan, & Sandstrom,

2011). The downfield shift ($\delta > 0$) was observed for H-1 only which accords to the de-shielding effects of the van der Waals force between drug and γ CD, or a variation in local polarity (Djedaini, Lin, Perly, & Wouessidjewe, 1990; H.M.Cabral Marques, Hadgraft, & Kellaway, 1990; R. Zhao et al., 2011).

All resonance protons for γ CD complex with drug and HDMBr shifted upfield similarly to the γ CD/HDMBr complex. The shielding effect became stronger when HDMBr was present.

These multicomponent complexes suggest the existence of the host-guest interaction with a partial inclusion in the torus.

The ^1H NMR chemical shifts corresponding to dovitinib were also monitored (Table 16). The free dovitinib gave NMR spectrum with signals at $\delta = 2.2167\text{-}7.5258$ (s). COSY spectroscopy confirmed the proton assignments on drug molecule (data not shown). The visible resonance protons are mainly from methyl groups (-CH) attached to methyl-piperazine ring (H-1' and H-2'), benzimidazole ring (H-3', H-4', and H-5'), and quinoline ring (H-6', H-7', H-8'). However, the hindered rotation of water molecule caused the signals for R-NH₂ and R₂-NH groups to disappear.

Both upfield and downfield shifts were observed in the chemical shifts of dovitinib/ γ CD complex. The H-1', H-2', and H-5' were displaced upfield, indicating the proximity of these protons to an electronegative atom like oxygen (L. Ribeiro et al., 2005; R. Zhao et al., 2011). The H-3', H-4', H-6', H-7', and H-8' were located in downfield, which could be ascribed to van der Waals force between the drug and hydrophobic carbohydrate chains (F. J. Veiga, Fernandes, Carvalho, & Geraldés, 2001), and a variation of local polarity when guest molecules were inside the central cavity (Djedaini, Lin, Perly, & Wouessidjewe, 1990; Zornoza, Martín, Sánchez, Vélaz, & Piquer, 1998).

In the case of dovitinib in the ternary dovitinib/ γ CD/HDMBr complex, majority of resonance protons shifted downfield except for H-2'. HDMBr changed the signal pattern, especially at H-1' and H-5' to achieve deshielding in the same way as in the case of the dovitinib/HDMBr complex. Nonetheless, this polymer not only induced the conformational change in complex but also resulted in stronger magnitude of signal shifts.

This confirms that this hydrophilic polymer effectively enhanced drug- γ CD interaction. However, drug protons at H-6', H-7', and H-8' were still located downfield when HDMBr was added. Thus, dovitinib enters the γ CD cavity via the quinoline ring towards to partial benzimidazole ring (Fig.16).

The assignments of ^1H NMR signals of HDMBr and its complexes are shown in Table 17. The H-1" to H-4" of all systems had large upfield shifts that were attributed to the anisotropic shielding effect of the π -electron cloud or conformation changes in polymer chain (H. M. Cabral Marques, Hadgraft, Kellaway, & Pugh, 1990; L. Ribeiro et al., 2005; R. Zhao et al., 2011). When compared between the two binary systems, γ CD prefers HDMBr over dovitinib, as shown by the higher shielding effect.

All ^1H -NMR data discussed above can be demonstrated that dovitinib molecules bound to the γ CD in two ways. Firstly, the drug inserted its quinolone moiety into the γ CD cavity from a larger rim. Secondly, the remaining part of drug molecules aligned with outer surface of the torus. The molecular interactions of dovitinib with γ CD were stronger both inside and outside of the torus when HDMBr was present. The nitrogen atom with a permanent positively charge in this polymer can provoke the effect of neighboring electronegative groups (i.e. oxygen atom or phenyl ring) via π -electron cloud between host and guest molecules that leads to the shielding effect in most cases (E Mohr, 2006; Mahadevi & Sastry, 2013; Reddy & Sastry, 2005). Thus, the complex formation with three components including dovitinib, γ CD, and HDMBr is schematically proposed on basis of results as depicted in Fig. 17.

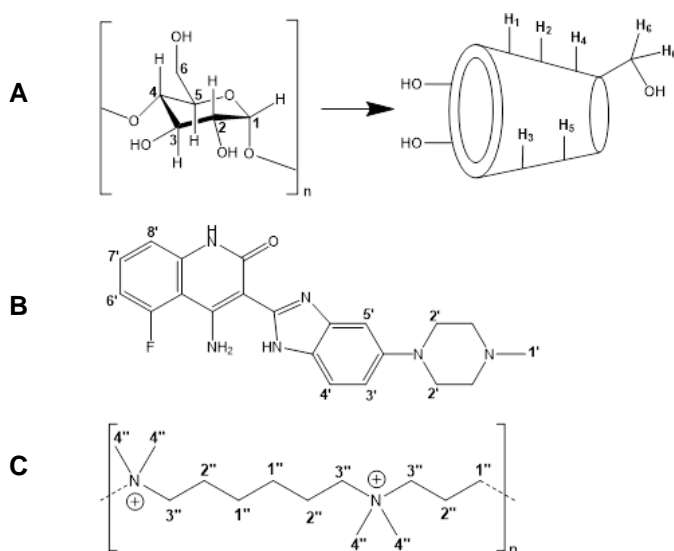


Figure 15. Structure of (A) γ CD, (B) dovitinib, (C) HDMBr and their protons probed in the NMR experiment.

Table 15. ^1H NMR chemical shift difference ($\Delta\delta$, ppm) of free γCD and in the binary (i.e. dovitinib/ γCD and HDMBr/ γCD) and ternary dovitinib/ γCD /HDMBr complexes.

| ^1H assignment ^a | δ free | | $\Delta\delta$ ^b | |
|--------------------------------------|-------------------|--------------------------------|------------------------------|---|
| | γCD | $\gamma\text{CD}/\text{HDMBr}$ | dovitinib/ γCD | dovitinib/ $\gamma\text{CD}/\text{HDMBr}$ |
| H-1 | 4.8700 | -0.0008 | +0.0005 | -0.0004 |
| H-3 | 3.6025 | -0.0006 | -0.0005 | -0.0015 |
| H-5 | 3.5550 | -0.0005 | -0.0004 | -0.0013 |
| H-6 | 3.5032 | -0.0008 | -0.0005 | -0.0015 |
| H-2 | 3.3298 | -0.0001 | 0.0000 | -0.0002 |
| H-4 | 3.3058 | -0.0002 | -0.0001 | -0.0002 |

^a DMSO- d_6 signal used as reference at 2.5000 ppm.

^b $\Delta\delta = \delta$ complex - δ free.

Table 16. ^1H NMR chemical shift difference ($\Delta\delta$, ppm) of dovitinib (D) in free-state and in the complexes.

| ^1H assignment ^a | δ free | | $\Delta\delta$ ^b | |
|--------------------------------------|---------------|-----------------|------------------------------|---|
| | dovitinib | dovitinib/HDMBr | dovitinib/ γCD | dovitinib/ $\gamma\text{CD}/\text{HDMBr}$ |
| H-1' | 2.2167 | 0.0578 | -0.0056 | 0.0880 |
| H-2' | 3.1083 | -0.0448 | -0.0024 | -0.0561 |
| H-3' | 6.9330 | 0.0050 | 0.0037 | 0.0121 |
| H-6' | 7.0083 | 0.0003 | 0.0030 | 0.0042 |
| H-5' | 7.0824 | 0.0115 | -0.0022 | 0.0175 |
| H-7' | 7.1800 | 0.0012 | 0.0006 | 0.0001 |
| H-8' | 7.4452 | 0.0057 | 0.0015 | 0.0112 |
| H-4' | 7.5258 | 0.0052 | 0.0001 | 0.0090 |

^a DMSO- d_6 signal used as reference at 2.5000 ppm

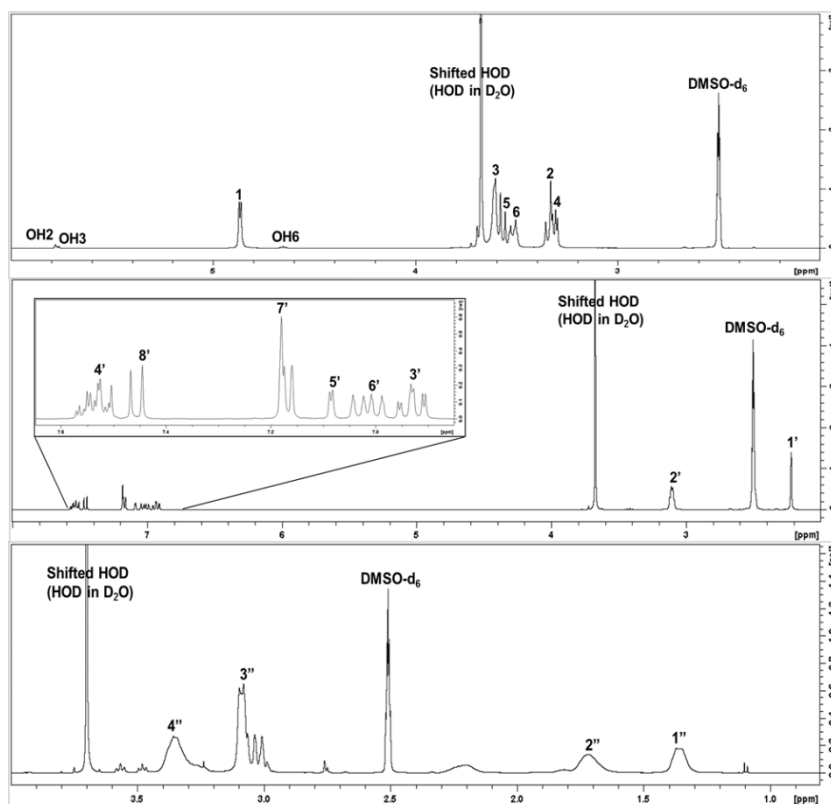
^b $\Delta\delta = \delta$ complex - δ free

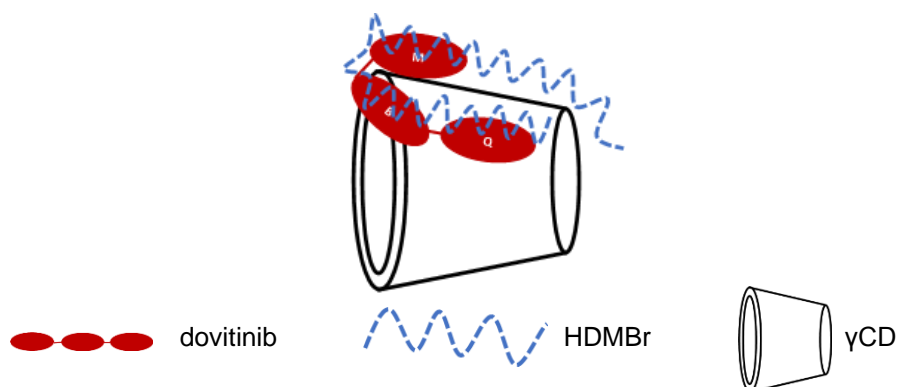
Table 17. ^1H NMR chemical shift difference ($\Delta\delta$, ppm) of HDMBr in free-state and in complex.

| ^1H assignment ^a | $\bar{\delta}$ free | | $\Delta\bar{\delta}$ ^b | |
|--------------------------------------|---------------------|-----------------|-----------------------------------|---|
| | HDMBr | dovitinib/HDMBr | $\gamma\text{CD}/\text{HDMBr}$ | dovitinib/ $\gamma\text{CD}/\text{HDMBr}$ |
| H-1'' | 1.3613 | -0.0094 | -0.0230 | -0.0220 |
| H-2'' | 1.7069 | -0.0056 | -0.0082 | -0.0118 |
| H-3'' | 3.0713 | -0.0182 | -0.0190 | -0.0192 |
| H-4'' | 3.3472 | -0.0110 | - | - |

^a DMSO- d_6 signal used as reference at 2.5000 ppm

^b $\Delta\bar{\delta} = \bar{\delta}$ complex - $\bar{\delta}$ free

**Figure 16.** Representative NMR spectrum of (A) γCD , (B) dovitinib, (C) HDMBr and their protons.



where M is methyl-piperazine ring, B is benzimidazole ring, and Q is quinoline ring

Figure 17. Proposed complex formation of dovitinib /HDMBr/γ-CD ternary system.

4.1.8 Physicochemical characteristics of solid dovitinib/γCD and dovitinib/γCD/HDMBr complex

The XRPD diffractogram of the pure substances (i.e. dovitinib, γCD, and HDMBr), physical mixtures, dovitinib/γCD binary complex, and dovitinib/γCD/HDMBr ternary complex are all presented in Fig. 18. The diffraction patterns of drug and γCD predictably show an intense crystallinity with sharp peaks while HDMBr produced a broad halo-pattern typical of an amorphous compound. The reduction of the degree of crystallinity of the drug and CD is observed in the binary and ternary physical mixtures. The characteristic peaks relevant to crystalline molecules were no longer detectable in all lyophilized complexes, and thus indicate the complex formation (Cavalli, Trotta, Trotta, Pastero, & Aquilano, 2007; Jansook, Muankaew, Stefansson, & Loftsson, 2015; Jansook, Pichayakorn, Muankaew, & Loftsson, 2016a).

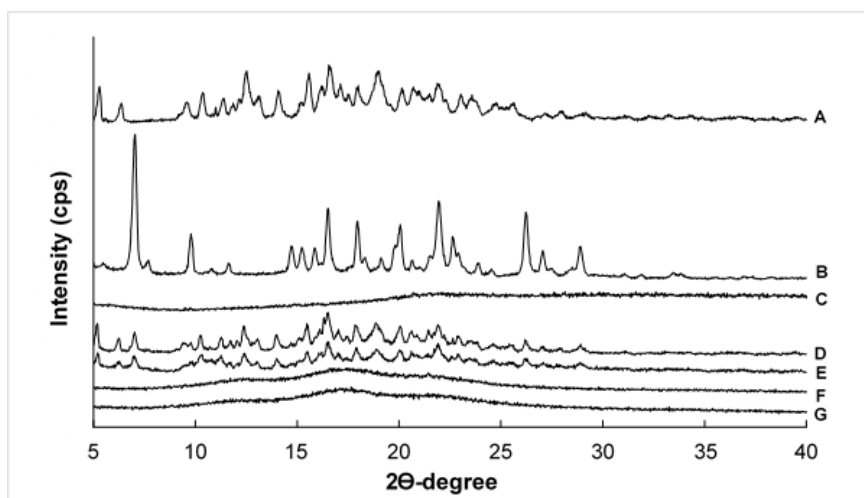


Figure 18. XRPD spectra of (A) γ CD, (B) pure dovitinib, (C) HDMBR, (D) Dovitinib/ γ CD physical mixture, (E) Dovitinib/ γ CD/HDMBR physical mixture, (F) Dovitinib/ γ CD complex, (G) Dovitinib/ γ CD/HDMBR complex.

DSC was applied to evaluate the solid-state characterization of γ CD, pure dovitinib, HDMBR, their physical mixtures, and their complexes (Fig. 19). The thermogram observed for γ CD exhibited broad bands due to dehydration at 90.4°C and decomposition at 320.4°C. The very broad peak was also found for HDMBR at 280.4°C, probably related to decomposition phenomena. The thermal curve of the pure drug was typical of a crystalline substance with a sharp endotherm at 332.9°C corresponding to its melting point. The overlap between this drug melting peak and γ CD decompositions bands made it difficult to detect changes in the binary and ternary mixtures. However, other KIs such as axitinib or motesanib mixtures were tested following this experiment, and the thermal curve displayed well-distinct melting peaks for the crystalline pure drugs whereas their complexes did not present that endothermic peak due to drug inclusion into γ CD indicating complex formation (Fig. 20-21). The dovitinib complexes showed similar DSC thermogram indicating complex formation. In addition to physical mixtures, the exothermic peak for binary system (at 327.9°C) and ternary system (at 302.9°C) suggested decomposition of the compound (Jansook et al., 2016a).

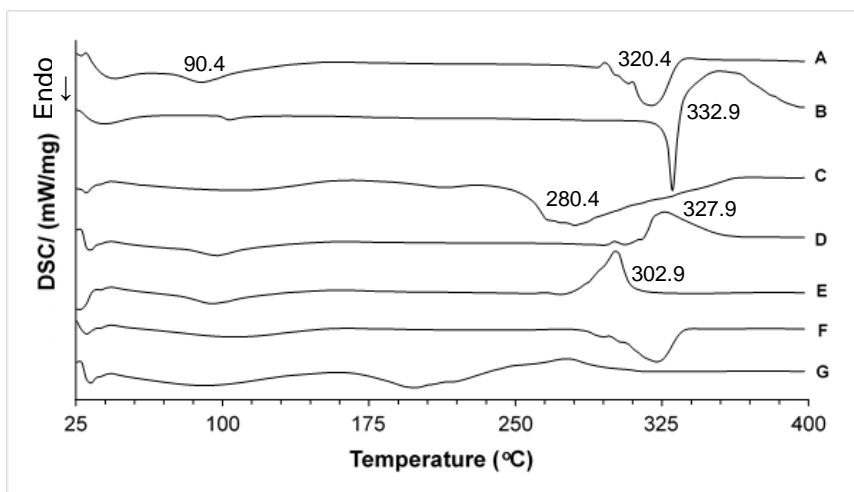


Figure 19. DSC of (A) γ CD, (B) pure dovitinib, (C) HDMBR, (D) dovitinib/ γ CD physical mixture, (E) dovitinib/ γ CD/HDMBR physical mixture, (F) dovitinib/ γ CD complex, (G) dovitinib/ γ CD/HDMBR complex.

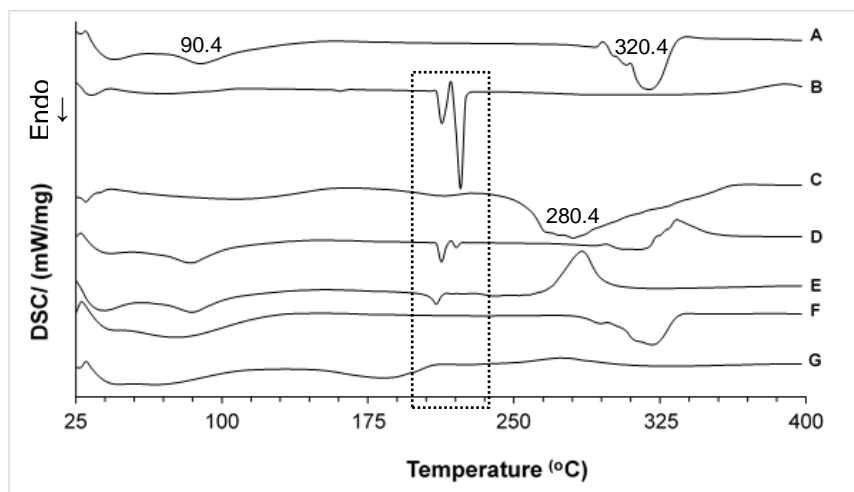


Figure 20. DSC of (A) γ CD, (B) pure axitinib, (C) HDMBR, (D) axitinib/ γ CD physical mixture, (E) axitinib/ γ CD/HDMBR physical mixture, (F) axitinib/ γ CD complex, (G) axitinib/ γ CD/HDMBR complex.

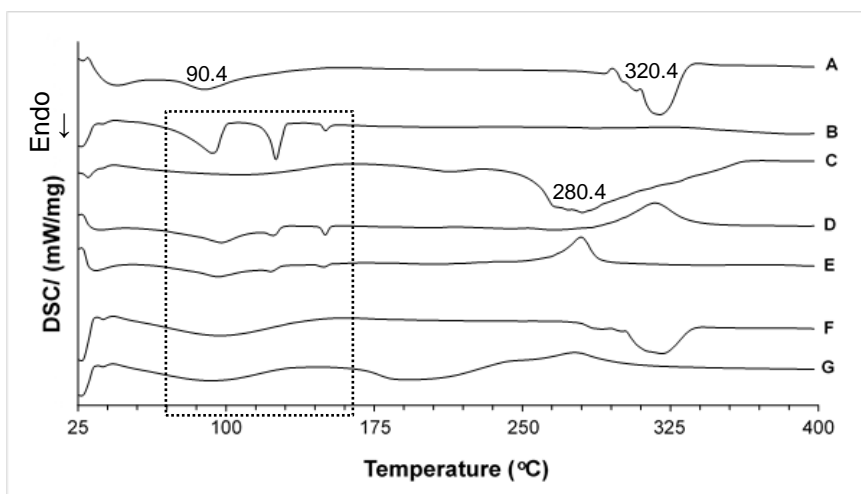


Figure 21. DSC of (A) γ CD, (B) pure motesanib, (C) HDMBr, (D) motesanib/ γ CD physical mixture, (E) motesanib/ γ CD/HDMBr physical mixture, (F) motesanib/ γ CD complex, (G) motesanib/ γ CD/HDMBr complex.

FT-IR spectroscopic analysis can provide useful information on the host-guest interaction in a solid state. Fig. 22 presents the FTIR spectra of dovitinib/ γ CD binary complex, dovitinib/ γ CD/HDMBr ternary complex, their physical mixtures, and pure substances. The spectral changes were observed in term of γ CD and dovitinib.

The IR spectrum of γ CD showed strong and wide characteristic bands belong to the free $-\text{OH}$ stretching vibration at 3293 cm^{-1} . The absorption observed in physical mixtures ($3320\text{--}3322\text{ cm}^{-1}$) was found to be less narrow and shifted to the higher wavenumber, and this band was down-shifted even further in lyophilized complexes ($3331\text{--}3347\text{ cm}^{-1}$). The change of these hydroxyl bands proved the existence of dovitinib/ γ CD complex formation (Goswami, Majumdar, & Sarkar, 2017; Sambasevam, Mohamad, Sarih, & Ismail, 2013). The frequency for free γ CD observed at 2902 cm^{-1} corresponds to $-\text{CH}$ and $-\text{CH}_2$ vibration. Only dovitinib complexes gave the shifts in this respective functional groups at 2971 cm^{-1} . Another large band assigned to the C-O-C stretching vibration is observed at 1020 cm^{-1} . The C-O-C stretching vibration of physical mixtures was upper-shifted to 1009 cm^{-1} while that of dovitinib complexes was down-shifted to 1045 cm^{-1} . Moreover, this band was narrowed when HDMBr presented in complex. This phenomenon indicated that hydrophilic polymer like HDMBr participated in the complex formation between γ CD and drug. Dovitinib complexes were observed to have some increases of frequency values which was due to the

insertion of an electron-rich group into the CD cavity (Goswami et al., 2017; Sambasevam et al., 2013; Tang, Chen, Zhang, Zhang, & Wang, 2006). The insertion behavior was agreeable to the $^1\text{H-NMR}$ data.

Several characteristic IR absorption bands of dovitinib were observed: 3502 cm^{-1} (N-H stretching vibration), 2837 cm^{-1} (aliphatic C-H stretching vibration), 1645 cm^{-1} (C=O stretching frequency), 1612 cm^{-1} (C=C of aromatic ring), and $753, 793\text{ cm}^{-1}$ (1, 2 di-substituted benzene ring). In lyophilized samples, the disappearance of these absorption frequencies and the shift of aliphatic C-H stretching might be explained by the complex formation between drug and γCD . Besides that, the characteristic bands were found to be less intense in FT-IR spectra of the physical mixtures (Chutimon Muankaew, Jansook, & Loftsson, 2016; C. Muankaew, Jansook, Stefansson, & Loftsson, 2014b). In summary, FTIR observation is supported by the XRPD and DSC results indicating complex formation in both binary and ternary systems.

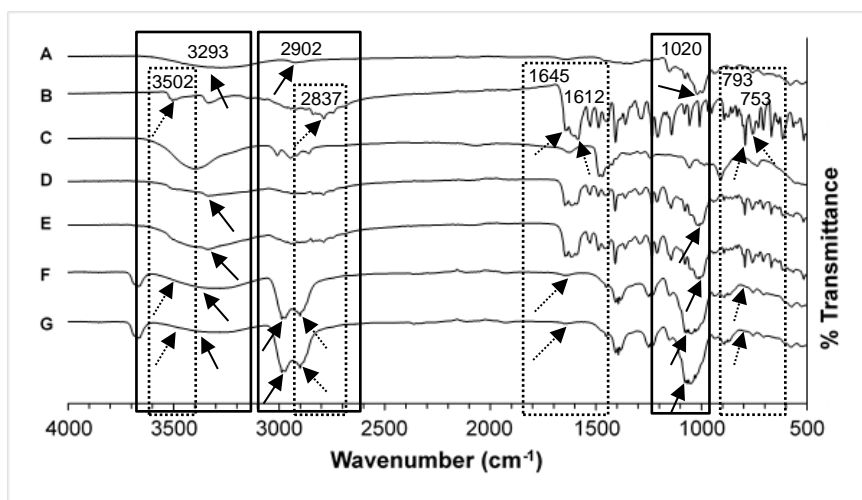


Figure 22. FT-IR spectra of 8(A) γCD , (B) pure dovitinib, (C) HDMBr, (D) Dovitinib/ γCD physical mixture, (E) Dovitinib/ γCD /HDMBr physical mixture, (F) Dovitinib/ γCD complex, (G) Dovitinib/ γCD /HDMBr complex.

4.1.9 *In vitro* dissolution studies (dovitinib/ γ CD and dovitinib/ γ CD/HDMBr complexes)

The advantage of the ternary drug/CD/polymer complexes in terms of enhanced aqueous KI solubility was clearly observed during the solubility experiments when the effects of different types of polymer were tested. HDMBr produced the highest solubilizing potency for most of the drug candidates. The following study was performed to evaluate the dissolution performance of optimum ternary system in comparison with that of the pure drug and binary complexes. This study tested only by γ CD concentrations of maximum drug solubility that is 5% (w/v) and 8% (w/v). A modified dissolution test with small volumes of dissolution medium was used, due to the limited availability of the test material.

The dissolution profiles in Fig. 23 show that dovitinib binary complexes were able to increase the extent and rate of dissolution, and the effect was independent of the amount of γ CD present. Those amorphous complexes dissolved completely within approximately 2 min (Chutimon Muankaew et al., 2016). The addition of HDMBr to form the ternary complexes somewhat retarded the release rate, probably due to polymer matrix formation (Loftsson & Masson, 2004; Mura, Faucci, & Bettinetti, 2001).

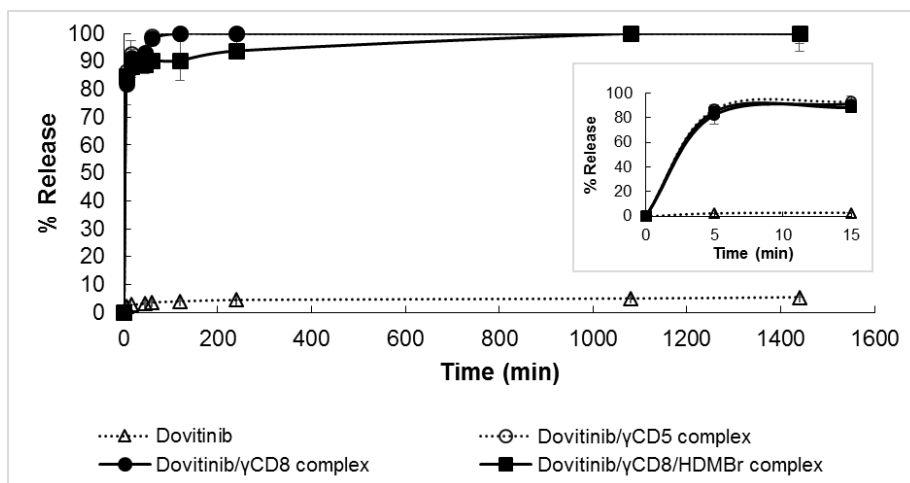


Figure 23. *In vitro* dissolution of dovitinib in solid complexes with γ CD at a concentration of 5% or 8% (w/v) (mean \pm standard deviation; n=3).

4.2 Effect of acidic counter ion on the dovitinib/ γ CD solubilization and complexation

Previous studies showed that natural γ CD can enhance the aqueous solubility of KIs especially that of dovitinib, but the complexation efficacy (CE) is relatively low. EDTA in formulation vehicle increased the solubilization through salt formation, and it also increased the γ CD solubilization of KIs. Therefore, the salt formation was investigated further. The main idea was to form dovitinib salt (i.e. increase the S_0) and to enhance the CE of the dovitinib/ γ CD complex. These complexes were also prepared by ultrasonication with mild heat and, thus, the degree of solubility enhancement between two additional techniques which are addition of hydrophilic polymers and salt formation, can be comparable.

4.2.1 pH-solubility studies (pure dovitinib and dovitinib/ γ CD complexes)

The solubility of dovitinib in pure water and aqueous γ CD solutions depended on the pH of the media (Fig.24). The drug was very soluble under acidic conditions due to the ionization of the nitrogen group (Budha et al., 2012; Zhang et al., 2014). The nitrogen in position 4 of the 4-methyl-1-piperazinyl (estimated pK_a 6.5), was protonated at low pH (Fig. 25). However, the drug was degraded (i.e. color change was observed) in the strong acidic medium (e.g., at pH 1) when γ CD was absent. The presence of γ CD at 5% (w/v) not only improved the solubility of dovitinib but also protected the drug from acidic degradation at pH lower than 3.

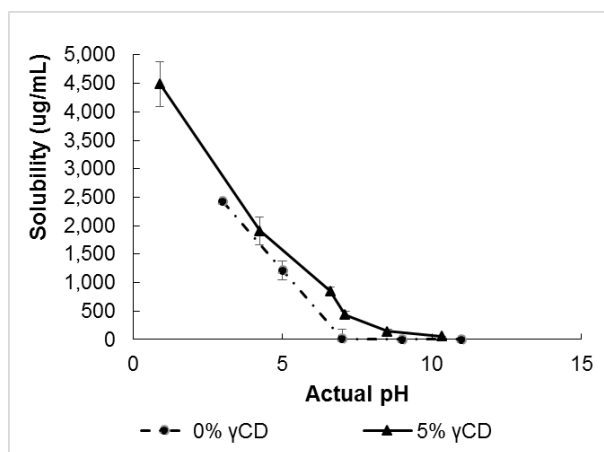


Figure 24. pH-solubility profiles of dovitinib in pure water and in 5% (w/v) aqueous γ CD solutions (mean \pm standard deviation; $n=3$).

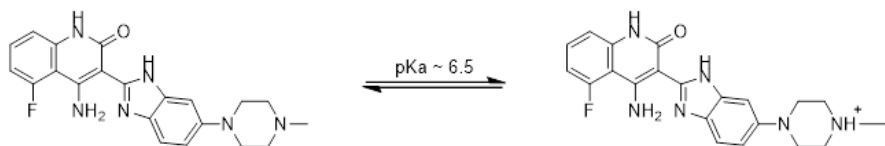


Figure 25. Ionization of dovitinib assuming the nitrogen in position 4 of the 4-methyl-1-piperazinyl moiety is the most basic one.

4.2.2 Phase-solubility studies (dovitinib/ γ CD complex)

The phase-solubility profiles under ambient conditions showed that the solubility of dovitinib was limited in aqueous media at γ CD concentrations above 5% (w/v), thus the diagram is of B_s -type (Fig. 26). Without pH adjustment, the media pH was 6.86. Hydrochloric acid (HCl) was used to adjust the pH of complexation media to 6. The addition of inorganic acid slightly lowered the pH while also greatly enhancing the large enhancement of drug solubility. Although at pH 6 the ionized dovitinib was more soluble, the stability constant ($K_{1:1}$) of the complex was decreased from 684 M^{-1} to 145 M^{-1} due to the ionization effect (Table 18). In general, the more hydrophilic ionized form of a given drug molecule has a lower affinity for the hydrophobic CD cavity than the unionized form, and therefore, the ionized form generally has a lower $K_{1:1}$ value (Loftsson & Brewster, 2012). Here the drug was practically more soluble due to HCl. However, this ionized molecule had less affinity to γ CD.

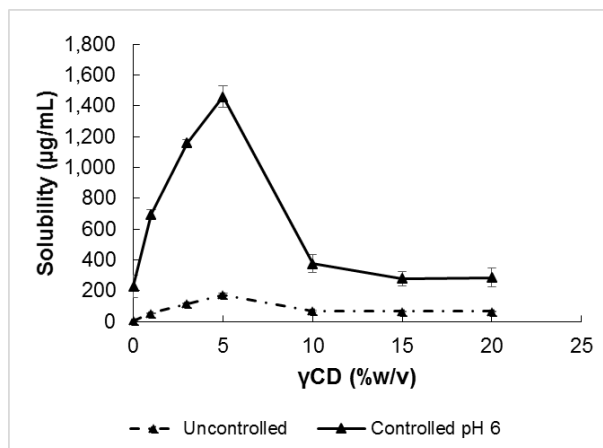


Figure 26. Phase-solubility profiles of dovitinib complexes in pure water (pH about 6.86) and in aqueous hydrochloric acid solution, at pH 6 (mean \pm standard deviation; $n=3$).

Table 18. Solubilization efficacy of dovitinib in different CD solution.

| Counter ion | pH | S ₀ (µg/mL) | Phase solubility parameters | | | | | | | | |
|----------------|-----------|---------------------------|-----------------------------|--|------|--------------------|--|------|---------------------|--|----|
| | | | γCD ^a | | | HPγCD ^a | | | SBEγCD ^a | | |
| | | | PS- type | K _{1:1} (M ⁻¹) | CE | PS- type | K _{1:1} (M ⁻¹) | CE | PS- type | K _{1:1} (M ⁻¹) | CE |
| No Counter ion | 6.86 | 6.34 | B _s | 684 | 0.01 | - | - | - | - | - | - |
| Hydrochloride | 6.0 ± 0.1 | 229 | B _s | 145 | 0.08 | A _N | 44 | 0.03 | - | - | - |

4.2.3 Effect of acidic counter ion on drug solubility

The aqueous solubility of dovitinib in binary and ternary systems containing 1% (w/v) of a given acid, both with and without the presence of 8% (w/v) γ CD was determined at pH 6. Here the solubility determinations were performed at a γ CD concentration above the determined maximum dovitinib solubility according to the phase-solubility profile (see Fig. 26). If formation of the complex provided for an effective solubilization in the presence of an organic counter ion, then the observed drug solubility should be greater than the maximum solubility of dovitinib in a complex media without the counter ion. Hydrochloride was used as a control.

The drug solubility of ionized systems is presented in Fig. 27, and the solubilizing ratio was also calculated (Table 19). The solubility is always greater when a counter ion is present in the complexation media. In pure water, hydrochloride (control) showed the highest solubilizing power. In presence of γ CD, the drug solubility was increased by about 3 to 95 units (Table 19) depending on counter ions except, for formate. Although lactate had the greatest performance with 94-fold increases in solubility, the candidate still had less solubilizing power than hydrochloride. Citrate, acetate, edetate and hydrochloride intensified γ CD solubilization (Fig.27 and Table 19). However, the solubility enhancement of dovitinib hydrochloride (which formed upon the addition of HCl) was less pronounced in the aqueous γ CD complexation media. Typically, for effective salt formation, the pK_a difference (ΔpK_a) between the drug and the counter ion should be at least 2 to 3 units (D. Gupta, Bhatia, Dave, Sutariya, & Varghese Gupta, 2018; H. Lee, 2014). Although the ΔpK_a value between dovitinib (estimated pK_a 6.5) and HCl (pK_a -10) is larger, it is not insufficient when γ CD is dissolved in that aqueous environment. Here, even if dovitinib salt could form, it might rapidly break down into individual species in γ CD complexation media. In this instance, the relationship between ionization and ΔpK_a is not always clear cut. However, the ionization can depend on structural features of the basic drug and acidic counter ion (Moreira et al., 2015). It is known that these hydroxyl acids can participate in the complex formation (Fenyvesi et al., 1999; Loftsson & Brewster, 2012) and therefore, increase the apparent $K_{1:1}$ value, in addition to the salt effect. Thus, these acids can sometimes increase both S_0 and $K_{1:1}$.

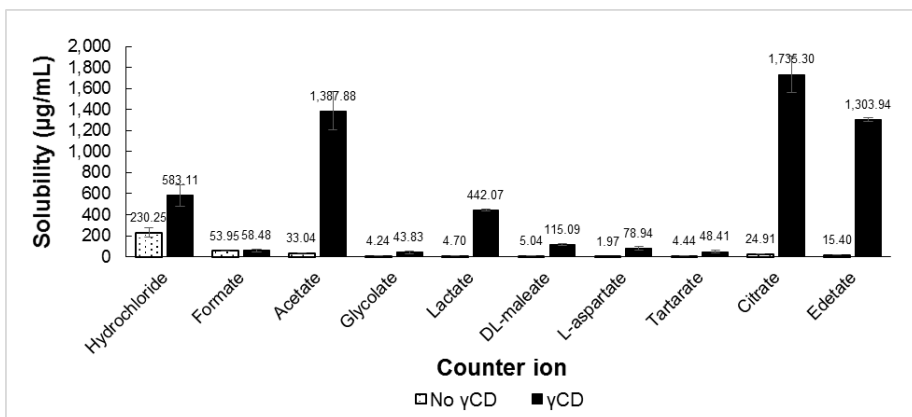


Figure 27. Aqueous solubility of the dovitinib in buffered aqueous 1% (w/v) acidic counter ion solution at pH 6.0 with and without 8% (w/v) γ CD at room temperature (mean \pm standard deviation; n=3).

Table 19. Solubilizing ratio of ionized dovitinib at pH 6 in comparison of control, and the ratio between presence and absence of γ CD.

| Counter ion | Solubilizing ratio | | |
|----------------------------|-----------------------------------|--------------------------------|--|
| | Comparison with control | | Comparison between γ CD group and no γ CD group ^c |
| | No γ CD group ^a | γ CD group ^b | |
| Hydrochloride (control) | 1.00 | 1.00 | 2.53 |
| Formate | 0.23 | 0.10 | 1.08 |
| Acetate | 0.14 | 2.38 ^d | 42.01 ^e |
| Glycolate | 0.02 | 0.08 | 10.33 |
| Lactate | 0.02 | 0.76 | 94.01 ^d |
| DL-malate | 0.02 | 0.20 | 22.82 |
| L-aspartate | 0.01 | 0.14 | 39.97 |
| Tartarate | 0.02 | 0.08 | 10.90 |
| Citrate | 0.11 | 2.98 ^e | 69.66 ^e |
| Edetate | 0.07 | 2.24 ^d | 84.69 ^e |

^a refers to *solubilizing ratio* = $\frac{\text{drug solubility of drug/counter ion}}{\text{drug solubility of drug/hydrochloride}}$

^b refers to *solubilizing ratio* = $\frac{\text{drug solubility of drug/}\gamma\text{CD/counter ion}}{\text{drug solubility of drug/}\gamma\text{CD/hydrochloride}}$

^c refers to *solubilizing ratio* = $\frac{\text{drug solubility in presence of CD}}{\text{drug solubility in absence of CD}}$

^d refers to maximum solubilizing ratio

^e refers to very high solubilizing ratio

4.2.4 Effect of acidic counter ion on phase-solubility profile

Citrate, acetate, and edetate were selected to determine the phase-solubility behavior in aqueous complexation media containing neutral CD and charged CD in comparison to hydrochloride. The ionized form of dovitinib has a positive charge, the negatively charged γ CD, in this case SBE γ CD, was used to improve drug solubility through charge-charge interaction.

The phase-solubility profiles of ternary complexes due to counter ion were varied depending on the type of CD. Here the natural γ CD gave B_s-type profiles whereas A_N-type were observed in the more water-soluble γ CD derivatives, that is HP γ CD and SBE γ CD (data not shown). Many studies have shown that the natural CDs formed B-type phase-solubility profiles while their more water-soluble derivatives display formed A-type profiles (Loftsson, Jarho, Masson, & Jarvinen, 2005). The SBE γ CD complex systems gave had the highest drug solubility, followed by HP γ CD, and γ CD. The acidic counter ion had an intensive influence on the K_{1:1} values of dovitinib-CD complexes and the CE (Table 20). Salt formation improved both the aqueous solubility of the drug and its apparent K_{1:1} value. Moreover, charge-charge interaction between SBE γ CD and the protonized dovitinib highly increased the CE. Hydrochloride had the least tendency to solubilize the drug, consequently, it was not included in SBE γ CD system. The highest solubilizing power of any given counter ion was citric acid. It enhanced the phase solubility parameters, especially that of the SBE γ CD ternary complex, giving K_{1:1} 8350 M⁻¹ and CE 0.63. However, the aqueous solubility of dovitinib due to corresponding counter ion is lower than that from acetate. In case of edetate, the dovitinib salt resulted in good high solubility. This was also the case for the acetate. Those two acidic counter ions may play a role of space-regulating molecule between host and ionized guest (Ueno, Takahashi, & Osa, 1981). These ions can participate in the complex, not only increasing S₀ but also K_{1:1}. In addition, the highest CE was obtained for the most soluble salt. This may indicate that those counter ions participate directly in the complex formation, or that they may form a ternary drug CD-salt complex (Loftsson & Brewster, 2012; Mura, Faucci, Manderioli, & Bramanti, 2001; Redenti, Szente, & Szejtli, 2000).

Table 20. Solubilization efficacy of dovitinib in different CD solution.

| Counter ion | pH | S ₀ ($\mu\text{g/mL}$) | Phase solubility parameters | | | | | | | | |
|----------------|---------------|--|-----------------------------|---|------|------------------------|---|------|-------------------------|---|------|
| | | | γCD^a | | | HP γCD^a | | | SBE γCD^a | | |
| | | | PS-type | K _{1:1} (M^{-1}) | CE | PS-type | K _{1:1} (M^{-1}) | CE | PS-type | K _{1:1} (M^{-1}) | CE |
| No Counter ion | 6.86 | 6.34 | B _s | 684 | 0.01 | - | - | - | - | - | - |
| Hydrochloride | 6.0 \pm 0.1 | 229 | B _s | 145 | 0.08 | A _N | 44 | 0.03 | - | - | - |
| Edetate | 6.0 \pm 0.1 | 28.5 | B _s | 1590 | 0.12 | A _N | 1490 | 0.11 | A _N | 3960 | 0.44 |
| Acetate | 6.0 \pm 0.1 | 41.7 | B _s | 2110 | 0.22 | A _N | 1250 | 0.13 | A _N | 4680 | 0.70 |
| Citrate | 6.0 \pm 0.1 | 33.9 | B _s | 2270 | 0.20 | A _N | 1630 | 0.14 | A _N | 8350 | 0.63 |

^a Based on the slope of the initial linear phase-solubility diagram observed between 0% and 5% (w/v) CD.

4.2.5 Physicochemical properties of dovitinib/CD and dovitinib/CD/counter ion complex aggregates

Salts can significantly alter the physicochemical properties of drug molecules that expedites the drug development process (D. Gupta et al., 2018). The suitable counter ions will be determined depending on particle sizes, zeta potential, electrical conductivity, and osmolality.

Particle size

The ternary complexes formed nano-sized aggregates approximately 100-900 nm in diameter (Fig. 28a). The aggregate size became larger in the presence of a counter ion as well as in the case of increased dovitinib/ γ CD solubilization. Other investigators previously found that hydroxyl acids, and other low MW organic acids, increase the aqueous solubility of the poorly soluble β CD (Fenyvesi et al., 1999). The solubility enhancement in this present study may be related to the tendency of γ CD and their complexes to form nanoparticles in aqueous solution, and the ability of a counter ion to solubilize and stabilize these aggregates (Loftsson & Brewster, 2012; Messner et al., 2010). The natural γ CD ternary system had larger sized aggregates than were present in γ CD derivatives. CD derivatives such as HP β CD, HP γ CD, and SBE γ CD are mixtures of geometrical and optical isomers. Such CD molecules may lose their hydrogen-bond donor (i.e. -OH groups) on derivation. This fact decreases their ability to self-assemble and form aggregates than their parent CDs (Loftsson, 2014b; Messner et al., 2010; Puskás, Schrott, Malanga, & Szente, 2013; Ryzhakov et al., 2016). Each of the carboxylic counter ions, i.e. edetate, acetate, and citrate, showed a similar pattern of aggregate size.

Zeta potential

Zeta potential (ZP) is the electric potential at the interfacial double layer (also called “slipping plan”) of a dispersed particle versus a point in the bulk medium (Pate & Safier, 2016). The ZP of dispersed particle in solution describes the overall effect net charge of the particle under the sample environments. The effect net charge refers to all charges (including counter ions) that are held around the particle. The ZP value of samples with acidic counter ion in Fig. 28b except that of hydrochloride, is fairly negative due to the excess amount of counter ion. It also implies an effective ionization between dovitinib and those counter ions. No large differences in ZP are observed between samples. However, the presence of hydrochloride in pure water influences the ZP in different way. It is known that Cl⁻ ions are

chemisorbed, but this chemisorption is enhanced by adsorbed H^+ ions. When the concentration of hydrochloride is relatively low, the adsorbed H^+ ions cannot stimulate the adsorption of Cl^- ion near a surface (Logtenberg & Stein, 1986). Therefore, the net charge behind the slipping plane is positive.

Electrical conductivity

Electrical conductivity is a simple technique that provides information on the structure of ionic solutions, and the degree of counter ion dissociation for diluted solutions. This technique measures the ability of an aqueous solution to carry an electric current depending on the concentration, mobility, ionized species in a solution, and the temperature (Barthel et al., 1998; Robinson & Stokes, 2002). The presence of an acidic counter ion in CD ternary complexes induced a higher conductivity as shown in Fig 28c. The signals were even strong when the solution contained carboxylic derivatives compounds such as edetate, acetate, and citrate. It indicated that soluble drug molecules were in salt form that dissociated into ionized species in aqueous solution. Thus, the higher conductivity reflected the higher concentration of such ions. Unlike the uncharged CDs, SBE γ CD increased a tendency to induce the good conductivity due to the influence of charge-charge interaction.

Osmolality

Osmolality refers to the concentration of all dissolved substrates (i.e. drug, counter ion, salt, CD, and complexes) in pure water. It is proportional to the osmoles of solute per kilogram of solvent (E Mohr, 2006). Higher osmolality means more amounts of dissolved substances in the solution while lower osmolality means they are more diluted. Each counter ion presented osmolality in a comparable pattern (Fig. 28d) which corresponded to the conductivity results (Fig. 28c). An increase of drug solubility in γ CD derivatives complexation media increased this parameter.

Additionally, acetate systems appeared darker in color after they had been kept in ambient condition for a couple of months. In summary, acetate was not a good choice due to stability problem. Thus, only citrate was selected for further study.

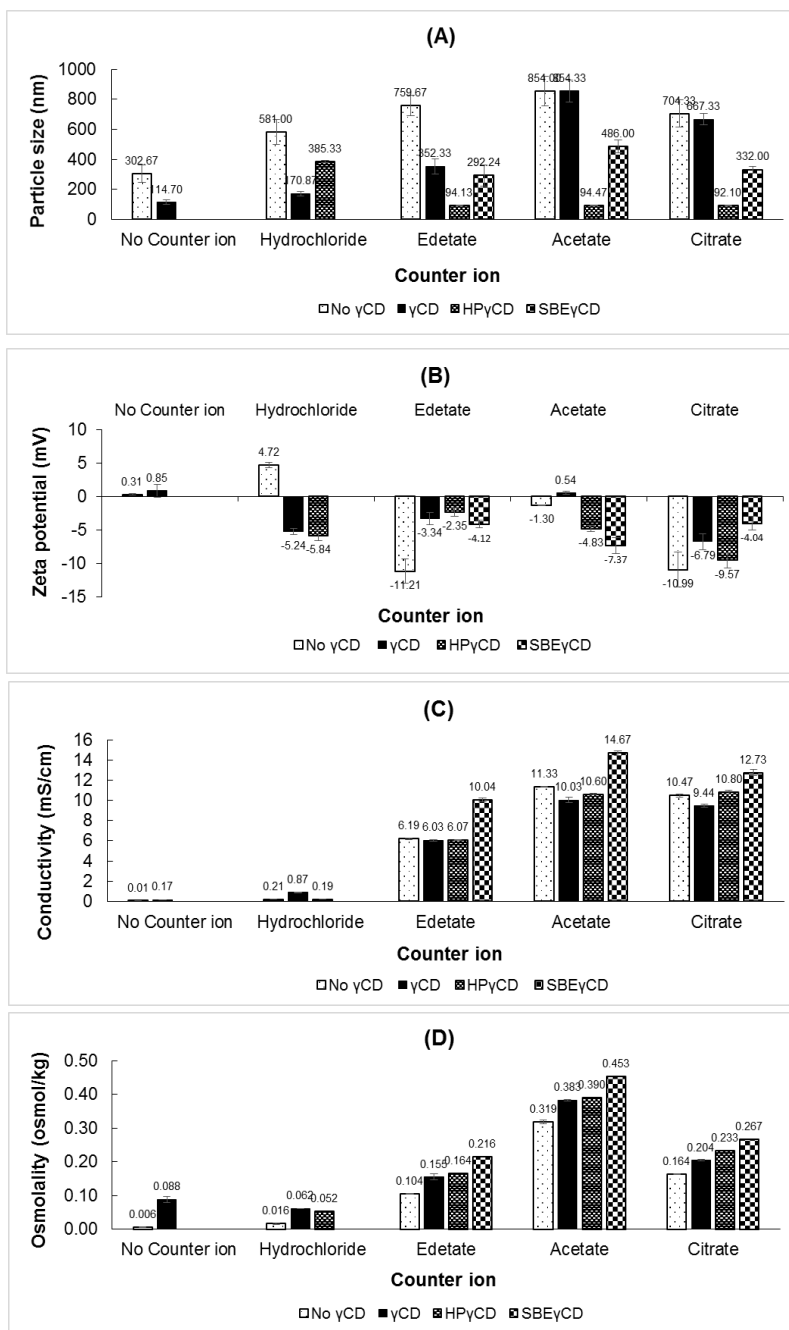


Figure 28. Characteristics of pure dovitinib and dovitinib complexes (A) particle size, (B) zeta potential, (C) electrical conductivity, and (D) osmolality (mean \pm standard deviation; n=3).

4.2.6 ¹H-NMR Spectroscopic studies (dovitinib/CD and dovitinib/CD/counter ion complexes)

The chemical shifts for CDs were calculated in free and bound states as shown in Table 21-23. In the case of the natural γ CD, the proton signals on the exterior rim are H-1, H-2, H-4, and H-6, and the interior of the cavity are H-3, and H-5 (Amiri & Amiri, 2017; C. Muankaew et al., 2014a). However, the γ CD derivatives have proton resonances located on both the cavity region and the substituent chain. The number of protons present depends on the length of the side chain. For example, HP γ CD which consists of short side chain, only has H-1' located near the ring (Dufour, Evrard, & de Tullio, 2015) while the substituent group of SBE γ CD is longer, with the proton signals at H-2', H-3', and H-4' (Luna et al., 1997; Maeda, Tanaka, & Nakayama, 2015).

The chemical shift changes of γ CD in the presence of dovitinib and citric acid are shown in Table 21. H-2 and H-4 show no relative displacement. The only upfield shift ($\Delta\delta < 0$) is very slight and due to shielding effect; it occurs at the H-3, H-5, and H-6 protons. The signal changes indicate that the guest molecules, that are dovitinib and citric acid, are located at the internal and external γ CD cavity. When citric acid is the ternary component, the shielding effect of guest molecules is elevated (oxygen atom and aromatic moieties of dovitinib) or, in other words, the molecular conformation is particularly altered due to the ternary complex formation. (Prapahnwittaya, Saokham, Jansook, & Loftsson, 2020b; L. Ribeiro et al., 2005). Furthermore, citric acid may change the ionization of the drug and/or the polarity of the medium that increases the drug-CD association constant, thus, the shifts is larger after addition of citric acid.

The changes in the ¹H NMR chemical shifts of the HP γ CD protons (Table 22) when dovitinib and citric acid are present, occur both upfield ($\Delta\delta < 0$) and downfield ($\Delta\delta > 0$). The H-2 and H-4 displace in an upfield shift ($\Delta\delta < 0$) due to shielding effect, as previously described. The downfield displacements ($\Delta\delta > 0$) at H-1, H-5, H-6, and H-1' all relate to de-shielding effects of the local polarity variation after complex formation, or the van der Waals binding between drug molecules and γ CD (Djedaïni et al., 1990; Prapahnwittaya et al., 2020b; R. Zhao et al., 2011). The shielding effect became more intense when citric acid was added. The signal shift of the H-2 and H-4 protons was stronger than that of the H-3 and H-5 protons. Thus, the host-guest interactions probably occur both inside and outside of the γ CD cavity, and majority of such bindings is at the external rim.

The ^1H NMR chemical shifts corresponding to SBE γ CD in free-state and in complexes are listed in Table 23. The changes in proton resonance are mainly upfield shifts ($\Delta\delta < 0$) but only H-3 shows a downfield shift ($\Delta\delta > 0$). Each displacement is due to the aforementioned shielding/de-shielding effects. The H-4 proton has the highest intensity, follow by H-2, and H-3, H-4', and H-2'. The molecular interaction covers not only the ring but also the negatively charged side chain. The ionic pairing between the anionic CD substituent and the cationic drug increases the higher affinity for the complex. This is indicated that strong bindings exist primarily at the surface of CD cavity and occurring in the hydrophobic interior in some parts.

Briefly, the complex formation was confirmed by ^1H -NMR determination. The acidic counter ion like citric acid enhanced the interaction between drug and CDs. These ternary systems generally formed a partial inclusion complex. However, the binding affinity depended on the type of host molecules. The proposed complex formation of the dovitinib/CD/citric acid ternary system is schematically depicted in Fig. 29.

Table 21. ^1H NMR chemical shift difference ($\Delta\delta$, ppm) of free γ CD and in the binary (i.e. dovitinib/ γ CD and citric acid/ γ CD) and ternary dovitinib/ γ CD/citric acid complexes.

| ^1H assignment ^a | δ free | | $\Delta\delta$ ^b | |
|--------------------------------------|---------------|--------------------------|-----------------------------|------------------------------------|
| | γ CD | citric acid/ γ CD | dovitinib/ γ CD | dovitinib/ γ CD/citric acid |
| H-1 | 4.8700 | -0.0022 | 0.0005 | -0.0002 |
| H-3 | 3.6025 | -0.0022 | -0.0005 | -0.0010 |
| H-5 | 3.5550 | -0.0023 | -0.0004 | -0.0010 |
| H-6 | 3.5032 | -0.0029 | -0.0005 | -0.0010 |
| H-2 | 3.3298 | -0.0004 | 0.0000 | 0.0001 |
| H-4 | 3.3058 | -0.0004 | -0.0001 | 0.0002 |

^a DMSO- d_6 signal used as reference at 2.5000 ppm.

^b $\Delta\delta = \delta$ complex - δ free.

Table 22. ^1H NMR chemical shift difference ($\Delta\delta$, ppm) of free HP γ CD and in the binary (i.e. dovitinib/HP γ CD and citric acid/HP γ CD) and ternary dovitinib/HP γ CD/citric acid complexes.

| ^1H assignment ^a | δ free | | $\Delta\delta$ ^b | |
|--------------------------------------|----------------|----------------------------|-----------------------------|--------------------------------------|
| | HP γ CD | Citric acid/HP γ CD | Dovitinib/HP γ CD | Dovitinib/Citric acid/HP γ CD |
| H-1 | 4.8571 | -0.0002 | 0.0003 | 0.0012 |
| H-3 | 3.6776 | N/A | 0.0101 | N/A |
| H-5 | 3.6094 | 0.0006 | 0.0006 | 0.0020 |
| H-6 | 3.5255 | -0.0007 | -0.0015 | 0.0012 |
| H-4 | 3.3070 | -0.0002 | 0.0007 | -0.0364 |
| H-2 | 3.2329 | -0.0005 | 0.0002 | -0.1529 |
| H-1' | 1.0083 | 0.0002 | -0.0005 | 0.0004 |

^a DMSO- d_6 signal used as reference at 2.5000 ppm.

^b $\Delta\delta = \delta$ complex - δ free.

Table 23. ^1H NMR chemical shift difference ($\Delta\delta$, ppm) of free SBE γ CD and in the binary (i.e. dovitinib/SBE γ CD and citric acid/SBE γ CD) and ternary dovitinib/SBE γ CD/citric acid complexes.

| ^1H assignment ^a | δ free | | $\Delta\delta$ ^b | |
|--------------------------------------|-----------------|-----------------------------|-----------------------------|---------------------------------------|
| | SBE γ CD | Citric acid/SBE γ CD | Dovitinib/SBE γ CD | Dovitinib/Citric acid/SBE γ CD |
| H-1 | 4.8589 | 0.0014 | 0.0014 | -0.0008 |
| H-3 | 3.6732 | N/A | -0.0002 | 0.0028 |
| H-5 | 3.6079 | 0.0005 | 0.0008 | -0.0006 |
| H-6 | 3.5247 | 0.0008 | 0.0010 | -0.0006 |
| H-2 | 3.3283 | 0.0005 | 0.0007 | -0.0051 |
| H-4 | 3.2354 | -0.0004 | 0.0005 | -0.0228 |
| H-4' | 2.0661 | 0.0001 | -0.0003 | -0.0025 |
| H-3' | 1.5794 | -0.0056 | 0.0000 | -0.0009 |
| H-2' | 1.5181 | -0.0012 | 0.0000 | -0.0024 |

^a DMSO- d_6 signal used as reference at 2.5000 ppm.

^b $\Delta\delta = \delta$ complex - δ free.

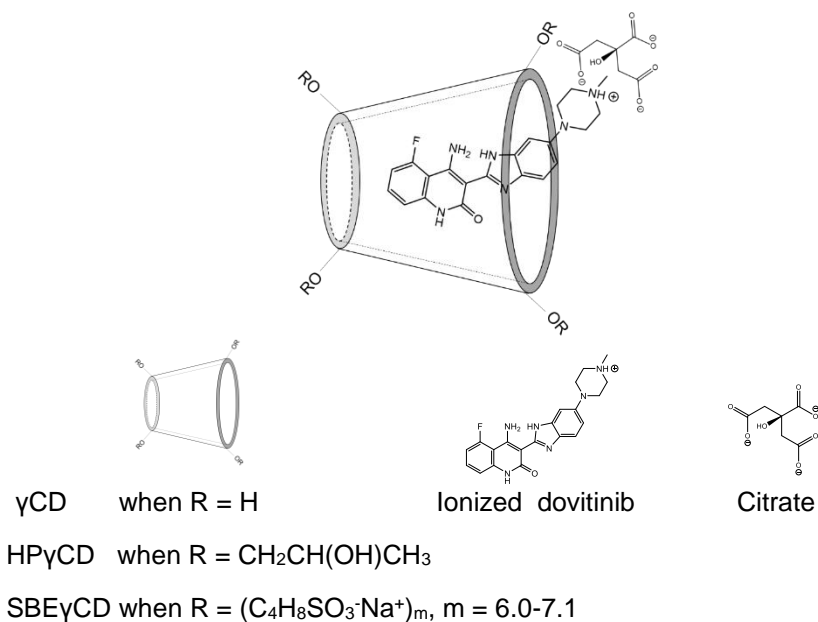


Figure 29. Proposed complex formation of dovitinib/CD/citric acid ternary system.

4.2.7 *In vitro* permeation studies (dovitinib/CD and dovitinib/CD/counter ion complex aggregates)

An increase of drug solubility (Fig. 30a) resulted in an increasing dovitinib flux at the semi-permeable MWCO 12-14k membrane, as shown in Fig. 30b. The flux became steady when CD concentration was above 5% (w/v) due to the formation of water-soluble complex aggregates that were too large to permeate the membrane. SBE γ CD ternary system containing citric acid resulted in the greatest solubility enhancement in dovitinib. In addition to the calculated parameters in Table 19, citric acid significantly enhanced the CE of drug/CD complexes, especially in the case of SBE γ CD. The elevated CE enhanced the flux of drug molecules through the MWCO 12-14k membrane. The flux pattern revealed how the permeation coefficient (Fig. 30c) is influenced by the amount of CD. When the higher CD concentration was used, a lower apparent permeability was observed due to the spontaneous self-assembly of both the CDs and the drug/CD complexes (Fig. 30d). Unexpectedly, relatively large dovitinib/citric acid aggregates were formed. It has been reported that citric acid can form complexes or aggregates with mono-, and multivalent metal ions (Zabizszak et al., 2018; Zelenina & Zelenin, 2005). Here such aggregation could be induced by an interaction between the positively ionized drug molecules and the negatively carboxyl groups of citric acid.

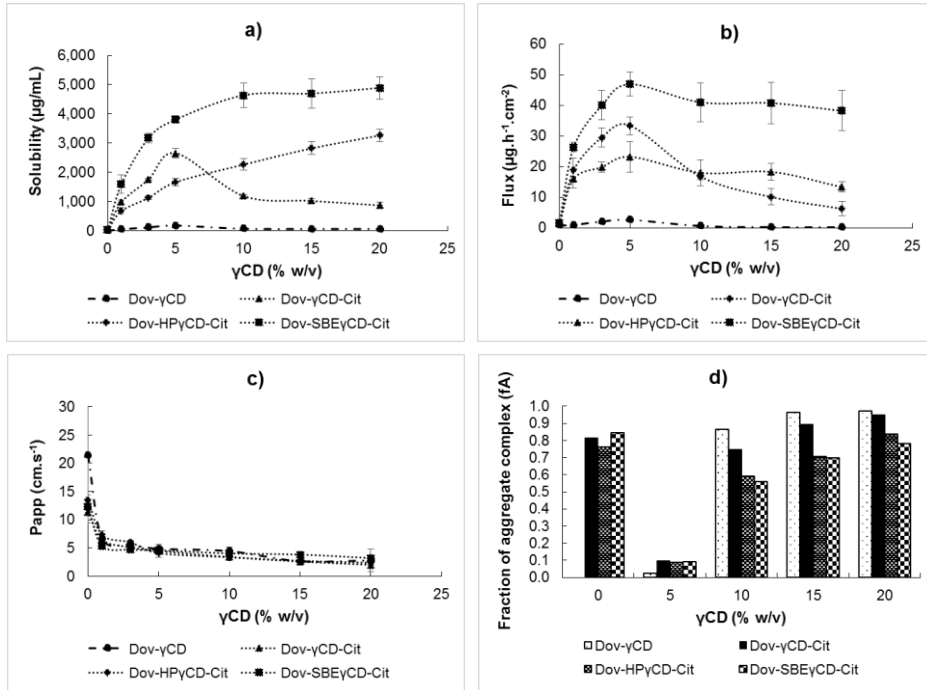


Figure 30. Permeation parameters a) solubility, b) flux through a MWCO 12-14k semi-permeable membrane, c) apparent permeation (P_{app}), and d) fraction of aggregate complex (f_A) calculated from dovitinib ternary complexes with citric acid (mean \pm standard deviation; $n=3$).

4.3 Development of thermally stable formulation of cediranib maleate based γ CD for ophthalmic drug delivery

Different attempts were made to overcome solubility problems in the poorly water-soluble KIs. The ability of γ CD as a complexing agent to solubilize the drug was limited. Thus, two additional techniques were tested, including the addition of hydrophilic polymers and salt formation. KI salt formation, or ion pairing together with solubilization through γ CD complexation, gave the best results. However, the target solubility was not attained or about 5 mg/mL (Table 2). The low aqueous solubility of the penetrating molecules seriously hampers the ocular bioavailability. Therefore, the commercial KI salt was used in further studies. However, dovitinib lactate had some technical problems during the preliminary studies. Cediranib base can be a good choice due to its higher intrinsic solubility. Thus, cediranib maleate (CM) was selected for the preparation of the ophthalmic suspensions.

Ophthalmic products are required to be sterile. An official report confirmed that CM is not sensitive to moisture and heat (EMA, 2016). Therefore, it can undergo the thermal sterilization. Here, autoclaving technique was used to prepare the complexes as well as to sterilize the aqueous formulation in a single process. The desirable CM formulation contained high amount of γ CD that enabled formulation of drug/CD aggregates, and micro- or nanoparticles for targeted drug delivery. However, the preliminary CM/ γ CD formulation resulted in drug loss of up to 23% during the sterilization process (data not shown). Although CDs are used to protect the drug against degradation, they can also induce an adversary effect in concentrated complexation media. Hence, the preparation of γ CD-based aqueous suspensions by autoclaving required the use of thermal stabilizers.

4.3.1 Effect of stabilizer on thermal stability of CM/CD complex aggregates in solution-state

Suspensions consist of one solid and one liquid phase. In general, chemical degradation of the active ingredient in the solid-state frequently follows the same degradation mechanisms as drug degradation in concentrated aqueous solutions (Loftsson, 2014a). Therefore, the improvement of drug stability during autoclaving can be initially conducted in solution-state. Furthermore, drug degradation in the solid-state is always significantly slower than in the solution-state.

The idea of this study was to find a suitable stabilizer to prevent or retard the thermal degradation of CM in concentrated aqueous complexation media.

4.3.1.1 pH-solubility studies of CM

The aqueous solubility of CM is pH-dependent. As the drug is a weak base, it was more soluble in acidic media (Fig. 31). However, the solubility tended to decrease at pH 3. A change in the color of the sample was observed changing from colorless to pink, and it became darkening further in strong acidic conditions due to degradation.

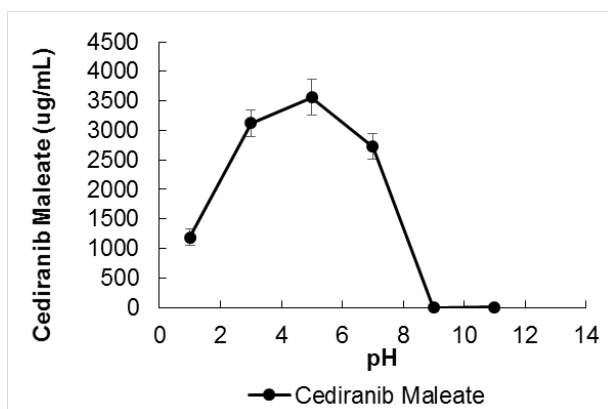


Figure 31. The pH profile of CM in pure water (mean \pm standard deviation; n=3).

4.3.1.2 Thermal stability study (CM/ γ CD and CM/ γ CD/stabilizer complex aggregates)

The thermal stability data in Fig. 32 showed that CM was slightly sensitive to heat (about 5% drug loss during autoclaving), but stable in the presence of 5% (w/v) γ CD. The remaining drug amount was significantly lower in 15% (w/v) aqueous γ CD solution. In brief, CM is unstable in aqueous solution at high γ CD concentrations.

The application of CD technology has been investigated as a nanocarrier for targeted drug delivery due to their self-assembling ability. CD drug delivery platforms can be formed in concentrated CD solutions (Loftsson et al., 2004; Messner et al., 2010). However, the results indicated that CM underwent thermal degradation in the presence of higher γ CD concentration. The underlying mechanism remains unknown. The destabilization of drug may involve catalysis due to metal impurities in γ CD (Jansook, Praphanwittaya, Sripecth, & Loftsson, 2020). Other possible hypotheses are oxidation, excessive aggregation, and unsuitable conformation change. Thus, the stabilizer, which can affect those factors, was added to prevent drug degradation in concentrated complexation media.

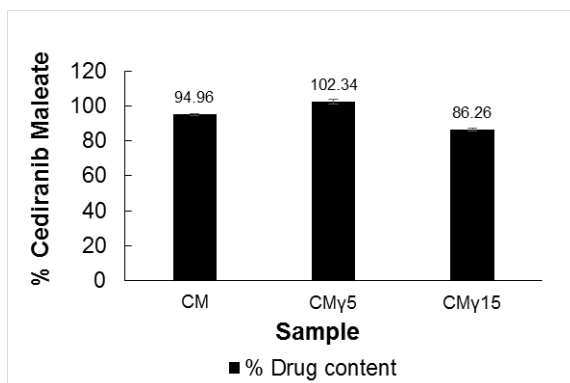


Figure 32. Thermal stability of CM in aqueous γ CD solutions at concentration of 0%, 5%, and 15% (w/v) under autoclaving (mean \pm standard deviation; n=3).

The addition of stabilizer to systems containing the binary complex increased the amount of remaining drug (Fig. 33). According to European Pharmacopeia general text (Ph. Eur. 2.9.40), the drug concentration should be within 95 to 105% of the declared content in units of mass/volume (e.g. mg/ml). This official criterion was applied in this study. The stabilizer has a good potency against thermal degradation of CM when less than 5% is degraded during autoclaving. In other words, at least 95% of the drug should be present in the formulation after autoclaving (i.e. heating to 121°C for 20 min). Riboflavin was the most effective stabilizer preventing drug loss (100.50%) during autoclaving, followed by EDTA (96.26%), and L-arginine (95.55%). Urea had the lowest ability (87.27%) to protect the drug during heating and this was associated to the ability of urea to disrupt CD aggregates (Sá Couto, Ryzhakov, & Loftsson, 2018). Enhanced aggregation was excluded as the main cause of thermal degradation. Thus, two possible roles of effective stabilizers are inhibiting oxidative stress probably caused by metal ions, and changes in the conformation of drug/CD complexes.

Trace metal ions may remain from CD synthesis. The amount of these impurities can increase with increasing γ CD concentration. EDTA is a very powerful chelating agent for divalent metals and, thus, can literally reduce radical reactions and slow the oxidation process (Flora & Pachauri, 2010). In pharmaceutical formulations, EDTA is applied to prevent oxidative degradation of drug by chelating metal ion impurities (E Mohr, 2006). Jansook and colleagues reported that EDTA might protect dovitinib from thermal degradation via metal chelation (Jansook et al., 2020). In the present study, the inhibition of reactions (usually oxidations) by EDTA is presumed to

be the mechanism that improves the thermal stability of CM. Furthermore, L-arginine and riboflavin can also act as chelating agents. For example, L-arginine inhibited the oxidation of lipids and proteins in emulsion sausage by chelating ferrous ions, and scavenging free radicals (Xu, Zheng, Zhu, Li, & Zhou, 2018). Riboflavin has the ability to chelate or complex various metal ions such as Fe(II), Mn(II), Co(II), Ni(II), Cu(II) and Zn(II) (Harkins & Freiser, 1959; Khan & Mohan, 1973).

The change in complex conformation may also affect the thermal behavior of the drug. The driving forces for formation of the drug/CD complex include expulsion of enthalpy-rich water molecules from the cavity, hydrogen bonding, van der Waals interaction, electrostatic interactions, and charge-transfer interactions (Liu & Guo, 2002; Loftsson, Jarho, et al., 2005). L-arginine has been found to improve drug stability when drug/CD inclusion complexes are formed. For example, the direct interaction between L-arginine and omeprazole attributes to hydrogen bonds in the drug molecule, and a significant desolvation of the omeprazole molecule. This amino acid plays an active role in the multicomponent complex formation by having a tendency to be located near the inner surface of the host cavity (Figueiras, Sarraguca, Pais, Carvalho, & Veiga, 2010). A simulation study showed that one feature of aqueous arginine solutions is the self-association of arginine molecules. Stronger arginine-arginine hydrogen bonds replace the weak hydrogen bonds between arginine and water. The carboxylate group of such arginine clusters is found to interact with the aromatic and charged sides of protein via cation- π interactions and hydrogen bonding, respectively (Shukla & Trout, 2010). For the present study, it might be anticipated that L-arginine thermally stabilized the drug/CD complex by intermolecular interactions between single L-arginine molecule as well as L-arginine clusters.

In an aqueous environment, riboflavin can interact with small molecules. For example, several indoles form a weak complex with riboflavin in acidic solution due to charge transfer forces (Mitsuda, Tsuge, Kawai, & Tanaka, 1970). Hydrogen bonds and van der Waals interactions played major roles in stabilizing the complex between quinine sulfate and riboflavin (Patil, Bhattar, Kolekar, & Patil, 2011). The case of acidic drugs like salicylic acid, charge transfer or stacking interactions may take place during complex formation (Bhattar, Kolekar, & Patil, 2010). Riboflavin mainly forms partial inclusion complexes with β CD, γ CD and their hydroxypropyl derivatives (Loukas, Jayasekera, & Gregoriadis, 1995; Terekhova, Koźbiał, Kumeev, & Alper, 2011). The aromatic ring is suitably accommodated within the CD cavity while the other part, such as ribityl chain, is located in the bulk solvent (Terekhova

et al., 2011). However, ternary drug/CD/riboflavin complexes have not been previously described. CM is an indole ether quinazoline derivative and, thus, its structure has some similarities to those drug molecules with which riboflavin can potentially form a complex. Consequently, riboflavin may somehow interrupt the formation of CM/ γ CD complex. In these screening data, riboflavin was the best candidate, thus the investigation of its binary and ternary complexes was further studied.

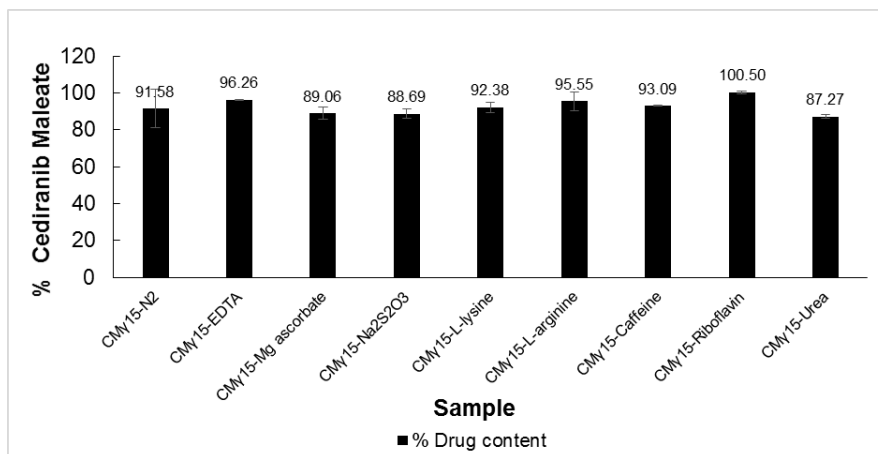


Figure 33. Thermal stabilizer of CM in 15% (w/v) γ CD aqueous solution in presence of 0.1% (w/v) stabilizer (mean \pm standard deviation; n=3).

The amount of drug remaining after 1-3 cycles of the autoclaving process are presented in Fig. 34. In plain CM solution, the drug degraded slightly. The presence of γ CD affected the drug amount in different way. In the aqueous 5% (w/v) γ CD medium, CM was stable during the first cycle, then tended to degrade in next cycles. In the aqueous 15% (w/v) γ CD medium, the drug loss was about 10-12% during each cycle. All systems became more stable for at least during the first cycle when riboflavin was present. In brief, it was shown that riboflavin had the potential to thermally stabilize CM in aqueous γ CD solution.

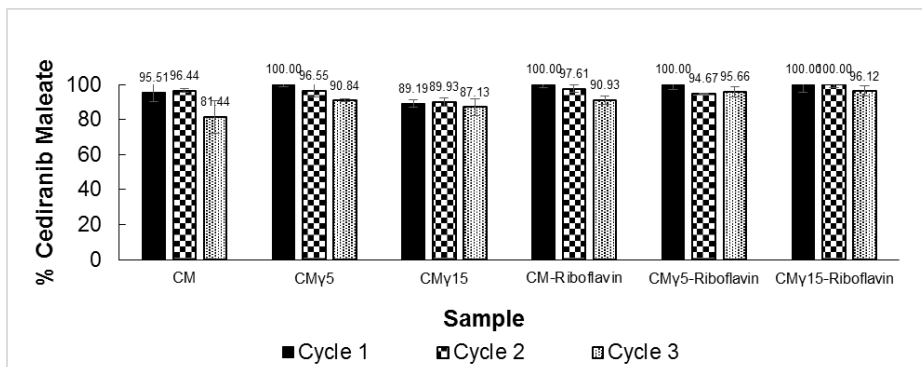


Figure 34. Thermal stability of CM after 3 cycles of autoclaving in aqueous γ CD solutions and 0.1 % (w/v) stabilizer (mean \pm standard deviation; n=3).

4.3.1.3 Degradation products of CM

Previously, drug degradation was observed in CM solutions that underwent strong acidic conditions (pH 1) or were exposed to autoclaving process for 3 cycles. Their appearance changed from colorless to purple in color. Thus, the degradation products were investigated in this study.

HPLC chromatogram of those samples showed an identical degradation peak with the same λ_{\max} and R_t (data not shown). The strong acid and heating in autoclave can induce drug degradation in a similar manner. However, faster degradation was observed under acidic conditions as observed by the larger degradation peak (Fig. 35) and the darker color of the solution.

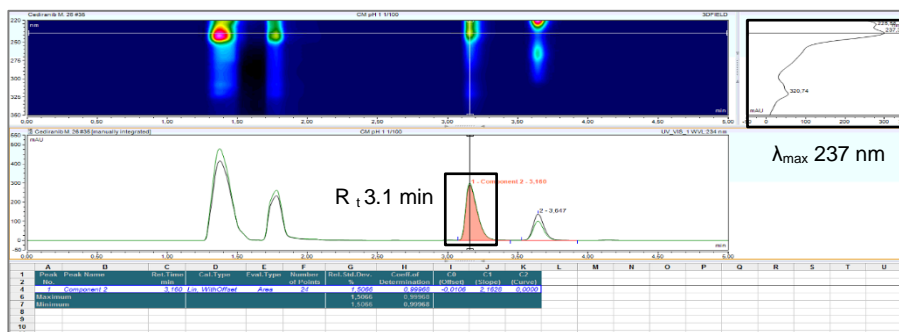
LC/PDA/MS showed a similar UV spectrum pattern of CM and its degradation products as the one revealed by LC-UV (Fig. 36). Both instruments indicated that the drug degradation pathway is similar during autoclaving and storage under strong acidic condition. The m/z of the drug peak included 451 and its one half that was 226 - the other half is the electron which was removed in the ionization process. The m/z of the degradation peak could be 166, 214.04 and 304.08 or 309 (Fig. 35 and Table 24). The possible degradation products under strong acid or autoclaving process are proposed in Fig. 37.

The rate and extent of drug degradation depends invariably on the acidic medium and the temperature of exposure. The breakdown of ether linkage (solid line) under vigorous condition points towards hydrolysis (Fig. 37). However, CM is also observed to degrade into products (dashed line), which route cannot be justified. Although their bond cleavage looks like N-

dealkylation, this reaction frequently occurs in living organisms, usually through specialized enzymatic systems (Markey, 2007).

Due to degradation products, the previous hypothesis that oxidation causes drug degradation turns out to be inaccurate. Hydrolysis is the main reaction in this scenario. Thus, EDTA and riboflavin were applied to inhibit hydrolysis by chelating metal ions.

A) Drug peak



B) Degradation peak

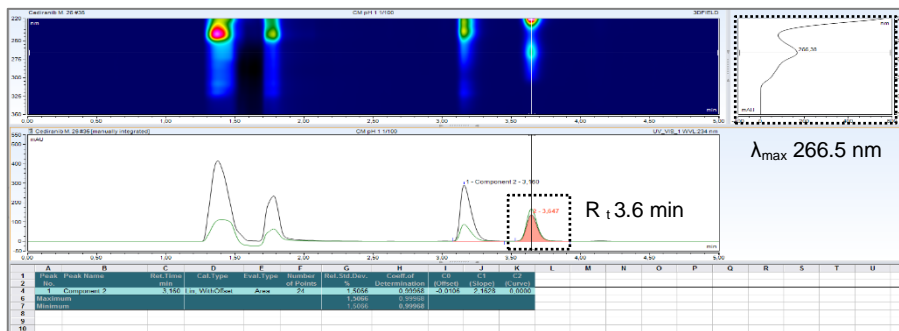


Figure 35. LC/UV chromatogram of CM in pure water at pH 1; A) Drug peak, B) Degradation peak.

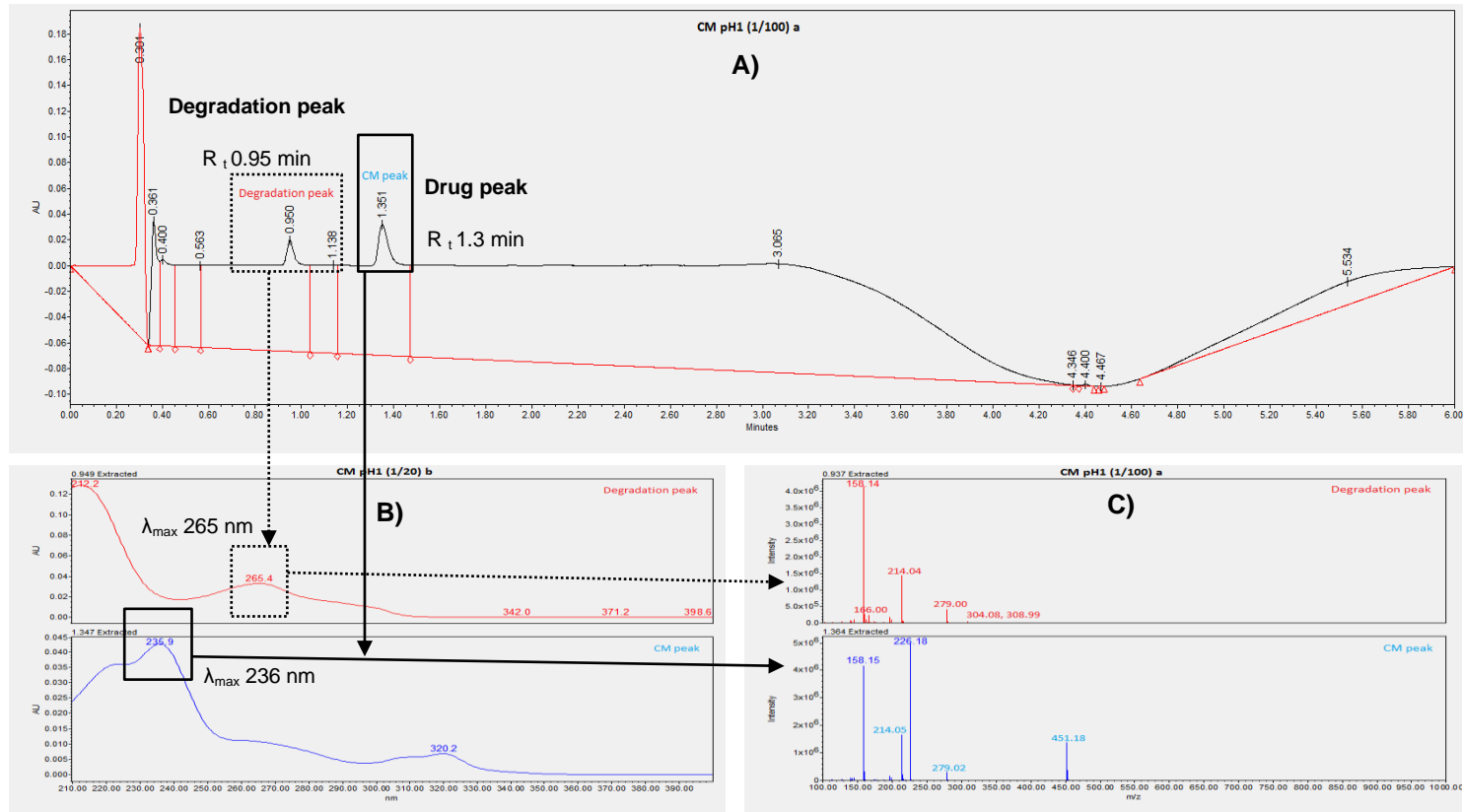


Figure 36. LC/PDA/MS spectra of CM in pure water at pH 1; A) UV chromatogram, B) UV absorbance, C) mass spectra.

Table 24. Peak characteristics of CM determined by LC/PDA/MS.

| Sample | Drug peak | | | Degradation peak | | |
|-------------|-----------------------------|----------------------|----------|-----------------------------|----------------------|----------------------------|
| | λ_{max} (nm) | R _t (min) | m/z | λ_{max} (nm) | R _t (min) | m/z |
| CM | 236 | 1.3 | 226, 451 | - | - | - |
| CM 3 cycles | 236 | 1.3 | N/A | 265 | 0.95 | N/A |
| CM pH1 | 236 | 1.3 | 226, 451 | 265 | 0.95 | 166, 214.04, 304.08 or 309 |

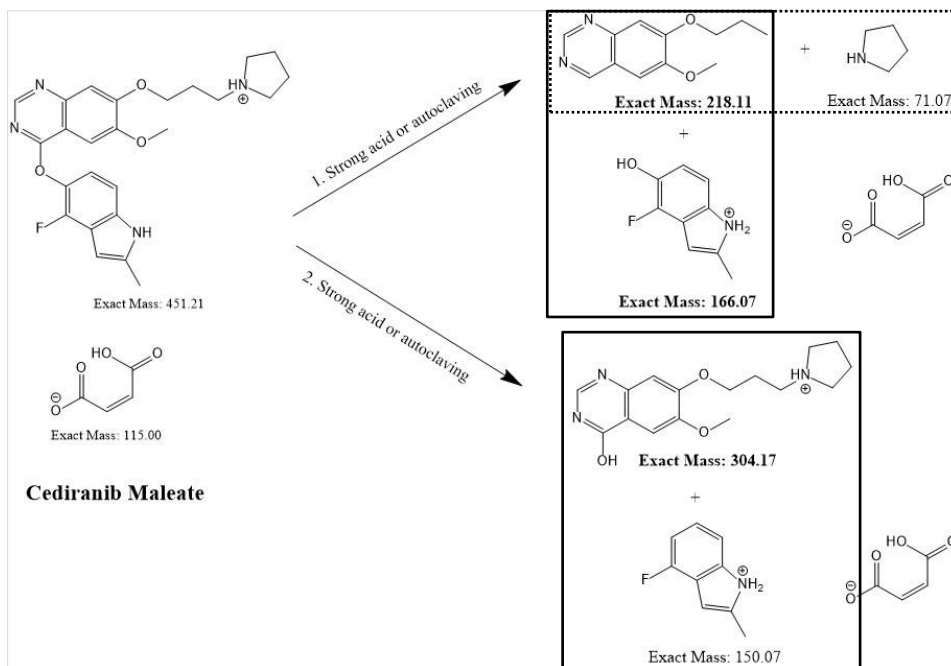


Figure 37. Possible degradation products of CM after storage in strong acid or exposure to autoclaving.

4.3.1.4 Phase-solubility studies (CM/ γ CD and CM/ γ CD/riboflavin complexes)

The phase-solubility profiles (Fig. 38) showed that the formation of binary CM/ γ CD complex and ternary CM/ γ CD/riboflavin complexes of B_s type. The solubility tended to be limited when increasing γ CD concentration above 10% (w/v). Riboflavin slightly decreased the amount of dissolved CM. However, the concentration of dissolved drug was greater in the presence of riboflavin in aqueous 15% (w/v) γ CD solution, and it might relate to thermal stabilization. The calculated phase solubility (PS) parameters in Table 25 indicated that riboflavin did not affect the interaction between CM and γ CD, and complex stability significantly.

The γ CD started precipitating at concentrations $\geq 10\%$ (w/v) due to the formation of larger aggregates and nanoparticles (Fig.39). The optimal γ CD concentration was determined to be 15% (w/v) γ CD. The pattern of dissolved γ CD in aqueous solution did not change upon the addition of riboflavin (Fig. 39).

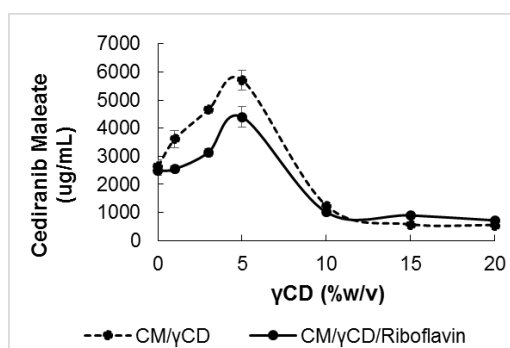


Figure 38. Phase solubility profile of CM containing 0.1% (w/v) riboflavin in aqueous γ CD solution (mean \pm standard deviation; n=3).

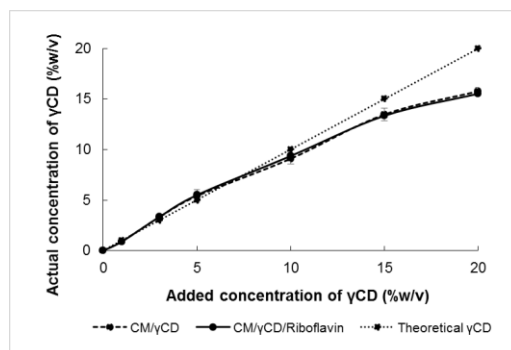


Figure 39. Amount of dissolved γ CD from CM/ γ CD/Riboflavin complexes in pure water (mean \pm standard deviation; $n=3$).

Table 25. Estimated phase-solubility parameters of CM/ γ CD complex and CM/ γ CD/riboflavin complex in pure water.

| System | pH | S_0 ($\mu\text{g/mL}$) | Phase-solubility parameters | | |
|----------------------------|---------------|-------------------------------|-----------------------------|-------------------------------|------|
| | | | PS-type | $K_{1:1}$ (M^{-1}) | CE |
| CM/ γ CD | 4.9 ± 0.5 | 2,639 | B_s | 33.70 | 0.16 |
| CM/ γ CD/riboflavin | 4.8 ± 0.4 | 2,486 | B_s | 22.03 | 0.10 |

4.3.1.5 NMR studies (CM/ γ CD and CM/ γ CD/riboflavin complexes)

This study aimed to investigate how heat affects the behavior of complexes, and how stabilizer can protect the drug in complexation media from thermal degradation. The NMR samples were divided into two groups following preparation conditions at room temperature and autoclaving.

The $^1\text{H-NMR}$ spectra of pure substances including γ CD, CM, and riboflavin prepared in room temperature along with their labelled chemical structure are presented in Fig. 40. Only the CM spectrum was slightly changed due to the autoclaving treatment; its proton signals (i.e. H-1', H-9', and H-11') disappeared (Fig. 41).

Table 26a shows the $\Delta\delta$ shifts of γ CD for the binary and ternary complexes prepared under different conditions. Complexes prepared at room temperature, the proton resonances are at the γ CD cavity (H-3 and H-5) and the external rim (H-1, H-2, H-4, and H-6) (Schneider, Hacket, Rudiger, & Ikeda, 1998). Those signals displaces downfield shift ($\Delta\delta > 0$) due to the deshielding effect caused by changes in local polarity, or the van der Waals interaction between host and guest molecules (Djedaini et al., 1990). In

ambient condition, the partial inclusion complex was formed between γ CD and guest molecules i.e. CM and riboflavin.

For complexes prepared by autoclaving (Table 26b), the assigned protons located in both within the γ CD cavity and externally, as was observed for complexes prepared in room temperature. However, the chemical shifts behave differently in the case of binary complexes. In the case of riboflavin/ γ CD complexes, the majority of proton signals shifts to upfield ($\Delta\delta < 0$) due to shielding effect of the guest molecule (i.e. flavin moiety of riboflavin) (L. Ribeiro et al., 2005). For CM/ γ CD complex, the upfield ($\Delta\delta < 0$) presents at H-1 only, and H-6 has no proton replacement. In other words, a conformation of γ CD was changed when autoclaving was applied to such systems containing riboflavin or CM. The introduction of riboflavin in that binary complex returns those proton signals to downfield shift ($\Delta\delta > 0$), or it allows γ CD behaved as it did in the ambient condition and formed a partial inclusion complex. Therefore, it is highly possible that there may be some molecular interactions among CM, riboflavin and γ CD which can protect the drug from thermal degradation.

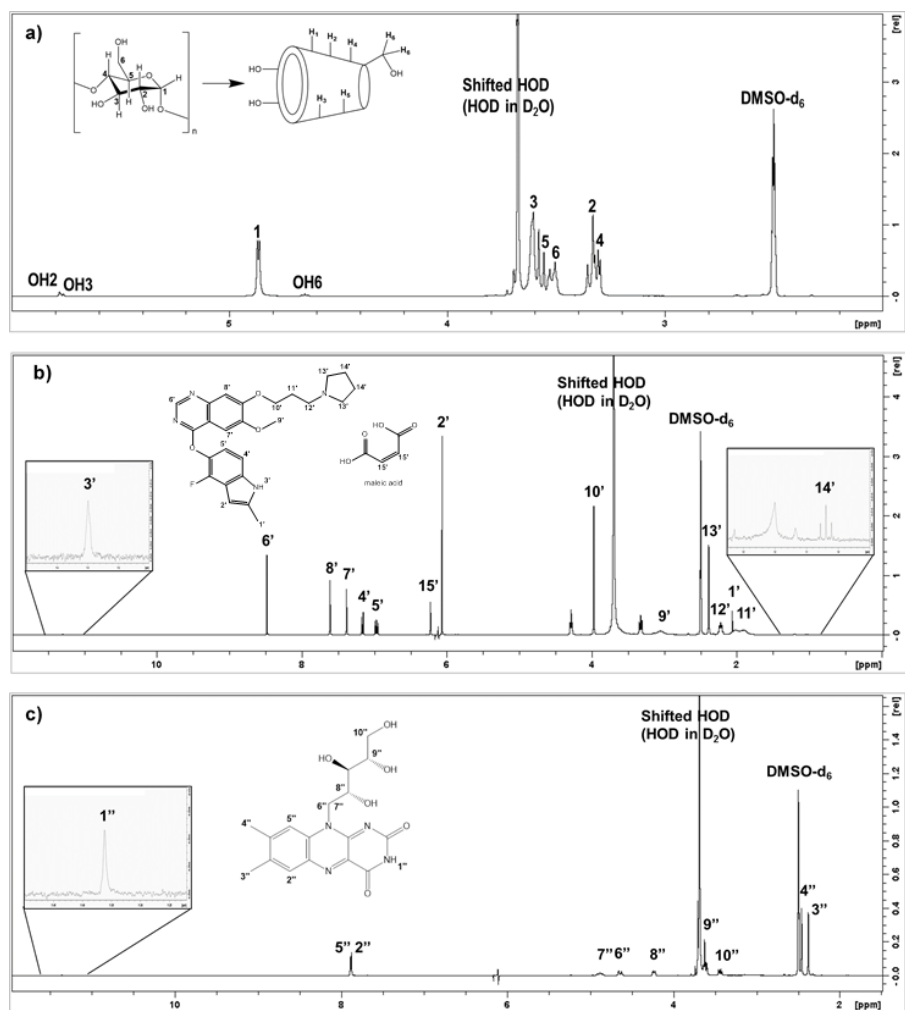


Figure 40. $^1\text{H-NMR}$ spectra and proton assignments of a) γCD , b) CM, and c) riboflavin prepared under room temperature.

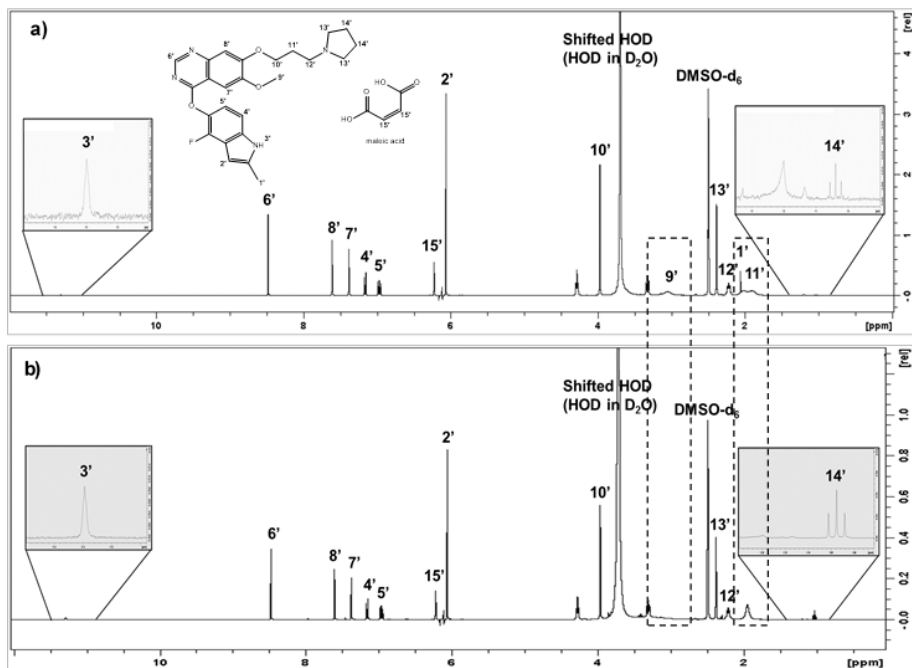


Figure 41. ¹H-NMR spectra and proton assignments of CM prepared under a) room temperature, and b) autoclaving.

Table 26. ^1H NMR chemical shift of γCD containing riboflavin in free-state and in complex by preparing under a) room temperature, and b) autoclave.

| ^1H assignment ^a | δ free | | a) $\Delta\delta$ ^b | |
|--------------------------------------|-------------------|-------------------------------|--------------------------------|----------------------------------|
| | γCD | Riboflavin/ γCD | CM/ γCD | CM/Riboflavin/ γCD |
| H1 | 4.8686 | 0.0007 | 0.0010 | 0.0013 |
| H3 | 3.6003 | 0.0007 | 0.0009 | 0.0011 |
| H5 | 3.5528 | 0.0006 | 0.0009 | 0.0010 |
| H6 | 3.5011 | 0.0005 | 0.0009 | 0.0010 |
| H2 | 3.3288 | 0.0004 | 0.0006 | 0.0006 |
| H4 | 3.3048 | 0.0004 | 0.0008 | 0.0006 |

| H assignment ^a | δ free | | b) $\Delta\delta$ ^b | |
|---------------------------|-------------------|-------------------------------|--------------------------------|----------------------------------|
| | γCD | Riboflavin/ γCD | CM/ γCD | CM/Riboflavin/ γCD |
| H1 | 4.8689 | <u>-0.0011</u> | <u>-0.0004</u> | 0.0006 |
| H3 | 3.6005 | 0.0005 | 0.0003 | 0.0006 |
| H5 | 3.5529 | <u>-0.0005</u> | 0.0003 | 0.0007 |
| H6 | 3.5012 | <u>-0.0005</u> | <u>0.0000</u> | 0.0006 |
| H2 | 3.3288 | <u>-0.0007</u> | 0.0008 | 0.0008 |
| H4 | 3.3047 | <u>-0.0006</u> | 0.0009 | 0.0009 |

^a DMSO- d_6 signal used as reference at 2.5000 ppm.

^b $\Delta\delta = \delta$ complex - δ free.

The expansion of the NOESY spectra of the ternary system exposed to heat is presented in Fig. 42, and the observed molecular NOE cross-peaks were marked by the dotted line. Firstly, the riboflavin- γCD interactions were observed between H-6'', H-7'', H-10'' of riboflavin (RF) and the H-1, H-2 protons located on surface of γCD . Secondly, some cross-peaks occurred where the H-12' and H-14' protons of CM interacted with the external rim H-1, H-2, H-4, H-6 protons of γCD . Lastly, interactions between the guest molecules appeared at the H-1' and H-14' protons of CM and the H-4'', H-7'' and H-10'' protons of riboflavin (RF). These results indicated that the pyrrolidinyl-propoxy group of CM and the ribityl chain of riboflavin were both located near the outer cavity of γCD . These functional groups shared some intermolecular interactions. However, the partial inclusion into the CD cavity could be assumed according to $^1\text{H-NMR}$, since the expansion of the NOESY spectra was limited and did not present the protons of phenyl moieties which were located in the range of 6.0-12.0 ppm.

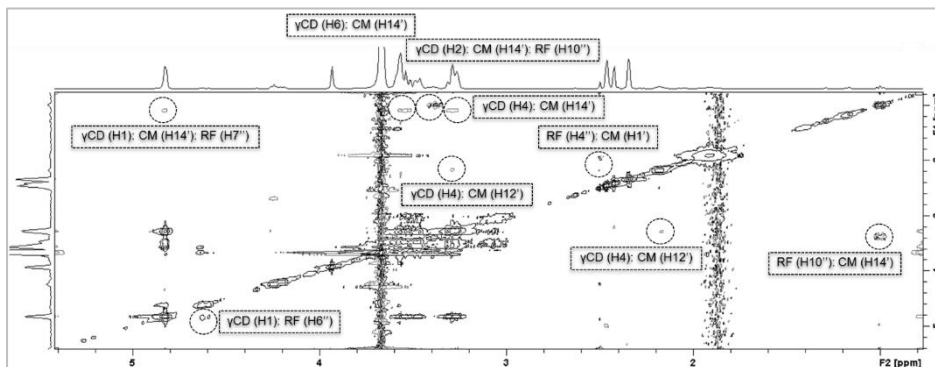


Figure 42. NOESY spectra of ternary CM/ γ CD/riboflavin (RF) complex prepared under autoclaving.

In summary, NMR studies confirmed the formation of partial inclusion complexes in aqueous solutions. The phenyl moieties are inserted to its host cavity whereas the alkyl side groups stand outside. The pyrrolidinyl-propoxy group of CM can undergo thermal destruction due to by the location on the outer γ CD ring. This group may be shielded by ribityl side chain of riboflavin and, thus, the thermal degradation is prevented or retarded.

4.3.1.6 *In vitro* permeation (CM/ γ CD and CM/ γ CD/riboflavin nanoparticles)

The flux profiles of CM with and without 0.1% (w/v) riboflavin, are shown in Fig. 43a. Increased CM flux is a result of increased CM solubility as observed from the phase solubility profile. However, the patterns level off CD concentration above 10% (w/v) due to the formation of water-soluble complex aggregates and nanoparticles. Riboflavin slightly decreased that the flux of CM at lower concentrations. The permeability coefficient (P_{app}) is affected by the CD concentration and riboflavin (Fig. 43b). Increased γ CD concentration reduced the apparent permeability due to the self-assembly of CM/ γ CD or CM/riboflavin/ γ CD complexes (Fig. 43c). The presence of riboflavin resulted in decreased aggregation as well as aggregates size, especially at 5-15% (w/v) of CD, resulting in their increased permeation coefficient (P_{app}). However, the formation of small CM and CM/riboflavin aggregates was unexpected. Maleic acid, a commercial salt of CM, has been reported to form complex with mono-, di-, and trivalent metal ions (Bychkova, Katrovitseva, & Kozlovskii, 2008) as well as riboflavin (Foye & Lange, 1954). Here, the aggregation could be due to an interaction of carboxyl groups of maleic acid and positively ionized cediranib molecules, or flavin moiety of riboflavin and the drug in ionized form. In brief, riboflavin did not alter the pattern of permeation.

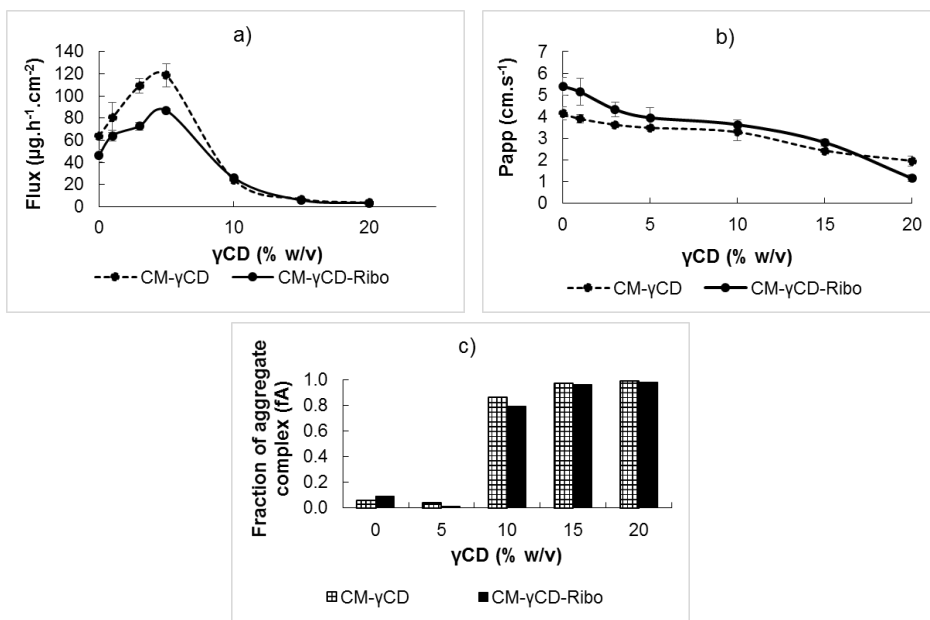


Figure 43. Permeation parameters of CM/ γCD and CM/ γCD /Riboflavin complexes a) flux, b) apparent permeation coefficient, and c) fraction of aggregate complex (mean \pm standard deviation; $n=3$).

4.3.1.7 TEM analysis of CM/ γCD and CM/ γCD /riboflavin nanoparticles

Direct morphological information about the pure substances (i.e. 15% (w/v) γCD , 0.1% (w/v) riboflavin, saturated CM solution), and their binary or ternary systems is provided by TEM images in Fig. 44. For pure substances, 15% (w/v) γCD aqueous solution presents with large nanocrystal characteristics with a diameter of 500 nm to 1,000 nm, while sphere-like particles are found in both the CM solution (300-500 nm) and the riboflavin solution (200-300 nm). The binary and ternary samples display both nanocrystals and nanoparticles between 200-500 nm and 500-1,000 nm in diameter due to the formation of complex aggregates and the precipitation of particles. The presence of riboflavin did not change the morphology of the drug/ γCD nanoparticles.

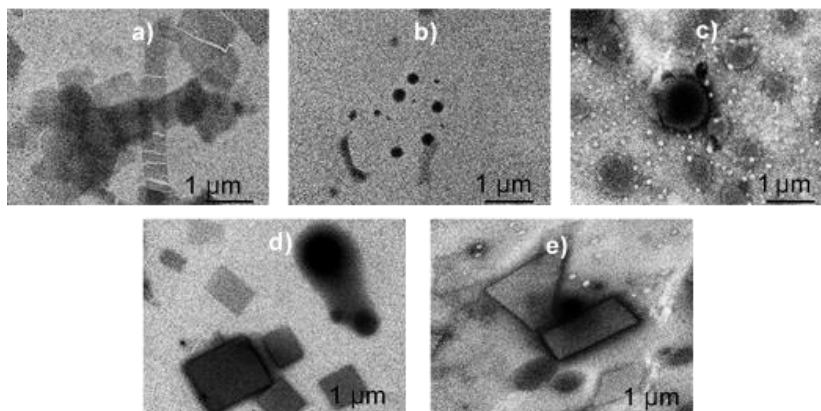


Figure 44. TEM images at magnitude of 10,000 a) 15% (w/v) γ CD, b) 0.1% (w/v) riboflavin, c) CM, d) CM/ γ CD15, e) CM/ γ CD15/riboflavin.

4.3.2 Development and characterization of ophthalmic formulation

Solutions, suspensions, and ointments are three types of topical ophthalmic dosage forms which are mainly applied in clinical usage. Many studies have shown that low viscosity aqueous eye drops containing drug/ γ CD nano- and micro- suspensions enhance drug delivery to the back of the eye (Johannsdottir et al., 2018; Loftsson, Hreinsdóttir, & Stefánsson, 2007; Loftsson et al., 2008).

In general, an aqueous eye drop solution provides a pulse drug permeation, and its concentration rapidly declines after administration (Patel, Cholkar, Agrahari, & Mitra, 2013). Although various additives have been used to improve drug contact time, permeation and ocular bioavailability, this dosage form cannot, in general, deliver therapeutic drug concentrations to the retina (Soubrane, Coscas, & Voigt, 2010). In addition, insufficient chemical drug stability (e.g., CM) in aqueous solutions can limit eye drop efficacy in ophthalmology.

Formulating the drug as a suspension containing both solid drug/CD complex particles and dissolved drug/CD complexes will increase the concentration gradient of lipophilic drugs like CM over an extended time. This gradient is the driving force of passive diffusion of drug molecules through the water layer to the epithelial surface of the eye without decreasing the ability of the drug to partition into and penetrate through the lipophilic member barriers such as the cornea and the conjunctiva (Loftsson et al., 2008). The aqueous drug/CD suspension keeps the aqueous tear fluid saturated with the

drug, and thus, the maximum drug permeation is obtained (Saokham, Muankaew, Jansook, & Loftsson, 2018).

Here, the thermally stable CM/ γ CD eye drop will be formulated as a suspension. This formulation will result in sustain high concentrations of dissolved drug in the tear fluid and, consequently, increase the ocular drug bioavailability. In some ways these systems behave more like dispersed systems such as nano-suspension, liposome, rather than a true solution due to aggregate formation (Loftsson, 2014b). To be precise, this ophthalmic product is classified as a micro- or nano-suspension.

Furthermore, the charge of the drug is another concern for ocular penetration. CM is a drug salt in which the drug molecule carries a positive charge. Corneal epithelial bears an overall negative charge at physiological pH, thus positively charged molecules such as CM tend to penetrate at a faster rate compared to negatively charged molecules (Rabinovich-Guilatt, Couvreur, Lambert, & Dubernet, 2004).

4.3.2.1 Selection of supportive thermal stabilizers

The thermal stability data in Fig. 45 showed that the presence of stabilizers such as co-solubilizers (e.g. PG, PEG400, and glycerin), and polymers (e.g. PVA, HPMC, tyloxapol, and poloxamer 407) in the CM/ γ CD complex media could protect the drug from thermal degradation.

The co-solubilizers can change the polarity of the complexation media (Loftsson, Jarho, et al., 2005). Here, drug stability up on heating is dependent on the polarity of the solubilizer. The dielectric constant (ϵ) of a compound is an index of its polarity. For example, glycerin (46 ϵ), PG (32.1 ϵ), and PEG400 (12.4 ϵ) at 20°C. Increasing polarity showed a serial decrease in drug loss. Glycerin and PG are more polar than PEG400. The drug was thermally stabilized in the presence of glycerin followed by PG, and PEG400 due to solvent effect. The effect of dielectric constant (ϵ) on drug degradation rate can be explained by the Bronsted-Christiansen-Scatchard equation (Eq. 12) (Loftsson, 2014a).

$$\log k = \log k_{\epsilon=\infty} = -\frac{KZ_A Z_B}{\epsilon} \quad (12)$$

Where k is rate constant, $k_{\epsilon=\infty}$ is the rate constant in a theoretical solvent of infinite dielectric constant, K is a constant for a particular reaction at a given temperature, and Z_A and Z_B are the charge numbers of the two interacting ions.

A relationship of $\log k$ against the reciprocal of the ϵ of the solvent should be linear with a gradient $-KZ_AZ_B$. Based on Eq. 12, the interacting ions in complexation media are protonated cediranib (positively charged) and maleate (negatively charged). Since the two ions have different charges, the gradient of the line will be positive. Thus, the rate constant of reaction (e.g., drug degradation) will decrease with increasing ϵ (Attwood & Florence, 2008; Loftsson, 2014a). In summary, when CM is in the ionized form, the presence of higher polar co-solvent could prevent or retard the drug degradation during autoclaving.

In case of the polymers, the drug was stabilized by two different mechanisms. Hydrophilic polymers are known to stabilize various types of aqueous particulated or dispersed systems (Fendler, 1996; Malmsten, 2002). Cellulose derivatives and other polymers may act as a steric stabilizer (Parfitt & Barnes, 1992). They have also been shown to have a stabilizing effect on CD aggregates (Loftsson, Frikdriksdóttir, Sigurkdardóttir, & Ueda, 1994; Ryzhakov et al., 2016). The interaction between polymers and CDs and drug/CD complexes occurs on the external surface of the CD molecule via van der Waal and hydrogen bonding (Loftsson & Duchêne, 2007). In aqueous solutions, it is believed that polymers reduce CD mobility by changing the hydration properties of CD molecules (Loftsson, Jarho, et al., 2005; F. Veiga et al., 2006). The steric inclusion-dissociation behaviors between host and guest molecules responds to temperature change (Amiri & Amiri, 2017). Thus, the elevated temperature from the autoclaving process may change the rotation of the polymer i.e. PVA, HPMC, tyloxapol, or poloxamer 407 to γ CD and CM/ γ CD complexes, causing a steric barrier against the thermal degradation of CM.

The stabilizers that prevented at least 5% drug degradation, such as PG, glycerol, PVA, HPMC, and poloxamer 407, were selected for further formulation studies. Although tyloxapol was a good choice, CM itself can form air bubbles in pure water as well as this polymer. For this reason, tyloxapol was excluded from the study.

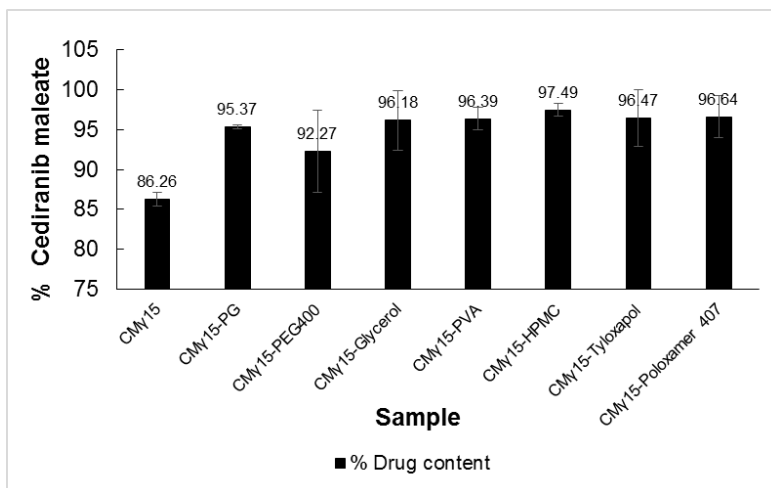


Figure 45. Thermal stability of CM/ γ CD complex in presence of 0.1% (w/v) stabilizer after 1-cycle autoclaving (mean \pm standard deviation; n=3).

The pH of the binary complex apparently affected the thermal stability of CM (Fig. 46). In general, the pH of unbuffered CM solution containing 15% (w/v) γ CD was about 5.5. The desired pH was adjusted by dropwise titration of 0.1 N HCl to pH 5, and that of 0.1 N NaOH to pH 6, and 7. Cediranib (free base) has pKa 10.1 (most basic) (ACS, 2019). The drug was in ionized form at those pH values. Upon autoclaving, drug degradation was increased with increasing of pH and NaOH. This is worth noting that the degradation rate is influenced by the ionic strength effect (or also called the salt effect) which is the electrostatic interaction between the drug and other reacting ions (i.e. maleate, Na^+ , OH^-). Ionic strength (I) of an aqueous solution is a measure of the concentration of charges (Loftsson, 2014a). Here, CM had lower thermal degradation in an acidic environment due to less ionic strength. Thus, pH 5 was the optimal and selected for further formulation studies.

Besides that, the adjustment from hypotonic to isotonic solutions for ocular preparations may affect the ionic strength, and then drug stability during autoclaving. Common tonicity agents for pharmaceutical formulation are dextrose, glycerin, mannitol, potassium chloride, and sodium chloride (E Mohr, 2006). In order to prevent too high ionic strength, non-ionic types can be a good choice.

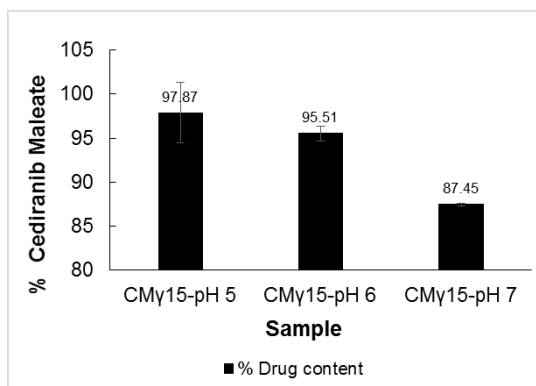


Figure 46. Thermal stability of CM/γCD complex in different pH after 1-cycle autoclaving (mean ± standard deviation; n=3).

4.3.2.2 Preparation of CM eye drop formulations

All CM suspensions were formulated at pH 5 where CM displays the highest stability. The total drug concentration in the formulation was set at 3% (w/v). This composition was based on values shown in Table 3. In two patents (Table 3), cediranib (free base) eye drops were prepared in non-aqueous suspension at concentration of 2% (w/v) (Böttger M., 2013, 2015). In addition to other researches in our group, prepared and tested CD-based formulations containing 1.5-3.0% (w/v) of various drugs such as dexamethasone and dorzolamide, shown that the formulation successfully delivered the drugs to the back of eye (Loftsson & Stefansson, 2017). These drugs have an MW between 320 and 390 while MW of cediranib and CM is 450.5 and 566.6, respectively. Thus, 3% (w/v) CM was used in the present project to assure the success rate. Previous study revealed that riboflavin could lower the thermal degradation of the drug in concentrated γCD solutions. Riboflavin and supportive stabilizers such as L-arginine, polymers at a concentration of 0.1% (w/v) were introduced step by step to protect the drug from thermal degradation. After mixing those substances, nitrogen (N₂) was used for removal of oxygen from the finished products. Although N₂ provided slightly less thermal protection to CM, it was still selected to protect the products from oxidation during storage. The selection of polymers was based on the thermal stability study. Three polymers (i.e. PVA, HPMC, and poloxamer 407) were shown to enhance the thermally stability of CM during autoclaving. However, the addition of hydrophilic polymers can either increase or decrease the drug solubility (Loftsson & Masson, 2004; Praphanwittaya, Saokham, Jansook, & Loftsson, 2020a). Previously, a study on stability

enhancement revealed that cediranib (free base) was solubilized by PVA, whereas HPMC and poloxamer 407 tended to decrease the drug solubility (Praphanwittaya et al., 2020a). Thus, the concentration of PVA was elevated to 0.2% (w/v) in such formulations to maintain the drug amount in solid and solution phases according to the criteria in Table 27. Drug content was improved by up to 90-100% when those different thermal stabilizers were added to the media (Table 27). The combination of stabilizers, especially polymers might enhance the steric network which hindered the thermal degradation of the drug in the complexation media. Overall, the solid fraction meets the criteria for about 70-75% or two-third of the total drug in the solid-state as drug/ γ CD complex. Studies have shown that the eye drops containing about one-third of the drug in solution as free drug molecule, solubilized drug/ γ CD complexes, and solubilized drug/ γ CD nanoparticles, and about two-third of drug (i.e. dorzolamide, dexamethasone) as solid drug/ γ CD complexes, can deliver the drug to the back of eye (Jansook et al., 2010; Jóhannesson et al., 2014; Johannsdottir et al., 2018). The high ratio of drug in solid part provided high sustained concentrations of dissolved drug over time. This enhanced the drug absorption from the aqueous tear fluid through the lipophilic membranes barriers that is cornea and conjunctiva cornea (Loftsson & Stefansson, 2017). Thus, the criteria in present study were set up according to those successful formulations. CM-F6 is the optimal formulation with acceptable values of 102% drug content, 23% liquid fraction, and 74% solid fraction. This formula was selected for further study.

Table 27. CM eye drop formula containing 15% (w/v) γ CD.

| No. | Ingredient | Purpose | Concentration (% w/v) | | | | | |
|-------------------|-------------------|-----------------------|-----------------------|--------|--------|--------|--------|--------|
| | | | CM-F1 | CM-F2 | CM-F3 | CM-F4 | CM-F5 | CM-F6 |
| 1 | Cediranib Maleate | API | 3 | 3 | 3 | 3 | 3 | 3 |
| 2 | gCD | Solubilizer | 15 | 15 | 15 | 15 | 15 | 15 |
| 3 | PG | Supportive stabilizer | - | - | - | - | - | 0.1 |
| 4 | Glycerol | Supportive stabilizer | - | - | - | - | 0.1 | 0.1 |
| 5 | PVA (30-70k) | Supportive stabilizer | - | - | 0.2 | 0.2 | 0.2 | 0.2 |
| 6 | HPMC (50 cP) | Supportive stabilizer | - | - | 0.1 | 0.1 | 0.1 | 0.1 |
| 7 | Poloxamer 407 | Supportive stabilizer | - | - | 0.1 | 0.1 | 0.1 | 0.1 |
| 8 | EDTA | Chelating agent | 0.1 | 0.1 | 0.1 | 0.1 | 0.1 | 0.1 |
| 9 | Riboflavin | Main stabilizer | - | 0.1 | 0.1 | 0.1 | 0.1 | 0.1 |
| 10 | L-arginine | Supportive stabilizer | - | - | - | 0.1 | 0.1 | 0.1 |
| 11 | NaCl | Isotonicity agent | 0.5 | 0.5 | 0.5 | 0.5 | 0.5 | 0.5 |
| 12 | HCl/NaOH | pH adjustment | pH 5 | pH 5 | pH 5 | pH 5 | pH 5 | pH 5 |
| 14 | Purified water | Vehicle | qs 100 | qs 100 | qs 100 | qs 100 | qs 100 | qs 100 |
| 15 | N ₂ | Oxidation inhibitor | purge | purge | purge | purge | purge | purge |
| % Drug content | | | 82.99 | 90.02 | 92.31 | 93.92 | 97.67 | 102.68 |
| % Liquid fraction | | | 30.88 | 27.30 | 28.91 | 25.41 | 25.32 | 23.46 |
| % Solid fraction | | | 69.12 | 72.70 | 71.09 | 74.59 | 74.68 | 76.54 |

4.3.2.3 Physicochemical properties of formulation

CM-F6 had a yellow color due to the presence of riboflavin. The formulation was thick and homogeneous. The suspended particles settled out of the fluid after storage overnight at room temperature, and that sediment was easily re-suspended by shaking. Table 28 shows that drug assay, pH, osmolality, and viscosity are all within the acceptable range. The drug content of CM-F6 was equal to the theoretical value. The main particle diameter is 340 nm, only about 2% of particles have diameter of 1.6 μ m, thus this eye drops are a micro-suspension. However, the zeta potential is very low which might affect the long-term stability of the colloidal system.

Table 28. Physicochemical data of CM-F6 suspension (n =3).

| No. | Physicochemical properties | Part | mean | SD | Criteria |
|-----|---|-------------------------------|--|-----------------|---------------------------|
| 1 | Assay at initial | Suspension | 30.69 mg/mL 102.27% LA ^d | 0.10 | 27-33 mg/mL 90-110% LA |
| | | Supernatant | 24.14% F ^e | 0.07 | 10-30% Fraction (F) |
| | | Solid | 75.86% F | 0.07 | 70-90% Fraction (F) |
| | Assay 3 months (ambient condition) | Suspension | 30.07 mg/mL 100.24% LA | 0.05 | 27-33 mg/mL 90-110% LA |
| | | Supernatant | 24.19% F | 0.05 | 10-30% Fraction (F) |
| | | Solid | 75.81% F | 0.05 | 70-90% Fraction (F) |
| 2 | pH ^a | Suspension | 5.02 | 0.03 | min 4.0-5.0 |
| 3 | Osmolality ^b | Suspension | 257 | 2 | 200-280 mOsm/kg |
| | | Supernatant | 262 | 2 | |
| 4 | Viscosity at 25°C ^c Viscosity at 37°C | Suspension | 13.463 | 0.345 | 2-20 cP at 25°C |
| | | Suspension | 5.757 | 0.256 | |
| 5 | Particle size by DLS (nm) | Suspension (Dilution 1/20) | Diameter (nm) | % Vol | - |
| | | | 356 | 85.80% | - |
| | | | 1.06 1689 | 12.20% 2.00% | - |
| 6 | Zeta potential | Suspension (Dilution 1/20) | 1.20 | 0.11 | - |

^a refers to Ph.Eur.07/2016:20203 used as reference.

^b refers to Ph.Eur.01/2010:20235 used as reference.

^c refers to Ph. Eur.01/2008:20210 used as reference.

^d % Label amount

^e Fraction

4.3.2.4 Stability studies of the optimal formulation

Table 29 shows that % drug content of CM-F6 at 5°C is stable throughout 6 months, the drug starts degrading after storage for 1 months at 40°C, and for 6 months at 25°C. Furthermore, the micro-suspension is still stable when stored at ambient condition up to 4 months (data not shown).

Table 29. Drug assay of CM-F6 in 6 months (mean \pm standard deviation; n=2).

| Formulation | Cediranib maleate assay | | | | | |
|----------------------|-------------------------|------|----------------|------|-------------|------|
| | Drug amount (mg/mL) | | % Drug content | | % Drug loss | |
| | mean | SD | mean | SD | mean | SD |
| <u>CM-F6 at 5°C</u> | | | | | | |
| 0 month | 30.56 | 1.54 | 101.87 | 5.12 | - | - |
| 1 month | 30.46 | 1.59 | 101.54 | 5.30 | - | - |
| 2 months | 31.24 | 0.24 | 104.12 | 0.81 | - | - |
| 3 months | 30.74 | 1.46 | 102.47 | 4.86 | - | - |
| 6 months | 29.78 | 0.23 | 99.27 | 0.76 | 0.73 | 0.08 |
| <u>CM-F6 at 25°C</u> | | | | | | |
| 0 month | 31.18 | 0.57 | 103.91 | 1.86 | - | - |
| 1 month | 30.30 | 0.06 | 100.98 | 0.16 | - | - |
| 2 months | 30.25 | 0.19 | 100.81 | 0.59 | - | - |
| 3 months | 30.05 | 0.05 | 100.15 | 0.20 | - | - |
| 6 months | 29.60 | 1.87 | 98.64 | 6.22 | 1.36 | 0.62 |
| <u>CM-F6 at 40°C</u> | | | | | | |
| 0 month | 30.84 | 0.40 | 102.81 | 1.35 | - | - |
| 1 month | 29.26 | 0.11 | 97.52 | 0.35 | 2.48 | 0.35 |
| 2 months | 27.02 | 0.16 | 90.06 | 0.53 | 9.94 | 0.53 |
| 3 months | 26.28 | 0.37 | 87.59 | 1.22 | 12.41 | 1.22 |
| 6 months | 16.45 | 1.09 | 54.84 | 3.64 | 45.16 | 3.64 |

At 5°C, CM-F6 micro-suspension has a good appearance with a thick texture, stable bright yellow color, and a slow sedimentation rate after gentle shaking. However, this formulation cannot tolerate high temperature, particularly at 40°C. The color becomes much darker. The sedimentation volume of micro-suspension was up to 40% of the total volume. Although storing CM-F6 at 25°C still does not change %drug content (data not shown), its color darkens slightly over time. Storage temperature does not affect the

pH of CM-F6 during the 6 months stability study (Fig. 47). The particle size and distribution in CM-F6 are larger at 5°C and 40°C (Fig. 48). The particle sizes of the micro-suspension remain stable at 25°C.

According to collision theory, the chemical reaction will occur when the reacting molecules must collide to one another with a certain minimum energy called the activation energy (E_a), and with proper orientation. As the temperature rises, the proportion of molecules with higher kinetic energy is also increased (Loftsson, 2014a). Therefore, a higher storage temperature, especially 40°C has a greater number of collisions resulting in a faster reaction (i.e. faster drug degradation). Although the reaction proceeds slower at 5°C, the diameter of particles tends to increase, probably due to crystallization of γ CD. In brief, the storage temperature of 25°C is the most suitable condition for CM-F6 in term of stable particle size and acceptable %drug content.

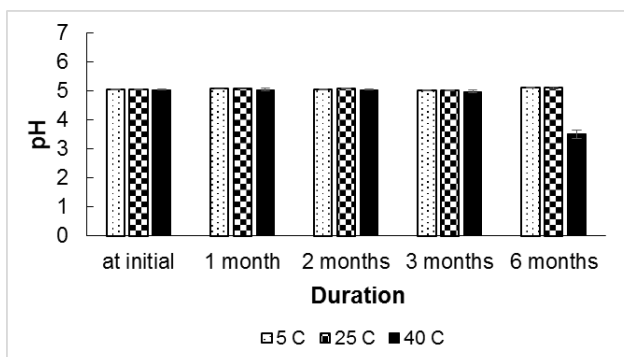


Figure 47. pH of CM-F6 in 3 months (mean \pm standard deviation; n=2).

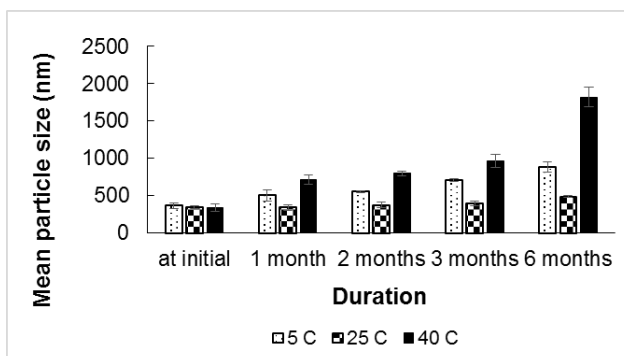


Figure 48. Mean particle diameter (nm) of CM-F6 in 3 months (mean \pm standard deviation; n=2).

4.3.2.5 Morphology studies of the optimal formulation

Light microscopy

The examination of CM-F6 by light microscope in Fig. 49 shows that 15% (w/v) γ CD-based formulation produced irregular spherical particles, indicating the formation of an amorphous complex. Both undiluted micro-suspension (Fig. 49a) and diluted micro-suspension (Fig. 49b) display similar size of particles with diameters of less than 1 μm . For supernatant (Fig. 49c), those particles formed a cluster-like shape with larger size.

The official specification (Ph. Eur.01/2008:1163) for eye drop suspension requires that in each 10 μg of solid active substance, not more than 20 particles have a maximum dimension greater than 25 μm , and not more than 2 of these particles have a maximum dimension greater than 50 μm . None of the particles has a maximum dimension greater than 90 μm . Thus, all types of CM-F6 samples obtain particles within acceptable range according to Ph. Eur.01/2008:1163.

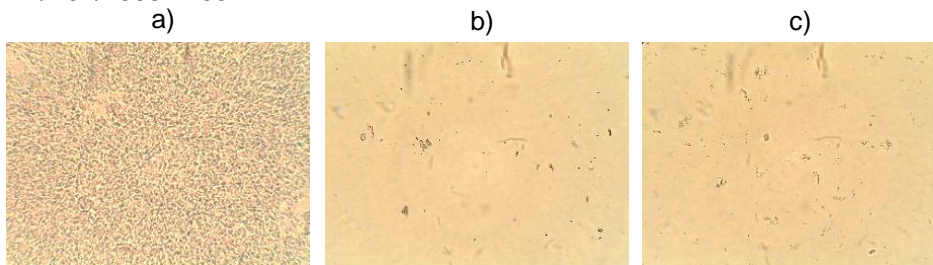


Figure 49. Light microscope images of a) undiluted micro-suspension, b) diluted micro-suspension (dilution of 1/20), and c) supernatant at 400X magnitude.

TEM

In order to get more information about complex formation, TEM measurements were also employed to investigate the morphological features of CM-F6 containing 15% (w/v) γ CD as shown in Fig. 50. TEM micrograms demonstrate that CM-F6 samples at the initial stage obtain spherical particles with an average size of hundreds of nanometers. For diluted suspension, not only spherical nanoparticles but also irregular nanocrystals (see close arrow) can be seen. The size of those crystals varies up to 1-2 μm , while spherical particles are between 100 and 300 nm in diameter; comparable to the nanoparticles found in a typical suspension. This indicated that diluting the sample with pure water did not change the particle size. Supernatant shows a greater diameter of spherical particles about 300-500 nm and up to 800 nm in diameter.

After a 3-month storage period, nanoparticles behaved differently (Fig. 51). Temperature is a critical factor affecting the morphologies of suspension. The sample has good stability at 25°C. Particles become larger at lower and higher temperatures. The micro-suspension becomes crystalline (see close arrow) at 5°C, whereas it tends to produce irregular debris (see close arrow) due to thermal degradation from incubation at 40°C. All results are nearly the same as those derived from DLS observation.

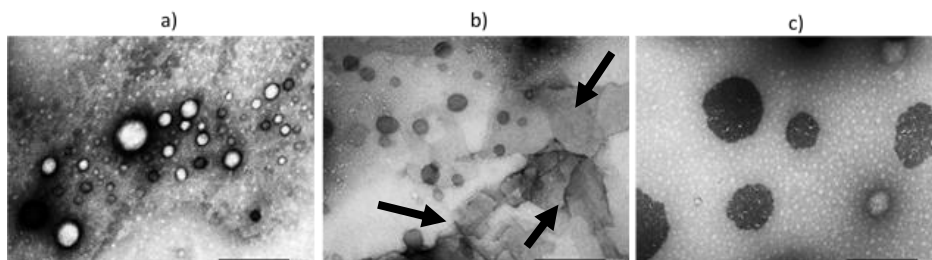


Figure 50. TEM image at magnitude 25,000x of CM-F6 a) undiluted micro-suspension, b) diluted micro-suspension (dilution of 1/20), c) supernatant.

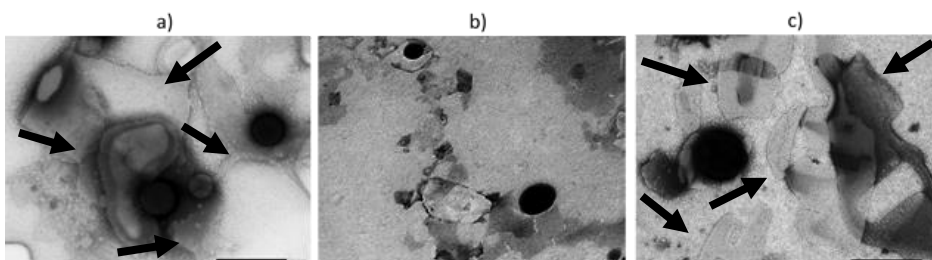


Figure 51. TEM images at magnitude 25,000x of 3-month CM-F6 at a) 5°C, b) 25°C, and c) 40°C.

4.3.2.6 *In vivo* permeation of the optimal formulation

Briefly, thermally stable eye drops could deliver CM to the back of eye. The details of permeation performance in the rabbit model are confidential.

5 Summary and conclusions

The focus of this dissertation is the development of cyclodextrin (CD) nanoparticles for targeted ocular delivery of kinase inhibitors (KIs). The critical difficulty in this research is very low aqueous solubility of the KIs which decreases their ability to permeate a biological membrane. The use of γ CD to solubilize the drug through complexation was still inadequate. Hence, the early phase-solubility studies involved supplementary techniques such as the addition of a small amount of hydrophilic polymer, drug ionization and salt formation. In the solubility studies, the complexes were prepared under mild heating during ultrasonication because some KIs are heat-labile. However, the moist heating (i.e. autoclaving) was applied as sterilization during eye drop preparation. The γ CD aggregate and nanoparticles formed at higher concentrations were applied as a micro- or nanoparticle drug delivery platform. The thermal stability of KI salt in concentrated complexation media was an obstacle during product development. In summary, the research framework is divided into three tasks that are influenced by hydrophilic polymers, counter ions, and thermal stabilizers.

1. Hydrophilic polymers

The main task in the first part was to screen the aqueous solubility of six different KIs (i.e. axitinib, cediranib, dovitinib, motesanib, pazopanib, and regorafenib) upon complex formation with γ CD and hydrophilic polymer, and to evaluate of their characteristics both in solution and solid state. The main findings are as follows:

- All six KIs formed B_s-type phase-solubility profiles in the aqueous γ CD media. The KI/ γ CD complexes were more soluble in acidic conditions or, in other words, their aqueous solubility is pH-dependent. Dovitinib had the greatest interaction with γ CD ($K_{1:1}$ 684 M⁻¹, and CE 0.011), then motesanib. The γ CD was an excellent complexing agent to solubilize dovitinib.
- The tested hydrophilic polymers had a specific solubilizing effect on the KIs in the γ CD complexation media. HDMBr generally promoted the γ CD solubilization on KI solubility via a synergist effect.

- The formulation vehicle containing BAC and EDTA could also solubilize drug/ γ CD complexes. Drug solubility improved with increasing EDTA concentrations whereas BAC limited the enhancement of solubility at a certain amount.
- Dovitinib was the optimal candidate for further studies.
- The formation of dovitinib/ γ CD nanosized aggregates and dovitinib/ γ CD/HDMBr nanosized aggregates was confirmed by DLS and TEM studies.
- The ternary complexes with HDMBr still formed B_s-type profiles. HDMBr enhanced the solubility of the dovitinib/ γ CD complex, and CE increased from 0.0110 to 0.0391.
- The formation of a dovitinib/ γ CD complex was confirmed by XRPD, DSC, and FTIR in solid state.
- The γ CD could stabilize the supersaturated dovitinib solution and enhance the dissolution rate, but the presence of HDMBr reduced this rate due to formation of a polymeric matrix.

2. Counter ions

Previously, EDTA also had potential to solubilize the KI in complexation media. This acidic compound may function as a counter ion which increases the solubility of weakly basic drug/ γ CD complex through salt formation. Thus, the second task was mainly investigating how counter ions improved the KI solubility, and affected γ CD solubilization and complexation. The most effective counter ion further determined the permeation. The following conclusions were reached:

- Citrate led to the greatest CD solubilization and complexation on dovitinib via salt formation and/or charge-charge interactions.
- Drug permeation through a semi-permeable membrane was opposed to the CD solubilization.

3. Thermal stabilizers

According to solubility enhancement studies, salt formation was more powerful than the addition of hydrophilic polymers. Although dovitinib

obtained the greatest performance, cediranib was also a good choice to form salt due to high intrinsic solubility. Unexpectedly, dovitinib lactate had some technical problems during the preliminary study. Hence, eye drops were formulated containing CM salt only. In the third part, the major tasks were the essential thermal stabilizer for CM in concentrated γ CD complexation media and formulating the thermally stable eye drops. Additionally, formulation compositions such as polymers and other excipients were selected from previous data. The main observations were made in the studies presented herein:

- Riboflavin is the most effective thermal stabilizer for CM in concentrated γ CD solution. In the multicomponent system, it could decrease thermal degradation of CM during at least one cycle of autoclaving.
- Hydrolysis is the main reaction in drug degradation due to the breakdown of ether linkage under vigorous condition i.e. strong acid and high temperature.
- The 15% (w/v) γ CD is optimal where γ CD precipitated, and then formed nanoparticles as a drug delivery platform.
- Riboflavin did not interfere with the pattern of phase-solubility, *in-vitro* permeation, and morphology of nanoparticles.
- NMR studies confirmed the formation of partial inclusion complex between γ CD and guest molecules (i.e. CM and riboflavin). The ribityl side chain of riboflavin may shield the pyrrolidinyloxy group of CM, and thus, thermal degradation is retarded or prevented.
- Micro-suspension formulations containing riboflavin and other excipients (i.e. co-stabilizer, polymers) did retard or prevent drug loss during the heating process.
- A temperature of 25°C is an appropriate storage condition. The pH, particle size and shape of micro-suspensions remained unchanged over six months. The drug loss still met the acceptable criteria.
- The optimal formulation can deliver the drug to the target site.

In conclusion, γ CD enhanced the KIs solubility through complex formation, and additional techniques (e.g. by hydrophilic polymers, and counter ions) solubilized the drug even further. The thermal degradation of KI salt in concentrated complexation media was reduced in the presence of an appropriate stabilizer. The final product was thermally stable during an autoclaving. The product shelf stability should be a concern after six months. The possible solution may be separating the solid complexes from the formulation vehicle and mixing these two parts prior to administration. The ocular KI delivery of this suspension has been successful.

References

- ACS. (2019). SciFinder (scifinder.cas.org). from American Chemical Society
- The Age-Related Eye Disease Study (AREDS): design implications. AREDS report no. 1. (1999). *Controlled Clinical Trials*, 20(6), 573-600. doi:10.1016/s0197-2456(99)00031-8
- Ahmad, I., Ahmed, S., Sheraz, M. A., Aminuddin, M., & Vaid, F. H. (2009). Effect of caffeine complexation on the photolysis of riboflavin in aqueous solution: a kinetic study. *Chemical and Pharmaceutical Bulletin (Tokyo)*, 57(12), 1363-1370. doi:10.1248/cpb.57.1363
- Al-Ani, M. R. (2006). A Review of: "Vitamins in Foods/Analysis, Bioavailability, and Stability". *International Journal of Food Properties*, 9(4), 927-928. doi:10.1080/10942910600853899
- Ambati, J., & Fowler, B. J. (2012). Mechanisms of age-related macular degeneration. *Neuron*, 75(1), 26-39. doi:10.1016/j.neuron.2012.06.018
- Amiri, S., & Amiri, S. (2017). *Cyclodextrins: Properties and Industrial Applications*: Wiley.
- Arora, A., & Scholar, E. M. (2005). Role of Tyrosine Kinase Inhibitors in Cancer Therapy. *Journal of Pharmacology and Experimental Therapeutics*, 315(3), 971. doi:10.1124/jpet.105.084145
- Attwood, D., & Florence, A. T. (2008). *Physical Pharmacy*: Pharmaceutical Press.
- Avis, K. E., Lachman, L., & Lieberman, H. A. (1986). *Pharmaceutical Dosage Forms: Parenteral Medications* (first ed. Vol. 2). New York Marcel Dekker Inc.
- Badrinarayan, P., & Sastry, G. N. (2011). Sequence, Structure, and Active Site Analyses of p38 MAP Kinase: Exploiting DFG-out Conformation as a Strategy to Design New Type II Leads. *Journal of Chemical Information and Modeling*, 51(1), 115-129. doi:10.1021/ci100340w
- Badrinarayan, P., & Sastry, G. N. (2012). Virtual screening filters for the design of type II p38 MAP kinase inhibitors: A fragment based library generation approach. *Journal of Molecular Graphics and Modelling*, 34, 89-100. doi:https://doi.org/10.1016/j.jm gm.2011.12.009
- Barak, Y., Heroman, W. J., & Tezel, T. H. (2012). The past, present, and future of exudative age-related macular degeneration treatment.

- Middle East African journal of ophthalmology*, 19(1), 43-51.
doi:10.4103/0974-9233.92115
- Barba, A. A., d'Amore, M., Chirico, S., Lamberti, G., & Titomanlio, G. (2009). Swelling of cellulose derivative (HPMC) matrix systems for drug delivery. *Carbohydrate Polymers*, 78, 469-474.
doi:10.1016/j.carbpol.2009.05.001
- Barthel, J. M. G., Krienke, H., Kunz, W., Baumgartel, H., Franck, E. U., & Grunbein, W. (1998). *Physical Chemistry of Electrolyte Solutions: Modern Aspects*: U.S. Government Printing Office.
- Bekiroglu, S., Kenne, L., & Sandstrom, C. (2003). ¹H NMR studies of maltose, maltoheptaose, alpha-, beta-, and gamma-cyclodextrins, and complexes in aqueous solutions with hydroxy protons as structural probes. *Journal Organic Chemistry*, 68(5), 1671-1678.
doi:10.1021/jo0262154
- Bergers, G., Song, S., Meyer-Morse, N., Bergsland, E., & Hanahan, D. (2003). Benefits of targeting both pericytes and endothelial cells in the tumor vasculature with kinase inhibitors. *The Journal of clinical investigation*, 111(9), 1287-1295. doi:10.1172/JCI17929
- Bhattacharjee, S. (2016). DLS and zeta potential - What they are and what they are not? *Journal of Controlled Release*, 235, 337-351.
doi:10.1016/j.jconrel.2016.06.017
- Bhattar, S. L., Kolekar, G. B., & Patil, S. R. (2010). Spectroscopic studies on the molecular interaction between salicylic acid and riboflavin (B2) in micellar solution. *Journal of Luminescence*, 130(3), 355-359.
doi:https://doi.org/10.1016/j.jlumin.2009.09.019
- Bhutto, I., & Luttly, G. (2012). Understanding age-related macular degeneration (AMD): Relationships between the photoreceptor/retinal pigment epithelium/Bruch's membrane/choriocapillaris complex. *Molecular Aspects of Medicine*, 33(4), 295-317. doi:https://doi.org/10.1016/j.mam.2012.04.005
- Böttger M., D. G. V., Freundlieb J., Hirth-Dietrich C., Keldenich J., Klar J., Muenster U., Ohm A., Richter A., Riedl B.,Telser J. (2013). US Patent No. WO 2013188279 A1. with international search report (Art. 21(3)).
- Böttger M., D. G. V., Freundlieb J., Hirth-Dietrich C., Keldenich J., Klar J., Muenster U., Ohm A., Richter A., Riedl B.,Telser J. (2015). US Patent No. US 2015/0165028A1 with international search report (Art. 21(3)).
- Brackman, J. C., & Engberts, J. B. F. N. (1993). Polymer-micelle interactions: physical organic aspects. *Chemical Society Reviews*, 22(2), 85-92. doi:10.1039/CS9932200085

- Bressler, N. M., Bressler, S. B., & Fine, S. L. (1988). Age-related macular degeneration. *Survey of Ophthalmology*, 32(6), 375-413. doi:10.1016/0039-6257(88)90052-5
- Brewster, M. E., & Loftsson, T. (2007). Cyclodextrins as pharmaceutical solubilizers. *Advanced Drug Delivery Reviews*, 59(7), 645-666. doi:10.1016/j.addr.2007.05.012
- Budha, N. R., Frymoyer, A., Smelick, G. S., Jin, J. Y., Yago, M. R., Dresser, M. J., . . . Ware, J. A. (2012). Drug absorption interactions between oral targeted anticancer agents and PPIs: is pH-dependent solubility the Achilles heel of targeted therapy? *Clinical Pharmacology & Therapeutics*, 92(2), 203-213. doi:10.1038/clpt.2012.73
- Bychkova, S. A., Katrovitseva, A. V., & Kozlovskii, E. V. (2008). Complex formation of maleic acid with the Zn²⁺, Ni²⁺, Co²⁺, Cu²⁺ in aqueous solution. *Russian Journal of Coordination Chemistry*, 34(2), 93-96. doi:10.1134/S1070328408020036
- Carrier, R. L., Miller, L. A., & Ahmed, I. (2007). The utility of cyclodextrins for enhancing oral bioavailability. *Journal of Controlled Release*, 123(2), 78-99. doi:https://doi.org/10.1016/j.jconrel.2007.07.018
- Cavalli, R., Trotta, F., Trotta, M., Pastero, L., & Aquilano, D. (2007). Effect of alkylcarbonates of γ -cyclodextrins with different chain lengths on drug complexation and release characteristics. *International Journal of Pharmaceutics*, 339(1), 197-204. doi:https://doi.org/10.1016/j.ijpharm.2007.03.001
- Cerreia Vioglio, P., Chierotti, M. R., & Gobetto, R. (2017). Pharmaceutical aspects of salt and cocrystal forms of APIs and characterization challenges. *Advanced Drug Delivery Reviews*, 117, 86-110. doi:10.1016/j.addr.2017.07.001
- Chappelow, A. V., & Kaiser, P. K. (2008). Neovascular age-related macular degeneration: potential therapies. *Drugs*, 68(8), 1029-1036. doi:10.2165/00003495-200868080-00002
- Chen, Y., Tortorici, M. A., Garrett, M., Hee, B., Klamerus, K. J., & Pithavala, Y. K. (2013). Clinical Pharmacology of Axitinib. *Clinical Pharmacokinetics*, 52(9), 713-725. doi:10.1007/s40262-013-0068-3
- Cho, E.-C. (2012). Effect of Polymer Characteristics on the Thermal Stability of Retinol Encapsulated in Aliphatic Polyester Nanoparticles. *Bulletin of the Korean Chemical Society*, 33. doi:10.5012/bkcs.2012.33.8.2560
- Combs, G. F., & McClung, J. P. (2017). Chapter 12 - Riboflavin. In G. F. Combs & J. P. McClung (Eds.), *The Vitamins (Fifth Edition)* (pp. 315-329): Academic Press.

- Cruz-Cabeza, A. J. (2012). Acid–base crystalline complexes and the pKa rule. *CrystEngComm*, 14(20), 6362-6365. doi:10.1039/C2CE26055G
- Danis, R., McLaughlin, M. M., Tolentino, M., Staurengi, G., Ye, L., Xu, C.-F., . . . Johnson, M. W. (2014). Pazopanib eye drops: a randomised trial in neovascular age-related macular degeneration. *British Journal of Ophthalmology*, 98(2), 172. doi:10.1136/bjophthalmol-2013-303117
- Delplace, V., Payne, S., & Shoichet, M. (2015). Delivery strategies for treatment of age-related ocular diseases: From a biological understanding to biomaterial solutions. *Journal of Controlled Release*, 219, 652-668. doi:10.1016/j.jconrel.2015.09.065
- Deng, Y., Sychterz, C., Suttle, A. B., Dar, M. M., Bershas, D., Negash, K., . . . Ho, M. Y. K. (2013). Bioavailability, metabolism and disposition of oral pazopanib in patients with advanced cancer. *Xenobiotica*, 43(5), 443-453. doi:10.3109/00498254.2012.734642
- Desai, A., & Lee, M. (2007). *Gibaldi's Drug Delivery Systems in Pharmaceutical Care*. Maryland: American Society of Health-System Pharmacists Inc.
- Deygen, I., Skuredina, A., & Kudryashova, E. (2017). Drug delivery systems for fluoroquinolones: New prospects in tuberculosis treatment. *Russian Journal of Bioorganic Chemistry*, 43, 487-501. doi:10.1134/S1068162017050077
- Djedaini, F., Lin, S. Z., Perly, B., & Wouessidjewe, D. (1990). High-field nuclear magnetic resonance techniques for the investigation of a β -cyclodextrin:indomethacin inclusion complex. *Journal of Pharmaceutical Sciences*, 79(7), 643-646.
- Doguizi, S., Ozdek, S., & Yuksel, S. (2015). Tachyphylaxis during ranibizumab treatment of exudative age-related macular degeneration. *International journal of ophthalmology*, 8(4), 846-848. doi:10.3980/j.issn.2222-3959.2015.04.37
- Donaubauer, H. H., Fuchs, H., Langer, K. H., & Bär, A. (1998). Subchronic Intravenous Toxicity Studies with γ -Cyclodextrin in Rats. *Regulatory Toxicology and Pharmacology*, 27(2), 189-198. doi:https://doi.org/10.1006/rtph.1998.1224
- Dong, Y., Ng, W. K., Shen, S., Kim, S., & Tan, R. B. H. (2009). Preparation and characterization of spironolactone nanoparticles by antisolvent precipitation. *International Journal of Pharmaceutics*, 375(1), 84-88. doi:https://doi.org/10.1016/j.ijpharm.2009.03.013
- Doukas, J., Mahesh, S., Umeda, N., Kachi, S., Akiyama, H., Yokoi, K., . . . Campochiaro, P. (2008). Topical Administration of a Multi-Targeted Kinase Inhibitor Suppresses Choroidal Neovascularization and

- Retinal Edema. *Journal of cellular physiology*, 216, 29-37.
doi:10.1002/jcp.21426
- Dufour, G., Evrard, B., & de Tullio, P. (2015). Rapid quantification of 2-hydroxypropyl- β -cyclodextrin in liquid pharmaceutical formulations by ^1H nuclear magnetic resonance spectroscopy. *European Journal of Pharmaceutical Sciences*, 73, 20-28.
doi:<https://doi.org/10.1016/j.ejps.2015.03.005>
- E Mohr, M. (2006). *Remington: The Science and Practice of Pharmacy, 21st Edition* (Vol. 22).
- EFSA. (2009). Scientific Opinion of the Panel on Food Additives and Nutrient Sources added to Food on a request from the Commission on magnesium ascorbate, zinc ascorbate and calcium ascorbate added for nutritional purposes in food supplements. *EFSA Journal*, 994, 1-22.
- EMA, E. M. A. (2016) EMA/CHMP/616303/2016. In. *Assessment Report: Cediranib maleate*.
- Fahmy, S. A., Br  bler, J., Alawak, M., El-Sayed, M. M. H., Bakowsky, U., & Shoeib, T. (2019). Chemotherapy Based on Supramolecular Chemistry: A Promising Strategy in Cancer Therapy. *Pharmaceutics*, 11(6), 292. doi:10.3390/pharmaceutics11060292
- Falavarjani, K. G., & Nguyen, Q. D. (2013). Adverse events and complications associated with intravitreal injection of anti-VEGF agents: a review of literature. *Eye (Lond)*, 27(7), 787-794.
doi:10.1038/eye.2013.107
- Faria, D. K., Mendes, M. E., & Sumita, N. M. (2017). The measurement of serum osmolality and its application to clinical practice and laboratory: literature review. *Jornal Brasileiro de Patologia e Medicina Laboratorial*, 53, 38-45.
- Fauci, M. T., & Mura, P. (2001). Effect of water-soluble polymers on naproxen complexation with natural and chemically modified beta-cyclodextrins. *Drug Development and Industrial Pharmacy*, 27(9), 909-917.
- Fendler, J. H. (1996). Self-assembled nanostructured materials. *Chemistry of Materials*, 8(8), 1616-1624. doi:10.1021/cm960116n
- Fenyvesi, E., Vikmon, M., Szeman, J., Redenti, E., Delcanale, M., Ventura, P., & Szejtli, J. (1999). Interaction of Hydroxy Acids with β -Cyclodextrin. *Journal of inclusion phenomena and macrocyclic chemistry*, 33(3), 339-344. doi:10.1023/A:1008094702632
- Ferris, F. L., 3rd, Wilkinson, C. P., Bird, A., Chakravarthy, U., Chew, E., Csaky, K., & Sadda, S. R. (2013). Clinical classification of age-

- related macular degeneration. *Ophthalmology*, 120(4), 844-851. doi:10.1016/j.ophtha.2012.10.036
- Figueiras, A., Sarraguca, J. M., Pais, A. A., Carvalho, R. A., & Veiga, J. F. (2010). The role of L-arginine in inclusion complexes of omeprazole with cyclodextrins. *AAPS PharmSciTech*, 11(1), 233-240. doi:10.1208/s12249-009-9375-2
- Flora, S. J. S., & Pachauri, V. (2010). Chelation in metal intoxication. *International journal of environmental research and public health*, 7(7), 2745-2788. doi:10.3390/ijerph7072745
- Fong, C. (2016). *Drug discovery model using molecular orbital computations: tyrosine kinase inhibitors*. Retrieved from <https://hal.archives-ouvertes.fr/hal-01350862>
- Foss, A. J. E., Childs, M., Reeves, B. C., Empeslidis, T., Tesha, P., Dhar-Munshi, S., . . . Montgomery, A. (2015). Comparing different dosing regimens of bevacizumab in the treatment of neovascular macular degeneration: study protocol for a randomised controlled trial. *Trials*, 16, 85-85. doi:10.1186/s13063-015-0608-2
- Foye, W. O., & Lange, W. E. (1954). Metal Chelates of Riboflavin1. *Journal of the American Chemical Society*, 76(8), 2199-2201. doi:10.1021/ja01637a050
- Georgiev, G. A., Yokoi, N., Koev, K., Kutsarova, E., Ivanova, S., Kyumurkov, A., . . . Lalchev, Z. (2011). Surface Chemistry Study of the Interactions of Benzalkonium Chloride with Films of Meibum, Corneal Cells Lipids, and Whole Tears. *Investigative Ophthalmology & Visual Science*, 52(7), 4645-4654. doi:10.1167/iovs.10-6271
- Giani, A., Linde, A., Laverde, N., Colauto, G., & Linde, G. (2011). *Changes to Taste Perception in the Food Industry: Use of Cyclodextrins**.
- Giddabasappa, A., Lalwani, K., Norberg, R., Gukasyan, H. J., Paterson, D., Schachar, R. A., . . . Eswaraka, J. (2016). Axitinib inhibits retinal and choroidal neovascularization in in vitro and in vivo models. *Experimental Eye Research*, 145, 373-379. doi:10.1016/j.exer.2016.02.010
- González-Gaitano, G., Rodríguez, P., Isasi, J. R., Fuentes, M., Tardajos, G., & Sánchez, M. (2002). The Aggregation of Cyclodextrins as Studied by Photon Correlation Spectroscopy. *Journal of inclusion phenomena and macrocyclic chemistry*, 44(1), 101-105. doi:10.1023/a:1023065823358
- Goswami, S., Majumdar, A., & Sarkar, M. (2017). Painkiller Isoxicam and Its Copper Complex Can Form Inclusion Complexes with Different Cyclodextrins: A Fluorescence, Fourier Transform Infrared Spectroscopy, and Nuclear Magnetic Resonance Study. *Journal of*

Physical Chemistry B, 121(36), 8454-8466.
doi:10.1021/acs.jpcc.7b05649

- Gragoudas, E. S., Adamis, A. P., Cunningham, E. T., Feinsod, M., Guyer, D. R., & Group, V. I. S. i. O. N. C. T. (2004). Pegaptanib for neovascular age-related macular degeneration. *The New England journal of medicine*, 351(27), 2805-2816. doi:10.1056/nejmoa042760
- Gupta, D., Bhatia, D., Dave, V., Sutariya, V., & Varghese Gupta, S. (2018). Salts of Therapeutic Agents: Chemical, Physicochemical, and Biological Considerations. *Molecules*, 23(7). doi:10.3390/molecules23071719
- Gupta, M., Chauhan, D. N., Sharma, V., & Chauhan, N. S. (2019). *Novel Drug Delivery Systems for Phytoconstituents*: CRC Press.
- Guttman, D. E. (1962). Complex formation influence on reaction rate. I. Effect of caffeine on riboflavin base-catalyzed degradation rate. *Journal of Pharmaceutical Sciences*, 51, 1162-1166. doi:10.1002/jps.2600511211
- Hannink, M., & Donoghue, D. J. (1989). Structure and function of platelet-derived growth factor (PDGF) and related proteins. *Biochimica et Biophysica Acta*, 989(1), 1-10. doi:10.1016/0304-419x(89)90031-0
- Hanout, M., Ferraz, D., Ansari, M., Maqsood, N., Kherani, S., Sepah, Y. J., . . . Nguyen, Q. D. (2013). Therapies for Neovascular Age-Related Macular Degeneration: Current Approaches and Pharmacologic Agents in Development. *BioMed Research International*, 2013, 830837. doi:10.1155/2013/830837
- Harkins, T. R., & Freiser, H. (1959). The Chelating Tendency of Riboflavin. *The Journal of Physical Chemistry*, 63(2), 309-311. doi:10.1021/j150572a047
- Heier, J. S., Brown, D. M., Chong, V., Korobelnik, J.-F., Kaiser, P. K., Nguyen, Q. D., . . . Schmidt-Erfurth, U. (2012). Intravitreal Aflibercept (VEGF Trap-Eye) in Wet Age-related Macular Degeneration. *Ophthalmology*, 119(12), 2537-2548. doi:https://doi.org/10.1016/j.ophtha.2012.09.006
- Herbrink, M., Nuijen, B., Schellens, J. H., & Beijnen, J. H. (2015). Variability in bioavailability of small molecular tyrosine kinase inhibitors. *Cancer Treatment Reviews*, 41(5), 412-422. doi:10.1016/j.ctrv.2015.03.005
- Herbrink, M., Schellens, J. H., Beijnen, J. H., & Nuijen, B. (2016). Inherent formulation issues of kinase inhibitors. *Journal of Controlled Release*, 239, 118-127. doi:10.1016/j.jconrel.2016.08.036
- Higuchi, T., & Connors, K. A. (1965). Phase-solubility techniques. In C. N. R. (Ed.) (Ed.), *Advances in Analytical Chemistry and Instrumentation* (Vol. 4, pp. 117-212): Wiley-Interscience, New York.

- Hirlekar, R. S., Sonawane, S. N., & Kadam, V. J. (2009). Studies on the effect of water-soluble polymers on drug-cyclodextrin complex solubility. *AAPS PharmSciTech*, *10*(3), 858-863. doi:10.1208/s12249-009-9274-6
- Holash, J., Davis, S., Papadopoulos, N., Croll, S. D., Ho, L., Russell, M., . . . Rudge, J. S. (2002). VEGF-Trap: a VEGF blocker with potent antitumor effects. *Proceedings of the National Academy of Sciences of the United States of America*, *99*(17), 11393-11398. doi:10.1073/pnas.172398299
- Holz, F. G., Dugel, P. U., Weissgerber, G., Hamilton, R., Silva, R., Bandello, F., . . . Souied, E. (2016). Single-Chain Antibody Fragment VEGF Inhibitor RTH258 for Neovascular Age-Related Macular Degeneration: A Randomized Controlled Study. *Ophthalmology*, *123*(5), 1080-1089. doi:https://doi.org/10.1016/j.ophtha.2015.12.030
- Honda, M., Asai, T., Oku, N., Araki, Y., Tanaka, M., & Ebihara, N. (2013). Liposomes and nanotechnology in drug development: Focus on ocular targets. *International journal of nanomedicine*, *8*, 495-504. doi:10.2147/IJN.S30725
- Horita, S., Watanabe, M., Katagiri, M., Nakamura, H., Haniuda, H., Nakazato, T., & Kagawa, Y. (2019). Species differences in ocular pharmacokinetics and pharmacological activities of regorafenib and pazopanib eye-drops among rats, rabbits and monkeys. *Pharmacology Research & Perspectives*, *7*(6), e00545. doi:10.1002/prp2.545
- Hovorka, S. W., & Schöneich, C. (2001). Oxidative degradation of pharmaceuticals: Theory, mechanisms and inhibition. *Journal of Pharmaceutical Sciences*, *90*(3), 253-269. doi:https://doi.org/10.1002/1520-6017(200103)90:3<253::AID-JPS1>3.0.CO;2-W
- Irie, T., & Uekama, K. (1997). Pharmaceutical applications of cyclodextrins. III. Toxicological issues and safety evaluation. *Journal of Pharmaceutical Sciences*, *86*(2), 147-162. doi:10.1021/js960213f
- Jambhekar, S. S., & Breen, P. (2016). Cyclodextrins in pharmaceutical formulations II: solubilization, binding constant, and complexation efficiency. *Drug Discovery Today*, *21*(2), 363-368. doi:10.1016/j.drudis.2015.11.016
- Jansook, P., Muankaew, C., Stefansson, E., & Loftsson, T. (2015). Development of eye drops containing antihypertensive drugs: formulation of aqueous irbesartan/ γ CD eye drops. *Pharmaceutical Development and Technology*, *20*(5), 626-632. doi:10.3109/10837450.2014.910811

- Jansook, P., Ogawa, N., & Loftsson, T. (2018). Cyclodextrins: structure, physicochemical properties and pharmaceutical applications. *International Journal of Pharmaceutics*, 535(1-2), 272-284. doi:10.1016/j.ijpharm.2017.11.018
- Jansook, P., Pichayakorn, W., Muankaew, C., & Loftsson, T. (2016). Cyclodextrin-poloxamer aggregates as nanocarriers in eye drop formulations: dexamethasone and amphotericin B. *Drug Development and Industrial Pharmacy*, 42, 1446-1454.
- Jansook, P., Praphanwittaya, P., Sripetch, S., & Loftsson, T. (2020). Solubilization and in vitro permeation of dovitinib/cyclodextrin complexes and their aggregates. *Journal of inclusion phenomena and macrocyclic chemistry*, 97(3), 195-203. doi:10.1007/s10847-020-00995-y
- Jansook, P., Stefánsson, E., Thorsteinsdóttir, M., Sigurdsson, B. B., Kristjánisdóttir, S. S., Bas, J. F., . . . Loftsson, T. (2010). Cyclodextrin solubilization of carbonic anhydrase inhibitor drugs: Formulation of dorzolamide eye drop microparticle suspension. *European Journal of Pharmaceutics and Biopharmaceutics*, 76(2), 208-214. doi:https://doi.org/10.1016/j.ejpb.2010.07.005
- Jóhannesson, G., Moya-Ortega, M. D., Asgrímsdóttir, G. M., Agnarsson, B. A., Lund, S. H., Loftsson, T., & Stefánsson, E. (2014). Dorzolamide cyclodextrin nanoparticle suspension eye drops and Trusopt in rabbit. *Journal of Ocular Pharmacology and Therapeutics*, 30(6), 464-467. doi:10.1089/jop.2013.0164
- Johannsdottir, S., Jansook, P., Stefansson, E., Kristinsdottir, I. M., Fulop, Z., Asgrimsdottir, G. M., . . . Loftsson, T. (2018). Topical drug delivery to the posterior segment of the eye: Dexamethasone concentrations in various eye tissues after topical administration for up to 15 days to rabbits. *Journal of Drug Delivery Science and Technology*, 45, 449-454. doi:https://doi.org/10.1016/j.jddst.2018.04.007
- Jones, D. (2004). *Pharmaceutical Applications of Polymers for Drug Delivery*: Rapra Technology Limited.
- Joussen, A. M., Wolf, S., Kaiser, P. K., Boyer, D., Schmelter, T., Sandbrink, R., . . . Boettger, M. K. (2019). The Developing Regorafenib Eye drops for neovascular Age-related Macular degeneration (DREAM) study: an open-label phase II trial. *British Journal of Clinical Pharmacology*, 85(2), 347-355. doi:10.1111/bcp.13794
- Kang, S., Park, K. C., Yang, K. J., Choi, H. S., Kim, S. H., & Roh, Y. J. (2013). Effect of cediranib, an inhibitor of vascular endothelial growth factor receptor tyrosine kinase, in a mouse model of choroidal neovascularization. *Clinical & Experimental Ophthalmology*, 41(1), 63-72. doi:10.1111/j.1442-9071.2012.02813.x

- Khan, M., Agarwal, K., Loutfi, M., & Kamal, A. (2014). Present and possible therapies for age-related macular degeneration. *ISRN ophthalmology*, 2014, 608390-608390. doi:10.1155/2014/608390
- Khan, M. M. T., & Mohan, M. S. (1973). The metal chelates of riboflavin and riboflavin monophosphate. *Journal of Inorganic and Nuclear Chemistry*, 35(5), 1749-1755. doi:https://doi.org/10.1016/0022-1902(73)80275-1
- Kim, J., Schlesinger, E. B., & Desai, T. A. (2015). Nanostructured materials for ocular delivery: nanodesign for enhanced bioadhesion, transepithelial permeability and sustained delivery. *Therapeutic delivery*, 6(12), 1365-1376. doi:10.4155/tde.15.75
- Kim, K.-H., Xing, H., Zuo, J.-M., Zhang, P., & Wang, H. (2015). TEM based high resolution and low-dose scanning electron nanodiffraction technique for nanostructure imaging and analysis. *Micron*, 71, 39-45. doi:https://doi.org/10.1016/j.micron.2015.01.002
- Klar, J., Boettger, M. K., Freundlieb, J., Keldenich, J., Elena, P.-P., & von Degenfeld, G. (2015). Effects of the multi-kinase inhibitor regorafenib on ocular neovascularization. *Investigative Ophthalmology & Visual Science*, 56(7), 246-246.
- Klein, R. (2007). Overview of progress in the epidemiology of age-related macular degeneration. *Ophthalmic Epidemiology*, 14(4), 184-187. doi:10.1080/09286580701344381
- Kuno, N., & Fujii, S. (2012). Clinical Application of Drug Delivery Systems for Treating AMD. In.
- Küpper, T. E. A. H., Schraut, B., Rieke, B., Hemmerling, A. V., Schöffl, V., & Steffgen, J. (2006). Drugs and Drug Administration in Extreme Environments. *Journal of Travel Medicine*, 13(1), 35-47. doi:10.1111/j.1708-8305.2006.00007.x
- Kwak, N., Okamoto, N., Wood, J. M., & Campochiaro, P. A. (2000). VEGF is major stimulator in model of choroidal neovascularization. *Investigative Ophthalmology & Visual Science*, 41(10), 3158-3164.
- Lackey, K. (2008). *Gene Family Targeted Molecular Design*: Wiley.
- Lee, H. (2014). *Pharmaceutical Industry Practices on Genotoxic Impurities*: CRC Press.
- Lee, P. K. (2009). US Patent No. WO2009054841A2.
- Lee, Y.-C., Zocharski, P. D., & Samas, B. (2003). An intravenous formulation decision tree for discovery compound formulation development. *International Journal of Pharmaceutics*, 253(1), 111-119. doi:https://doi.org/10.1016/S0378-5173(02)00704-4

- Li, J., Chu, M. K., Lu, B., Mirzaie, S., Chen, K., Gordijo, C. R., . . . Wu, X. Y. (2017). Enhancing thermal stability of a highly concentrated insulin formulation with Pluronic F-127 for long-term use in microfabricated implantable devices. *Drug Delivery and Translational Research*, 7(4), 529-543. doi:10.1007/s13346-017-0381-8
- Lieberman, H., & Murti Vemuri, N. (2015). Chapter 32 - Chemical and Physicochemical Approaches to Solve Formulation Problems. In C. G. Wermuth, D. Aldous, P. Raboisson, & D. Rognan (Eds.), *The Practice of Medicinal Chemistry (Fourth Edition)* (pp. 767-791). San Diego: Academic Press.
- Lin, N., & Dufresne, A. (2013). Supramolecular hydrogels from in situ host-guest inclusion between chemically modified cellulose nanocrystals and cyclodextrin. *Biomacromolecules*, 14(3), 871-880. doi:10.1021/bm301955k
- Liu, E., Morimoto, M., Kitajima, S., Koike, T., Yu, Y., Shiiki, H., . . . Fan, J. (2007). Increased expression of vascular endothelial growth factor in kidney leads to progressive impairment of glomerular functions. *Journal of the American Society of Nephrology*, 18(7), 2094-2104. doi:10.1681/asn.2006010075
- Liu, L., & Guo, Q.-X. (2002). The Driving Forces in the Inclusion Complexation of Cyclodextrins. *Journal of inclusion phenomena and macrocyclic chemistry*, 42(1), 1-14. doi:10.1023/A:1014520830813
- Loftsson, T. (2014a). *Drug Stability for Pharmaceutical Scientists*.
- Loftsson, T. (2014b). Self-assembled cyclodextrin nanoparticles and drug delivery. *Journal of inclusion phenomena and macrocyclic chemistry*, 80(1), 1-7. doi:10.1007/s10847-013-0375-1
- Loftsson, T., & Brewster, M. E. (1996). Pharmaceutical Applications of Cyclodextrins. 1. Drug Solubilization and Stabilization. *Journal of Pharmaceutical Sciences*, 85(10), 1017-1025. doi:https://doi.org/10.1021/js950534b
- Loftsson, T., & Brewster, M. E. (2010). Pharmaceutical applications of cyclodextrins: basic science and product development. *Journal of Pharmacy and Pharmacology*, 62(11), 1607-1621. doi:10.1111/j.2042-7158.2010.01030.x
- Loftsson, T., & Brewster, M. E. (2012). Cyclodextrins as functional excipients: methods to enhance complexation efficiency. *Journal of Pharmaceutical Sciences*, 101(9), 3019-3032. doi:10.1002/jps.23077
- Loftsson, T., & Duchêne, D. (2007). Cyclodextrins and their pharmaceutical applications. *International Journal of Pharmaceutics*, 329(1), 1-11. doi:https://doi.org/10.1016/j.ijpharm.2006.10.044

- Loftsson, T., Frikdriksdóttir, H., Sigurkdardóttir, A. M., & Ueda, H. (1994). The effect of water-soluble polymers on drug-cyclodextrin complexation. *International Journal of Pharmaceutics*, 110(2), 169-177. doi:[https://doi.org/10.1016/0378-5173\(94\)90155-4](https://doi.org/10.1016/0378-5173(94)90155-4)
- Loftsson, T., Hreinsdóttir, D., & Másson, M. (2005). Evaluation of cyclodextrin solubilization of drugs. *International Journal of Pharmaceutics*, 302(1), 18-28. doi:<https://doi.org/10.1016/j.ijpharm.2005.05.042>
- Loftsson, T., Hreinsdóttir, D., & Stefánsson, E. (2007). Cyclodextrin microparticles for drug delivery to the posterior segment of the eye: aqueous dexamethasone eye drops. *Journal of Pharmacy and Pharmacology*, 59(5), 629-635. doi:10.1211/jpp.59.5.0002
- Loftsson, T., Jarho, P., Masson, M., & Jarvinen, T. (2005). Cyclodextrins in drug delivery. *Expert Opinion on Drug Delivery*, 2(2), 335-351. doi:10.1517/17425247.2.1.335
- Loftsson, T., Leeves, N., Sigurjonsdottir, J. F., Sigurdsson, H. H., & Masson, M. (2001). Sustained drug delivery system based on a cationic polymer and an anionic drug/cyclodextrin complex. *Pharmazie*, 56(9), 746-747.
- Loftsson, T., Magnusdottir, A., Masson, M., & Sigurjonsdottir, J. F. (2002). Self-association and cyclodextrin solubilization of drugs. *Journal of Pharmaceutical Sciences*, 91(11), 2307-2316. doi:10.1002/jps.10226
- Loftsson, T., & Masson, M. (2004). The effects of water-soluble polymers on cyclodextrins and cyclodextrin solubilization of drugs. *Journal of Drug Delivery Science and Technology*, 14(1), 35-43. doi:[https://doi.org/10.1016/S1773-2247\(04\)50003-5](https://doi.org/10.1016/S1773-2247(04)50003-5)
- Loftsson, T., Másson, M., & Brewster, M. E. (2004). Self-Association of Cyclodextrins and Cyclodextrin Complexes. *Journal of Pharmaceutical Sciences*, 93(5), 1091-1099. doi:<https://doi.org/10.1002/jps.20047>
- Loftsson, T., Matthíasson, K., & Másson, M. (2003). The effects of organic salts on the cyclodextrin solubilization of drugs. *International Journal of Pharmaceutics*, 262(1-2), 101-107. doi:10.1016/s0378-5173(03)00334-x
- Loftsson, T., Saokham, P., & Sá Couto, A. R. (2019). Self-association of cyclodextrins and cyclodextrin complexes in aqueous solutions. *International Journal of Pharmaceutics*, 560, 228-234. doi:<https://doi.org/10.1016/j.ijpharm.2019.02.004>
- Loftsson, T., Sigurdsson, H. H., Konrádsdóttir, F., Gísladóttir, S., Jansook, P., & Stefánsson, E. (2008). Topical drug delivery to the posterior segment of the eye: anatomical and physiological considerations. *Pharmazie*, 63(3), 171-179.

- Loftsson, T., & Stefansson, E. (2017). Cyclodextrins and topical drug delivery to the anterior and posterior segments of the eye. *International Journal of Pharmaceutics*, 531(2), 413-423. doi:10.1016/j.ijpharm.2017.04.010
- Loftssona, T., & Järvinen, T. (1999). Cyclodextrins in ophthalmic drug delivery. *Advanced Drug Delivery Reviews*, 36(1), 59-79. doi:10.1016/s0169-409x(98)00055-6
- Logtenberg, E. H. P., & Stein, H. N. (1986). Zeta potential and coagulation of ZnO in alcohols. *Colloids and Surfaces*, 17(3), 305-312. doi:https://doi.org/10.1016/0166-6622(86)80254-2
- Loukas, Y. L., Jayasekera, P., & Gregoriadis, G. (1995). Novel liposome-based multicomponent systems for the protection of photolabile agents. *International Journal of Pharmaceutics*, 117(1), 85-94. doi:https://doi.org/10.1016/0378-5173(94)00320-5
- Lumholdt, L. R., Holm, R., Jorgensen, E. B., & Larsen, K. L. (2012). In vitro investigations of alpha-amylase mediated hydrolysis of cyclodextrins in the presence of ibuprofen, flurbiprofen, or benzo[a]pyrene. *Carbohydrate Research*, 362, 56-61. doi:10.1016/j.carres.2012.09.018
- Luna, E. A., Vander Velde, D. G., Tait, R. J., Thompson, D. O., Rajewski, R. A., & Stella, V. J. (1997). Isolation and characterization by NMR spectroscopy of three monosubstituted 4-sulfobutyl ether derivatives of cyclomaltoheptaose (beta-cyclodextrin). *Carbohydrate Research*, 299(3), 111-118. doi:10.1016/s0008-6215(97)00006-2
- Maeda, H., Tanaka, R., & Nakayama, H. (2015). Inclusion complexes of trihexyphenidyl with natural and modified cyclodextrins. *Springerplus*, 4(1), 218. doi:10.1186/s40064-015-0986-7
- Mahadevi, A. S., & Sastry, G. N. (2013). Cation- π Interaction: Its Role and Relevance in Chemistry, Biology, and Material Science. *Chemical Reviews*, 113(3), 2100-2138. doi:10.1021/cr300222d
- Malmsten, M. (2002). *Surfactants and polymers in drug delivery*.
- Markey, S. P. (2007). CHAPTER 11 - Pathways of Drug Metabolism. In A. J. Atkinson, D. R. Abernethy, C. E. Daniels, R. L. Dedrick, & S. P. Markey (Eds.), *Principles of Clinical Pharmacology (Second Edition)* (pp. 143-162). Burlington: Academic Press.
- Marques, H. M. C., Hadgraft, J., & Kellaway, I. W. (1990). Studies of cyclodextrin inclusion complexes. I. The salbutamol-cyclodextrin complex as studied by phase solubility and DSC. *International Journal of Pharmaceutics*, 63(3), 259-266.
- Marques, H. M. C., Hadgraft, J., Kellaway, I. W., & Pugh, W. J. (1990). Studies of cyclodextrin inclusion complexes. II. Molecular modelling

- and ¹H-NMR evidence for the salbutamol- β -cyclodextrin complex. *International Journal of Pharmaceutics*, 63(3), 267-274. doi:[https://doi.org/10.1016/0378-5173\(90\)90133-O](https://doi.org/10.1016/0378-5173(90)90133-O)
- Martin, D. F., Maguire, M. G., Fine, S. L., Ying, G.-s., Jaffe, G. J., Grunwald, J. E., . . . Ferris, F. L. (2012). Ranibizumab and Bevacizumab for Treatment of Neovascular Age-related Macular Degeneration: Two-Year Results. *Ophthalmology*, 119(7), 1388-1398. doi:<https://doi.org/10.1016/j.ophtha.2012.03.053>
- Másson, M., Loftsson, T., & Stefánsson, E. (1999). How Do Cyclodextrins Enhance Drug Permeability through Biological Membranes? In (pp. 363-366).
- Meier, M., Bordignon-Luiz, M., Farmer, P., & Szpoganicz, B. (2001). The Influence of β - and γ -Cyclodextrin Cavity Size on the Association Constant with Decanoate and Octanoate Anions. *Journal of Inclusion Phenomena*, 40, 291-295. doi:10.1023/A:1012705301448
- Messner, M., Kurkov, S. V., Jansook, P., & Loftsson, T. (2010). Self-assembled cyclodextrin aggregates and nanoparticles. *International Journal of Pharmaceutics*, 387(1), 199-208. doi:<https://doi.org/10.1016/j.ijpharm.2009.11.035>
- Meyer, C., Rodrigues, E., Michels, S., Mennel, S., Schmidt, J., Helb, H.-M., . . . Eid, F. (2010). Incidence of Damage to the Crystalline Lens During Intravitreal Injections. *Journal of ocular pharmacology and therapeutics : the official journal of the Association for Ocular Pharmacology and Therapeutics*, 26, 491-495. doi:10.1089/jop.2010.0045
- Mitsuda, H., Tsuge, H., Kawai, F., & Tanaka, K. E. N. (1970). Riboflavin-Indoles Interaction in Acid Solution. *The Journal of Vitaminology*, 16(3), 215-218. doi:10.5925/jnsv1954.16.215
- Moreira, D. N., Fresno, N., Pérez-Fernández, R., Frizzo, C. P., Goya, P., Marco, C., . . . Elguero, J. (2015). Brønsted acid–base pairs of drugs as dual ionic liquids: NMR ionicity studies. *Tetrahedron*, 71(4), 676-685. doi:<https://doi.org/10.1016/j.tet.2014.12.003>
- Moutray, T., & Chakravarthy, U. (2011). Age-related macular degeneration: current treatment and future options. *Therapeutic advances in chronic disease*, 2(5), 325-331. doi:10.1177/2040622311415895
- Moya-Ortega, M., Messner, M., Jansook, P., Nielsen, T., Wintgens, V., Larsen, K., . . . Loftsson, T. (2011). Drug loading in cyclodextrin polymers: Dexamethasone model drug. *Journal OF Inclusion Phenomena and Macrocyclic Chemistry*, 69, 377-382. doi:10.1007/s10847-010-9758-8

- Muankaew, C., Jansook, P., & Loftsson, T. (2016). Evaluation of γ -cyclodextrin effect on permeation of lipophilic drugs: application of cellophane/fused octanol membrane. *Pharmaceutical Development and Technology*, 22, 562-570. doi:10.1080/10837450.2016.1180394
- Muankaew, C., Jansook, P., Stefansson, E., & Loftsson, T. (2014). Effect of gamma-cyclodextrin on solubilization and complexation of irbesartan: influence of pH and excipients. *International Journal of Pharmaceutics*, 474(1-2), 80-90. doi:10.1016/j.ijpharm.2014.08.013
- Munro, I. C., Newberne, P. M., Young, V. R., & Bar, A. (2004). Safety assessment of gamma-cyclodextrin. *Regulatory Toxicology and Pharmacology*, 39 Suppl 1, S3-13. doi:10.1016/j.yrtph.2004.05.008
- Mura, P., Faucci, M. T., & Bettinetti, G. P. (2001). The influence of polyvinylpyrrolidone on naproxen complexation with hydroxypropyl-beta-cyclodextrin. *European Journal of Pharmaceutical Sciences*, 13(2), 187-194.
- Mura, P., Faucci, M. T., Manderioli, A., & Bramanti, G. (2001). Multicomponent Systems of Econazole with Hydroxyacids and Cyclodextrins. *Journal of inclusion phenomena and macrocyclic chemistry*, 39(1), 131-138. doi:10.1023/A:1008114411503
- NCBI. (2019). PubChem(Pubchem.ncbi.nlm.nih.gov). from National Center for Biotechnology Information
- Nguyen, Q. D., Das, A., Do, D. V., Dugel, P. U., Gomes, A., Holz, F. G., . . . Maurer, P. (2020). Brolucizumab: Evolution through Preclinical and Clinical Studies and the Implications for the Management of Neovascular Age-Related Macular Degeneration. *Ophthalmology*. doi:https://doi.org/10.1016/j.opthta.2019.12.031
- Niazi, S. K. (2016). *Handbook of Pharmaceutical Manufacturing Formulations: Volume Three, Liquid Products*: CRC Press.
- Nogueiras-Nieto, L., Alvarez-Lorenzo, C., Sandez-Macho, I., Concheiro, A., & Otero-Espinar, F. J. (2009). Hydrosoluble cyclodextrin/poloxamer polypseudorotaxanes at the air/water interface, in bulk solution, and in the gel state. *Journal of Physical Chemistry B*, 113(9), 2773-2782. doi:10.1021/jp809806w
- Nogueiras-Nieto, L., Sobarzo-Sanchez, E., Gomez-Amoza, J. L., & Otero-Espinar, F. J. (2012). Competitive displacement of drugs from cyclodextrin inclusion complex by polypseudorotaxane formation with poloxamer: implications in drug solubilization and delivery. *European Journal of Pharmaceutics and Biopharmaceutics*, 80(3), 585-595. doi:10.1016/j.ejpb.2011.12.001
- Parfitt, G. D., & Barnes, H. A. (1992). Chapter 6 - The dispersion of fine particles in liquid media. In N. Harnby, M. F. Edwards, & A. W.

- Nienow (Eds.), *Mixing in the Process Industries* (pp. 99-117). Oxford: Butterworth-Heinemann.
- Pate, K., & Safier, P. (2016). 12 - Chemical metrology methods for CMP quality. In S. Babu (Ed.), *Advances in Chemical Mechanical Planarization (CMP)* (pp. 299-325): Woodhead Publishing.
- Patel, A., Cholkar, K., Agrahari, V., & Mitra, A. K. (2013). Ocular drug delivery systems: An overview. *World journal of pharmacology*, 2(2), 47-64. doi:10.5497/wjp.v2.i2.47
- Patil, D. T., Bhattar, S. L., Kolekar, G. B., & Patil, S. R. (2011). Spectrofluorimetric Studies of the Interaction Between Quinine Sulfate and Riboflavin. *Journal of Solution Chemistry*, 40(2), 211-223. doi:10.1007/s10953-010-9643-5
- Pessine, F., Calderini, A., & Alexandrino, G. (2012). Review: Cyclodextrin Inclusion Complexes Probed by NMR Techniques. In.
- Pinto, J. T., & Zempleni, J. (2016). Riboflavin. *Advances in Nutrition*, 7(5), 973-975. doi:10.3945/an.116.012716
- Praphanwittaya, P., Saokham, P., Jansook, P., & Loftsson, T. (2020a). Aqueous solubility of kinase inhibitors: I the effect of hydrophilic polymers on their γ -cyclodextrin solubilization. *Journal of Drug Delivery Science and Technology*, 55, 101462. doi:https://doi.org/10.1016/j.jddst.2019.101462
- Praphanwittaya, P., Saokham, P., Jansook, P., & Loftsson, T. (2020b). Aqueous solubility of kinase inhibitors: II the effect of hexadimethrine bromide on the dovitinib/ γ -cyclodextrin complexation. *Journal of Drug Delivery Science and Technology*, 55, 101463. doi:https://doi.org/10.1016/j.jddst.2019.101463
- Puskás, I., Schrott, M., Malanga, M., & Szente, L. (2013). Characterization and control of the aggregation behavior of cyclodextrins. *Journal of inclusion phenomena and macrocyclic chemistry*, 75(3), 269-276. doi:10.1007/s10847-012-0127-7
- Qiu, N., Li, X., & Liu, J. (2017). Application of cyclodextrins in cancer treatment. *Journal of inclusion phenomena and macrocyclic chemistry*, 89(3-4), 229-246. doi:10.1007/s10847-017-0752-2
- Rabinovich-Guilatt, L., Couvreur, P., Lambert, G., & Dubernet, C. (2004). Cationic Vectors in Ocular Drug Delivery. *Journal of drug targeting*, 12, 623-633. doi:10.1080/10611860400015910
- Raphael, K. L., Murphy, R. A., Shlipak, M. G., Satterfield, S., Huston, H. K., Sebastian, A., . . . Fried, L. F. (2016). Bicarbonate Concentration, Acid-Base Status, and Mortality in the Health, Aging, and Body Composition Study. *Clinical Journal of the American Society of Nephrology*, 11(2), 308-316. doi:10.2215/cjn.06200615

- Reddy, A. S., & Sastry, G. N. (2005). Cation [M = H⁺, Li⁺, Na⁺, K⁺, Ca²⁺, Mg²⁺, NH₄⁺, and NMe₄⁺] Interactions with the Aromatic Motifs of Naturally Occurring Amino Acids: A Theoretical Study. *The Journal of Physical Chemistry A*, 109(39), 8893-8903. doi:10.1021/jp0525179
- Reddy, E. P., & Aggarwal, A. K. (2012). The ins and outs of bcr-abl inhibition. *Genes & cancer*, 3(5-6), 447-454. doi:10.1177/1947601912462126
- Redenti, E., Szente, L., & Szejtli, J. (2000). Drug/cyclodextrin/hydroxy acid multicomponent systems. Properties and pharmaceutical applications. *Journal of Pharmaceutical Sciences*, 89(1), 1-8. doi:10.1002/(sici)1520-6017(200001)89:1<1::Aid-jps1>3.0.Co;2-w
- Rho, C. R., Kang, S., Park, K. C., Yang, K.-J., Choi, H., & Cho, W.-K. (2015). Antiangiogenic effects of topically administered multiple kinase inhibitor, motesanib (AMG 706), on experimental choroidal neovascularization in mice. *Journal of ocular pharmacology and therapeutics : the official journal of the Association for Ocular Pharmacology and Therapeutics*, 31(1), 25-31. doi:10.1089/jop.2014.0023
- Ribeiro, L., Carvalho, R. A., Ferreira, D. C., & Veiga, F. J. (2005). Multicomponent complex formation between vinpocetine, cyclodextrins, tartaric acid and water-soluble polymers monitored by NMR and solubility studies. *European Journal of Pharmaceutical Sciences*, 24(1), 1-13. doi:10.1016/j.ejps.2004.09.003
- Ribeiro, L. S., Ferreira, D. C., & Veiga, F. J. (2003). Physicochemical investigation of the effects of water-soluble polymers on vinpocetine complexation with beta-cyclodextrin and its sulfobutyl ether derivative in solution and solid state. *European Journal of Pharmaceutical Sciences*, 20(3), 253-266.
- Robinson, R. A., & Stokes, R. H. (2002). *Electrolyte Solutions: Second Revised Edition*: Dover Publications.
- Rodrigues, G. A., Lutz, D., Shen, J., Yuan, X., Shen, H., Cunningham, J., & Rivers, H. M. (2018). Topical Drug Delivery to the Posterior Segment of the Eye: Addressing the Challenge of Preclinical to Clinical Translation. *Pharm Res*, 35(12), 245. doi:10.1007/s11095-018-2519-x
- Rosenfeld, P. J., Brown, D. M., Heier, J. S., Boyer, D. S., Kaiser, P. K., Chung, C. Y., & Kim, R. Y. (2006). Ranibizumab for neovascular age-related macular degeneration. *The New England journal of medicine*, 355(14), 1419-1431. doi:10.1056/NEJMoa054481
- Rowe, R. C., Sheskey, P. J., Quinn, M. E., & Association, A. P. (2009). *Handbook of pharmaceutical excipients* (R. C. Rowe, P. J. Sheskey, & M. E. Quinn Eds. 6th ed. ed.): London ; Chicago : Washington, DC : Pharmaceutical Press ; American Pharmacists Association.

- Ryzhakov, A., Do Thi, T., Stappaerts, J., Bertoletti, L., Kimpe, K., Sa Couto, A. R., . . . Loftsson, T. (2016). Self-Assembly of Cyclodextrins and Their Complexes in Aqueous Solutions. *Journal of Pharmaceutical Sciences*, *105*(9), 2556-2569. doi:10.1016/j.xphs.2016.01.019
- Sá Couto, A. R., Ryzhakov, A., & Loftsson, T. (2018). Disruption of α - and γ -cyclodextrin aggregates promoted by chaotropic agent (urea). *Journal of Drug Delivery Science and Technology*, *48*, 209-214. doi:https://doi.org/10.1016/j.jddst.2018.09.015
- Sahoo, S. K., Dilnawaz, F., & Krishnakumar, S. (2008). Nanotechnology in ocular drug delivery. *Drug Discovery Today*, *13*(3), 144-151. doi:https://doi.org/10.1016/j.drudis.2007.10.021
- Salimiaghdam, N., Riazi-Esfahani, M., Fukuhara, P., Schneider, K., & Kenney, C. (2019). Age-related Macular Degeneration (AMD): A Review on its Epidemiology and Risk Factors. *The Open Ophthalmology Journal*, *13*, 90-99. doi:10.2174/1874364101913010090
- Sambasevam, K. P., Mohamad, S., Sarih, N. M., & Ismail, N. A. (2013). Synthesis and Characterization of the Inclusion Complex of beta-cyclodextrin and Azomethine. *International Journal of Molecular Sciences*, *14*(2), 3671-3682. doi:10.3390/ijms14023671
- Saokham, P., & Loftsson, T. (2015). A New Approach for Quantitative Determination of γ -Cyclodextrin in Aqueous Solutions: Application in Aggregate Determinations and Solubility in Hydrocortisone/ γ -Cyclodextrin Inclusion Complex. *Journal of Pharmaceutical Sciences*, *104*(11), 3925-3933. doi:https://doi.org/10.1002/jps.24608
- Saokham, P., & Loftsson, T. (2017). γ -Cyclodextrin. *International Journal of Pharmaceutics*, *516*(1), 278-292. doi:https://doi.org/10.1016/j.ijpharm.2016.10.062
- Saokham, P., Muankaew, C., Jansook, P., & Loftsson, T. (2018). Solubility of Cyclodextrins and Drug/Cyclodextrin Complexes. *Molecules*, *23*(5). doi:10.3390/molecules23051161
- Schneider, H. J., Hacket, F., Rudiger, V., & Ikeda, H. (1998). NMR Studies of Cyclodextrins and Cyclodextrin Complexes. *Chemical Reviews*, *98*(5), 1755-1786.
- Serajuddin, A. T. (2007). Salt formation to improve drug solubility. *Advanced Drug Delivery Reviews*, *59*(7), 603-616. doi:10.1016/j.addr.2007.05.010
- Shukla, D., & Trout, B. L. (2010). Interaction of arginine with proteins and the mechanism by which it inhibits aggregation. *Journal of Physical Chemistry B*, *114*(42), 13426-13438. doi:10.1021/jp108399g

- Sigurdsson, H. H., Knudsen, E., Loftsson, T., Leeves, N., Sigurjonsdottir, J. F., & Másson, M. (2002). Mucoadhesive Sustained Drug Delivery System Based on Cationic Polymer and Anionic Cyclodextrin/Triclosan Complex. *Journal of inclusion phenomena and macrocyclic chemistry*, 44(1), 169-172. doi:10.1023/A:1023098730627
- Sigurdsson, H. H., Konráethsdóttir, F., Loftsson, T., & Stefánsson, E. (2007). Topical and systemic absorption in delivery of dexamethasone to the anterior and posterior segments of the eye. *Acta Ophthalmologica Scandinavica*, 85(6), 598-602. doi:10.1111/j.1600-0420.2007.00885.x
- Soubrane, G., Coscas, G. J., & Voigt, M. (2010). CHAPTER 1 - Evolving knowledge in pharmacologic treatments. In Q. D. Nguyen, E. B. Rodrigues, M. E. Farah, & W. F. Mieler (Eds.), *Retinal Pharmacotherapy* (pp. 1-4). Edinburgh: W.B. Saunders.
- Stetefeld, J., McKenna, S. A., & Patel, T. R. (2016). Dynamic light scattering: a practical guide and applications in biomedical sciences. *Biophysical Reviews*, 8(4), 409-427. doi:10.1007/s12551-016-0218-6
- Stewart, M. W., Grippon, S., & Kirkpatrick, P. (2012). Aflibercept. *Nature Reviews Drug Discovery*, 11(4), 269-270. doi:10.1038/nrd3700
- Subrizi, A., del Amo, E. M., Korzhikov-Vlakh, V., Tennikova, T., Ruponen, M., & Urtti, A. (2019). Design principles of ocular drug delivery systems: importance of drug payload, release rate, and material properties. *Drug Discovery Today*, 24(8), 1446-1457. doi:https://doi.org/10.1016/j.drudis.2019.02.001
- Suebsuwong, C., Pinkas, D. M., Ray, S. S., Bufton, J. C., Dai, B., Bullock, A. N., . . . Cuny, G. D. (2018). Activation loop targeting strategy for design of receptor-interacting protein kinase 2 (RIPK2) inhibitors. *Bioorganic & medicinal chemistry letters*, 28(4), 577-583. doi:10.1016/j.bmcl.2018.01.044
- Surber, C., Abels, C., & Maibach, H. (2018). *pH of the Skin: Issues and Challenges*: S. Karger AG.
- Sweeney, T. E., & Beuchat, C. A. (1993). Limitations of methods of osmometry: measuring the osmolality of biological fluids. *American Journal of Physiology*, 264(3 Pt 2), R469-480. doi:10.1152/ajpregu.1993.264.3.R469
- Szente, L., Szejtli, J., & Kis, G. L. (1998). Spontaneous Opalescence of Aqueous γ -Cyclodextrin Solutions: Complex Formation or Self-Aggregation? *Journal of Pharmaceutical Sciences*, 87(6), 778-781. doi:https://doi.org/10.1021/js9704341

- Takahashi, K., Saishin, Y., Saishin, Y., King, A. G., Levin, R., & Campochiaro, P. A. (2009). Suppression and regression of choroidal neovascularization by the multitargeted kinase inhibitor pazopanib. *Archives of Ophthalmology*, 127(4), 494-499. doi:10.1001/archophthalmol.2009.27
- Tang, B., Chen, Z. Z., Zhang, N., Zhang, J., & Wang, Y. (2006). Synthesis and characterization of a novel cross-linking complex of beta-cyclodextrin-o-vanillin furfuralhydrazone and highly selective spectrofluorimetric determination of trace gallium. *Talanta*, 68(3), 575-580. doi:10.1016/j.talanta.2005.04.070
- Tang, W., McCormick, A., Li, J., & Masson, E. (2017). Clinical Pharmacokinetics and Pharmacodynamics of Cediranib. *Clinical Pharmacokinetics*, 56(7), 689-702. doi:10.1007/s40262-016-0488-y
- Terekhova, I. V., Koźbiał, M., Kumeev, R. S., & Alper, G. A. (2011). Inclusion Complex Formation Between Modified Cyclodextrins and Riboflavin and Alloxazine in Aqueous Solution. *Journal of Solution Chemistry*, 40(8), 1435. doi:10.1007/s10953-011-9724-0
- Thakur, A., Scheinman, R. I., Rao, V. R., & Kompella, U. B. (2011). Pazopanib, a multitargeted tyrosine kinase inhibitor, reduces diabetic retinal vascular leukostasis and leakage. *Microvascular Research*, 82(3), 346-350. doi:10.1016/j.mvr.2011.09.001
- Thomas, G. (2011). *Medicinal Chemistry: An Introduction*: Wiley.
- Tietz, J., Spohn, G., Schmid, G., Konrad, J., Jampen, S., Maurer, P., . . . Escher, D. (2015). Affinity and Potency of RTH258 (ESBA1008), a Novel Inhibitor of Vascular Endothelial Growth Factor A for the Treatment of Retinal Disorders. *Investigative Ophthalmology & Visual Science*, 56(7), 1501-1501.
- Tiwari, G., Tiwari, R., & Rai, A. K. (2010). Cyclodextrins in delivery systems: Applications. *Journal of pharmacy & bioallied sciences*, 2(2), 72-79. doi:10.4103/0975-7406.67003
- Tong, W. Q., & Whitesell, G. (1998). In situ salt screening--a useful technique for discovery support and preformulation studies. *Pharmaceutical Development and Technology*, 3(2), 215-223. doi:10.3109/10837459809028498
- Tóth, G., Jánoska, Á., Szabó, Z.-I., Völgyi, G., Orgován, G., Szenté, L., & Noszál, B. (2016). Physicochemical characterisation and cyclodextrin complexation of erlotinib. *Supramolecular Chemistry*, 28(7-8), 656-664. doi:10.1080/10610278.2015.1117083
- Tóth, G., Jánoska, Á., Völgyi, G., Szabó, Z. I., Orgován, G., & Mirzahassemi, A. (2017). Physicochemical characterization and cyclodextrin

- complexation of the anticancer drug lapatinib. *Journal of Chemistry*. doi:10.1155/2017/4537632.
- Traynor, K. (2012). Afibercept approved for macular degeneration. *American Journal of Health-System Pharmacy*, 69(1), 6-6. doi:10.2146/news120001
- Ueno, A., Takahashi, K., & Osa, T. (1981). Photocontrol of catalytic activity of capped cyclodextrin. *Journal of the Chemical Society, Chemical Communications*(3), 94-96. doi:10.1039/C39810000094
- Veiga, F., Pecorelli, C., & Ribeiro, L. (2006). *As ciclodextrinas em tecnologia farmacêutica*: MinervaCoimbra
- Veiga, F. J., Fernandes, C. M., Carvalho, R. A., & Geraldes, C. F. (2001). Molecular modelling and ¹H-NMR: ultimate tools for the investigation of tolbutamide: beta-cyclodextrin and tolbutamide: hydroxypropyl-beta-cyclodextrin complexes. *Chemical & pharmaceutical bulletin*, 49(10), 1251-1256.
- Viernstein, H., Weiss-Greiler, P., & Wolschann, P. (2003). Solubility enhancement of low soluble biologically active compounds—temperature and cosolvent dependent inclusion complexation. *International Journal of Pharmaceutics*, 256(1), 85-94. doi:https://doi.org/10.1016/S0378-5173(03)00065-6
- Waterman, K. C., Adami, R. C., Alsante, K. M., Hong, J., Landis, M. S., Lombardo, F., & Roberts, C. J. (2002). Stabilization of Pharmaceuticals to Oxidative Degradation. *Pharmaceutical Development and Technology*, 7(1), 1-32. doi:10.1081/PDT-120002237
- Waugh, A., & Grant, A. (2007). *Anatomy and Physiology in Health and Illness* (Vol. 10th edition). Philadelphia, Pa, USA: Churchill Livingstone Elsevier.
- Weisberg, E., Choi, H. G., Ray, A., Barrett, R., Zhang, J., Sim, T., . . . Griffin, J. D. (2010). Discovery of a small-molecule type II inhibitor of wild-type and gatekeeper mutants of BCR-ABL, PDGFRalpha, Kit, and Src kinases: novel type II inhibitor of gatekeeper mutants. *Blood*, 115(21), 4206-4216. doi:10.1182/blood-2009-11-251751
- Xiao-ming, C. (2011). Inclusion Complex of β-cyclodextrin with CTAB in Aqueous Solution. *Chinese Journal of Chemical Physics*, 24(4), 484.
- Xu, P., Zheng, Y., Zhu, X., Li, S., & Zhou, C. (2018). L-lysine and L-arginine inhibit the oxidation of lipids and proteins of emulsion sausage by chelating iron ion and scavenging radical. *Asian-Australasian journal of animal sciences*, 31(6), 905-913. doi:10.5713/ajas.17.0617
- Yoshioka, S., & Stella, V. J. (2007). *Stability of Drugs and Dosage Forms*: Springer US.

- Zabiszak, M., Nowak, M., Taras-Goslinska, K., Kaczmarek, M. T., Hnatejko, Z., & Jastrzab, R. (2018). Carboxyl groups of citric acid in the process of complex formation with bivalent and trivalent metal ions in biological systems. *Journal of Inorganic Biochemistry*, 182, 37-47. doi:<https://doi.org/10.1016/j.jinorgbio.2018.01.017>
- Zelenina, T. E., & Zelenin, O. Y. (2005). Complexation of citric and tartaric acids with Na and K ions in aqueous solution. *Russian Journal of Coordination Chemistry*, 31(4), 235-242. doi:10.1007/s11173-005-0083-5
- Zhang, L., Wu, F., Lee, S. C., Zhao, H., & Zhang, L. (2014). pH-dependent drug-drug interactions for weak base drugs: potential implications for new drug development. *Clinical Pharmacology & Therapeutics*, 96(2), 266-277. doi:10.1038/clpt.2014.87
- Zhao, R., Tan, T., & Sandstrom, C. (2011). NMR studies on puerarin and its interaction with beta-cyclodextrin. *Journal of Biological Physics*, 37(4), 387-400. doi:10.1007/s10867-011-9221-0
- Zhao, X., Zhu, S., Song, Y., Zhang, J., & Yang, B. (2015). Thermal responsive fluorescent nanocomposites based on carbon dots. *RSC Advances*, 5(20), 15187-15193. doi:10.1039/C4RA13417F
- Zhou, G., & Yang, J. C. (2004). In situ UHV-TEM investigation of the kinetics of initial stages of oxidation on the roughened Cu(110) surface. *Surface Science*, 559(2), 100-110. doi:<https://doi.org/10.1016/j.susc.2004.04.046>
- Zhou, X., Shi, K., Hao, Y., Yang, C., Zha, R., Yi, C., & Qian, Z. (2020). Advances in nanotechnology-based delivery systems for EGFR tyrosine kinases inhibitors in cancer therapy. *Asian Journal of Pharmaceutical Sciences*, 15(1), 26-41. doi:<https://doi.org/10.1016/j.ajps.2019.06.001>
- Zimmermann, T., Höchel, J., Becka, M., Boettger, M. K., Rohde, B., Schug, B., . . . Donath, F. (2018). Topical administration of regorafenib eye drops: phase I dose-escalation study in healthy volunteers. *British Journal of Clinical Pharmacology*, 84(5), 865-875. doi:10.1111/bcp.13502
- Zlotogorski, A. (1987). Distribution of skin surface pH on the forehead and cheek of adults. *Archives of Dermatological Research*, 279(6), 398-401.
- Zornoza, A., Martín, C., Sánchez, M., Vélaz, I., & Piquer, A. (1998). Inclusion complexation of glisentide with α -, β - and γ -cyclodextrins. *International Journal of Pharmaceutics*, 169(2), 239-244. doi:[https://doi.org/10.1016/S0378-5173\(98\)00124-0](https://doi.org/10.1016/S0378-5173(98)00124-0)

Paper I



Aqueous solubility of kinase inhibitors: I the effect of hydrophilic polymers on their γ -cyclodextrin solubilization

Pitsiree Praphanwittaya^a, Phennapha Saokham^b, Phatsawee Jansook^c, Thorsteinn Loftsson^{a,*}

^a Faculty of Pharmaceutical Sciences, University of Iceland, Hofsvallagata 53, IS-107, Reykjavik, Iceland

^b Department of Manufacturing Pharmacy, Faculty of Pharmacy, Rangsit University, Pathum Thani, 12000, Thailand

^c Faculty of Pharmaceutical Sciences, Chulalongkorn University, 254 Payathai Road, Pathumwan, Bangkok, 10330, Thailand

ARTICLE INFO

Keywords:

Kinase inhibitor
 γ -Cyclodextrin
 Complexation
 Complexation efficacy
 Polymer
 Solubility

ABSTRACT

Most small-molecule protein kinase inhibitors (KIs) are neutral or weakly basic lipophilic compounds with very poor solubility in aqueous media that decreases their ability to permeate biological membranes from an aqueous exterior and consequently bestow them with low bioavailability after oral and topical administration. Cyclodextrin (CD) complexation can increase water-solubility of poorly soluble drugs without affecting their ability to permeate biological membranes. The aim of the present study was to enhance aqueous solubility of six KIs that is axitinib, cediranib, dovitinib, motesanib, pazopanib and regorafenib, through formation of drug/ γ -cyclodextrin (γ CD)/polymer ternary complexes. The complexes were prepared in an aqueous environment by heating technique. The phase-solubility profiles showed formation of binary KI/ γ CD complexes of B_s-type. γ CD alone had significant solubilizing effect on dovitinib (stability constant ($K_{1:1}$) = 684 M⁻¹ and complexation efficacy (CE) = 0.011). The aqueous solubility of the binary KI/ γ CD complexes was pH-dependent. Hexadimethrine bromide (HDMBr) was the most effective polymer of the ones tested. The ternary complexes formed nano-sized aggregates with diameter between 200 and 400 nm. Osmolarity and pH were also monitored. TEM study showed formation of complex aggregates in aqueous media.

1. Introduction

In general, protein kinase inhibitors are neutral or weakly basic lipophilic compounds with very poor solubility in aqueous media and are classified as Class II (i.e. high permeability, low solubility) or Class IV (i.e. low permeability, low solubility) drugs according to the Biopharmaceutics Classification System [2,46]. In other words, the relatively high lipophilicity and low aqueous solubility of the small-molecule protein kinase inhibitors decreases their ability to permeate biological membranes from an aqueous exterior (e.g., from the aqueous tear fluid into the eye) and consequently bestow them with low bioavailability after oral and topical administration.

Small-molecule protein kinase inhibitors (KIs) have been shown to play a role in virtually all major disease areas [14,21]. For example, in a list of FDA-approved oncology drugs axitinib and pazopanib are used to treat advanced renal cell carcinoma (ARCC) [3,49,55] while regorafenib has been approved for treatment of metastatic colorectal cancer and gastrointestinal stromal tumor [16,49]. However, most small molecule KIs are practically insoluble in aqueous media with intrinsic solubility in the low μ g/ml range [43]. Their low intrinsic solubility

decreases their ability to permeate biological membranes and consequently bestow them with somewhat low bioavailability after oral and topical administration. In general, biomembranes are lipophilic with hydrophilic exterior. For example, mucous membrane (mucosa) consists of epithelial cell layers that form a lipophilic permeation barrier. The exterior of this lipophilic membrane is frequently protected with mucus, a viscous aqueous layer, which forms an aqueous permeation barrier. Thus, the permeating drug molecules must be hydrophilic and water-soluble to be able to permeate the mucus layer but at the same time, they must possess some lipophilicity to be able to permeate the epithelial cell layers. For successful topical and oral administration, the aqueous solubility of poorly soluble KIs has to be increased without affecting their lipophilic characteristics. This can be achieved by various formulation techniques such as through the use of surface-active compounds or complexing agents. Here cyclodextrins (CDs) are investigated as solubilizing complexing agents. Many studies have shown that CDs can be used to enhance water-solubility of KIs such as erlotinib, lapatinib and gefitinib [12,40,53,54]. Physicochemical properties, such as the melting point (T_m) and logP, are generally considered during selection of promising drug candidates for formulation

* Corresponding author.

E-mail address: thorstlo@hi.is (T. Loftsson).

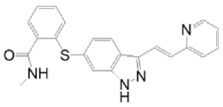
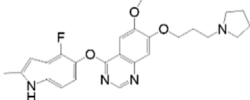
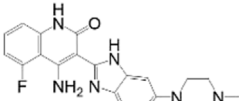
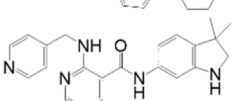
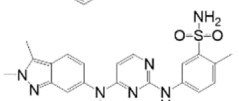
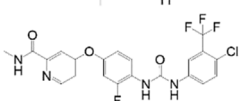
<https://doi.org/10.1016/j.jddst.2019.101462>

Received 31 October 2019; Received in revised form 9 December 2019; Accepted 10 December 2019

Available online 14 December 2019

1773-2247/ © 2019 Elsevier B.V. All rights reserved.

Table 1
The structure, physicochemical properties, and bioavailability of the KIs [1].

| Composition | Chemical structure | MW | Melting point (° C) | Log P _{o/w} ^a | pK _a ^b | S _o (µg/mL) in water ^c | S _o (µg/mL) in water ^d | BA ^e (%) |
|-------------|---|--------|---------------------|-----------------------------------|------------------------------|--|--|---------------------|
| Axitinib |  | 386.47 | 184–282 | 2.4 | 4.3 | 40 | 0.37 | 58 |
| Cediranib |  | 450.51 | 158–257 | 0.8 | 10.1 | 190 | 1154.63 | ND ^f |
| Dovitinib |  | 392.43 | 285–310 | 0.48 | 7.7 | 350 | 6.34 | ND ^f |
| Motesanib |  | 373.45 | 140–151 | 3.9 | 5.2 | 12 | 13.98 | ND ^f |
| Pazopanib |  | 437.52 | 285–289 | 3.1 | 5.6 | 1.7 | 0.55 | 14–39 |
| Regorafenib |  | 482.82 | 141–206 | 4.2 | 2.3 | 0.13 | 0.12 | 69 |

^a Calculated octanol-water partition coefficient at pH 7 and 25 °C.

^b Calculated value of the protonated base at 25 °C.

^c Calculated solubility at pH 7 and 25 °C.

^d Experimental solubility at approximately pH 6.5 and 22–23 °C.

^e Mean absolute bioavailability in human after oral administration [8,9,15,52].

^f No data available.

development [4]. T_m is a characteristic of crystal lattice energy involving solvate molecules while logP is the octanol-water partition coefficient [11]. High T_m and log P values usually results in limited aqueous solubility [5,48]. Ditzinger et al. investigated logP as a function of T_m and showed that commercial drugs formulated with CDs tend to have a logP value from 2 to 4.5 and a T_m between 473 and 573 K or between 200 and 300 °C (Ditzinger et al., 2019). Thus, in KI candidates in the mid-range spectrum of these limits were selected for this study as listed in Table 1.

CDs are cyclic torus-shaped oligosaccharides with a hydrophobic central cavity and hydrophilic exterior [19]. Monographs for the three natural CDs, that is α -cyclodextrin (α CD), β -cyclodextrin (β CD) and γ -cyclodextrin (γ CD), are in all major pharmacopoeias and they are on FDA's generally recognized as safe (GRAS) list of food additives. Essentially only γ CD is susceptible to hydrolysis catalyzed by human α -amylase that is found in the tear fluid, saliva, and gastrointestinal tract [32]. γ CD induced changes of the human erythrocyte shape and cytotoxicity less than both α CD and β CD in *in vitro* study [23,39]. Of the three CDs, γ CD has the most favorable toxicological profile [47]. γ CD has a relatively large hydrophobic central cavity that can accommodate a wide range of molecular structures such as KIs. In aqueous solutions, drug/ γ CD complexes have tendency to form nano-size aggregates that have been developed into effective drug delivery systems [20,29,35,47]. Water-soluble CD derivatives, such as HP β CD (2-hydroxypropyl- β CD), RM β CD (randomly methylated β CD), HP γ CD (2-hydroxypropyl- γ CD), do also form such aggregates but most have relatively low tendency to form aggregates in dilute aqueous solutions [19,47]. For this study the natural γ CD was selected as a solubilizer.

The solubilizing efficacy of CDs is the product of the intrinsic drug solubility and the stability constant of the drug/CD complex [28]. In case of the KIs, the intrinsic solubility is very low. Thus, even if the

stability constant of the KI/ γ CD complex is relatively high the γ CD solubilization can be seriously hampered by the very low intrinsic solubility. Various techniques can be applied to increase the solubilizing efficacy of CDs such as drug ionization and addition of co-complexing agents [25]. Addition of a small amount of water-soluble polymer, such as water-soluble cellulose derivative, enhances formation of drug/CD complexes and, thus, increases the CD solubilization [7,31]. The increase is due to the synergistic effects of the polymer and CD on the drug solubilization through formation of ternary complex or co-complex consisting of drug, CD and polymer [18,31]. It is thought that these complexes may have different solubilizing and physicochemical properties than those of binary drug/CD complexes [7]. We will investigate the effects of various water-soluble polymers on γ CD solubilization of KIs. Six KIs were selected for this study that is axitinib, cediranib, dovitinib, motesanib, pazopanib and regorafenib.

2. Materials and methods

2.1. Materials

Axitinib (A), cediranib (C), motesanib (M), pazopanib (P), and regorafenib (R) were purchased from Molekula (Newcastle, UK) whereas dovitinib (D) was purchased from Reagents Direct (Encinitas, CA, USA). γ -Cyclodextrin (γ CD) and 2-hydroxypropyl- γ -cyclodextrin, molecular weight 1540, (HP γ CD) was purchase from Wacker Chemie (Munich, Germany). Hexadimethrine bromide $\geq 94\%$ pure by titration with molecular weight 374 kDa (HDMBR), poly (vinyl pyrrolidone) molecular weight 10 kDa (PVP), low viscosity carboxymethyl cellulose (viscosity of a 4% solution in water at 25 °C is 50–200 cps) (CMC), poloxamer 407, poly(vinyl alcohol) molecular weight 30–70 kDa (PVA), hydroxypropyl methylcellulose (HPMC), viscosity of 2%

aqueous solution at 25 °C is approximately 50 cP, poly(ethylene glycol 400) (PEG400), tyloxapol and benzalkonium chloride (BAC) were purchased from Sigma-Aldrich (St. Louis, MO, USA). Disodium edetate dihydrate (EDTA) was purchased from Merck (Darmstadt, Germany). Other reagents were commercial products of analytical grade. Milli-Q water (Millipore, Billerica, MA) was used throughout the study.

2.2. Phase-solubility studies

The aqueous solubility of the KIs was determined by a heating technique as previously described [27]. The media were unbuffered aqueous γ CD solutions and the pH was between 6.3 and 6.8. Each experiment was performed in triplicate and the values reported are the mean values \pm the standard deviation. Initial testing of KI in aqueous γ CD solutions showed up to 60% degradation during heating in an autoclave and, thus, mild heating was selected. Briefly, excess amount of the KI to be investigated was added to aqueous γ CD solutions of given concentration. The suspension formed was placed in an ultrasonic bath (Branson Branson®, CPX3800H ultrasonic bath, USA) where it was sonicated at 30 °C for 30 min to avoid thermal degradation of the drug. After cooling to room temperature (22–23 °C) the vial was opened and small amount of the pure drug added to the media to promote drug precipitation and equilibrated in a shaker (KS 15 A Shaker, EB Edmund Bühler GmbH, Germany) at room temperature under constant agitation for 7 days. Finally, the suspension was centrifuged at 12000 rpm for 15 min (Heraeus Pico 17 Centrifuge, Thermo Fisher Scientific, Germany), the supernatant diluted with Milli-Q water and analyzed by HPLC.

Phase-solubility analysis was performed according to method described by Higuchi and Connors [17]. The value of the apparent stability constant ($K_{1:1}$) (Eq. (1)) and the complexation efficiency (CE) (Eq. (2)) were calculated from slope of the initial linear portion of KI concentration against γ CD concentration profiles assuming KI- γ CD 1:1 complex formation (i.e. that the molar ration of KI and γ CD in the complex is one-to-one).

$$K_{1:1} = \frac{\text{slope}}{S_0(1 - \text{slope})} \quad (1)$$

$$CE = S_0 K_{1:1} = \frac{\text{slope}}{(1 - \text{slope})} = \frac{[\text{KI}/\gamma\text{CD complex}]}{[\gamma\text{CD}]} \quad (2)$$

where S_0 is solubility of the KI in pure water, $[\text{KI}/\gamma\text{CD complex}]$ is the concentration of dissolved complex and $[\gamma\text{CD}]$ is the concentration of dissolved γ CD in the aqueous complexation media.

2.3. pH solubility profiles

The solubilities of the KIs were determined at different pH values. Excess amount of drug was added to aqueous 5% (w/v) HP γ CD or 5% (w/v) γ CD solutions. Addition of CDs increased the very limited drug solubility and facilitated detection by HPLC. The pH ranged from 1 to 11. It was obtained by dropwise titration of the media with concentrated aqueous sodium hydroxide or hydrochloric acid solutions. The suspensions formed were treated as described in Section 2.2. The pH was constantly monitored (Thermo Orion 3 Star™ bench top pH meter, Thermo Fisher Scientific, USA) and, if necessary, corrected with those concentrated aqueous hydrochloric acid or sodium hydroxide solution during the agitation. After equilibration, samples were centrifuged, and the KI concentration in the supernatant determined HPLC. Each experiment was performed in triplicate and the values reported are the mean values \pm the standard deviation.

2.4. Ternary hydrophilic polymer complexes preparation

Ternary KI/ γ CD/polymer complexes were prepared in triplicate by adding 1% (w/v) neutral, positively charged or negatively charged

polymer to the complexation medium. The amount of γ CD dissolved in the ternary complex medium was determined from the phase solubility profiles prepared according to Section 2.2. Each KI has maximum aqueous solubility at some given γ CD concentration. This γ CD concentration of maximum KI solubility was used in the medium during the ternary complex preparation. The previously described heating technique was used to determine the KI solubility (see Section 2.2). Those ternary hydrophilic polymer complexes were determined in comparison to controls that are drug in pure water, binary drug/ γ CD complexes, and drug/ γ CD in formulation vehicle. The formulation vehicle contains 0.1% EDTA, 0.02% benzalkonium chloride, and 0.05% sodium chloride (%w/v) in pure water. Although small amounts of polymers (i.e. HMPC and PVP) enhance the drug solubility through drug/polymer complex formation in aqueous solutions [26], other investigators have shown that mixtures of polymers (e.g. CMC, HPMC, PEG and PVP) and CDs solubilize the drug more effectively than either polymers or CDs when used alone [13,31,36]. Thus, the binary drug/polymer complexes were not introduced as a control.

2.5. Determination of KI solubility in formulation vehicle

Main excipients in the formulation vehicle are EDTA and benzalkonium chloride. The effects of these excipients on the KI solubility were investigated further. From 0 to 1% (w/v) of EDTA or benzalkonium chloride was dissolved in pure water or aqueous γ CD solution and the KI solubility determined as described in Section 2.2. The γ CD concentration was that of maximum solubility of the KI to be tested (see Section 2.4). Excess amount of solid drug was added to those aqueous systems.

2.6. Quantitative determination

Quantitative determination of the different KIs was accomplished by reversed-phase high performance liquid chromatographic method (HPLC) (Dionex, Softron GmbH Ultimate 3000 series, Germany). The equipment consisted of a P680 pump with a DG-1210 degasser, an ASI-100 autosampler and VWD-3400 UV-VIS detector. The column used was Kinetex Core-shell technology C18 100A 150 \times 4.6 mm, 5 μ m column connected to guard column (Phenomenex, UK) and operated at 30 °C. The compositions of isocratic mobile phases are shown in Table 2. All HPLC methods displayed good selectivity and were operated at 1 mL/min of flow rate.

2.7. Characterization of complexes in solution state

2.7.1. pH and osmolarity

The pH values of the ternary complex media were determined by

Table 2
The chromatographic conditions.

| KI | Mobile phase | | Wavelength (nm) | Injection volume (μ L) |
|-------------|----------------------------------|------------------------------------|-----------------|-----------------------------|
| | Non-aqueous:Aqueous ^a | pH ^b Ratio ^c | | |
| Axitinib | ACN:0.1%AC | 3.45 40:60 | 337 | 20 |
| Cediranib | ACN:0.05%PA | 2.8 35:65 | 234 | 20 |
| Dovitinib | ACN:MeOH:10 mM AF buffer | 4.5 20:40:40 | 233 | 20 |
| Motesanib | ACN:10 mM AA | 6.4 55:45 | 260 | 20 |
| Pazopanib | ACN:10 mM AA | 6.4 60:40 | 270 | 20 |
| Regorafenib | ACN:MeOH:0.05% PA | 2.8 65:10:25 | 265 | 100 |

^a ACN: acetonitrile; MeOH: methanol; AC: acetic acid; PA: phosphoric acid; AF: ammonium formate; AA: ammonium acetate.

^b pH of the aqueous phase before mixing with the non-aqueous phase.

^c Volume ratio of the phases before mixing.

Thermo Orion Star TM Series pH meter (Thermo Scientific, USA) at ambient temperature (22–23 °C) and the osmolality with a Knauer K-7000 vapor pressure osmometer (Germany) operated at 25 °C.

2.7.2. Dynamic light scattering (DLS)

The particle size of ternary γ CD complex aggregates were determined by dynamic light scattering (DLS) using Nanotracs Wave particle size analyzer (Microtrac Inc., York, PA). The diluted sample was illuminated by a laser beam at wavelength of 780 nm and its intensity fluctuation in scattered lights from Brownian motion of particles was detected at known scattering angle θ of 180° at 25 ± 0.2 °C. The size population of the complexes was interpreted via following equation:

$$M_i = \frac{A_i/R_i^a}{\sum A_i/R_i^a} \times 100 \quad (3)$$

where M_i is the mass distribution percentage, A_i is the intensity area, R_i is the hydrodynamic radius of the size population i , and a is the shape parameter that equals 3, assuming spherical shaped particles [6,51].

2.7.3. Transmission electron microscopy (TEM) analysis

The morphology of selected KI/ γ CD aggregates in aqueous solutions were evaluated using Model JEM-1400 transmission electron microscope (JEOL, Tokyo, Japan). The negative straining technique was used. First, a small amount of clear liquid (i.e. the aggregate solution) was dropped on a 200 mesh coated grid and dried at 37–40 °C for 1 h. Then a drop of centrifuged 4%w/w uranyl acetate was added to the loaded grid. After 6 min of straining, the sample was dried overnight at room temperature. Finally, the strained specimen was placed in holder and inserted into the microscope.

3. Results and discussions

The structures and physicochemical properties of the six KIs selected for this study are shown in Tables 1 and 3.

3.1. Phase-solubility studies

The phase-solubility profiles in Fig. 1 shows formation of binary KI/ γ CD complexes that have limited solubility in water or, in other words, the profiles are of Bs-type. Complexation efficiency (CE) is a more accurate parameter to determine the solubilizing effect of various CDs, especially for drugs with $S_0 < 1$ mg/mL. This is mainly because the estimation of CE from phase-solubility profiles is independent of S_0 . Solubility of very poorly soluble drugs are difficult to determine since such drugs frequently form small water-soluble oligomers (aggregates) in aqueous solutions whereas generally only the dissolve monomer forms a CD complex [27]. γ CD had the highest solubilizing effect on cediranib (CE 0.0578), then dovitinib (CE 0.0110), and motesanib (CE 0.0052) (Fig. 1 and Table 4). The observed stability constant ($K_{1:1}$) should show the strength of the drug-CD interaction (Jambhekar and Breen, 2016; Loftsson et al., 2004). The calculated data in Table 4 revealed that cediranib has much less affinity ($K_{1:1}$ 23 M⁻¹) for γ CD than dovitinib ($K_{1:1}$ 684 M⁻¹) and motesanib ($K_{1:1}$ 138 M⁻¹).

3.2. pH solubility profiles

The aqueous solubility of the binary KI/ γ CD complexes was pH-dependent with a relative high solubility under acidic conditions (Fig. 2) due to the nitrogen-based heterocyclic core structure and secondary amine moieties (Herbrink et al., 2016). The ionizable nitrogen groups can acquire a positive charge from proton in acidic medium (Budha et al., 2012; Zhang et al., 2014). Both cediranib and motesanib have maximum solubility between pH 3 and 5. However, acid-induced degradation occurred in some KIs including cediranib, motesanib, and pazopanib at pH ≤ 3 (Fig. 2).

3.3. Effect of hydrophilic polymer on drug solubility

Here each solubility determination was performed at γ CD above the determined maximum KI solubility according to the phase-solubility profile (see Fig. 1). For example, dovitinib and motesanib had maximum solubility at 5% (w/v) γ CD and, thus, 8% (w/v) γ CD was selected for investigation of the ternary KI/ γ CD/polymer complex. If formation of the ternary complex provided for an effective solubilization, the observed KI solubility in the ternary complex medium should be higher than the maximum solubility of the KI in the binary complex medium.

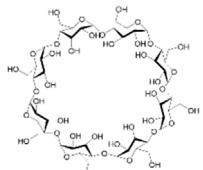
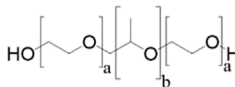
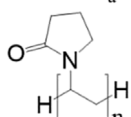
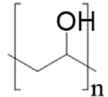
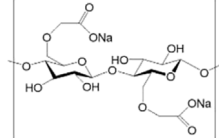
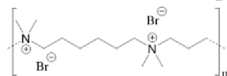
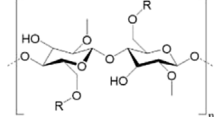
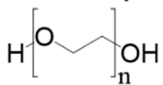
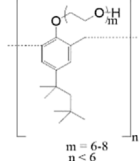
Formation of ternary complexes, either increased or decreased the KI solubility (Fig. 3, Table 5). Only HPMC could increase the solubility of pazopanib/ γ CD binary complex (52.67 μ g/mL), whereas the regorafenib/ γ CD complex was solubilized by tyloxapol (5.29 μ g/mL), yet their final solubility was rather low. Only tyloxapol and hexadimethrine bromide (HDMBr) were able to solubilize axitinib/ γ CD complex to 8.19 μ g/mL and 17.28 μ g/mL respectively. Some hydrophilic polymers slightly increased the solubility of cediranib/ γ CD binary complex. Their final solubility was relatively high or in range of mg/mL but with the exception of HDMBr where the solubility enhancement was insignificant. The solubility of the dovitinib/ γ CD complex and motesanib/ γ CD complex were mainly increased due to the synergistic effects of γ CD and the hydrophilic polymers. For example, HDMBr enhanced solubility of dovitinib to 798 μ g/mL and that of motesanib to 339 μ g/mL. In summary, HDMBr was the most effective polymer for water-soluble ternary KI/ γ CD/polymer complex formation, especially in the case of dovitinib, motesanib, axitinib, and cediranib. Formation of the dovitinib/ γ CD/HDMBr ternary complex resulted in maximum 160-fold solubility increase compared to the pure drug (Fig. 3, Table 5). HDMBr was shown to increase the solubilization efficacy of γ CD by 15% in presence of excess dexamethasone in the complexation medium [24,34]. This cationic polymer can be used at concentrations up to 3% (w/v) to promote mucoadhesive property of particulate CD-based drug delivery system without affecting the buccal mucosa [30,50]. Moreover, KIs were effectively solubilized in the control formulation vehicle. The effect of this vehicle on drug solubility is discussed further in the following section. HDMBr is a quaternary ammonium compound capable of interaction with various functions such as electron-donating moieties while tyloxapol is a nonionic surface active polymer.

Such observations led to the hypothesis that HDMBr may play the role in the KIs solubilization via cation- and electrostatic interactions. The KIs structure consists of nitrogen-based heterocyclic system (Herbrink et al., 2016). The unsaturated ring structures and amine moieties can interact with the quaternary ammonium ions, and the phenyl groups may form non-covalent bonding with the quaternary ammonium group via cation-interactions [10,10,33,42]. However, the cation-effect of the phenyl moieties could be shielded by the sulfonamide moiety in pazopanib, or the 3-fluoromethylene moiety in regorafenib. Quaternary ammonium compounds are highly water-soluble, and frequently somewhat surface active, and frequently solvate hydrophobic drug molecules (Badrinarayan and Sastry, 2011, 2012; [33]. HDMBr may also interact with KI/CD complex aggregates through formation of CD-polymer hydrogen bonds [44] or by reducing the mobility of γ CD (Veiga et al., 2006).

Interestingly, poloxamer reduces the aqueous solubility of all KIs/ γ CD in complexation media. Other investigators found that poloxamer is a competitive molecule that can displace drug molecules from the CD cavity through formation of soluble polypseudorotaxanes [37,38]. This CD-poloxamer interactions hamper drug solubilization [20].

The CE, strength of KI/ γ CD interaction, solubilizing ratio, and the maximum solubility upon ternary complex formation are all parameters that need to be considered during screening. Pazopanib and regorafenib do not readily form a complex with γ CD and the various polymers failed to increase their interaction with γ CD. Cediranib displays a relatively high CE compared to the other KIs tested, and high solubility in binary complexes and ternary complexes. However, only about 1 out of every

Table 3The structure and physicochemical properties of γ CD (i.e. the complexing agent) and the polymers (co-complexing agents) used [45].

| Compound | Chemical structure | MW | Melting point | Solubility in water at RT (mg/mL) |
|--------------------------------|---|-------------|---------------|-----------------------------------|
| γ CD |  | 1297.1 | ≥ 200 | 232 |
| Poloxamer 407 |  a = 101, b = 56 | 9840–14,600 | 53–57 | Miscible > 175 g/L |
| Poly(vinyl pyrrolidone) (PVP) |  | 10 k | 130–150 | Soluble > 130 g/L |
| poly(vinyl alcohol) (PVA) |  | 30-70 k | 180–190 | Soluble |
| Carboxymethyl cellulose (CMC) |  | 90 kDa | 300 | Soluble |
| Hexadimethrine bromide (HDMBr) |  | 374 kDa | – | Soluble 10%w/v |
| HPMC |  R = -CH ₂ CHOHCH ₃ | 17-20 k | 190–200 | Varies with the molecular weight |
| PEG400 |  | 380–420 | 4–8 | 0.232 |
| Tyloxapol |  m = 6-8 n < 6 | 298.4 | – | Miscible |

18 γ CD molecules in the complexation medium is forming a complex with cediranib [29]. Besides HDMBr, the polymers tested did not improve the CE and even in the case of HDMBr the increase was insignificant. Although axitinib had the lowest CE, it had good affinity to γ CD and so did dovitinib and motesanib (base on the $K_{1:1}$ values in Table 4). HDMBr enhanced the aqueous solubility of axitinib but it is still very slightly soluble in water. HDMBr had the highest solubilizing effect on dovitinib and motesanib and, consequently, dovitinib/ γ CD/HDMBr and motesanib/ γ CD/HDMBr ternary complexes were selected for further characterization.

3.4. Effect of formulation vehicle on drug solubility

In the previous section the effects of water-soluble polymers are described. However, it was also observed that simple aqueous formulation vehicle containing EDTA and benzalkonium chloride has significant effect on the aqueous solubilities of KIs, particularly on the solubilities of dovitinib and motesanib. Therefore, the effect of those

two excipients on KI solubility was investigated further.

EDTA and benzalkonium chloride significantly increased the aqueous solubility of pure motesanib in non-complexes system. Benzalkonium chloride had higher solubilization power in general. However, ternary complexes showed different pattern. EDTA enhanced the solubilizing effect of γ CD whereas benzalkonium chloride decreased that effect (Figs. 4 and 5). EDTA is an anionic chelating agent whereas benzalkonium chloride is a cationic surface-active antibacterial agent. EDTA is able to form salt with positively charged KIs.

3.5. Characterization of complexes in solution state

Physicochemical properties and mean particle size of pure dovitinib, pure motesanib, and their complexes in solution state are summarized in Table 6.

3.5.1. pH

The pH of human serum is between 7.35 and 7.45 [56], while the

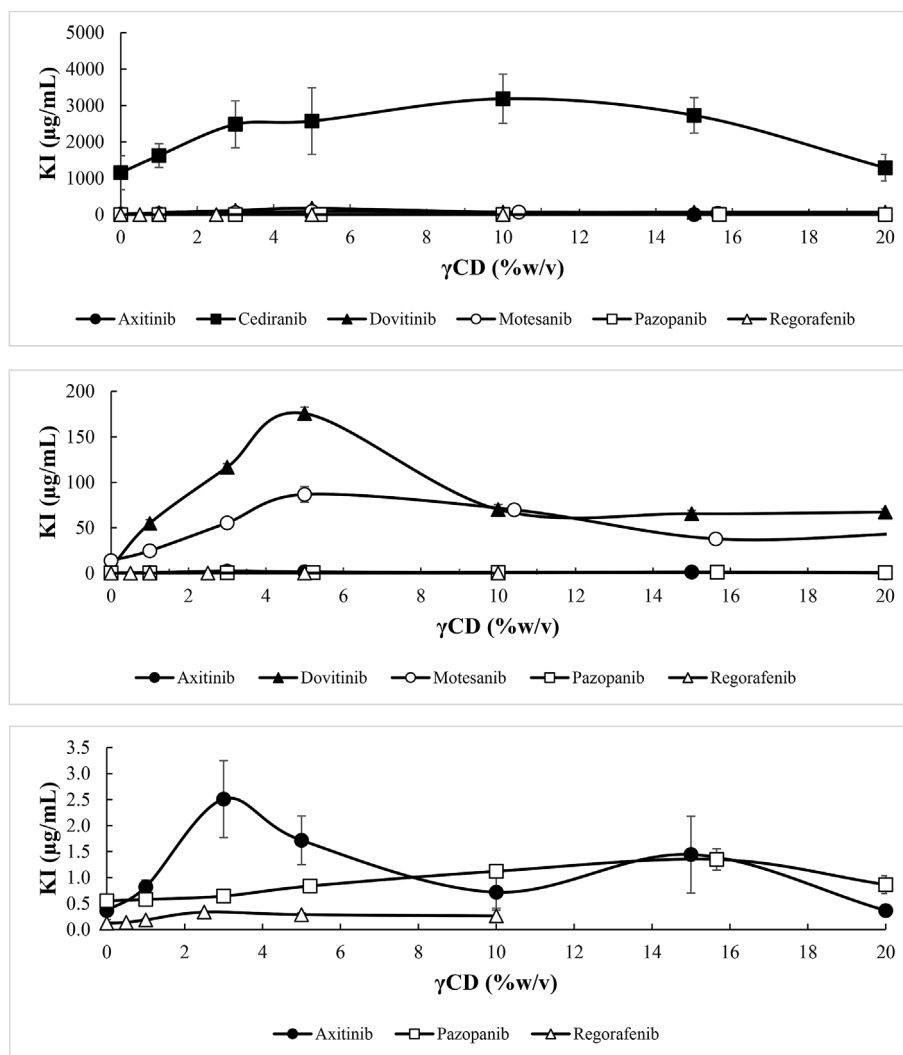


Fig. 1. The phase-solubility profiles of the KIs in unbuffered pure aqueous γ CD media (pH 6.3 to 6.8) at room temperature (\pm standard deviation; $n = 3$).

skin pH is generally somewhat acidic or between 4 and 6 [41,57]. pH of a pharmaceutical formulation should generally be adjusted within these physiological values [22]. However, at lower pH the buffer capacity should be low to avoid irritation. Pure KIs and their complexes in aqueous media obtained pH in the range of 5.5–7, except that of the motesanib/ γ CD/HDMBR complex. The presence of HDMBR in unbuffered motesanib system lowered the pH to 3.7 which is unsuitable for drug dosages, whereas the unbuffered dovitinib system gave pH 6.2 as well as that of pazopanib (data not shown). In ternary complex with HDMBR, dovitinib was more soluble than motesanib, although it resulted higher pH (i.e. should result in lower solubility). Thus, the solubility of KIs was increased due to ternary complex formation.

3.5.2. Osmolality

Osmolality refers to the number of dissolved particles or solutes in solution (Sweeney and Beuchat, 1993). It is an important attribute to have desired product, especially parenteral formulation, match physiological osmotic conditions (Desai and Lee, 2007). Serum osmolality is often estimated to be approximately 300 mOsmol/L [10]. Various references report the actual range as 280 to 295 mOsmol/L (Atkinson et al., 2013), 275 to 300 mOsmol/L (Wu, 2006), 290 mOsmol/L, 306 mOsmol/L, and 275 to 295 mOsmol/kg (Faria et al., 2017). All samples tested had osmolality within those physiological criteria or defined as hypotonic, and can be adjusted to appropriate osmolality by addition of, for example sodium chloride (Avis et al., 1986).

Table 4
Solubilization efficacy of six KIs in pure water (pH between 6.3 and 6.8).

| Drug | pH | PS ^a type | S ₀ (µg/mL) | Maximum solubility | | PS ^a parameter | | | |
|-------------|------|----------------------|------------------------|--------------------|--------------|---------------------------|----------------|-------------------------------------|----------|
| | | | | γ CD (%w/v) | drug (µg/mL) | Slope | r ² | K _{1,1} (M ⁻¹) | CE |
| Axitinib | 6.42 | B _s | 0.37 | 3.0 | 2.51 | 0.0004 | 0.9831 | 260.67 | 0.0002 |
| Cediranib | 6.31 | B _s | 1154.63 | 10.0 | 3184.57 | 0.0546 | 0.8649 | 22.54 | 0.0578 |
| Dovitinib | 6.86 | B _s | 6.34 | 5.0 | 175.66 | 0.0109 | 0.9911 | 684.42 | 0.0110 |
| Motesanib | 6.51 | B _s | 13.98 | 5.0 | 86.73 | 0.0051 | 0.9971 | 137.70 | 0.0052 |
| Pazopanib | 6.57 | B _s | 0.55 | 15.7 | 1.35 | 0.000016 | 0.9873 | 12.65 | 0.000016 |
| Regorafenib | 6.65 | B _s | 0.12 | 2.5 | 0.33 | 0.000024 | 0.9812 | 94.45 | 0.000024 |

^a PS is abbreviation of phase solubility.

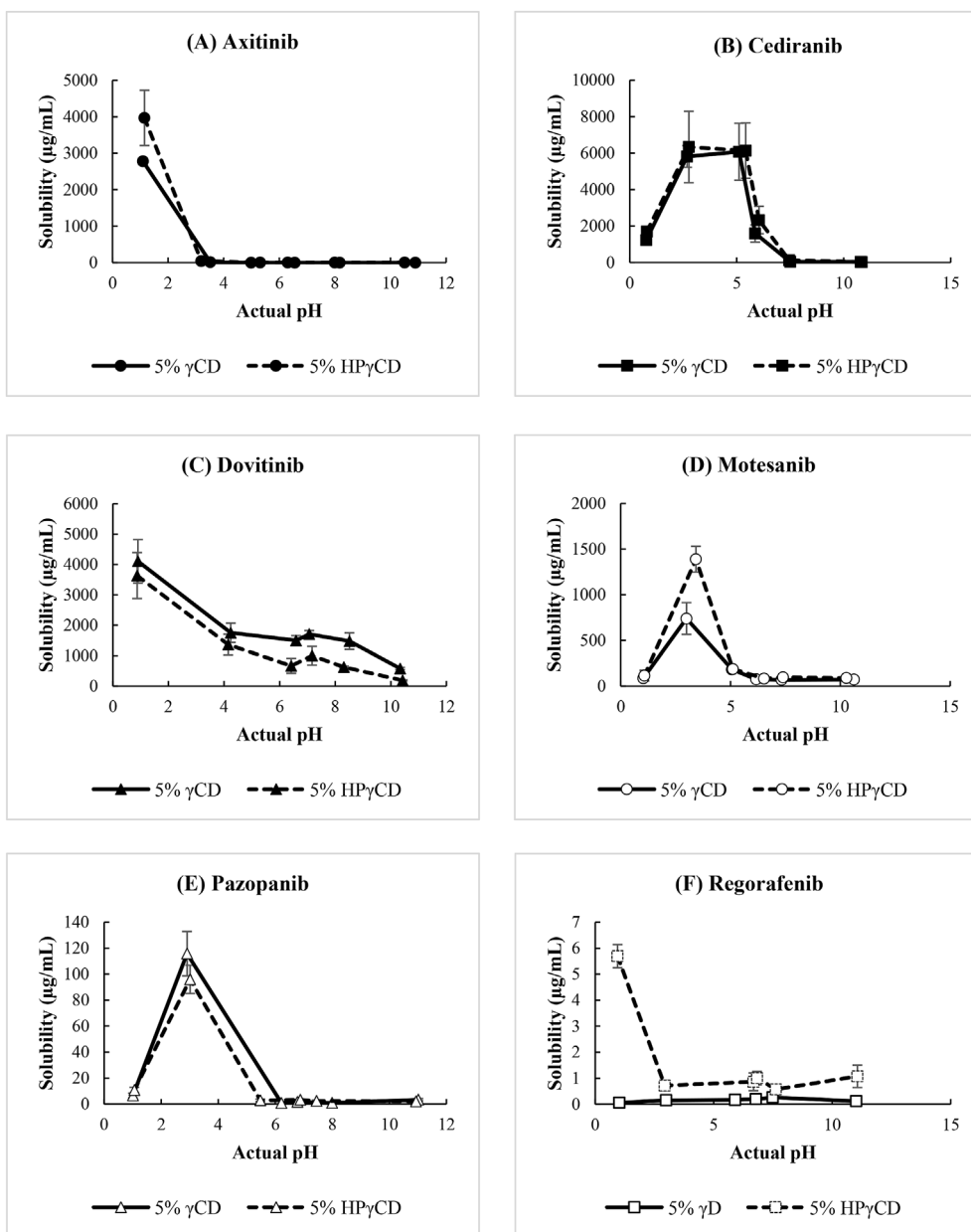


Fig. 2. The pH-solubility profiles of the KIs in pure aqueous 5% (w/v) γ CD and 5% (w/v) HP γ CD solutions at room temperature (\pm standard deviation; $n = 3$).

3.5.3. Particle size

Particle size measurements were recorded as the mean particle diameter based on the major intensity peak area (%A). Both dovitinib and motesanib systems provided a multimodal size distribution (data not shown). In summary, they formed drug/ γ CD complexes and different size aggregates. The reported size distribution of CD aggregates can vary from 20 nm to few μm , but their average size is frequently between 90 and 300 nm (González-Gaitano et al., 2002; Ryzhakov et al., 2016; Szente et al., 1998). The larger aggregates were in aqueous media containing the pure drugs, motesanib binary system, and all HDMBr ternary systems and ranged from 200 to 400 nm. Several studies revealed that the native CDs such as γ CD can self-associate to form aggregates (González-Gaitano et al., 2002; Messner et al., 2010), and the hydrophilic polymers are known to have stabilizing effect on such aggregates (Brackman and Engberts, 1993; Xiao-ming, 2011).

3.5.4. Transmission electron microscopy (TEM) images

Dovitinib was shown to be the most promising candidate of the KIs

tested. HDMBr improve drug solubility through ternary complex formation. Hence binary dovitinib/ γ CD complex and dovitinib/ γ CD/HDMBr ternary complex were investigated visually. The size of all complexes was smaller than 100 nm (Fig. 6). An addition of HDMBr resulted slightly larger aggregates. Number of complexes appeared in TEM images corresponded to the solubility experiments. Firstly, at 5% (w/v) γ CD binary complex medium saturated with dovitinib, where maximum dovitinib solubility was observed, displays larger number of complex aggregates than 8% (w/v) γ CD complex medium. Secondly, ternary dovitinib/ γ CD/HDMBr complex displays the largest particle population as expected based on its dovitinib solubilization. However, the mean particle size in the TEM figures is smaller than determined by DLS as commonly observed by other investigators [6]. This inconsistency is due to the different principle of techniques. TEM is a number-based technique that presents the projected surface area depended on how much incident electrons transmit through dry sample under ultrahigh vacuum (Kim et al., 2015; Zhou and Yang, 2004). Whereas DLS measurement engages with intensity where

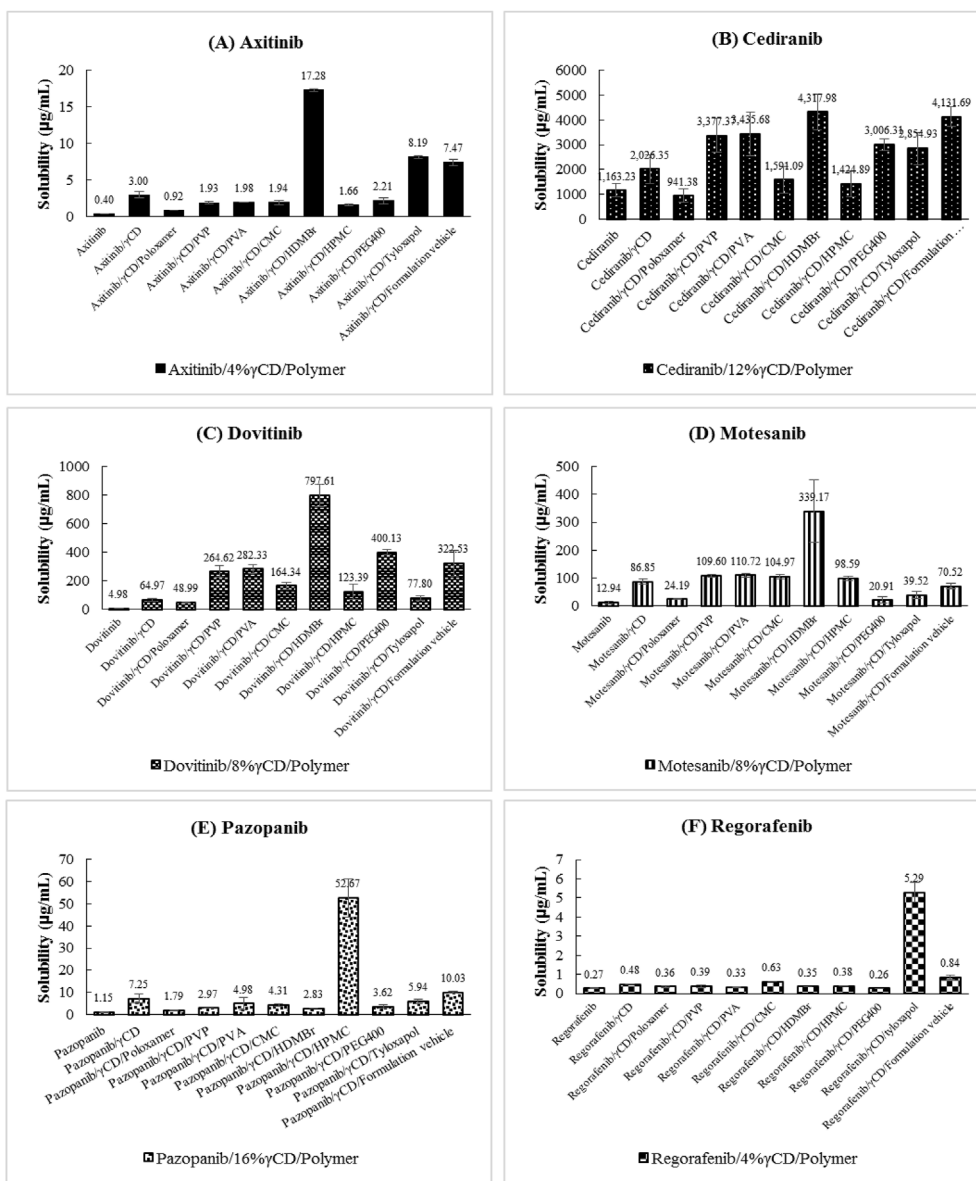


Fig. 3. Aqueous solubility of the KIs in unbuffered pure aqueous γ CD, (pH 6.3 to 6.8), with and without 1% (w/v) hydrophilic polymer solution at room temperature (\pm standard deviation; n = 3). The concentration of γ CD is shown below each figure.

Table 5

An increase of KI solubility in comparison of drug alone and drug/ γ CD complex (pH between 6.3 and 6.8).

| Sample | Solubilizing ratio | | | | | | | | | | | |
|-------------------------------------|--------------------|-------------------|-------------------|-------------------|---------------------|--------------------|--------------------|-------------------|--------------------|-------------------|--------------------|--------------------|
| | Axitinib (A) | | Cediranib (C) | | Dovitinib (D) | | Motesanib (M) | | Pazopanib (P) | | Regorafenib (R) | |
| | A | A/ γ CD | C | C/ γ CD | D | D/ γ CD | M | M/ γ CD | P | P/ γ CD | R | R/ γ CD |
| KI | - | - | - | - | - | - | - | - | - | - | - | - |
| KI/ γ CD | 7.50 | - | 1.74 | - | 13.04 | - | 6.71 | - | 6.31 | - | 1.78 | - |
| KI/ γ CD/Poloxamer | 2.30 | 0.31 | 0.81 | 0.46 | 9.83 | 0.75 | 1.87 | 0.28 | 1.56 | 0.25 | 1.33 | 0.74 |
| KI/ γ CD/PVP | 4.84 | 0.65 | 2.90 | 1.67 | 53.10 | 4.07 | 8.47 | 1.26 | 2.59 | 0.41 | 1.45 | 0.81 |
| KI/ γ CD/PVA | 4.95 | 0.66 | 2.95 | 1.70 | 56.65 | 4.35 | 8.56 | 1.27 | 4.33 | 0.69 | 1.21 | 0.68 |
| KI/ γ CD/CMC | 4.85 | 0.65 | 1.37 | 0.79 | 32.98 | 2.53 | 8.11 | 1.21 | 3.75 | 0.60 | 2.32 | 1.30 |
| KI/ γ CD/HDMBR | 43.20 ^a | 5.76 ^a | 3.71 ^a | 2.13 ^a | 160.05 ^a | 12.28 ^a | 26.21 ^a | 3.91 ^a | 2.46 | 0.39 | 1.31 | 0.74 |
| KI/ γ CD/HMPC | 4.15 | 0.55 | 1.22 | 0.70 | 24.76 | 1.90 | 7.62 | 1.14 | 45.84 ^a | 7.27 ^a | 1.42 | 0.80 |
| KI/ γ CD/PEG400 | 5.53 | 0.74 | 2.58 | 1.48 | 80.29 | 6.16 | 1.62 | 0.24 | 3.15 | 0.50 | 0.97 | 0.55 |
| KI/ γ CD/Tyloxapol | 20.49 | 2.73 | 2.45 | 1.41 | 15.61 | 1.20 | 3.05 | 0.45 | 5.17 | 0.82 | 19.62 ^a | 11.00 ^a |
| KI/ γ CD/Formulation vehicle | 18.67 | 2.49 | 3.55 | 2.04 | 64.72 | 4.96 | 5.45 | 0.81 | 8.73 | 1.38 | 3.11 | 1.75 |

^a Refers to maximum solubilizing ratio.

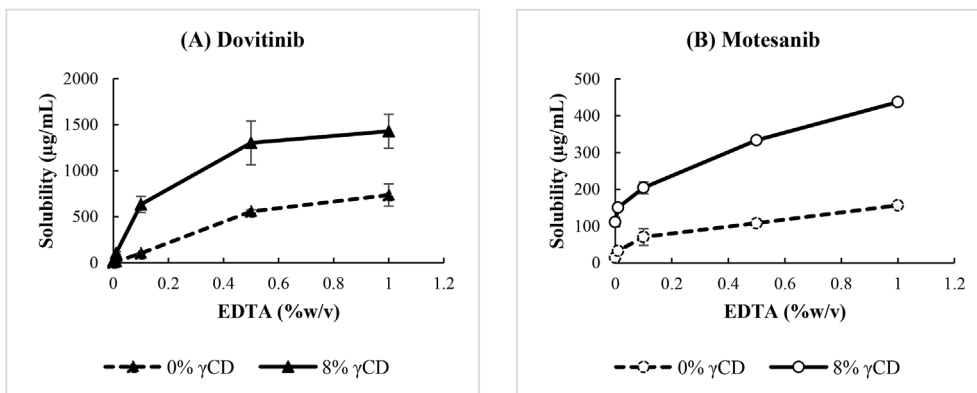


Fig. 4. Aqueous solubility of the KIs in EDTA solution and 0% or 8% (w/v) pure aqueous γ CD solution at room temperature (\pm standard deviation; n = 3).

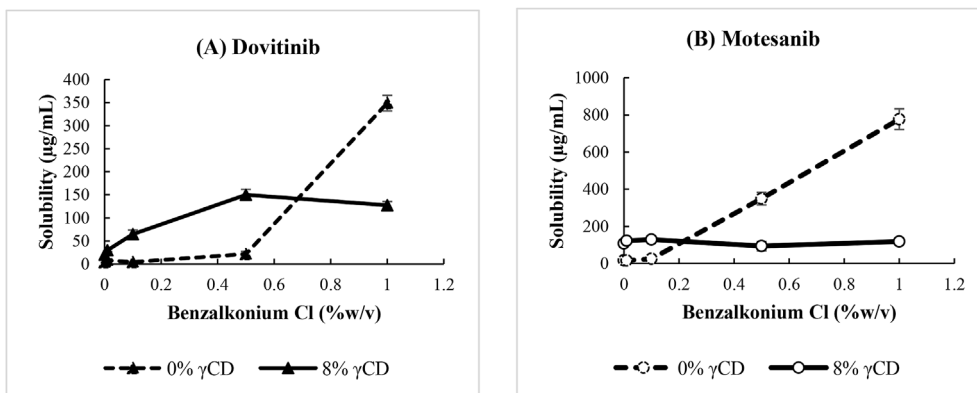


Fig. 5. Aqueous solubility of the KIs in benzalkonium chloride solution and 0% or 8% (w/v) pure unbuffered aqueous γ CD solution (pH 6.3–6.8) at room temperature (\pm standard deviation; n = 3).

Table 6
pH, Osmolality, DSL data of pure KI and KI complexes (n = 3).

| Sample | pH | | | Osmolality (Osmol/L) | | | Particle size (nm) | | |
|----------------------|------|-------|------|----------------------|-------|-------|--------------------|-------|------|
| | mean | \pm | SD | mean | \pm | SD | mean | \pm | SD |
| D | 6.81 | \pm | 0.01 | 0.001 | \pm | 0.001 | 283.4 | \pm | 12.6 |
| D/ γ CD | 7.04 | \pm | 0.04 | 0.063 | \pm | 0.002 | 114.7 | \pm | 16.9 |
| D/ γ CD/HDMBr | 6.22 | \pm | 0.36 | 0.094 | \pm | 0.001 | 406.7 | \pm | 90.7 |
| M | 5.54 | \pm | 0.63 | 0.007 | \pm | 0.001 | 355.7 | \pm | 62.7 |
| M/ γ CD | 5.48 | \pm | 0.09 | 0.068 | \pm | 0.001 | 417.3 | \pm | 51.5 |
| M/ γ CD/HDMBr | 3.71 | \pm | 0.45 | 0.103 | \pm | 0.002 | 273.8 | \pm | 30.3 |

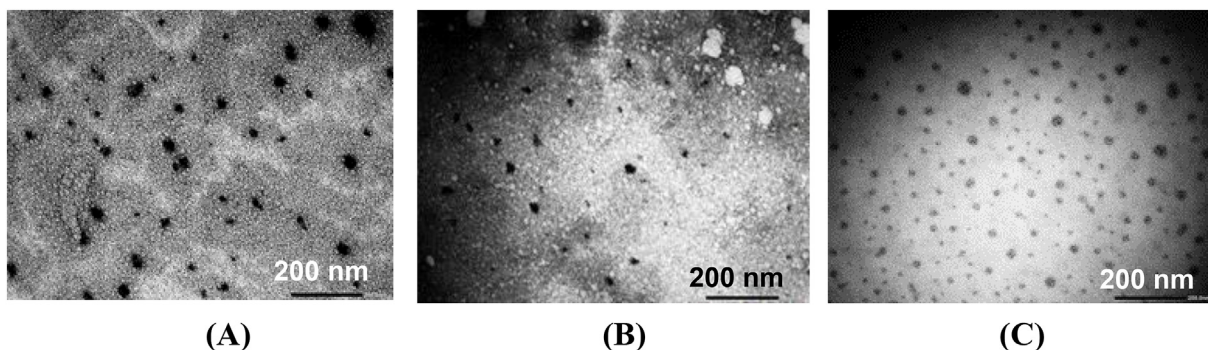


Fig. 6. Transmission electron microscopic images of dovitinib complexes with 5% or 8% (w/v) γ CD at magnitude of 50 k; (A) dovitinib/ γ CD5% complex, (B) dovitinib/ γ CD8% complex, and (C) dovitinib/ γ CD8%/HDMBr complex.

hydrodynamic radius of dispersed particles is detected under solvated condition (Zhao et al., 2015).

4. Conclusion

The phase solubility profiles of six KIs in aqueous γ CD solutions were classified as B_s-type. The aqueous solubility of the soluble KI/ γ CD complexes strongly depends on the pH of complexation media. Dovitinib interacted well with the complexing agent, γ CD, with high K_{1:1} value of 684 M⁻¹ and CE of 0.011, followed by motesanib. The water-soluble polymers tested increased or decreased the KI solubility in the aqueous γ CD media. In general HDMBR had synergistic effect on the KI solubilization. Dovitinib was selected to study further the KI- γ CD interaction. In liquid state, TEM imaging exhibited the complex formation.

CRedit authorship contribution statement

Pitsiree Praphanwittaya: Investigation, Data curation, Writing - original draft. **Phennapha Saokham:** Methodology. **Phatsawee Jansook:** Methodology. **Thorsteinn Loftsson:** Funding acquisition, Supervision, Writing - original draft.

Declaration of competing interest

The authors declare that there is no conflict of interest. The work was performed by Pitsiree Praphanwittaya and will be part of her PhD thesis.

Acknowledgement

This study was funded by the Icelandic center of Research, (RANNÍS), and the University of Iceland, Reykjavik, Iceland.

Appendix A. Supplementary data

Supplementary data to this article can be found online at <https://doi.org/10.1016/j.jddst.2019.101462>.

References

- [1] ACS, SciFinder (scifinder.cas.Org), American Chemical Society, 2019.
- [2] G.L. Amidon, H. Lennernas, V.P. Shah, J.R. Crison, A theoretical basis for a biopharmaceutical drug classification: the correlation of in vitro drug product dissolution and in vivo bioavailability, *Pharm. Res.* 12 (1995) 413–420.
- [3] A. Bellesoeur, E. Carton, J. Alexandre, F. Goldwasser, O. Huillard, Axitinib in the treatment of renal cell carcinoma: design, development, and place in therapy, *Drug Des. Dev. Ther.* 11 (2017) 2801–2811.
- [4] C.A.S. Bergstrom, W.N. Charman, C.J.H. Porter, Computational prediction of formulation strategies for beyond-rule-of-5 compounds, *Adv. Drug Deliv. Rev.* 101 (2016) 6–21.
- [5] C.A.S. Bergström, C.M. Wassvik, K. Johansson, I. Hubatsch, Poorly soluble marketed drugs display solvation limited solubility, *J. Med. Chem.* 50 (2007) 5858–5862.
- [6] S. Bhattacharjee, DLS and zeta potential - what they are and what they are not? *J. Control. Release : Off. J. Control. Release Soc.* 235 (2016) 337–351.
- [7] R.L. Carrier, L.A. Miller, I. Ahmed, The utility of cyclodextrins for enhancing oral bioavailability, *J. Control. Release* 123 (2007) 78–99.
- [8] Y. Chen, M.A. Tortorici, M. Garrett, B. Hee, K.J. Klamers, Y.K. Pithavala, Clinical pharmacology of axitinib, *Clin. Pharmacokinet.* 52 (2013) 713–725.
- [9] Y. Deng, C. Sychterz, A.B. Suttle, M.M. Dar, D. Bershas, K. Negash, Y. Qian, E.P. Chen, P.D. Gorycki, M.Y.K. Ho, Bioavailability, metabolism and disposition of oral pazopanib in patients with advanced cancer, *Xenobiotica* 43 (2013) 443–453.
- [10] M. E. Mohr, Remington: the Science and Practice of Pharmacy, twenty-first ed., (2006).
- [11] K. Edueng, D. Mahlin, C.A.S. Bergstrom, The need for restructuring the disordered science of amorphous drug formulations, *Pharm. Res.* 34 (2017) 1754–1772.
- [12] S.A. Fahmy, J. Brūšler, M. Alawak, M.M.H. El-Sayed, U. Bakowsky, T. Shoeb, Chemotherapy based on supramolecular chemistry: a promising strategy in cancer therapy, *Pharmaceutics* 11 (2019) 292.
- [13] M.T. Faucci, P. Mura, Effect of water-soluble polymers on naproxen complexation with natural and chemically modified beta-cyclodextrins, *Drug Dev. Ind. Pharm.* 27 (2001) 909–917.
- [14] F.M. Ferguson, N.S. Gray, Kinase inhibitors: the road ahead, *Nat. Rev. Drug Discov.* 17 (2018) 353.
- [15] C. Fong, Drug Discovery Model Using Molecular Orbital Computations: Tyrosine Kinase Inhibitors, (2016).
- [16] Z. He, R.A. Mitteer, Y. Mou, Y. Fan, Chapter 5 - Multimodality Targeting of Glioma Cells, *Glioblastoma*, Elsevier, 2016, pp. 55–72.
- [17] T. Higuchi, K.A. Connors, Phase-solubility techniques, in: C.N. R (Ed.), *Advances in Analytical Chemistry and Instrumentation*, Wiley-Interscience, New York, 1965, pp. 117–212.
- [18] R.S. Hirlekar, S.N. Sonawane, V.J. Kadam, Studies on the effect of water-soluble polymers on drug-cyclodextrin complex solubility, *AAPS PharmSciTech* 10 (2009) 858–863.
- [19] P. Jansook, N. Ogawa, T. Loftsson, Cyclodextrins: structure, physicochemical properties and pharmaceutical applications, *Int. J. Pharm.* 535 (2018) 272–284.
- [20] P. Jansook, W. Pichayakorn, C. Muangkaew, T. Loftsson, Cyclodextrin-poloxamer aggregates as nanocarriers in eye drop formulations: dexamethasone and amphotericin B, *Drug Dev. Ind. Pharm.* 42 (2016) 1446–1454.
- [21] P. Koch, S. Laufer, Special issue: kinase inhibitors, *Molecules* 23 (2018).
- [22] Y.-C. Lee, P.D. Zocharski, B. Samas, An intravenous formulation decision tree for discovery compound formulation development, *Int. J. Pharm.* 253 (2003) 111–119.
- [23] F. Leroy-Lechat, D. Wouessidjewe, J.-P. Andreux, F. Puisieux, D. Duchêne, Evaluation of the cytotoxicity of cyclodextrins and hydroxypropylated derivatives, *Int. J. Pharm.* 101 (1994) 97–103.
- [24] T. Loftsson, M.E. Brewster, Cyclodextrins as functional excipients: methods to enhance complexation efficiency, *J. Pharm. Sci.* 101 (2012) 3019–3032.
- [25] T. Loftsson, M.E. Brewster, Cyclodextrins as functional excipients: methods to enhance complexation efficiency, *J. Pharm. Sci.* 101 (2012) 3019–3032.
- [26] T. Loftsson, H. Friðriksdóttir, T.K. Guðmundsdóttir, The effect of water-soluble polymers on aqueous solubility of drugs, *Int. J. Pharm.* 127 (1996) 293–296.
- [27] T. Loftsson, D. Hreinsdóttir, M. Masson, Evaluation of cyclodextrin solubilization of drugs, *Int. J. Pharm.* 302 (2005) 18–28.
- [28] T. Loftsson, D. Hreinsdóttir, M. Másson, The complexation efficiency, *J. Incl. Phenom. Macrocycl. Chem.* 57 (2007) 545–552.
- [29] T. Loftsson, P. Jansook, E. Stefansson, Topical drug delivery to the eye: dorzolamide, *Acta Ophthalmol.* 90 (2012) 603–608.
- [30] T. Loftsson, N. Leevae, J.F. Sigurjonsdottir, H.H. Sigurdsson, M. Masson, Sustained drug delivery system based on a cationic polymer and an anionic drug/cyclodextrin complex, *Die Pharmazie* 56 (2001) 746–747.
- [31] T. Loftsson, M. Masson, The effects of water-soluble polymers on cyclodextrins and cyclodextrin solubilization of drugs, *J. Drug Deliv. Sci. Technol.* 14 (2004) 35–43.
- [32] L.R. Lumholdt, R. Holm, E.B. Jørgensen, K.L. Larsen, In vitro investigations of α -amylase mediated hydrolysis of cyclodextrins in the presence of ibuprofen, flurbiprofen, or benzo[a]pyrene, *Carbohydr. Res.* 362 (2012) 56–61.
- [33] A.S. Mahadevi, G.N. Sastry, Cation- π interaction: its role and relevance in chemistry, biology, and material science, *Chem. Rev.* 113 (2013) 2100–2138.
- [34] M. Moya-Ortega, M. Messner, P. Jansook, T. Nielsen, V. Wintgens, K. Larsen, C. Amiel, H. Sigurdsson, T. Loftsson, Drug loading in cyclodextrin polymers: dexamethasone model drug, *J. Incl. Phenom. Macrocycl. Chem.* 69 (2011) 377–382.
- [35] C. Muangkaew, P. Jansook, H.H. Sigurdsson, T. Loftsson, Cyclodextrin-based telmisartan ophthalmic suspension: formulation development for water-insoluble drugs, *Int. J. Pharm.* 507 (2016) 21–31.
- [36] P. Mura, M.T. Faucci, G.P. Bettinetti, The influence of polyvinylpyrrolidone on naproxen complexation with hydroxypropyl-beta-cyclodextrin, *Eur. J. Pharm. Sci. : Off. J. Eur. Fed. Pharm. Sci.* 13 (2001) 187–194.
- [37] L. Nogueiras-Nieto, C. Alvarez-Lorenzo, I. Sandez-Macho, A. Concheiro, F.J. Otero-Espinar, Hydro-soluble cyclodextrin/poloxamer polyseudorotaxanes at the air/water interface, in bulk solution, and in the gel state, *J. Phys. Chem. B* 113 (2009) 2773–2782.
- [38] L. Nogueiras-Nieto, E. Sobarzo-Sanchez, J.L. Gomez-Amoza, F.J. Otero-Espinar, Competitive displacement of drugs from cyclodextrin inclusion complex by polyseudorotaxane formation with poloxamer: implications in drug solubilization and delivery, *Eur. J. Pharm. Biopharm. : Off. J. Arbeitsgem. Pharm. Verfahrenstech. E.V.* 80 (2012) 585–595.
- [39] Y. Ohtani, T. Irie, K. Uekama, K. Fukunaga, J. Pitha, Differential effects of alpha-, beta- and gamma-cyclodextrins on human erythrocytes, *Eur. J. Biochem.* 186 (1989) 17–22.
- [40] N. Qiu, X. Li, J. Liu, Application of cyclodextrins in cancer treatment, *J. Incl. Phenom. Macrocycl. Chem.* 89 (2017) 229–246.
- [41] K.L. Raphael, R.A. Murphy, M.G. Shlipak, S. Satterfield, H.K. Huston, A. Sebastian, D.E. Sellmeyer, K.V. Patel, A.B. Newman, M.J. Sarnak, J.H. IX, L.F. Fried, Bicarbonate concentration, acid-base status, and mortality in the health, aging, and body composition study, *Clin. J. Am. Soc. Nephrol. : CJASN* 11 (2016) 308–316.
- [42] A.S. Reddy, G.N. Sastry, Cation [M = H⁺, Li⁺, Na⁺, K⁺, Ca²⁺, Mg²⁺, NH₄⁺, and NMe₄⁺] interactions with the aromatic motifs of naturally occurring amino Acids: A theoretical study, *J. Phys. Chem. A* 109 (2005) 8893–8903.
- [43] M. Remko, A. Boháč, L. Kováčiková, Molecular structure, pKa, lipophilicity, solubility, absorption, polar surface area, and blood brain barrier penetration of some antiangiogenic agents, *Struct. Chem.* 22 (2011) 635–648.
- [44] L.S. Ribeiro, D.C. Ferreira, F.J. Veiga, Physicochemical investigation of the effects of water-soluble polymers on vinpocetine complexation with beta-cyclodextrin and its sulfobutyl ether derivative in solution and solid state, *Eur. J. Pharm. Sci. : Off. J. Eur. Fed. Pharm. Sci.* 20 (2003) 253–266.
- [45] R.C. Rowe, P.J. Sheskey, M.E. Quinn, A.P. Association, Handbook of Pharmaceutical Excipients, sixth ed., Pharmaceutical Press ; American Pharmacists Association, London ; Chicago : Washington, DC, 2009.
- [46] A. Rowland, M. van Dyk, A.A. Mangoni, J.O. Miners, R.A. McKinnon, M.D. Wiese,

- A. Rowland, G. Kichenadasse, H. Gurney, M.J. Sorich, Kinase inhibitor pharmacokinetics: comprehensive summary and roadmap for addressing inter-individual variability in exposure, *Expert Opin. Drug Metabol. Toxicol.* 13 (2017) 31–49.
- [47] P. Saokham, T. Loftsson, γ -Cyclodextrin, *Int. J. Pharm.* 516 (2017) 278–292.
- [48] R. Savla, J. Browne, V. Plassat, K.M. Wasan, E.K. Wasan, Review and analysis of FDA approved drugs using lipid-based formulations, *Drug Dev. Ind. Pharm.* 43 (2017) 1743–1758.
- [49] N. Sekhon, R.A. Kumbla, M. Mita, Chapter 1 - current trends in cancer therapy, in: R.A. Gottlieb, P.K. Mehta (Eds.), *Cardio-Oncology*, Academic Press, Boston, 2017, pp. 1–24.
- [50] H.H. Sigurdsson, E. Knudsen, T. Loftsson, N. Leeves, J.F. Sigurjonsdottir, M. Másson, Mucoadhesive sustained drug delivery system based on cationic polymer and anionic cyclodextrin/triclosan complex, *J. Incl. Phenom. Macrocycl. Chem.* 44 (2002) 169–172.
- [51] J. Stetefeld, S.A. McKenna, T.R. Patel, Dynamic light scattering: a practical guide and applications in biomedical sciences, *Biophys. Rev.* 8 (2016) 409–427.
- [52] W. Tang, A. McCormick, J. Li, E. Masson, Clinical pharmacokinetics and pharmacodynamics of cediranib, *Clin. Pharmacokinet.* 56 (2017) 689–702.
- [53] G. Tóth, Á. Jánoska, Z.-I. Szabó, G. Völgyi, G. Orgován, L. Szente, B. Noszál, Physicochemical characterisation and cyclodextrin complexation of erlotinib, *Supramol. Chem.* 28 (2016) 656–664.
- [54] G. Tóth, Á. Jánoska, G. Völgyi, Z.I. Szabó, G. Orgován, A. Mirzahosseini, Physicochemical characterization and cyclodextrin complexation of the anticancer drug lapatinib, *J. Chem.* 2017 (2017) 4537632 <https://doi.org/10.1155/2017/4537632>.
- [55] K. Tzogani, V. Skibeli, I. Westgaard, M. Dalhus, H. Thoresen, K. Slot, P. Damkier, K. Hofland, J. Borregaard, J. Ersbøll, T. Salmonsøn, R. Pieters, R. Sylvester, G. Mickisch, J. Bergh, F. Pignatti, The European Medicines Agency Approval of Axitinib (Inlyta) for the Treatment of Advanced Renal Cell Carcinoma after Failure of Prior Treatment with Sunitinib or a Cytokine: Summary of the Scientific Assessment of the Committee for Medicinal Products for Human Use, *The oncologist*, 2015, p. 20.
- [56] A. Waugh, A. Grant, *Anatomy and Physiology in Health and Illness*, Churchill Livingstone Elsevier, Philadelphia, Pa, USA, 2007.
- [57] A. Zlotogorski, Distribution of skin surface pH on the forehead and cheek of adults, *Arch. Dermatol. Res.* 279 (1987) 398–401.

Paper II



Aqueous solubility of kinase inhibitors: II the effect of hexadimethrine bromide on the dovitinib/ γ -cyclodextrin complexation



Pitsiree Praphanwittaya^a, Phennapha Saokham^b, Phatsawee Jansook^c, Thorsteinn Loftsson^{a,*}

^a Faculty of Pharmaceutical Sciences, University of Iceland, Hofsvallagata 53, IS-107, Reykjavik, Iceland

^b Department of Manufacturing Pharmacy, Faculty of Pharmacy, Rangsit University, Pathum Thani, 12000, Thailand

^c Faculty of Pharmaceutical Sciences, Chulalongkorn University, 254 Payathai Road, Pathumwan, Bangkok, 10330, Thailand

ARTICLE INFO

Keywords:

Dovitinib
 γ -cyclodextrin
 Complexation
 Complexation efficacy
 Hexadimethrine
 Solubility

ABSTRACT

Dovitinib is a small molecule kinase inhibitor (KI) that is practically insoluble in water but demonstrates high antitumor activity. The aqueous solubility of dovitinib can be improved through formation of water-soluble γ -cyclodextrin (γ CD) complexes. However, the very low intrinsic solubility hampers the complex formation. The aim of the present study was to investigate dovitinib binary and ternary complexes with both γ CD and hexadimethrine bromide (HDMBr) in both aqueous solution and the solid state. The phase-solubility diagrams of dovitinib were of B_s-type. Addition of HDMBr to the complexation media, that is formation of ternary dovitinib/ γ CD/HDMBr complex, resulted in four-fold increase in the complexation efficacy (CE). The enhanced CE can decrease the amount of γ CD needed to solubilize given amount of dovitinib. The solid dovitinib complexes were characterized by differential scanning calorimetry (DSC), X-ray powder diffraction (XRPD), Fourier transform infrared spectroscopy (FTIR), and *in vitro* dissolution. The dissolution test showed that γ CD did stabilize supersaturated dovitinib solution.

1. Introduction

Dovitinib (D) is a tyrosine kinase inhibitor (KI) that has demonstrated antitumor activity in humans [1]. Like many other small molecule KIs, dovitinib is poorly soluble in water (solubility about 0.4 mg/ml) that can lead to limited and variable oral bioavailability [2]. There are only limited data available on the oral bioavailability of dovitinib in humans but the data available indicates that the drug is slowly absorbed from the gastrointestinal tract with maximum plasma concentration (t_{max}) at 4–7 h after administration and bioavailability of $\geq 75\%$ [3–6]. The rather lipophilic dovitinib molecule (molecular weight 392 Da; Log $P_{octanol/water}$ 1.7) consists of nitrogen-based heterocyclic rings (Fig. 1). Previously, cyclodextrin (CD) solubilization of KIs, such as erlotinib, lapatinib and gefitinib have been described [7–10]. Here, γ -cyclodextrin (γ CD) solubilization of dovitinib is described. Although dovitinib forms a water-soluble complex with the natural γ CD although the complexation efficacy is rather low. In the first part of this series it was shown that addition of polymers to the aqueous complexation medium enhanced significantly the γ CD solubilization of KIs such as dovitinib [11].

γ CD is one of the three most common natural CDs. It consists of 8 glucose subunits that form a cyclic doughnut shape oligosaccharide

with a somewhat lipophilic central cavity and a hydrophilic outer surface [12,13]. γ CD has the highest aqueous solubility of the three natural CDs (232 mg/ml at room temperature), the lowest critical aggregation concentration (cac about 8 mg/ml) and the most favorable toxicological profile of all natural CDs [14,15]. Self-assembled γ CD nano- and microparticles have been shown to be effective drug delivery systems [16].

Hexadimethrine bromide (HDMBr) consists of quaternary ammonium ion repeat units alternating with hydrophobic hexamethylene and trimethylene bridges (the chemical name is poly[(dimethyliminio)-1,3-propanediyl(dimethyliminio)-1,6-hexanedyl dibromide]). HDMBr was used to reverse heparin anticoagulation during surgery and is currently used at low doses to promote the efficiency of virus-mediated gene transfer both *in vitro* and *in vivo* [17]. HDMBr can cause life-threatening renal failure at doses > 5 mg/kg. Thus, when HDMBr is used as a heparin antagonist in human cardiovascular surgery the dose should not exceed 4–5 mg/kg [18,19]. This cationic polymer can be used to promote mucoadhesive sustained CD-based drug delivery system at a concentration of 3% (w/v) [20,21]. In the presence of 0.25% (w/v) HDMBr, the solubilization efficacy of γ CD was increased in presence of dexamethasone [22–24]. Here HDMBr is used to enhance the complexation efficacy and, consequently, the solubilizing effect of γ CD

* Corresponding author.

E-mail address: thorstlo@hi.is (T. Loftsson).

<https://doi.org/10.1016/j.jddst.2019.101463>

Received 31 October 2019; Received in revised form 9 December 2019; Accepted 10 December 2019

Available online 23 December 2019

1773-2247/ © 2019 Elsevier B.V. All rights reserved.

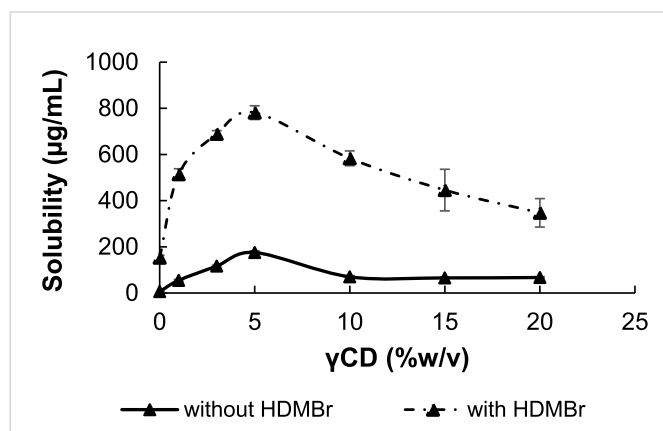


Fig. 1. Phase-solubility profiles of dovitinib complexes without and with HDMBr (mean \pm standard deviation; $n = 3$). The media was pure water.

through formation of ternary dovitinib/ γ CD/HDMBr complex.

2. Materials and methods

2.1. Materials

Dovitinib (D) was purchased from Reagents Direct (Encinitas, CA, USA). γ -cyclodextrin (γ CD) and 2-hydroxypropyl- γ -cyclodextrin, molecular weight 1540, (HP γ CD), were purchased from Wacker (München Germany). Hexadimethrine bromide (HDMBR, $\geq 94\%$ (titration) with molecular weight 374 kDa), was purchased from Sigma-Aldrich (St. Louis, MO, USA). Milli-Q water (Millipore, Billerica, MA) was used throughout the study.

2.2. Phase-solubility studies

The determination of drug solubility was performed by a heating technique in triplicate following previously described method [11]. Briefly, excess amount of dovitinib was added to aqueous 0–20% (w/v) γ CD solutions and to solutions containing 0–20% (w/v) γ CD solutions and 1% (w/v) HDMBR. The experiments were performed in unbuffered solutions. This was done to avoid salt and counterion effects of the buffer salts on the measured solubility value. The pH of aqueous media was closely monitored and was within acceptable range or between 6.11 and 6.86. The suspensions obtained were sonicated in sealed glass containers at 30 °C for half an hour. After they had cooled to ambient temperature (22–23 °C) the containers were opened, and small amount of solid drug added to the suspensions to promote drug precipitation. The resealed containers were placed in a shaker (KS 15 A Shaker, EB Edmund Bühler GmbH, Germany) and equilibrated at ambient temperature under constant agitation for 7 days. The saturated mixtures were centrifuged at 12000 rpm for 15 min (Heraeus Pico 17 Centrifuge, Thermo Fisher Scientific, Germany). Their supernatant was diluted with Milli-Q water and analyzed by HPLC.

Phase-solubility analysis was performed according to method described by Higuchi and Connors [25]. The value of the apparent stability constant ($K_{1:1}$) (Eq. (1)) and the complexation efficiency (CE) (Eq.

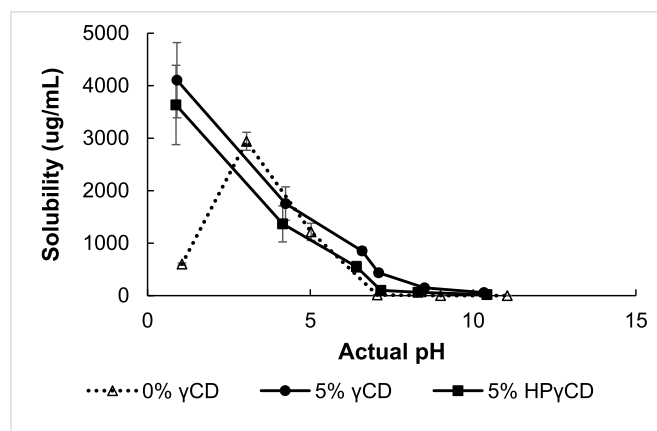


Fig. 2. pH-solubility profiles of dovitinib in pure water and in 5% (w/v) aqueous CD solutions (mean \pm standard deviation; $n = 3$).

(2)) were calculated from slope of the initial linear portion of KI concentration against γ CD concentration profiles assuming KI- γ CD 1:1 complex formation (i.e. that the molar ratio of KI and γ CD in the complex is one-to-one).

$$K_{1:1} = \frac{\text{slope}}{S_0(1 - \text{slope})} \quad (1)$$

$$CE = S_0 \cdot K_{1:1} = \frac{\text{slope}}{(1 - \text{slope})} = \frac{[\text{KI}/\gamma\text{CD complex}]}{[\gamma\text{CD}]} \quad (2)$$

where S_0 is the drug intrinsic solubility, $[\text{KI}/\gamma\text{CD complex}]$ is the concentration of dissolved complex and $[\gamma\text{CD}]$ is the concentration of dissolved γ CD in the aqueous complexation media.

2.3. pH-solubility profiles

Excess amount of dovitinib was added to different pH mediums in triplicate. Pure water, 5% (w/v) HP γ CD and 5% (w/v) γ CD solutions were adjusted to the desire pH ranging from 1 to 11 (Thermo Orion 3 Star™ bench top pH meter, Thermo Fisher Scientific, USA) by dropwise titration with concentrated aqueous sodium hydroxide solution or hydrochloric acid solution. In general, aqueous γ CD solutions form aggregates upon storage. The turbidity of γ CD solutions increased with increasing γ CD concentration while the HP γ CD solutions remained essentially non-turbid. The formation of drug/ γ CD complexes can enhance the aggregate formation [22]. The turbid appearance might affect the saturated point of dissolved drug at different pH values. Thus, HP γ CD was introduced in this study due to non-turbidity characteristic. The suspensions formed were sonicated at 30 °C as previously described (see Section 2.2). All suspensions in those mediums were equilibrated at room temperature (22–23 °C) under constant agitation for 7 days, and the pH readjusted pH if need. At the end of incubation, samples were harvested by centrifugation at 12,000 rpm for 15 min. The amount of dissolved drug in supernatant was determined by HPLC.

2.4. Ternary complex preparation

Dovitinib/ γ CD/HDMBr ternary complex was prepared by adding

Table 1
Solubilization efficacy of dovitinib complexes without and with HDMBr in pure water.

| Sample | pH | PS ^a type | S ₀ (µg/mL) | Maximum solubility | | PS ^a parameter | | | |
|------------------------------|------|----------------------|------------------------|--------------------|--------------|---------------------------|----------------|-------------------------------------|------|
| | | | | γ CD (%w/v) | drug (µg/mL) | Slope | r ² | K _{1:1} (M ⁻¹) | CE |
| Dovitinib/ γ CD | 6.86 | B _s | 6.34 | 5.0 | 175.66 | 0.01 | 0.99 | 684.42 | 0.01 |
| Dovitinib/ γ CD/HDMBR | 6.11 | B _s | 152.88 | 5.0 | 781.34 | 0.04 | 0.83 | 100.35 | 0.04 |

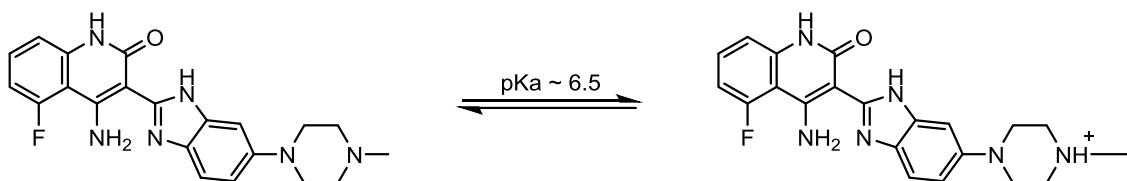


Fig. 3. Ionization of dovitinib assuming that the nitrogen in position 4 of the 4-methyl-1-piperazinyl moiety is the most basic one.

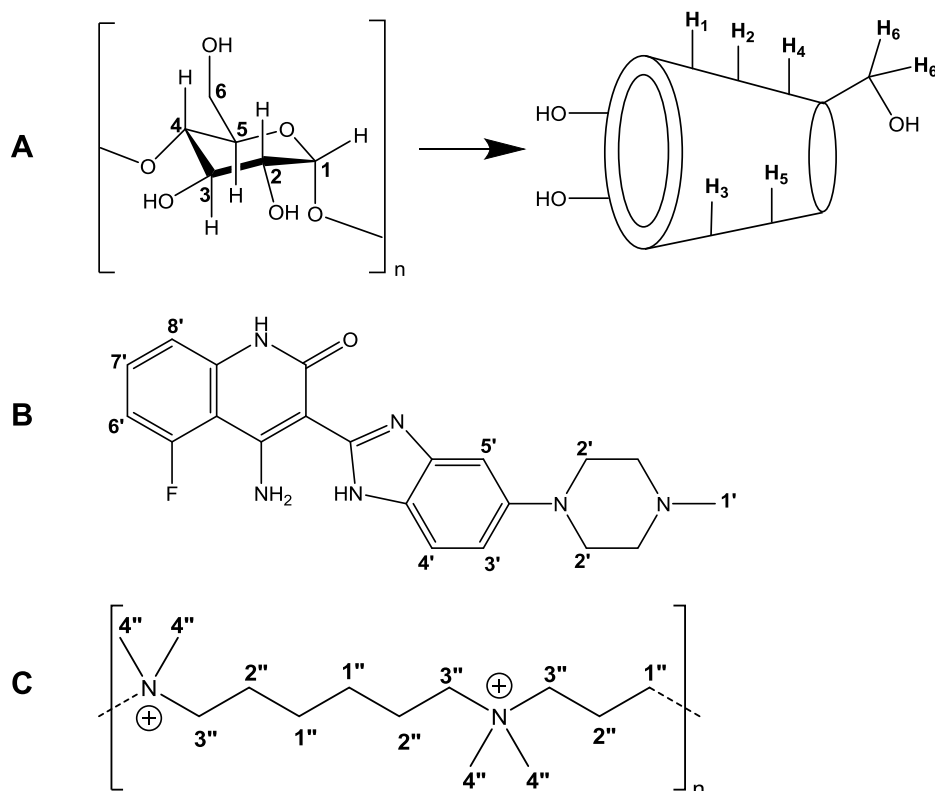


Fig. 4. Structure of (A) γ CD ($n = 8$), (B) dovitinib, (C) HDMBR and their protons probed in the NMR experiment.

0.15 mg of dovitinib to 10 mL of aqueous solution containing 5% (w/v) γ CD and 1% (w/v) HDMBR, applying the previously described heating method. The amount of drug and γ CD was adjusted to give 1:1:1 drug: γ CD:polymer molar ratio. Clear supernatant of the centrifuged suspension was collected and the amount of dissolved drug determined. The supernatant was lyophilized at $-52\text{ }^{\circ}\text{C}$ for 48 h (Snijders scientific 2040 Freeze dryer, Tilburg, Netherlands) to form complex powder for solid-state characterization. Physical mixture of drug, γ CD, and polymer, of equivalent molar ratio, was prepared in a mortar.

2.5. Quantitative determination method

Quantitative determination of dovitinib was performed in a reversed-phase high performance liquid chromatography (HPLC) system (Dionex, Softron GmbH Ultimate 3000 series, Germany). The equipment composed of a P680 pump, operated at 1.0 ml/min, with a DG-1210 degasser, an ASI-100 autosampler, VWD-3400 UV-VIS detector, operated at 233 nm, and a column heater, operated at $30\text{ }^{\circ}\text{C}$, containing a C18 column (100A $150 \times 4.6\text{ mm}$, $5\text{ }\mu\text{m}$) from Kinetex Core-shell technology and a guard column (Phenomenex, UK). The mobile phase consisted of acetonitrile, methanol, and 10 mM ammonium formate buffer pH 4.5 (volume ratio 20:40:40).

2.6. ^1H NMR spectroscopic studies

^1H NMR spectra of complexes were recorded in combined NMR solvents at 400 MHz and 298 K using Bruker AVANCE 400 instrument (Bruker Biospin GmbH, Karlsruhe, Germany). Solid samples of γ CD, dovitinib, dovitinib/ γ CD binary complex, and dovitinib/ γ CD/HDMBR ternary complex were dissolved separately in a mixture of deuterated dimethyl sulfoxide ($\text{DMSO-}d_6$) and deuterium dioxide (D_2O), volume ratio 9:1. The magnitude of chemical shifts was recorded in ppm (δ). The resonance at 2.5000 ppm, due to residual solvent ($\text{DMSO-}d_6$), was used as internal reference. ^1H NMR chemical shift change ($\Delta\delta$) caused upon complexation was calculated according to Eq. (3):

$$\Delta\delta = \delta_{\text{complex}} - \delta_{\text{free}} \quad (3)$$

2.7. Characterization of complexes in solid state

2.7.1. Differential scanning calorimetry (DSC)

DSC analysis of the pure dovitinib, pure γ CD, pure HDMBR, their physical mixture and the lyophilized ternary complex was performed in a Netzsch DSC 214 polyme calorimeter (GmbH, Germany). Accurately weighted amounts (3 mg) of the samples were placed in a perforated aluminium pan and scanned over the temperature range of $30\text{--}400\text{ }^{\circ}\text{C}$ at 10 K/min under a constant nitrogen purge. An identical aluminium pan was used as a reference.

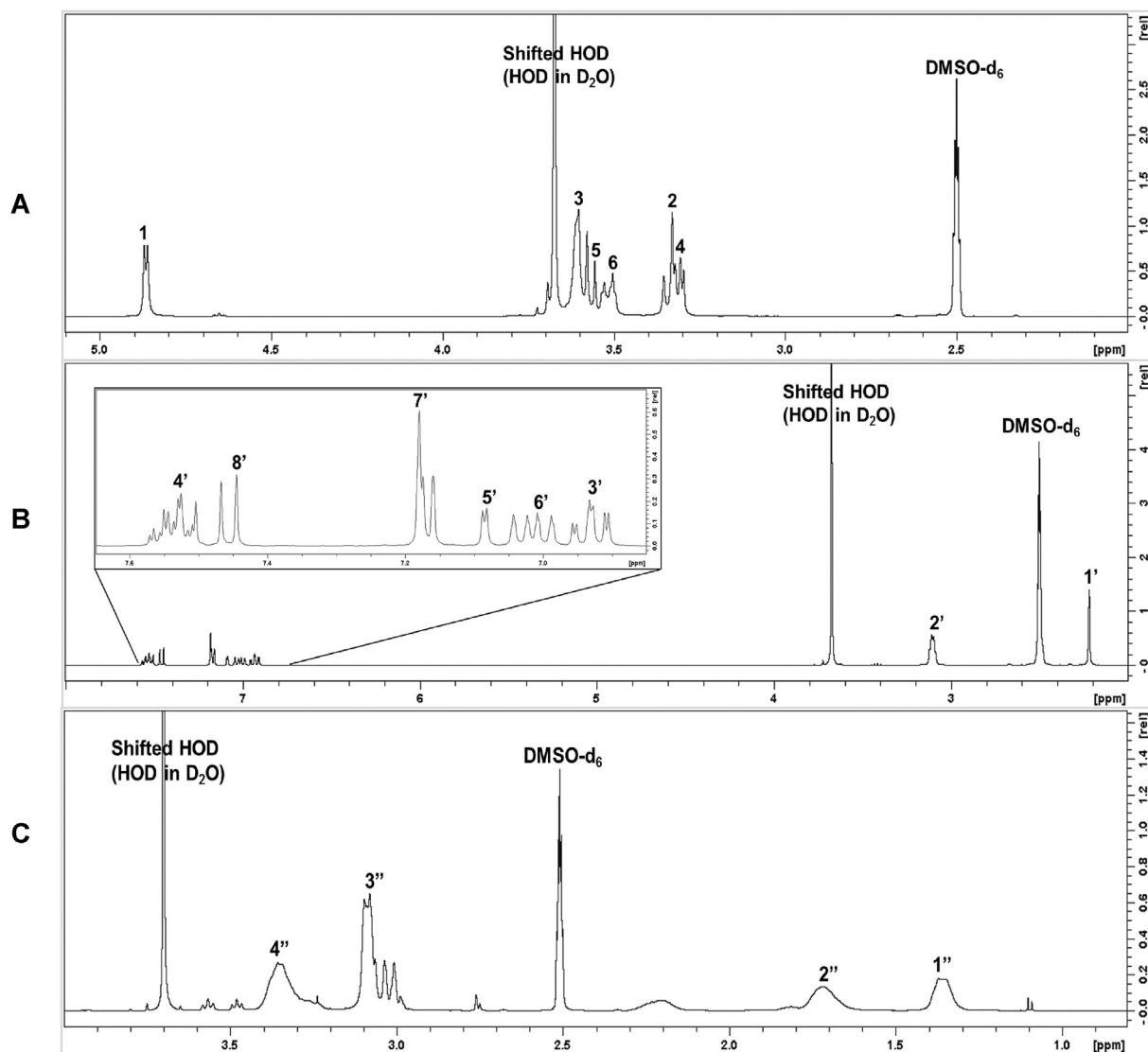


Fig. 5. Representative NMR spectrum of (A) γ CD ($n = 8$), (B) dovitinib, (C) HDMBr and their protons.

Table 2

^1H NMR chemical shift difference ($\Delta\delta$, ppm) of free γ CD and in the binary (i.e. dovitinib/ γ CD and HDMBr/ γ CD) and ternary dovitinib/ γ CD/HDMBr complexes.

| ^1H assignment ^a | δ free | | $\Delta\delta^b$ | |
|--------------------------------------|---------------|-------------------|------------------------|----------------------------------|
| | γ CD | γ CD/HDMBr | dovitinib/ γ CD | dovitinib/ γ CD/ HDMBr |
| H-1 | 4.8700 | -0.0008 | +0.0005 | -0.0004 |
| H-3 | 3.6025 | -0.0006 | -0.0005 | -0.0015 |
| H-5 | 3.5550 | -0.0005 | -0.0004 | -0.0013 |
| H-6 | 3.5032 | -0.0008 | -0.0005 | -0.0015 |
| H-2 | 3.3298 | -0.0001 | 0.0000 | -0.0002 |
| H-4 | 3.3058 | -0.0002 | -0.0001 | -0.0002 |

^a DMSO- d_6 signal used as reference at 2.5000 ppm.

^b $\Delta\delta = \delta \text{ complex} - \delta \text{ free}$.

2.7.2. X-ray powder diffraction (XRPD) studies

X-Ray powder diffractometry (XRPD) is a fundamental method for identification of internal crystal structure. The analysis is primarily used to distinguish between amorphous and crystalline materials. X-Ray diffractograms of pure dovitinib, pure γ CD, physical mixtures and lyophilized complexes were determined in a XRPD Bruker AXS D8

Table 3

^1H NMR chemical shift difference ($\Delta\delta$, ppm) of dovitinib (D) in free-state and in the complexes.

| $^1\text{H}^a$ assignment | δ free | | $\Delta\delta^b$ | |
|---------------------------|---------------|---------------------|------------------------|----------------------------------|
| | dovitinib | dovitinib/ HDMBr | dovitinib/ γ CD | dovitinib/ γ CD/ HDMBr |
| H-1' | 2.2167 | 0.0578 | -0.0056 | 0.0880 |
| H-2' | 3.1083 | -0.0448 | -0.0024 | -0.0561 |
| H-3' | 6.9330 | 0.0050 | 0.0037 | 0.0121 |
| H-6' | 7.0083 | 0.0003 | 0.0030 | 0.0042 |
| H-5' | 7.0824 | 0.0115 | -0.0022 | 0.0175 |
| H-7' | 7.1800 | 0.0012 | 0.0006 | 0.0001 |
| H-8' | 7.4452 | 0.0057 | 0.0015 | 0.0112 |
| H-4' | 7.5258 | 0.0052 | 0.0001 | 0.0090 |

^a DMSO- d_6 signal used as reference at 2.5000 ppm.

^b $\Delta\delta = \delta \text{ complex} - \delta \text{ free}$.

Focus instrument (Ser. no. 202418, Germany) with wide angle CuK α radiation at 40 kV and 40 mA. All scans were performed at 2θ range of 5–40 and scanning speed of $2^\circ/\text{min}$.

Table 4
 ^1H NMR chemical shift difference ($\Delta\delta$, ppm) of HDMBr in free-state and in complex.

| $^1\text{H}^a$ assignment | δ free | | $\Delta\delta^b$ | |
|---------------------------|---------------|---------------------|--------------------------------|--|
| | HDMBr | dovitinib/ HDMBr | $\gamma\text{CD}/\text{HDMBr}$ | dovitinib/ $\gamma\text{CD}/$ HDMBr |
| H-1 ^{''} | 1.3613 | -0.0094 | -0.0230 | -0.0220 |
| H-2 ^{''} | 1.7069 | -0.0056 | -0.0082 | -0.0118 |
| H-3 ^{''} | 3.0713 | -0.0182 | -0.0190 | -0.0192 |
| H-4 ^{''} | 3.3472 | -0.0110 | - | - |

^a DMSO- d_6 signal used as reference at 2.5000 ppm.

^b $\Delta\delta = \delta$ complex - δ free.

2.7.3. Fourier transform infrared (FT-IR)

FT-IR spectra from 4000 to 400 cm^{-1} (average of 32 scans) were recorded in Nicolet iZ10 FT-IR module coupled with an Attenuated Total Reflexion (ART) accessory (Thermo Scientific, USA). The solid specimen of pure drug, pure γCD , physical mixture, or the lyophilized complex was placed in direct contact with the crystal surface, and gently clamped with diamond ATR probe prior to analyze in transmission mode at room temperature.

2.7.4. In vitro dissolution

The dissolution method used was a modified method of Muankaew et al. [26,27]. The samples containing equivalent amounts of dovitinib, that is pure dovitinib (1 mg), binary complex powders (0.15 and 0.5 mg), ternary complex powders (2.5 mg) were added into 5 ml of phosphate buffer saline (pH 7.4). The sample was stirred at 50 rpm at 37 $^\circ\text{C}$, and 1 mL sample withdrawn at various time intervals. The sample was centrifuged at 12000 rpm for 15 min and analyzed by HPLC.

3. Results and discussions

3.1. The phase-solubility studies

The phase-solubility profiles of dovitinib binary and ternary complexes at pH between 6.11 and 6.86 are shown in Fig. 1, both of which are of B_s -type. Addition of 1% (w/v) HDMBr to the aqueous medium increased significantly the γCD solubilization of dovitinib. Addition of 1% (w/v) HDMBr to the media increased the apparent intrinsic solubility (S_0) of dovitinib from about 6.3 $\mu\text{g}/\text{ml}$ to about 150 $\mu\text{g}/\text{ml}$, and the total dovitinib solubility at 5% (w/v) γCD from 175 $\mu\text{g}/\text{ml}$ to

780 $\mu\text{g}/\text{ml}$. However, due to the increased S_0 value the $K_{1:1}$ value was decreased while the CE value was increased. The values of $K_{1:1}$ and the CE were determined to be 680 M^{-1} and 0.01 and 100 M^{-1} and 0.04 for the binary dovitinib/ γCD and ternary dovitinib/ $\gamma\text{CD}/\text{HDMBr}$ complexes, respectively (Table 1). Although $K_{1:1}$ is decreased the solubilizing effect of γCD is increased upon formation of ternary complex due to the increase in CE (CE is the product of $K_{1:1}$ and S_0 , see Eq. (2)).

3.2. The pH-solubility studies

The solubility of dovitinib in pure water and aqueous CDs solutions is pH-dependent (Fig. 2). The drug is very soluble at acidic pH due to the ionization of nitrogen group [28,29]. The nitrogen in position 4 of the 4-methyl-1-piperazinyl (estimated pKa 6.5) protonated at low pH (Fig. 3). The γCD and HP γCD prevented an acid-induced drug degradation under pH 3. Apparently the ionized dovitinib has much less affinity to the CD cavity than the unionized form and, thus, the CDs only had significant effect on the dovitinib solubility at pH above 4.

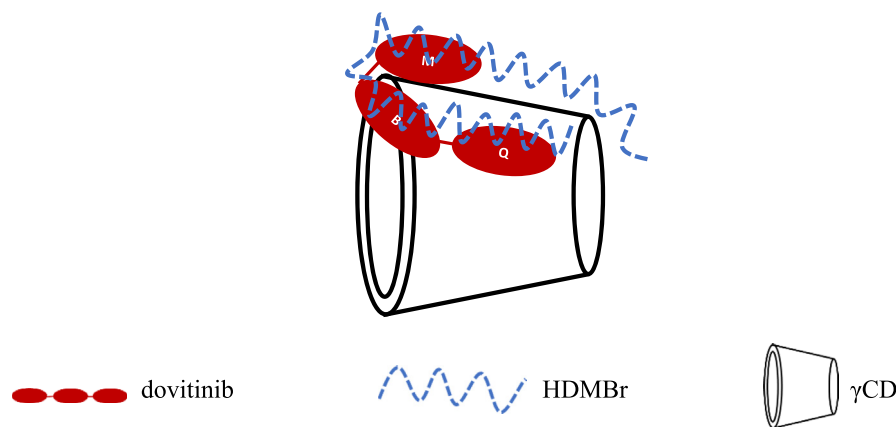
3.3. ^1H NMR spectroscopic studies

The difference in the chemical shifts of binary and ternary complexes were observed in comparison to free γCD , dovitinib, and HDMBr. The proton positions of each molecule are assigned to their chemical structures (Fig. 4) and representative NMR spectra (Fig. 5).

The ^1H NMR chemical shifts corresponding to γCD in free-state and in complexes are listed in Table 2. The 1H assignments relate to the six protons on the outer surface of the γCD molecule (i.e. H-1, H-2, H-4 and H-6) and inside the protons located inside the γCD cavity (i.e. H-3 and H-5) [30]. All these protons displayed significant resonance alternation in the presence of guest molecules (i.e. dovitinib and HDMBr). The downfield shift ($\delta > 0$) was observed for H-1 when dovitinib formed a binary complex with γCD . This is due to the de-shielding effects of the van der Waals interaction between γCD and dovitinib molecules or due to changes in local polarity upon complex formation [31–33]. The upfield signals ($\delta < 0$) of the H-3, H-5, H-6, and H-4 protons can be due to a shielding effect of the guest molecule (i.e. benzene ring and oxygen atom of dovitinib) or molecular conformation changes due to the complex formation [33,34].

In case of γCD in the ternary dovitinib/ $\gamma\text{CD}/\text{HDMBr}$ complex, resonance protons in both internal and external cavity underwent an upfield shift corresponding to the result of bound γCD with HDMBr. The addition of this hydrophilic polymer resulted in larger shielding effect of the characteristic protons.

Both the binary and ternary complexes had two indicative types of



where M is methyl-piperazine ring, B is benzimidazole ring, and Q is quinoline ring

Fig. 6. Proposed complex formation of dovitinib/HDMBr/ γCD ternary system. where M is methyl-piperazine ring, B is benzimidazole ring, and Q is quinoline ring.

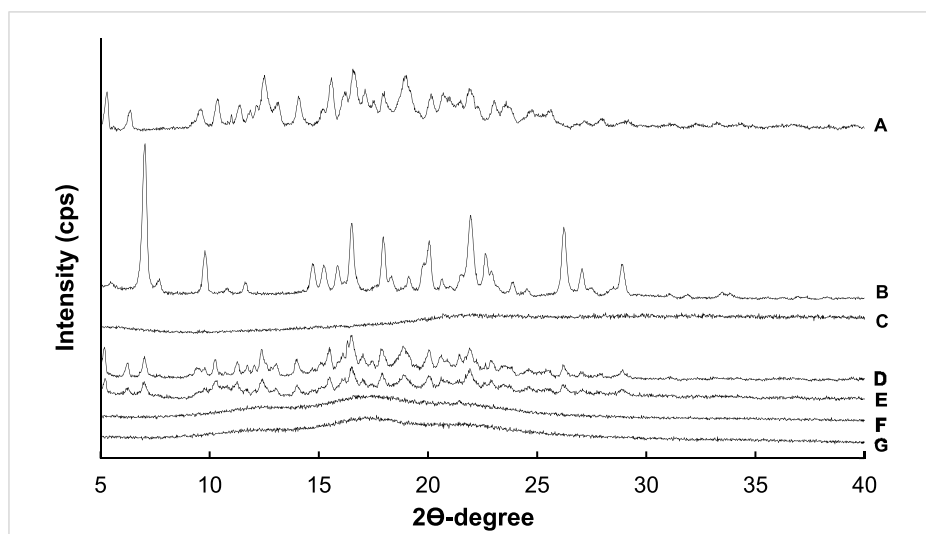


Fig. 7. XRPD spectra of (A) γ CD, (B) pure dovitinib, (C) HDMBr, (D) Dovitinib/ γ CD physical mixture, (E) Dovitinib/ γ CD/HDMBr physical mixture, (F) Dovitinib/ γ CD complex, (G) Dovitinib/ γ CD/HDMBr complex.

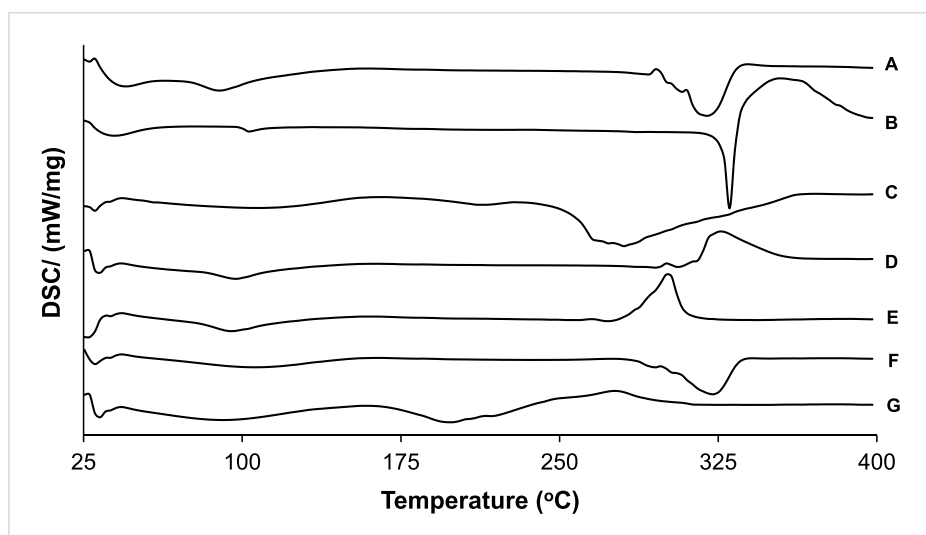


Fig. 8. DSC of (A) γ CD, (B) pure dovitinib, (C) HDMBr, (D) Dovitinib/ γ CD physical mixture, (E) Dovitinib/ γ CD/HDMBr physical mixture, (F) Dovitinib/ γ CD complex, (G) Dovitinib/ γ CD/HDMBr complex.

binding behavior, which include both the inner γ CD cavity and the exterior rim.

The assignments of ^1H NMR signals of drug alone, and in the binary (i.e. dovitinib/HDMBr and dovitinib/ γ CD) and ternary (dovitinib/ γ CD/HDMBr) complexes are listed in Table 3. The proton positions were confirmed by COSY spectroscopy (data not shown). NMR spectrum of free dovitinib is observed at $\delta = 2.2167\text{--}7.5258$ (s). Only protons from CH groups that are located at the methyl-piperazine ring (H-1' and H-2'), benzimidazole ring (H-3', H-4', and H-5'), and quinoline ring (H-6', H-7', H-8') are shown in Table 3. The R-NH_2 and $\text{R}_2\text{-NH}$ groups do practically disappear due to the water hindered rotation within the hydrogen-bond network.

The changes in chemical shift due to the dovitinib/ γ CD complex were both upfield and downfield. The upfield displacement of drug protons, that is H-1', H-2', and H-5', was probably due to an electro-negative effect of the γ CD oxygen atoms [33,34]. The downfield shifts (H-3', H-4', H-6', H-7', and H-8') indicate that local polarity changes when the protons were located inside the γ CD cavity [35,36], and weak van der Waals interaction between the drug and glucose subunits [37].

For ternary dovitinib/ γ CD/HDMBr complex, only chemical shifts of

the H-1' and H-5' moved downfield, hence the signals, except that of H-2', were deshielded in comparison to those of the dovitinib/HDMBr complex. The presence of HDMBr induced a larger resonance effect and altered the complex conformation.

This shows that HDMBr effectively enhance the drug- γ CD interaction. The NMR study shows that in the dovitinib/ γ CD complex the quinoline rings is located within γ CD cavity but the benzimidazole ring is only partly included in the cavity (Fig. 5).

Table 4 shows the chemical shifts of HDMBr upon formation of binary (i.e. dovitinib/HDMBr and γ CD/HDMBr) and ternary (i.e. dovitinib/ γ CD/HDMBr) complexes. Large upfield shifts were observed for H-1' to H-4' of the polymer subunit due to nearby π -electron cloud or the changes in molecular conformation [33,34,38]. In the binary system, HDMBr rather prefers γ CD than dovitinib. The magnitude of the shielding effect is larger when the polymer was presented.

In conclusion, the drug displays two types of binding behavior, that are incorporation of quinolone ring into the γ CD cavity, and alignment the other parts of the dovitinib molecule with the outer surface of the γ CD molecule. The presence of HDMBr increased the magnitude of all observed interactions between drug and γ CD, particularly the shielding

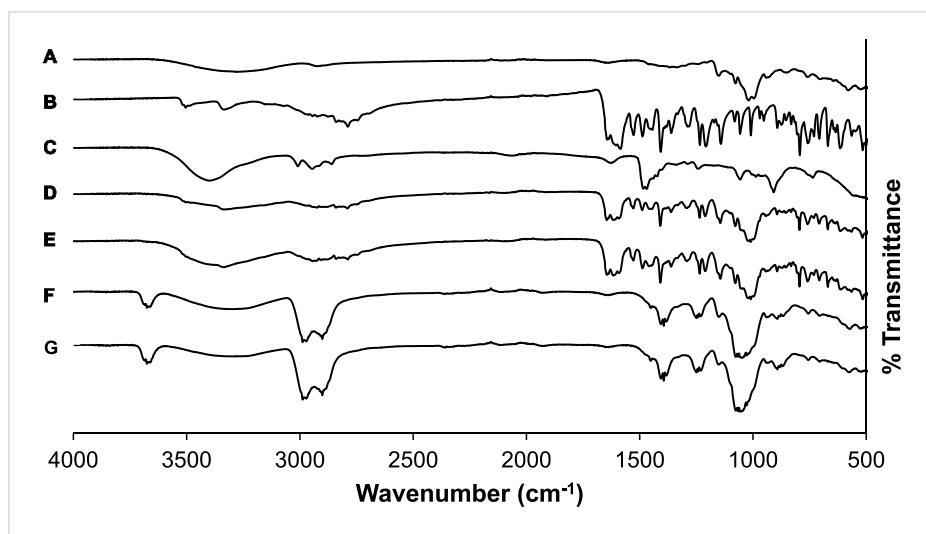


Fig. 9. FT-IR spectra of (A) γ CD, (B) pure dovitinib, (C) HDMBr, (D) Dovitinib/ γ CD physical mixture, (E) Dovitinib/ γ CD/HDMBr physical mixture, (F) Dovitinib/ γ CD complex, (G) Dovitinib/ γ CD/HDMBr complex.

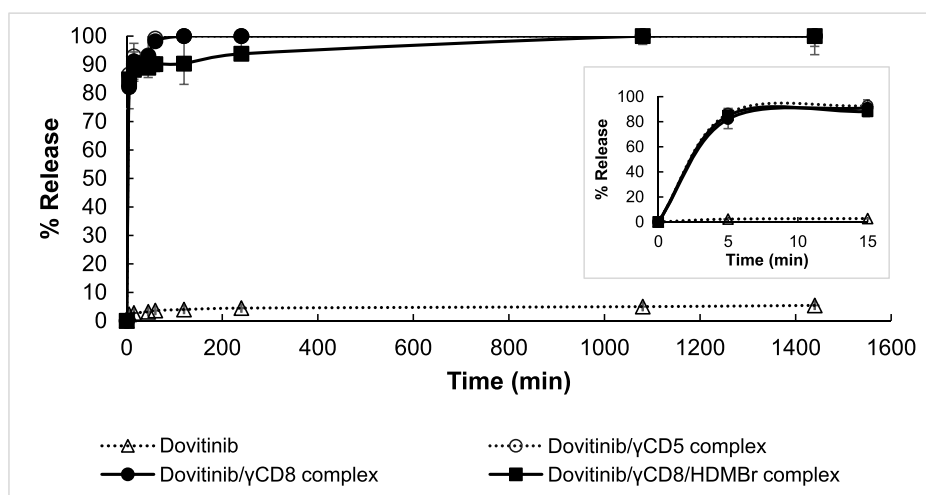


Fig. 10. *In vitro* dissolution of dovitinib in solid complexes with γ CD at concentration of 5% or 8% w/w ($n = 3$).

shifts. The permanent positively charge of the HDMBr's nitrogen atom might induce electronegative effect on via π -electron cloud in dovitinib and γ CD [39–41]. This polymer enhanced the interaction of dovitinib with both internal and external part of the γ CD molecule. The proposed complex formation of dovitinib/ γ CD/HDMBr ternary system is schematically depicted in Fig. 6.

3.4. Characterization of dovitinib/ γ CD/polymer complexes in solid state

3.4.1. Physicochemical characteristics of solid complexes

The XRPD pattern of dovitinib/ γ CD binary complex, dovitinib/ γ CD/HDMBr ternary complex, physical mixture of the binary and ternary systems, and the pure substances are shown in Fig. 7. The diffractograms of dovitinib and γ CD show their strongly crystallinity with a series of intense lines and well-defined peaks while that of HDMBr exhibited a broad shape, confirming its amorphous character. The observed patterns of the binary and ternary physical mixtures displayed all the drug characteristic peaks but with reduced intensities. However, these characteristic peaks had disappeared in the lyophilized binary and ternary complex samples indicating complex formation [26,42,43].

Pure γ CD, pure dovitinib, HDMBr, their physical mixtures, and their complexes were studied by DSC (Fig. 8). The thermal profile of γ CD

showed broad bands at 90.4 and 320.4 $^{\circ}$ C, corresponding to the γ CD dehydration and decomposition. HDMBr also showed very broad decomposition peak at 280.4 $^{\circ}$ C. The endothermic T_{max} of dovitinib alone was observed at 332.9 $^{\circ}$ C representing the melting point of crystalline drug. This drug melting peak overlapped with γ CD decomposition bands thus it was difficult to be detected in the binary and ternary mixtures. However, other related KIs that is axitinib, motesanib and their γ CD complexes were also tested, and both showed well-distinct endothermic peaks (i.e. melting points) whereas their complexes did not (data not shown). In case of dovitinib complexes, the DSC patterns were similar to the described result. Additionally, an exothermic peak appeared at 327.9 $^{\circ}$ C in binary mixture, and at 302.9 $^{\circ}$ C in ternary mixture, suggesting decomposition [26].

In attempt to examine host-guest interaction in a solid state, FTIR spectra of pure substances, physical mixtures, and complexes were compared (Fig. 9). The observation focused on the spectral changes of γ CD and dovitinib.

The free γ CD showed intense broad absorption bands at 3293 cm^{-1} related to the free $-\text{OH}$ stretching vibration. The observed spectra of dovitinib mixtures (3320–3322 cm^{-1}) was less narrowed and shifted to a higher wavenumber in the binary and ternary complexes (3331–3347 cm^{-1}). This change is an indicator of dovitinib/ γ CD complex

formation [44,45]. The vibration of the $-\text{CH}$ and $-\text{CH}_2$ groups in pure γCD appear at 2902 cm^{-1} , and another large band corresponding to the $\text{C}-\text{O}-\text{C}$ stretching vibration is observed at 1020 cm^{-1} . The shifts in $-\text{CH}$ and $-\text{CH}_2$ vibrations at approximately 2971 cm^{-1} occurred only in the dovitinib complexes. The $\text{C}-\text{O}-\text{C}$ stretching vibration of physical mixtures were shifted to lower frequency (1009 cm^{-1}) and that of dovitinib complexes to higher frequency (1045 cm^{-1}). In the dovitinib/ γCD /HDMBr ternary complexes this band had narrowed, which might be an influence of HDMBr. The changes indicated that γCD formed complex with drug that included the hydrophilic polymer. The increment observed in the dovitinib complexes corresponds to insertion of an electron-rich group into CD cavity which increases the electron density of the cavity [44–46]. This insertion behavior supported the results of the ^1H NMR study.

With respect to dovitinib spectrum, it had characteristic bands at 3502 cm^{-1} related to $\text{N}-\text{H}$ stretching vibration, 1645 cm^{-1} which is carbonyl group ($\text{C}=\text{O}$) stretching frequency, the aromatic ring ($\text{C}=\text{C}$) produced a peak at 1612 cm^{-1} , 2837 cm^{-1} related to aliphatic $\text{C}-\text{H}$ stretching vibration, and 1,2 di-substituted benzene ring at 753 and 793 cm^{-1} . All absorption frequencies disappeared upon complexation and the aliphatic $\text{C}-\text{H}$ stretching was shifted. Besides, the characteristic peaks exhibited less intensities in physical mixtures [47,48]. In summary, this observation indicated formation of binary and ternary complexes and support the XRPD and DSC data.

3.4.2. Dissolution studies

The enhanced aqueous solubility of the ternary dovitinib/ γCD /HDMBr complex should result in faster drug dissolution. The following step was to evaluate the dissolution performance of optimum ternary system in comparison with that of the pure drug and binary complexes. The ternary dovitinib/ γCD /HDMBr complexes were tested at 5% and 8% w/v γCD concentration due to different increase of drug solubility in previous study [11]. A modified dissolution test with small volume of dissolution medium was used.

The dissolution profiles in Fig. 10 show that the dissolution rate of dovitinib from the two amorphous binary complexes were equally fast from both complexes with 90% dissolution within 2 min [47]. Addition of HDMBr to form ternary complex lowered the release rate, probably due to polymer matrix formation [49,50]. Upon complete drug dissolution, the concentration of dissolved drug remained constant. It is known that CDs are able to stabilize supersaturated aqueous drug solutions [51,52].

4. Conclusion

The phase-solubility profiles of binary and ternary complexes were classified as B_3 -type. HDMBr increased the γCD solubilization of dovitinib and enhanced the CE from 0.0110 to 0.0391. Solid state characterizations by XRPD, DSC, and FTIR indicated the formation of dovitinib/ γCD complex. Furthermore, γCD was shown to stabilize supersaturated dovitinib solution and to enhance dissolution rate, yet this rate was slightly decreased from the ternary dovitinib/ γCD /HDMBr complex due to HDMBr matrix formation. γCD was shown to be an excellent complexing agent with solubilizer of dovitinib whereas addition of HDMBr resulted in synergistic solubilizing effect.

CRedit authorship contribution statement

Pitsiree Praphanwittaya: Investigation, Data curation, Writing - original draft. **Phennapha Saokham:** Methodology. **Phatsawee Jansook:** Methodology. **Thorsteinn Loftsson:** Funding acquisition, Supervision, Writing - original draft.

Declaration of competing interest

The authors declare that there is no conflict of interest. The work

was performed by Pitsiree Praphanwittaya and will be part of her PhD thesis.

Acknowledgement

This study was supported by a grant from Icelandic Center of Research, (RANNÍS), and gratefully supported by the University of Iceland. The authors acknowledge Sigurður Sveinn Jónsson, Iceland GeoSurvey (ÍSOR) for his technical assist during X-ray powder diffraction analysis (XRPD).

References

- [1] B. Escudier, V. Grunwald, A. Ravaud, Y.C. Ou, D. Castellano, C.C. Lin, J.E. Gschwend, A. Harzstark, S. Beall, N. Pirota, M. Squires, M. Shi, E. Angevin, Phase II results of dovitinib (TKI258) in patients with metastatic renal cell cancer, *Clin. Cancer Res.* 20 (2014) 3012–3022.
- [2] M. Herbrink, J.H. Schellens, J.H. Beijnen, B. Nuijen, Inherent formulation issues of kinase inhibitors, *J. Control. Release : Off. J. Control. Release Soc.* 239 (2016) 118–127.
- [3] A.C. Dubbelman, A. Uphagrove, J.H. Beijnen, S. Marchetti, E. Tan, K. Krone, S. Anand, J.H.M. Schellens, Disposition and metabolism of C-14-dovitinib (TKI258), an inhibitor of FGFR and VEGFR, after oral administration in patients with advanced solid tumors, *Cancer Chemother. Pharmacol.* 70 (2012) 653–663.
- [4] J.R. Infante, R.K. Ramanathan, D. George, E. Tan, M. Quinlan, A. Liu, J.W. Scott, S. Sharma, A randomized, crossover phase 1 study to assess the effects of formulation (capsule vs tablet) and meal consumption on the bioavailability of dovitinib (TKI258), *Cancer Chemother. Pharmacol.* 75 (2015) 729–737.
- [5] J. Sarantopoulos, S. Goel, V. Chung, P. Munster, S. Pant, M.R. Patel, J. Infante, H. Tawbi, C. Becerra, J. Bruce, F. Kabbinar, A.C. Lockhart, E. Tan, S. Yang, G. Carlson, J.W. Scott, S. Sharma, Randomized phase 1 crossover study assessing the bioequivalence of capsule and tablet formulations of dovitinib (TKI258) in patients with advanced solid tumors, *Cancer Chemother. Pharmacol.* 78 (2016) 921–927.
- [6] S. Sharma, R.K. Ramanathan, D.J. George, M. Quinlan, S. Kulkarni, A. Homs, J.W. Scott, J.R. Infante, A randomized, crossover phase 1 study to assess the effects of formulation and meal consumption on the bioavailability of dovitinib (TKI258), *J. Clin. Oncol.* 31 (2013).
- [7] S.A. Fahmy, J. Brüßler, M. Alawak, M.M.H. El-Sayed, U. Bakowsky, T. Shoeib, Chemotherapy based on supramolecular chemistry: a promising strategy in cancer therapy, *Pharmaceutics* 11 (2019) 292.
- [8] N. Qiu, X. Li, J. Liu, Application of cyclodextrins in cancer treatment, *J. Incl. Phenom. Macrocycl. Chem.* 89 (2017) 229–246.
- [9] G. Tóth, Á. Jánoska, Z.-I. Szabó, G. Völgyi, G. Orgován, L. Szente, B. Noszá, Physicochemical characterisation and cyclodextrin complexation of erlotinib, *Supramol. Chem.* 28 (2016) 656–664.
- [10] G. Tóth, Á. Jánoska, G. Völgyi, Z.I. Szabó, G. Orgován, A. Mirzahosseini, Physicochemical characterization and cyclodextrin complexation of the anticancer drug lapatinib, *J. Chem.* 2017 (2017) 4537632, <https://doi.org/10.1155/2017/4537632>.
- [11] P. Praphanwittaya, P. Saokham, P. Jansook, T. Loftsson, Aqueous Solubility of Kinase Inhibitors: I the Effect of Hydrophilic Polymers on Their γ -cyclodextrin Solubilization, (2019).
- [12] M.E. Brewster, T. Loftsson, Cyclodextrins as pharmaceutical solubilizers, *Adv. Drug Deliv. Rev.* 59 (2007) 645–666.
- [13] J.K. Kristinsson, H. Fridriksdottir, S. Thorisdottir, A.M. Sigurdardottir, E. Stefansson, T. Loftsson, Dexamethasone-cyclodextrin-polymer co-complexes in aqueous eye drops - aqueous humor pharmacokinetics in humans, *Investig. Ophthalmol. Vis. Sci.* 37 (1996) 1199–1203.
- [14] T. Loftsson, P. Saokham, A.R. Sá Couto, Self-association of cyclodextrins and cyclodextrin complexes in aqueous solutions, *Int. J. Pharm.* 560 (2019) 228–234.
- [15] P. Saokham, T. Loftsson, γ -Cyclodextrin, *Int. J. Pharm.* 516 (2017) 278–292.
- [16] T. Loftsson, E. Stefansson, Cyclodextrins and topical drug delivery to the anterior and posterior segments of the eye, *Int. J. Pharm.* 531 (2017) 413–423.
- [17] F.X. Bao, H.Y. Shi, M. Gao, L. Yang, L.Y. Zhou, Q.G. Zhao, Y. Wu, K.S. Chen, G. Xiang, Q. Long, J.Y. Guo, J. Zhang, X.G. Liu, Polybrene induces neural degeneration by bidirectional Ca^{2+} influx-dependent mitochondrial and ER-mitochondrial dynamics, *Cell Death Dis.* 9 (2018), <https://doi.org/10.1038/s41419-018-41009-41418>.
- [18] J.W. Pate, W.H. Lee Jr., Polybrene and renal toxicity, *J. Thorac. Cardiovasc. Surg.* 46 (1963) 390–392.
- [19] H.T. Ransdell, J.A. Haller, D. Stowens, P.B. Barton, Renal toxicity of polybrene (hexadimethrine bromide), *J. Surg. Res.* 5 (1965) 195–199.
- [20] T. Loftsson, N. Leevess, J.F. Sigurjonsdottir, H.H. Sigurdsson, M. Masson, Sustained drug delivery system based on a cationic polymer and an anionic drug/cyclodextrin complex, *Die Pharmazie* 56 (2001) 746–747.
- [21] H.H. Sigurdsson, E. Knudsen, T. Loftsson, N. Leevess, J.F. Sigurjonsdottir, M. Måsson, Mucoadhesive sustained drug delivery system based on cationic polymer and anionic cyclodextrin/triclosan complex, *J. Incl. Phenom. Macrocycl. Chem.* 44 (2002) 169–172.
- [22] P. Jansook, M. Moya-Ortega, T. Loftsson, Effect of self-aggregation of γ -cyclodextrin on drug solubilization, *J. Inclusion Phenom.* 68 (2010) 229–236.

- [23] T. Loftsson, M.E. Brewster, Cyclodextrins as functional excipients: methods to enhance complexation efficiency, *J. Pharm. Sci.* 101 (2012) 3019–3032.
- [24] M. Moya-Ortega, M. Messner, P. Jansook, T. Nielsen, V. Wintgens, K. Larsen, C. Amiel, H. Sigurdsson, T. Loftsson, Drug loading in cyclodextrin polymers: dexamethasone model drug, *J. Incl. Phenom. Macrocycl. Chem.* 69 (2011) 377–382.
- [25] T. Higuchi, K.A. Connors, Phase-solubility techniques, in: C.N. Reilly (Ed.), *Advances in Analytical Chemistry and Instrumentation*, Wiley-Interscience, New York, 1965, pp. 117–212.
- [26] P. Jansook, W. Pichayakorn, C. Muankaew, T. Loftsson, Cyclodextrin-poloxamer aggregates as nanocarriers in eye drop formulations: dexamethasone and amphotericin B, *Drug Dev. Ind. Pharm.* 42 (2016) 1446–1454.
- [27] C. Muankaew, P. Jansook, H.H. Sigurdsson, T. Loftsson, Cyclodextrin-based telmisartan ophthalmic suspension: formulation development for water-insoluble drugs, *Int. J. Pharm.* 507 (2016) 21–31.
- [28] N.R. Budha, A. Frymoyer, G.S. Smelick, J.Y. Jin, M.R. Yago, M.J. Dresser, S.N. Holden, L.Z. Benet, J.A. Ware, Drug absorption interactions between oral targeted anticancer agents and PPIs: is pH-dependent solubility the Achilles heel of targeted therapy? *Clin. Pharmacol. Ther.* 92 (2012) 203–213.
- [29] L. Zhang, F. Wu, S.C. Lee, H. Zhao, L. Zhang, pH-dependent drug-drug interactions for weak base drugs: potential implications for new drug development, *Clin. Pharmacol. Ther.* 96 (2014) 266–277.
- [30] S. Bekiroglu, L. Kenne, C. Sandstrom, ¹H NMR studies of maltose, maltoheptaose, alpha-, beta-, and gamma-cyclodextrins, and complexes in aqueous solutions with hydroxy protons as structural probes, *J. Org. Chem.* 68 (2003) 1671–1678.
- [31] F. Djedaini, S.Z. Lin, B. Perly, D. Wouessidjewe, High-field Nuclear Magnetic Resonance Techniques for the Investigation of a β -cyclodextrin:indomethacin Inclusion Complex vol. 79, (1990), pp. 643–646 Feb.
- [32] H.M.C. Marques, J. Hadgraft, I.W. Kellaway, Studies of cyclodextrin inclusion complexes. I. The salbutamol-cyclodextrin complex as studied by phase solubility and DSC, *Int. J. Pharm.* 63 (1990) 259–266.
- [33] R. Zhao, T. Tan, C. Sandstrom, NMR studies on puerarin and its interaction with beta-cyclodextrin, *J. Biol. Phys.* 37 (2011) 387–400.
- [34] L. Ribeiro, R.A. Carvalho, D.C. Ferreira, F.J. Veiga, Multicomponent complex formation between vinpocetine, cyclodextrins, tartaric acid and water-soluble polymers monitored by NMR and solubility studies, *Eur. J. Pharm. Sci. : Off. J. Eur. Fed. Pharm. Sci.* 24 (2005) 1–13.
- [35] F. Djedaini, S.Z. Lin, B. Perly, D. Wouessidjewe, High-field nuclear magnetic resonance techniques for the investigation of a β -cyclodextrin:indomethacin inclusion complex, *J. Pharm. Sci.* 79 (1990) 643–646.
- [36] A. Zornoza, C. Martín, M. Sánchez, I. Vélaz, A. Piquer, Inclusion complexation of glisentide with α -, β - and γ -cyclodextrins, *Int. J. Pharm.* 169 (1998) 239–244.
- [37] F.J. Veiga, C.M. Fernandes, R.A. Carvalho, C.F. Geraldes, Molecular modelling and ¹H-NMR: ultimate tools for the investigation of tolbutamide: beta-cyclodextrin and tolbutamide: hydroxypropyl-beta-cyclodextrin complexes, *Chem. Pharmaceut. Bull.* 49 (2001) 1251–1256.
- [38] H.M.C. Marques, J. Hadgraft, I.W. Kellaway, W.J. Pugh, Studies of cyclodextrin inclusion complexes. II. Molecular modelling and ¹H-NMR evidence for the salbutamol- β -cyclodextrin complex, *Int. J. Pharm.* 63 (1990) 267–274.
- [39] M. E Mohr, Remington: the Science and Practice of Pharmacy, twenty-first ed., (2006).
- [40] A.S. Mahadevi, G.N. Sastry, Cation- π interaction: its role and relevance in chemistry, biology, and material science, *Chem. Rev.* 113 (2013) 2100–2138.
- [41] A.S. Reddy, G.N. Sastry, Cation [M = H⁺, Li⁺, Na⁺, K⁺, Ca²⁺, Mg²⁺, NH₄⁺, and NMe₄⁺] interactions with the aromatic motifs of naturally occurring amino Acids: A theoretical study, *J. Phys. Chem. A* 109 (2005) 8893–8903.
- [42] R. Cavalli, F. Trotta, M. Trotta, L. Pastero, D. Aquilano, Effect of alkylcarbonates of γ -cyclodextrins with different chain lengths on drug complexation and release characteristics, *Int. J. Pharm.* 339 (2007) 197–204.
- [43] P. Jansook, C. Muankaew, E. Stefansson, T. Loftsson, Development of eye drops containing antihypertensive drugs: formulation of aqueous irbesartan/ γ CD eye drops, *Pharm. Dev. Technol.* 20 (2015) 626–632.
- [44] S. Goswami, A. Majumdar, M. Sarkar, Painkiller isoxicam and its copper complex can form inclusion complexes with different cyclodextrins: a fluorescence, fourier transform infrared spectroscopy, and nuclear magnetic resonance study, *J. Phys. Chem. B* 121 (2017) 8454–8466.
- [45] K.P. Sambasevam, S. Mohamad, N.M. Sarih, N.A. Ismail, Synthesis and characterization of the inclusion complex of beta-cyclodextrin and azomethine, *Int. J. Mol. Sci.* 14 (2013) 3671–3682.
- [46] B. Tang, Z.Z. Chen, N. Zhang, J. Zhang, Y. Wang, Synthesis and characterization of a novel cross-linking complex of beta-cyclodextrin-o-vanillin furfuralhydrazone and highly selective spectrofluorimetric determination of trace gallium, *Talanta* 68 (2006) 575–580.
- [47] C. Muankaew, P. Jansook, T. Loftsson, Evaluation of γ -cyclodextrin effect on permeation of lipophilic drugs: application of cellophane/fused octanol membrane, *Pharm. Dev. Technol.* 22 (2016) 562–570.
- [48] C. Muankaew, P. Jansook, E. Stefansson, T. Loftsson, Effect of γ -cyclodextrin on Solubilization and Complexation of Irbesartan: Influence of pH and Excipients vol. 474, (2014), pp. 80–90 Mar 15.
- [49] T. Loftsson, M. Masson, The effects of water-soluble polymers on cyclodextrins and cyclodextrin solubilization of drugs, *J. Drug Deliv. Sci. Technol.* 14 (2004) 35–43.
- [50] P. Mura, M.T. Fauci, G.P. Bettinetti, The influence of polyvinylpyrrolidone on naproxen complexation with hydroxypropyl-beta-cyclodextrin, *Eur. J. Pharm. Sci. : Off. J. Eur. Fed. Pharm. Sci.* 13 (2001) 187–194.
- [51] M.E. Brewster, R. Vandecruys, G. Verreck, J. Peeters, Supersaturating drug delivery systems: effect of hydrophilic cyclodextrins and other excipients on the formation and stabilization of supersaturated drug solutions, *Die Pharmazie* 63 (2008) 217–220.
- [52] J. Hong, J.C. Shah, M.D. McGonagle, Effect of cyclodextrin derivation and amorphous state of complex on accelerated degradation of ziprasidone, *J. Pharm. Sci.* 100 (2011) 2703–2716.

Paper III



Aqueous solubility of kinase inhibitors: III. The effect of acidic counter ion on the dovitinib/ γ -cyclodextrin complexation

Pitsiree Praphanwittaya¹ · Phatsawee Jansook² · Thorsteinn Loftsson¹

Received: 8 April 2020 / Accepted: 4 July 2020
© Springer Nature B.V. 2020

Abstract

Dovitinib, a hydrophobic kinase inhibitor (KI), is lipophilic anticancer agent that forms water-soluble complexes with cyclodextrins (CDs). However, dovitinib's very low intrinsic solubility hampers the complex formation and, consequently, the CD solubilization. The aim of the study was to enhance the CD solubilization through formation of more water soluble dovitinib salts. When dovitinib is unionized (i.e. at pH above its pKa value) the phase-solubility profile of the binary dovitinib/ γ CD complex is of B_s-type with K_{1:1} of 684 M⁻¹. Then the complex has limited solubility in water. Upon protonization, (i.e. at pH below the pKa value) the solubility of dovitinib was increased but the increase was dependent on the negatively charged counter ion. Citrate, acetate, EDTA and chloride resulted in the greatest solubility enhancement and, thus, were selected to further studies. The ternary phase-solubility profiles of dovitinib/ γ CD/counter ion were also of B_s-type while those of dovitinib/HP γ CD/counter ion and dovitinib/SBE γ CD/counter ion were of A_N-type. The counter ions had greater solubilizing effect in SBE γ CD solutions than in γ CD and HP γ CD solutions. This is due to the influence of charge-charge interaction between the positively charged dovitinib and negatively charged SBE γ CD. Citrate was the most effective counter ion particularly in aqueous SBE γ CD solutions. The complexation was verified by NMR. The highest dovitinib flux through semi-permeable membrane was observed from medium containing dovitinib/CDs/citrate complexes. In conclusion, citrate provided the highest dovitinib solubilization and complexation.

Keywords Dovitinib · γ -Cyclodextrin · Complexation · Salt formation · Counter ion · Solubility

1. Introduction

Dovitinib is biologically active small molecule that exhibits potent inhibitory activity against tyrosine kinase involved in tumor growth and angiogenesis [1]. In general, kinase inhibitors (KIs) are neutral or weakly basic lipophilic compounds with very poor solubility in aqueous media. The poor aqueous solubility can be one of the main causes for a low and variable uptake of a drug into the systemic circulation and consequently their low and variable bioavailability [2, 3]. Dovitinib contains nitrogen-based heterocyclic rings and is rather lipophilic [4]. Cyclodextrins (CDs) are complexing

agents and very effective pharmaceutical solubilizers. Previous study showed that the natural γ -cyclodextrin (γ CD) can enhance the aqueous solubility of KIs, especially that of dovitinib, but the complexation efficacy (CE) is relatively low [5]. Dovitinib is weak base with protonatable amino groups and estimated pKa of 6.5 [4]. Salt formation is an effective technique to increasing pH-dependent solubility of drugs [6]. Addition of organic salts (counter ions) can increase the complexation efficacy (CE) of CDs through stabilization and solubilization of drug/CD nanoparticles [7, 8].

γ CD is a cyclic oligosaccharide consisting of eight glucose units. Like other CDs, γ CD has a doughnut shape with a lipophilic central cavity and a hydrophilic outer surface, and can form inclusion complexes with a variety of drug molecules [9]. The natural γ CD has the highest aqueous solubility and the most favorable toxicological profile of the natural CDs which makes it very attractive as a pharmaceutical excipient [10, 11]. In addition, γ CD is known to self-assemble to form nano- and microparticles with the potential of being developed into novel drug delivery

✉ Thorsteinn Loftsson
thorstlo@hi.is

¹ Faculty of Pharmaceutical Sciences, University of Iceland, Hofsvallagata 53, 107 Reykjavik, Iceland

² Faculty of Pharmaceutical Sciences, Chulalongkorn University, 254 Payathai Road, Pathumwan, 10330 Bangkok, Thailand

54 systems [11–13]. Water-soluble γ CD derivatives such as
55 2-hydroxypropyl- γ -cyclodextrin (HP γ CD), sulfobutylether
56 γ -cyclodextrin (SBE γ CD) are also used in pharmaceutical
57 formulations [14]. Random substitution of hydroxyl groups
58 on the γ CD molecule results in improved CD solubility
59 [15, 16]. In addition, CD solubilization of a poorly soluble
60 drug can be enhanced by increasing its intrinsic solubil-
61 ity (S_0) and/or increasing the value of its apparent stabil-
62 ity constant ($K_{1:1}$) [17]. S_0 in aqueous complexation media
63 can be increased by, for example, adding cosolvents to the
64 media, formation of co-complexes, ionization of the drug
65 molecules and salt formations. Methods that increase $K_{1:1}$
66 include addition of water-soluble polymers to the aqueous
67 media, charge-charge interactions between ionized CDs and
68 ionic drug molecules and formation of ternary complexes
69 [18, 19]. Because of charge-charge attraction, the negatively
70 charged SBE γ CD frequently interacts somewhat stronger
71 with positively charged drug molecules than, for example,
72 the uncharged HP γ CD [17, 20, 21].

73 Counter ions especially that of organic acids, are fre-
74 quently used to improve aqueous solubility of protonizable
75 drugs [22]. The solubility of the salt is governed by the solu-
76 bility product constant of the salt, the solubility of the union-
77 ized drug, and the pKa value. In some cases the counter ion
78 is a buffer salt [17]. Weakly basic drugs such as dovitinib can
79 have higher apparent intrinsic solubility (S_0) at pH below
80 their pKa value. Appropriate pH adjustment with different
81 anionic species, or acidic counter ions such as hydroxyl and/
82 or polycarboxylic acids as ternary component, can enhance
83 CD solubilization of drugs through salt formation [17, 23].
84 One important criterion in the selection of counter ion is
85 to include candidates that have previously been used in
86 approved drug product, and/or generally recognized as safe
87 (GRAS) by authorities such as FDA [22, 24]. For a given
88 drug substance, the choices of counter ions that are feasible
89 for salt formation are limited by the basicity or acidity of the
90 ionizable drug moiety. According to the pKa rule, ideally,
91 the pKa of the counter ion should be two to three pH units
92 lower than the pKa of the basic drug to employ stable salt
93 formation [25–27]. Here dovitinib salts were formed using
94 different (mono-, di-, tri- and tetra-) carboxylic acid deriva-
95 tives with acceptable pKa in comparison to lactic acid which
96 is a commercial salt, and inorganic acid like hydrochloric
97 acid (HCl). Due to its very low pKa, HCl is the most com-
98 monly used acid for preparation of salts of basic drugs [28].
99 The aim of this present study was to enhance CD solubiliza-
100 tion of dovitinib in the aqueous complexation medium using
101 anionic counter ions. The CDs tested were γ CD, HP γ CD
102 and SBE γ CD.

Materials and methods 103

Materials 104

Dovitinib (D) was purchased from Reagents Direct 105
(Encinitas, CA, USA). γ -Cyclodextrin (γ CD) and 106
(2-hydroxypropyl)- γ -cyclodextrin (HP γ CD) were purchased 107
from Wacker (München, Germany). Sulfobutylether- γ - 108
cyclodextrin (SBE γ CD) was supplied by Ligand pharma- 109
ceuticals (Lawrence, KS, USA). 0.1 N Hydrochloric acid, 110
acetic acid, glycolic acid, DL-malic acid, L-aspartic acid, 111
tartaric acid, citric acid, disodium EDTA were purchased 112
from Sigma-Aldrich (St. Louis, MO, USA). Formic acid 113
was purchased from GmbH Chemicals GmbH (Hamburg, 114
Germany). Lactic acid was purchased from Fluka Chemie 115
GmbH (Barcelona, Spain). Milli-Q water (Millipore, Bill- 116
erica, MA) was used throughout the study. Semi-permea- 117
ble cellophane membrane with molecular weight cutoff 118
(MWCO) 12–14,000 Da were purchased from Biotech CE, 119
Spectrum Europe (Breda, The Netherlands). 120

pH-solubility profiles 121

Excess amount of dovitinib was added to aqueous medium 122
(pH 1 to 11). Pure water and aqueous 5% (w/v) γ CD solu- 123
tion were adjusted to the desire pH (Thermo Orion 3 Star™ 124
bench top pH meter, Thermo Fisher Scientific, USA) by 125
dropwise titration with concentrated hydrochloric acid and 126
sodium hydroxide solutions. The method applied has previ- 127
ously been described [5]. Briefly, the suspensions formed 128
were sonicated at 30 °C for 30 min. All suspensions were 129
allowed to equilibrate at room temperature (22–23 °C) 130
for 7 days under constant agitation, and the pH readjusted 131
periodically. The saturated suspensions were centrifuged 132
at 12,000 rpm for 15 min. (Heraeus Pico 17 Centrifuge, 133
Thermo Fisher Scientific, Germany). The supernatant was 134
then diluted with Milli-Q water and analyzed by HPLC. 135
Each experiment was performed in triplicate and the results 136
are the mean values \pm standard deviation (SD). 137

Phase-solubility studies 138

The determination of drug solubility was performed as 139
described above in Sect. 2.2. Briefly, excess amount of dovi- 140
tinib was added to aqueous complexation media containing 141
from 0 to 20% (w/v) γ CD, with and without 1% (w/v) acidic 142
counter ion at pH 6. 143

Phase-solubility analysis was conducted according to method described by Higuchi and Connors [29]. The value of the apparent stability constant ($K_{1:1}$) of the dovitinib/ γ CD 1:1 (mole ratio) complex (Eq. 1) and the complexation efficiency (CE) (Eq. 2) were calculated from slope of the initial linear portion of dovitinib concentration against γ CD concentration profiles.

$$K_{1:1} = \frac{\text{slope}}{S_0 \cdot (1 - \text{slope})} \quad (1)$$

$$CE = S_0 \cdot K_{1:1} = \frac{\text{slope}}{(1 - \text{slope})} = \frac{[KI/\gamma CD \text{ complex}]}{[\gamma CD]} \quad (2)$$

where S_0 is the intrinsic solubility of drug, [dovitinib/ γ CD complex] is the concentration of dissolved complex and $[\gamma CD]$ is the concentration of dissolved γ CD in the aqueous complexation media.

The counter ions that had the largest effect on the dovitinib solubility were selected for phase-solubility studies of the dovitinib/counter ion/CD ternary complexes.

Preparation of dovitinib salts ternary acidic counter ion complex

Binary dovitinib/counter ion salts and ternary dovitinib/ γ CD/counter ion complexes were prepared in triplicate by adding 1% (w/v) acidic counter ion to the aqueous medium as described in Sect. 2.2. The suspensions were adjusted at pH 6. The amount of γ CD dissolved in the ternary complex medium was determined from the phase solubility profiles prepared according to Sect. 2.3. This γ CD concentration of maximum dovitinib solubility was applied in the ternary complex preparation.

Quantitative determinations

The concentration of dovitinib was analyzed in a reversed-phase high performance liquid chromatography (HPLC) system (Dionex, Softron GmbH Ultimate 3000 series, Germany). The analytical instrument composed of a P680 pump with a DG-1210 degasser, an ASI-100 autosampler, VWD-3400 UV-Vis detector, and a column heater, containing a C18 column (100A 150 \times 4.6 mm, 5 μ m) from Kinetex

Core-shell technology and a guard column (Phenomenex, UK). The HPLC system was operated under 30 $^{\circ}$ C, isocratic condition, flow rate was 1.0 mL/min and detection wavelength was 233 nm. The mobile phase consisted of acetonitrile, methanol, and 10 mM ammonium formate buffer pH 4.5 (volume ratio 20:40:40).

$^1\text{H-NMR}$ Spectroscopic studies

$^1\text{H-NMR}$ spectra of complexes were recorded in combined NMR solvent of deuterated dimethyl sulfoxide (DMSO-d_6) and deuterium oxide (D_2O), volume ratio 9:1. at 400 MHz and 298 K using Bruker AVANCE 400 instrument (Bruker Biospin GmbH, Karlsruhe, Germany). Solid samples of CDs, dovitinib, dovitinib/CD binary complex (1:1 molar ratio), and dovitinib/CD/counter ion ternary complex (1:1:1 molar ratio) were subjected to analysis. The magnitudes of chemical shifts were recorded in ppm (δ). The resonance at 2.5000 ppm, due to residual solvent (DMSO-d_6), was used as internal reference. $^1\text{H-NMR}$ chemical shift change ($\Delta\delta$) caused upon complexation was calculated according to Eq. 3:

$$\Delta\delta = \delta_{\text{complex}} - \delta_{\text{free}} \quad (3)$$

In vitro permeation studies

The effect of CDs and counter ion on dovitinib permeation was conducted using unjacketed Franz diffusion cells (SES GmbH-Analysesysteme, Germany). The donor chamber and the receptor chamber were separated with a single layer of semi-permeable cellophane membrane with MWCO 12–14,000 Da (diffusion area of 1.77 cm^2). The membrane was soaked overnight in the receptor phase that consisted of aqueous solution containing phosphate buffer saline solution pH 7.4 and 2.5% (w/v) γ CD. γ CD was added to the receptor phase to ensure sufficient drug solubility. The receptor phase (12 ml) was sonicated under vacuum to remove dissolved gas. The sample (1 ml) was added to the donor chamber after filtration through 0.45 mm membrane filter. The study was carried out at ambient temperature (22–23 $^{\circ}$ C) under continuous stirring of the receptor phase by magnetic stirring bar rotating at 300 rpm. A 150 ml sample of receptor medium was withdrawn

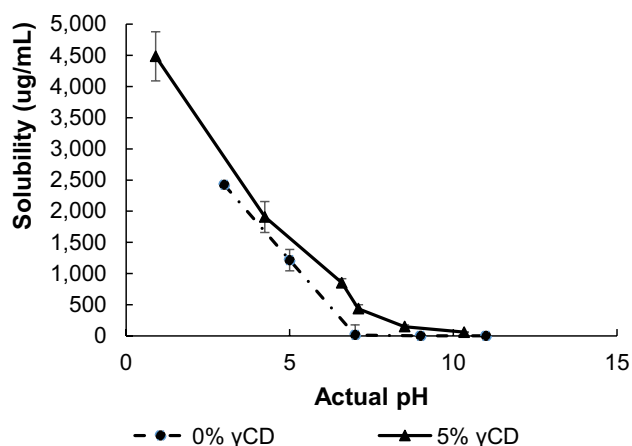


Fig. 1 pH-solubility profiles of dovitinib in pure water and in 5% (w/v) aqueous γ CD solutions (mean \pm standard deviation; $n=3$)

219 at 30, 60, 120, 180, 240, 300, and 360 min and replaced immediately with an equal volume of fresh receptor phase. The drug concentration was determined by HPLC.

222 The steady state flux was calculated as the slope (dq/dt) of linear section of the amount of drug in the receptor chamber (q) versus time (t) profiles, and the apparent permeability coefficient (P_{app}) was calculated from the flux (J) according to Eq. 4:

$$227 \quad J = \frac{dq}{A \times dt} = P_{app} \times C_d \quad (4)$$

228 where A is the surface area of mounted chamber (1.77 cm^2) and C_d is initial concentration of dovitinib in the donor phase. Each experiment was performed in triplicate and the results reported as the mean values \pm standard deviation (SD).

233 Results and discussions

234 The pH-solubility studies

235 The aqueous solubility of plain dovitinib and binary dovitinib/ γ CD complexes was pH-dependent (Fig. 1). The drug was more soluble at low pH, but it was degraded (i.e. color change was observed) at strong acidic conditions (e.g., at pH 1) when no γ CD was present. The presence of γ CD at 5% (w/v) can improve the solubility of dovitinib and protect the drug from acidic degradation lower pH 3.

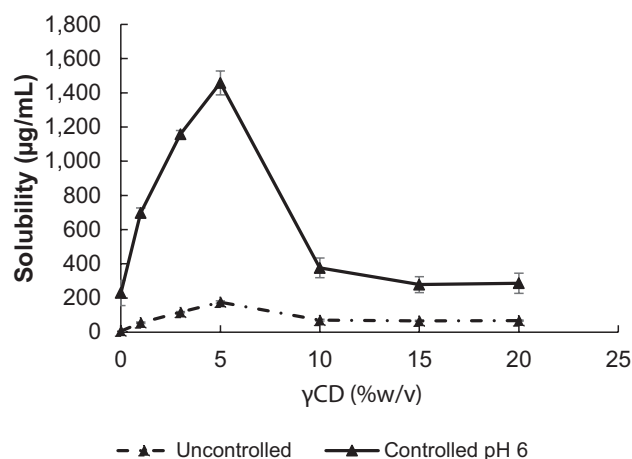


Fig. 2 Phase-solubility profiles of dovitinib complexes in pure water and in aqueous hydrochloric acid solution, at pH 6 (mean \pm standard deviation; $n=3$)

The phase solubility studies

242 In general, the phase-solubility profiles showed formation of dovitinib/ γ CD complexes that have limited solubility in water or, in other words, displayed B_s -type profiles (Fig. 2). Under ambient conditions, when the pH was not adjusted, the media pH was 6.86. Hydrochloric acid was used to adjust pH of the complexation media to pH 6. Although dovitinib was more soluble at pH 6, $K_{1:1}$ was decreased from 684 M^{-1} to 145 M^{-1} due to dovitinib ionization (Table 1). Normally, the more lipophilic unionized form of a drug molecule has a greater affinity for the hydrophobic CD cavity than the ionized form and, thus, the unionized form has a higher $K_{1:1}$ value [17].

Effect of acidic counter ion on drug solubility

256 In search of the optimal acidic counter ion, aqueous solubility of dovitinib in binary and ternary systems containing 8% (w/v) γ CD with and without 1% (w/v) of the given acid was determined at pH 6. Here the solubility determination was performed at γ CD concentration that is above the determined maximum dovitinib solubility according to the phase-solubility profile (see Fig. 2).

262 The drug solubility of ionized systems is presented in Fig. 3. The aqueous solubility of the ionized dovitinib is always greater than that of the unionized dovitinib (i.e.

Table 1 Solubilization efficacy of dovitinib in different CD solution

| Counter ion | pH | S_0 ($\mu\text{g/ml}$) | Phase solubility parameters | | | | | | | | |
|----------------|---------------|----------------------------|-----------------------------|-------------------------------|------|------------------------------|-------------------------------|------|-----------------------------|-------------------------------|------|
| | | | γCD^a | | | $\text{HP}\gamma\text{CD}^a$ | | | $\text{SBE}\gamma\text{CD}$ | | |
| | | | PS-type | $K_{1:1}$ (M^{-1}) | CE | PS-type | $K_{1:1}$ (M^{-1}) | CE | PS-type | $K_{1:1}$ (M^{-1}) | CE |
| No counter ion | 6.86 | 6.34 | B_s | 684 | 0.01 | – | – | – | – | – | – |
| HCl | 6.0 ± 0.1 | 229 | B_s | 145 | 0.08 | A_N | 44 | 0.03 | – | – | – |
| EDTA | 6.0 ± 0.1 | 28.5 | B_s | 1590 | 0.12 | A_N | 1490 | 0.11 | A_N | 3960 | 0.44 |
| Acetate | 6.0 ± 0.1 | 41.7 | B_s | 2110 | 0.22 | A_N | 1250 | 0.13 | A_N | 4680 | 0.70 |
| Citrate | 6.0 ± 0.1 | 33.9 | B_s | 2270 | 0.20 | A_N | 1630 | 0.14 | A_N | 8350 | 0.63 |

^aRefers to linear correlation calculated from 0 to 5% (w/v) CD

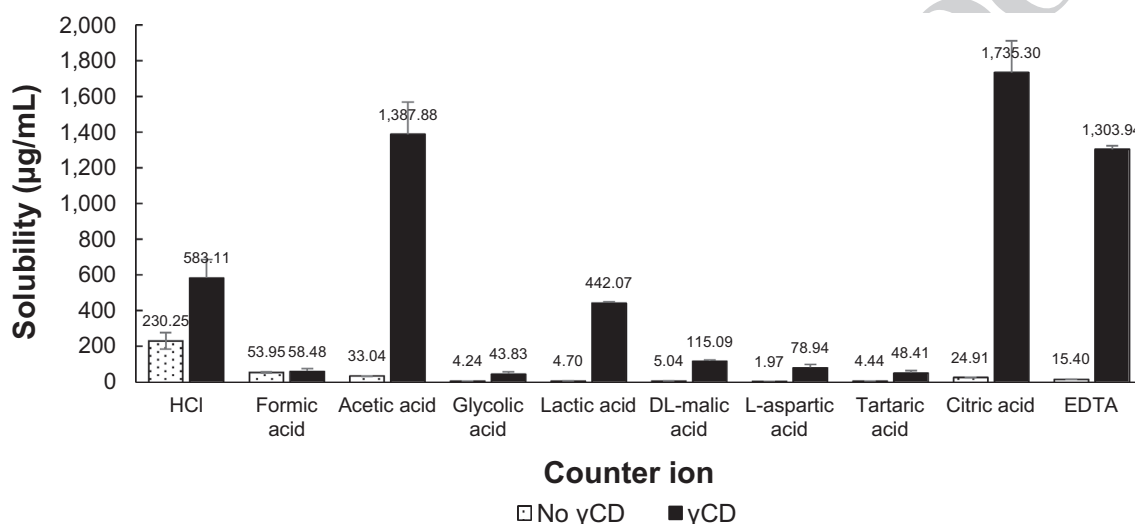


Fig. 3 Aqueous solubility of the dovitinib in buffered aqueous 8% w/v γCD at pH 6.0 with and without 1% (w/v) acidic counter ion solution at room temperature (\pm standard deviation; $n = 3$)

266 the S_0 value in Eq. 2) and, due to enhance complexation
 267 efficacy, the solubility of the ionized dovitinib in the aque-
 268 ous complexation medium will be greater as well. In pure
 269 water the chloride had the highest solubility (Fig. 3). Addi-
 270 tion of counter ions to the complexation media resulted in
 271 significant solubility enhancement. However, the solubility
 272 enhancement observed in the γCD complexation media was
 273 not always proportional to the observed S_0 increase. Citric
 274 acid, acetic acid, EDTA and HCl resulted in the greatest
 275 solubility enhancement. Although formation of dovitinib
 276 hydrochloride (upon addition of HCl) resulted in less solu-
 277 bility enhancement in the aqueous γCD complexation media.
 278 It is clear that pKa difference between dovitinib (estimated

279 pKa 6.5) and HCl (pKa – 10) is insufficient and, thus, even
 280 if a salt is formed it may readily break down into individual
 281 species in the γCD complexation media [22, 28]. Organic
 282 acids, especially hydroxyl and/or polycarboxylic acids such
 283 as citric acid, are known to increase the aqueous solubility
 284 of the poorly soluble β -cyclodextrin (βCD), possibly through
 285 modification of intramolecular and intermolecular hydrogen
 286 bonding system of βCD [17, 30]. It is possible that citric
 287 acid, acetic acid and EDTA interacted with CD molecules
 288 by forming hydrogen bonds with their numerous hydroxyl
 289 groups at the appropriate position. Thus, only three acids
 290 that is citric acid, acetic acid and EDTA, were selected for
 291 further studies.

Table 2 ^1H NMR chemical shift difference ($\Delta\delta$, ppm) of free γCD and in the binary (i.e. dovitinib/ γCD and citric acid/ γCD) and ternary dovitinib/ γCD /citric acid complexes

| ^1H assignment ^a | δ free | $\Delta\delta^b$ | | |
|--------------------------------------|-------------------|--------------------------------|------------------------------|---|
| | γCD | Citric acid/ γCD | Dovitinib/ γCD | Dovitinib/ γCD /citric acid |
| H-1 | 4.8700 | -0.0022 | 0.0005 | -0.0002 |
| H-3 | 3.6025 | -0.0022 | -0.0005 | -0.0010 |
| H-5 | 3.5550 | -0.0023 | -0.0004 | -0.0010 |
| H-6 | 3.5032 | -0.0029 | -0.0005 | -0.0010 |
| H-2 | 3.3298 | -0.0004 | 0.0000 | 0.0001 |
| H-4 | 3.3058 | -0.0004 | -0.0001 | 0.0002 |

^aResidual semideuterated DMSO used as reference at 2.5000 ppm^b $\Delta\delta = \delta$ complex - δ free**3.4 Effect of acidic counter ion on phase-solubility profile**

Citric acid, acetic acid, EDTA were selected to investigate the phase-solubility behavior in aqueous complexation media containing neutral CD and charged CD. HCl was used as a reference in comparison of those carboxylic acid derivatives. Since, the ionized form of dovitinib has positive charge, the negatively charged γCD derivative SBE γCD was used to study the effects of charge-charge interaction.

The ternary phase-solubility profiles of dovitinib/ γCD /counter ion were B_s-type meanwhile those of dovitinib/HP γCD /counter ion and dovitinib/SBE γCD /counter ion were A_N-type (data not shown). In general, cyclodextrin derivatives from A-type phase-solubility profiles while

Table 4 ^1H NMR chemical shift difference ($\Delta\delta$, ppm) of free SBE γCD and in the binary (i.e. dovitinib/SBE γCD and citric acid/SBE γCD) and ternary dovitinib/SBE γCD /citric acid complexes

| ^1H assignment ^a | δ free SBE γCD | $\Delta\delta = \delta$ complex - δ free | | |
|--------------------------------------|--|---|---------------------------------|---|
| | | Citric acid/SBE γCD | Dovitinib/SBE γCD | Dovitinib/citric acid/SBE γCD |
| H-1 | 4.8589 | 0.0014 | 0.0014 | -0.0008 |
| H-3 | 3.6732 | N/A | -0.0002 | 0.0028 |
| H-5 | 3.6079 | 0.0005 | 0.0008 | -0.0006 |
| H-6 | 3.5247 | 0.0008 | 0.0010 | -0.0006 |
| H-2 | 3.3283 | 0.0005 | 0.0007 | -0.0051 |
| H-4 | 3.2354 | -0.0004 | 0.0005 | -0.0228 |
| H-4' | 2.0661 | 0.0001 | -0.0003 | -0.0025 |
| H-3' | 1.5794 | -0.0056 | 0.0000 | -0.0009 |
| H-2' | 1.5181 | -0.0012 | 0.0000 | -0.0024 |

^aResidual semideuterated DMSO used as reference at 2.5000 ppm^b $\Delta\delta = \delta$ complex - δ free**Table 3** ^1H NMR chemical shift difference ($\Delta\delta$, ppm) of free HP γCD and in the binary (i.e. dovitinib/HP γCD and citric acid/HP γCD) and ternary dovitinib/HP γCD /citric acid complexes

| ^1H assignment ^a | δ free HP γCD | $\Delta\delta^b$ | | |
|--------------------------------------|---------------------------------------|----------------------------------|--------------------------------|--|
| | | Citric acid/HP γCD | Dovitinib/HP γCD | Dovitinib/citric acid/HP γCD |
| H-1 | 4.8571 | -0.0002 | 0.0003 | 0.0012 |
| H-3 | 3.6776 | N/A | 0.0101 | N/A |
| H-5 | 3.6094 | 0.0006 | 0.0006 | 0.0020 |
| H-6 | 3.5255 | -0.0007 | -0.0015 | 0.0012 |
| H-4 | 3.3070 | -0.0002 | 0.0007 | -0.0364 |
| H-2 | 3.2329 | -0.0005 | 0.0002 | -0.1529 |
| H-1' | 1.0083 | 0.0002 | -0.0005 | 0.0004 |

^aResidual semideuterated DMSO used as reference at 2.5000 ppm^b $\Delta\delta = \delta$ complex - δ free

the natural CDs frequently from B-type profiles [15]. The acids provided the highest drug solubility in phase-solubility diagram of SBE γ CD, followed by HP γ CD, and γ CD. Table 1 shows the effect of different counter ions on the $K_{1:1}$ of dovitinib-CD complexes and the CE. Increasing the water solubility of dovitinib through salt formation generally increased the value the apparent $K_{1:1}$. Charge-charge attraction between ionized drug and SBE γ CD enhanced the CE even further. HCl tended to obtain the lowest solubilizing power hence it was excluded from SBE γ CD system. The best solubilizing efficiency of ternary complex system containing citric acid (SBE γ CD: $K_{1:1} = 8350 \text{ M}^{-1}$, CE = 0.63), even though the solubility of the corresponding salt with dovitinib is less than that of acetate salt which generally resulted in the highest drug solubility in those CD systems. However, acetate salt also displayed high solubility as well as the EDTA salt. The acidic counter ion probably acts as a space-regulating molecule between ionized drug and CD [31]. The differences observed between $K_{1:1}$ values in presences of the acids did not result from either the different degree of drug ionization (the pH was maintained at 6.0) or from the different solubility of those salts and therefore they might be reasonably attributed to the more or less good steric fit with hydroxyl acid provides for the drug with CD [23]. Here the most soluble salt possesses the highest CE. This has been suggested that the counter ions participate directly in complex formation, or a ternary drug cyclodextrin-salt complex is being formed [17, 23, 32]. Dovitinib acetate displayed some instability (i.e. color changes) and, thus, only citric acid was selected for further study.

$^1\text{H-NMR}$ Spectroscopic studies

Chemical shift variations of a host or guest molecule can reveal the formation of complexes that occurs between the free and bound states in solution. Here only shift changes were observed in term of CD molecules as shown in Table 2, 3, 4. Basically, the natural γ CD region includes the proton resonances from the exterior of the cavity (H-1, H-2, H-4,

and H-6), and the interior of the cavity (H-3, and H-5) [33, 34]. In γ CD derivatives, the proton resonances are not only from the protons in the cavity region but also from the substituent chains. The number of proton resonances depends on the length of the side chain. For instances, the substituent group of HP γ CD presents the proton signal at H-1' which locates near the ring [35] while SBE γ CD consisted of longer side chain presents the signals at H-2', H-3', H-4' [36, 37].

The change in the ^1H NMR chemical shifts of the γ CD protons (Table 2), when with dovitinib and citric acid, showed that the H-3, H-5, and H-6 protons showed slightly upfield shifts ($\Delta\delta < 0$) due to shielding effect whereas H-2 and H-4 protons are relatively unaffected. It indicates that the guest molecules are inserted into the γ CD cavity. The addition of citric acid increased the shielding effect of the guest molecules (i.e. aromatic moieties of dovitinib), or some changes in molecular conformation due to the complex formation [38, 39]. Moreover, the increasing of the shifts after addition of citric acid is maybe due to an increase of the drug-CD association constant as a consequence of changes in the ionization of the drug and/or in the polarity of the medium.

The ^1H NMR chemical shifts corresponding to HP γ CD in free-state and in complexes are listed in Table 3. The changes in chemical shift due to the dovitinib/HP γ CD/citric acid complex were both upfield ($\Delta\delta < 0$) and downfield ($\Delta\delta > 0$). The upfield displacement ($\Delta\delta < 0$) of CD protons that is H-2 and H-4 according to shielding effect as described previously. The downfield shift ($\Delta\delta > 0$) is at H-1, H-5, H-6, and H-1' due to the de-shielding effects of the van der Waals interaction between γ CD and guest molecules or local polarity change after complex formation [38, 40, 41]. The magnitude of the shielding effect is larger when the citric acid was presented. The signal shift is rather intensive in H-2 and H-4 protons than H-3 and H-5 protons. This suggests that binding happens mainly at the external rim mainly rather than at the internal HP γ CD cavity.

The chemical shift changes of SBE γ CD in presence of dovitinib and citric acid are shown in Table 4. The

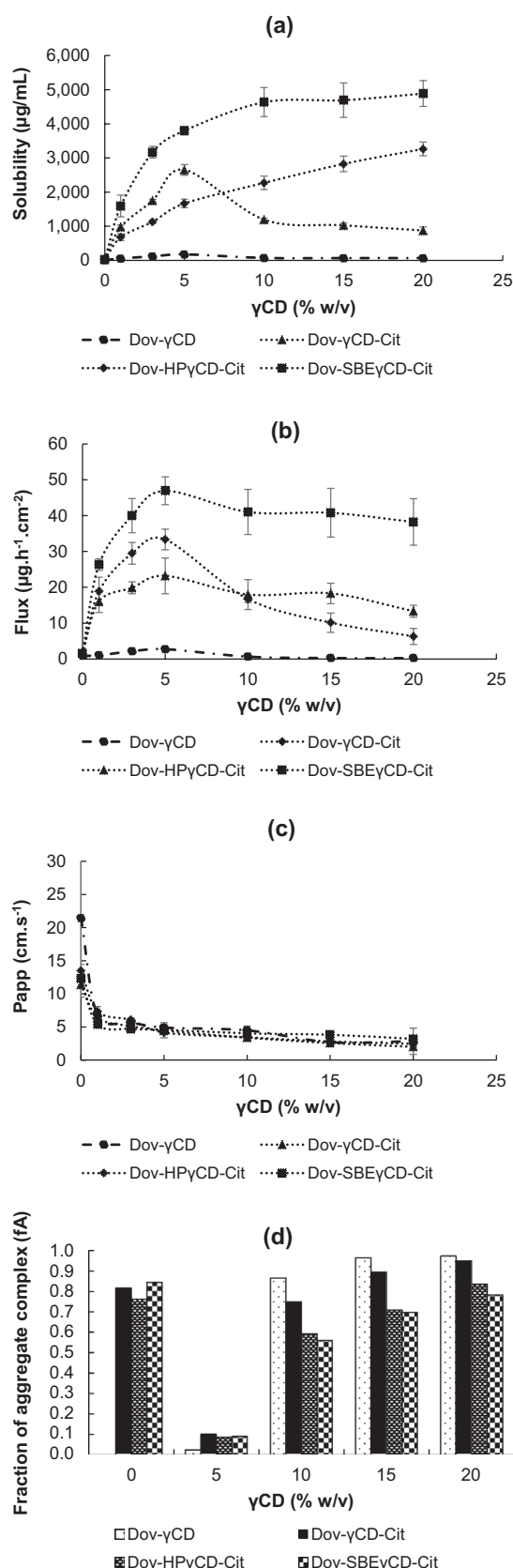


Fig. 4 Proposed complex formation of dovitinib/CD/citric acid ternary system

majority of characteristic protons shows upfield shifts ($\Delta\delta < 0$) but only H-3 displaces in downfield shift ($\Delta\delta > 0$). Each is due to the shielding or de-shielding effect as mentioned previously. The high intensity of chemical shift is at H-4, followed by H-2, and H-3, H-4', and H-2'. In case of SBE γ CD, the binding regions cover the negatively charged substituent chain where ionic pair could form between the drug cation and the CD anion resulted in totally higher affinity than neutral CDs. These provide the evidence for the existence of strong interaction between the guest molecules and especially the exterior rim of CD cavity, with a partial inclusion in the torus.

In summary, $^1\text{H-NMR}$ studies confirmed formation of complexes in aqueous solution. The change of intramolecular and intermolecular hydrogen bonding system of CDs increased when acidic counter ion such as citric acid was introduced to the complexation media. The presence of citric acid improved the interaction of guest molecules with internal or external part of the γ CD cavity depending on the type of host molecules. The proposed complex formation of dovitinib/CD/citric acid ternary system is schematically depicted in Fig. 4.

In vitro permeation studies

The flux profiles of dovitinib from aqueous complexation media containing different γ CD derivatives are shown in Fig. 5b. The increased flux is a result of increased drug solubility as shown in Fig. 5a. However, the patterns level off at CD concentrations above 5% (w/v) due to formation of water-soluble complex aggregates. The greatest increase in dovitinib solubility is obtained in aqueous SBE γ CD solutions containing citric acid. This could be attributed to ternary complex formation in aqueous medium, enhance complex efficiency and solubilization of the drug/CD complex. The enhanced CE leads to improve dovitinib flux through MWCO 12–14 k semi-permeable cellophane membrane. The plot of dovitinib flux showed how permeability coefficient (Fig. 5c) is affected only by the CD concentration. At higher CD concentrations the apparent permeability was lowered due to self-assemble of the dovitinib/CD complexes (Fig. 5d). However, formation of relatively large dovitinib-citric acid aggregates was unexpected. Citric acid has been reported to form complexes or aggregates with mono-, di-, and trivalent metal ions [42, 43]. Here the aggregation could be due to an interaction of carboxyl groups of citric acid and positively ionized dovitinib molecules.

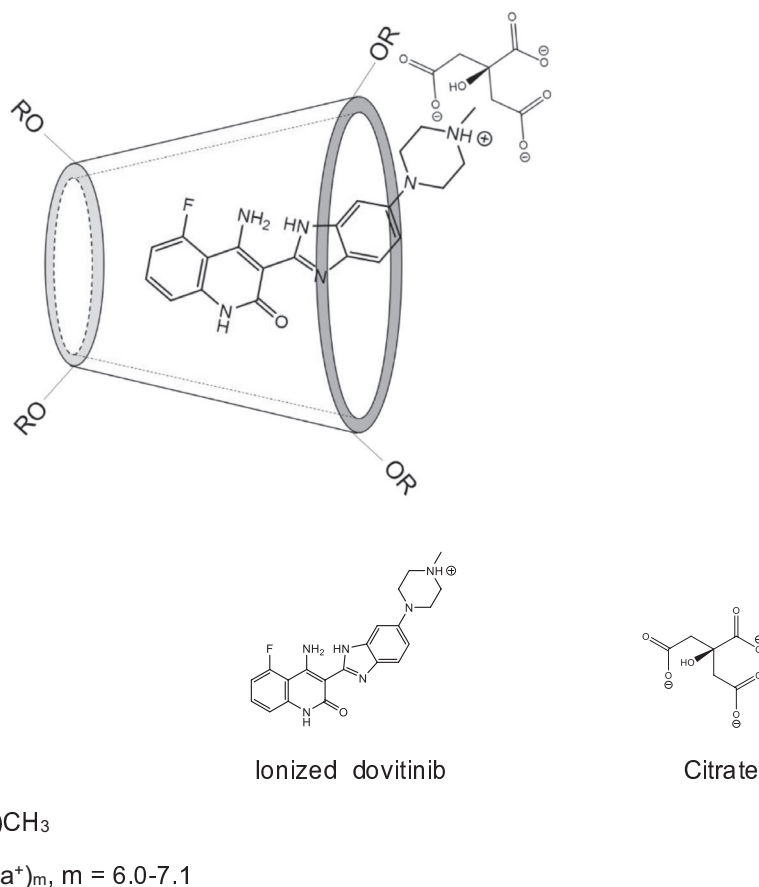


Fig. 5 Permeation parameters **a** solubility, **b** flux, **c** apparent permeation (P_{app}), and **d** fraction of aggregate complex (f_A) calculated from dovitinib ternary complexes with citric acid

430 Conclusion

431 Of the binary and ternary complexes evaluated citrate
 432 provided for the highest solubilization and complexation
 433 through salt formation and/or charge-charge interactions.
 434 However, the drug permeation through semi-permeable
 435 membrane was not always proportional to the CD
 436 solubilization.

437 **Acknowledgements** The authors are grateful for the support provided
 438 by the University of Iceland.

439 **Author contributions** Pitsiree Praphanwittaya: investigation, formal
 440 analysis, data curation, writing—original draft. Phatsawee Jansook:
 441 Methodology. Thorsteinn Loftsson: Funding acquisition, Supervision,
 442 Writing—original draft.

443 **Funding** This research was granted by Icelandic center of Research
 444 (RANNÍS).

445 **Data availability** All data generated or analyzed during this study are
 446 available within this published article and its supplementary informa-
 447 tion files.

448 Compliance with ethical standards

Conflict of interest The authors declare that there is no conflict of inter-
 449 est. The work was performed by Pitsiree Praphanwittaya and will be
 450 part of her PhD dissertation.
 451

452 References

1. Porta, C., Giglione, P., Liguigli, W., Paglino, C.: Dovitinib (CHIR258, TKI258): structure, development and preclinical and clinical activity. *Future Oncol.* (London, England). **11**(1), 39–50 (2015). <https://doi.org/10.2217/fon.14.208>
2. Benet, L.Z.: The role of BCS (biopharmaceutics classification system) and BDDCS (biopharmaceutics drug disposition classification system) in drug development. *J. Pharm. Sci.* **102**(1), 34–42 (2013). <https://doi.org/10.1002/jps.23359>
3. Herbrink, M., Schellens, J.H., Beijnen, J.H., Nuijen, B.: Inherent formulation issues of kinase inhibitors. *J. Controlled Release* **239**, 118–127 (2016). <https://doi.org/10.1016/j.jconrel.2016.08.036>
4. Remko, M., Boháč, A., Kováčiková, L.: Molecular structure, pKa, lipophilicity, solubility, absorption, polar surface area, and blood brain barrier penetration of some antiangiogenic agents. *Struct.* **453**
 454
 455
 456
 457
 458
 459
 460
 461
 462
 463
 464
 465
 466

- 467 Chem. **22**(3), 635–648 (2011). <https://doi.org/10.1007/s11224-011-9741-z>
- 468
- 469 5. Prapphanwittaya, P., Saokham, P., Jansook, P., Loftsson, T.: Aqueous solubility of kinase inhibitors: I the effect of hydrophilic polymers on their γ -cyclodextrin solubilization. *J. Drug Deliv. Sci. Technol.* **55**, 101462 (2020). <https://doi.org/10.1016/j.jddst.2019.101462>
- 470
- 471
- 472
- 473
- 474 6. Serajuddin, A.T.: Salt formation to improve drug solubility. *Adv. Drug Deliv. Rev.* **59**(7), 603–616 (2007). <https://doi.org/10.1016/j.addr.2007.05.010>
- 475
- 476
- 477 7. Loftsson, T., Magnusdottir, A., Masson, M., Sigurjonsdottir, J.F.: Self-association and cyclodextrin solubilization of drugs. *J. Pharm. Sci.* **91**(11), 2307–2316 (2002). <https://doi.org/10.1002/jps.10226>
- 478
- 479
- 480
- 481 8. Saokham, P., Muankaew, C., Jansook, P., Loftsson, T.: Solubility of cyclodextrins and drug/cyclodextrin complexes. *Molecules* (2018). <https://doi.org/10.3390/molecules23051161>
- 482
- 483
- 484 9. Brewster, M.E., Loftsson, T.: Cyclodextrins as pharmaceutical solubilizers. *Adv. Drug Deliv. Rev.* **59**(7), 645–666 (2007). <https://doi.org/10.1016/j.addr.2007.05.012>
- 485
- 486
- 487 10. Saokham, P., Loftsson, T.: γ -Cyclodextrin. *Int. J. Pharm.* **516**(1), 278–292 (2017). <https://doi.org/10.1016/j.ijpharm.2016.10.062>
- 488
- 489
- 490 11. Loftsson, T., Saokham, P., Sá Couto, A.R.: Self-association of cyclodextrins and cyclodextrin complexes in aqueous solutions. *Int. J. Pharm.* **560**, 228–234 (2019). <https://doi.org/10.1016/j.ijpharm.2019.02.004>
- 491
- 492
- 493 12. Loftsson, T., Stefansson, E.: Cyclodextrins and topical drug delivery to the anterior and posterior segments of the eye. *Int. J. Pharm.* **531**(2), 413–423 (2017). <https://doi.org/10.1016/j.ijpharm.2017.04.010>
- 494
- 495
- 496
- 497 13. Messner, M., Kurkov, S.V., Jansook, P., Loftsson, T.: Self-assembled cyclodextrin aggregates and nanoparticles. *Int. J. Pharm.* **387**(1), 199–208 (2010). <https://doi.org/10.1016/j.ijpharm.2009.11.035>
- 498
- 499
- 500
- 501 14. Loftsson, T., Duchêne, D.: Cyclodextrins and their pharmaceutical applications. *Int. J. Pharm.* **329**(1), 1–11 (2007). <https://doi.org/10.1016/j.ijpharm.2006.10.044>
- 502
- 503
- 504 15. Loftsson, T., Jarho, P., Masson, M., Jarvinen, T.: Cyclodextrins in drug delivery. *Expert Opin. Drug Deliv.* **2**(2), 335–351 (2005). <https://doi.org/10.1517/17425247.2.1.335>
- 505
- 506
- 507 16. Munro, I.C., Newberne, P.M., Young, V.R., Bar, A.: Safety assessment of gamma-cyclodextrin. *Regul. Toxicol. Pharmacol.* **39**(1), S3–S13 (2004). <https://doi.org/10.1016/j.yrtph.2004.05.008>
- 508
- 509
- 510 17. Loftsson, T., Brewster, M.E.: Cyclodextrins as functional excipients: methods to enhance complexation efficiency. *J. Pharm. Sci.* **101**(9), 3019–3032 (2012). <https://doi.org/10.1002/jps.23077>
- 511
- 512
- 513 18. Jansook, P., Ogawa, N., Loftsson, T.: Cyclodextrins: structure, physicochemical properties and pharmaceutical applications. *Int. J. Pharm.* **535**(1–2), 272–284 (2018). <https://doi.org/10.1016/j.ijpharm.2017.11.018>
- 514
- 515
- 516
- 517 19. Kurkov, S.V., Loftsson, T.: Cyclodextrins. *Int. J. Pharm.* **453**(1), 167–180 (2013). <https://doi.org/10.1016/j.ijpharm.2012.06.055>
- 518
- 519 20. Okimoto, K., Rajewski, R.A., Uekama, K., Jona, J.A., Stella, V.J.: The interaction of charged and uncharged drugs with neutral (HP-beta-CD) and anionically charged (SBE7-beta-CD) beta-cyclodextrins. *Pharm. Res.* **13**(2), 256–264 (1996). <https://doi.org/10.1023/a:1016047215907>
- 520
- 521
- 522 21. Zia, V., Rajewski, R.A., Stella, V.J.: Effect of cyclodextrin charge on complexation of neutral and charged substrates: comparison of (SBE)7M-beta-CD to HP-beta-CD. *Pharm. Res.* **18**(5), 667–673 (2001). <https://doi.org/10.1023/a:1011041628797>
- 523
- 524
- 525 22. Gupta, D., Bhatia, D., Dave, V., Sutariya, V., Varghese Gupta, S.: Salts of therapeutic agents: chemical, physicochemical, and biological considerations. *Molecules* (Basel, Switzerland) (2018). <https://doi.org/10.3390/molecules23071719>
- 526
- 527
- 528
- 529
- 530
- 531
23. Mura, P., Faucci, M.T., Manderioli, A., Bramanti, G.: Multicomponent systems of econazole with hydroxyacids and cyclodextrins. *J. Incl. Phenom. Macrocyclic Chem.* **39**(1), 131–138 (2001). <https://doi.org/10.1023/A:1008114411503>
- 532
- 533
- 534
- 535 24. Gould, P.L.: Salt selection for basic drugs. *Int. J. Pharm.* **33**(1), 201–217 (1986). [https://doi.org/10.1016/0378-5173\(86\)90055-4](https://doi.org/10.1016/0378-5173(86)90055-4)
- 536
- 537 25. Tong, W.Q., Whitesell, G.: In situ salt screening—a useful technique for discovery support and preformulation studies. *Pharm. Dev. Technol.* **3**(2), 215–223 (1998). <https://doi.org/10.3109/10837459809028498>
- 538
- 539 26. Cerreia Vioglio, P., Chierotti, M.R., Gobetto, R.: Pharmaceutical aspects of salt and cocrystal forms of APIs and characterization challenges. *Adv. Drug Deliv. Rev.* **117**, 86–110 (2017). <https://doi.org/10.1016/j.addr.2017.07.001>
- 540
- 541 27. Cruz-Cabeza, A.J.: Acid–base crystalline complexes and the pKa rule. *CrystEngComm* **14**(20), 6362–6365 (2012). <https://doi.org/10.1039/C2CE26055G>
- 542
- 543 28. Lee, H.: *Pharmaceutical Industry Practices on Genotoxic Impurities*. CRC Press, London (2014)
- 544
- 545 29. Higuchi, T., Connors, K.A.: Phase-solubility techniques. In: C.N.R. (ed.) *Advances in Analytical Chemistry and Instrumentation*, vol. 4. pp. 117–212. Wiley, New York (1965)
- 546
- 547 30. Fenyvesi, E., Vikmon, M., Szeman, J., Redenti, E., Delcanale, M., Ventura, P., Szejtli, J.: Interaction of hydroxy acids with β -cyclodextrin. *J. Incl. Phenom. Macrocyclic Chem.* **33**(3), 339–344 (1999). <https://doi.org/10.1023/A:1008094702632>
- 548
- 549 31. Ueno, A., Takahashi, K., Osa, T.: Photocontrol of catalytic activity of capped cyclodextrin. *J. Chem. Soc. Chem. Commun.* **3**, 94–96 (1981). <https://doi.org/10.1039/C39810000094>
- 550
- 551 32. Redenti, E., Szente, L., Szejtli, J.: Drug/cyclodextrin/hydroxy acid multicomponent systems. Properties and pharmaceutical applications. *J. Pharm. Sci.* **89**(1), 1–8 (2000).
- 552
- 553 33. Muankaew, C., Jansook, P., Stefansson, E., Loftsson, T.: Effect of gamma-cyclodextrin on solubilization and complexation of irbesartan: influence of pH and excipients. *Int. J. Pharm.* **474**(1–2), 80–90 (2014). <https://doi.org/10.1016/j.ijpharm.2014.08.013>
- 554
- 555 34. Amiri, S., Amiri, S.: *Cyclodextrins: Properties and Industrial Applications*. Wiley, New York (2017)
- 556
- 557 35. Dufour, G., Evrard, B., de Tullio, P.: Rapid quantification of 2-hydroxypropyl- β -cyclodextrin in liquid pharmaceutical formulations by ¹H nuclear magnetic resonance spectroscopy. *Eur. J. Pharm. Sci.* **73**, 20–28 (2015). <https://doi.org/10.1016/j.ejps.2015.03.005>
- 558
- 559 36. Luna, E.A., Vander Velde, D.G., Tait, R.J., Thompson, D.O., Rajewski, R.A., Stella, V.J.: Isolation and characterization by NMR spectroscopy of three monosubstituted 4-sulfobutyl ether derivatives of cyclomaltoheptaose (beta-cyclodextrin). *Carbohydr. Res.* **299**(3), 111–118 (1997). [https://doi.org/10.1016/s0008-6215\(97\)00006-2](https://doi.org/10.1016/s0008-6215(97)00006-2)
- 560
- 561 37. Maeda, H., Tanaka, R., Nakayama, H.: Inclusion complexes of trihexphenidyl with natural and modified cyclodextrins. *SpringerPlus* **4**(1), 218 (2015). <https://doi.org/10.1186/s40064-015-0986-7>
- 562
- 563 38. Prapphanwittaya, P., Saokham, P., Jansook, P., Loftsson, T.: Aqueous solubility of kinase inhibitors: II the effect of hexadimethrine bromide on the dovitinib/ γ -cyclodextrin complexation. *J. Drug Deliv. Sci. Technol.* **55**, 101463 (2020). <https://doi.org/10.1016/j.jddst.2019.101463>
- 564
- 565 39. Ribeiro, L., Carvalho, R.A., Ferreira, D.C., Veiga, F.J.: Multicomponent complex formation between vinpocetine, cyclodextrins, tartaric acid and water-soluble polymers monitored by NMR and solubility studies. *Eur. J. Pharm. Sci.* **24**(1), 1–13 (2005). <https://doi.org/10.1016/j.ejps.2004.09.003>
- 566
- 567 40. Djedaini, F., Lin, S.Z., Perly, B., Wouessidjewe, D.: High-field nuclear magnetic resonance techniques for the investigation of a
- 568
- 569
- 570
- 571
- 572
- 573
- 574
- 575
- 576
- 577
- 578
- 579
- 580
- 581
- 582
- 583
- 584
- 585
- 586
- 587
- 588
- 589
- 590
- 591
- 592
- 593
- 594
- 595
- 596

- 597 β -cyclodextrin:indomethacin inclusion complex. *J. Pharm. Sci.*
598 **79**(7), 643–646 (1990). <https://doi.org/10.1002/jps.2600790721>
- 599 41. Zhao, R., Tan, T., Sandstrom, C.: NMR studies on puerarin and its
600 interaction with beta-cyclodextrin. *J. Biol. Phys.* **37**(4), 387–400
601 (2011). <https://doi.org/10.1007/s10867-011-9221-0>
- 602 42. Zabiszak, M., Nowak, M., Taras-Goslinska, K., Kaczmarek, M.T.,
603 Hnatejko, Z., Jastrzab, R.: Carboxyl groups of citric acid in the
604 process of complex formation with bivalent and trivalent metal
ions in biological systems. *J. Inorg. Biochem.* **182**, 37–47 (2018).
<https://doi.org/10.1016/j.jinorgbio.2018.01.017>
- 605
606
607 43. Zelenina, T.E., Zelenin, O.Y.: Complexation of citric and tartaric
608 acids with Na and K ions in aqueous solution. *Russ. J. Coord.*
609 *Chem.* **31**(4), 235–242 (2005). <https://doi.org/10.1007/s11173-005-0083-5>
610

Publisher's Note Springer Nature remains neutral with regard to
jurisdictional claims in published maps and institutional affiliations.

613

UNCORRECTED PROOF

Paper IV

Effect of Stabilizer on Thermal Stability of Cediranib Maleate/Cyclodextrin Complexes in solution state

Pitsiree Praphanwittaya¹, Phennapha Saokham², Phatsawee Jansook³, Thorsteinn Loftsson^{1,*}

¹Faculty of Pharmaceutical Sciences, University of Iceland, Hofsvallagata 53, IS-107 Reykjavik, Iceland

²Department of Manufacturing Pharmacy, Faculty of Pharmacy, Rangsit University, Pathum Thani 12000, Thailand

³Faculty of Pharmaceutical Sciences, Chulalongkorn University, 254 Payathai Road, Pathumwan, Bangkok, 10330, Thailand

*Corresponding author. Tel.: +354 525 4464; Fax: +354 525 4071; E-mail: thorstlo@hi.is

Abstract

Cediranib maleate (CM), a protein kinase inhibitor (KI), is less soluble in aqueous medium. Its solubility can be enhanced by employing drug/cyclodextrin (CD) complexation technique. Heating is a common method to prepare such complexes both on laboratory scale and in industry. In general, CDs are used to protect compounds against light, heat, and oxygen. However, CD at higher concentration has tendency to form larger aggregates that probably induce an adversary effect instead. This present study was aimed to improve thermal stability of CM/gamma cyclodextrin (γ CD) complex by stabilizer in aqueous suspension. The complexes were prepared by autoclaving process at 121°C for 20 min. CM became more soluble in acidic aqueous environment. The pure drug was slightly sensitive to heat but it underwent thermal degradation when formed complex with γ CD at higher concentrations. Riboflavin acted as a good stabilizer preventing drug loss during heating. The phase-solubility profiles showed formation of binary CM/ γ CD complexes, and ternary complexes with riboflavin that have limited solubility in water (B_s type profiles). Riboflavin did not alter the pattern of phase-solubility, and permeation. The optimal γ CD concentration was determined to be 15% (w/v) γ CD. NMR spectra confirmed formation of binary and ternary complexes in aqueous solutions. TEM study displayed aggregates formation in solution state.

Keywords

Cediranib maleate, γ -cyclodextrin, complexation, complexation efficacy, thermal stability, stabilizer

1. Introduction

Cediranib maleate (CM) is the maleate salt of cediranib, which inhibits the activity of tyrosine kinase to prevent the growth of new blood vessels (EMA, 2016). Cediranib is developed as an anti-tumor agent for potential monotherapy and in combination with chemotherapy of ovarian cancer (Liu et al., 2014; Orbegoso et al., 2017). Cediranib is an indole-ether quinazoline molecule which slightly dissolves in water (EMA, 2016). However, the aqueous solubility of its maleate salt is not relatively high (about 2 mg/mL, pH 4.5, at 22-23°C) for that effective dose. Drug candidates with solubility of <10 mg/ml over the pH range of 1-7 at physiological temperature show bioavailability issues (Semalty, 2014). In the pharmaceutical area, cyclodextrins (CDs) have mainly been used as complexing agents to increase the aqueous solubility of poorly water soluble compounds, in order to increase their bioavailability and to improve stability (Loftsson and Duchêne, 2007). CD-based formulations have been applied through various drug delivery systems i.e. oral, nasal, dermal, rectal, and ocular (Loftsson et al., 2005; Loftsson and Stefansson, 2017; Matsuda and Arima, 1999; Merkus et al., 1999). CDs can be used to enhance aqueous solubility of KIs such as erlotinib, gefitinib, ibritinib, lapatinib (Fahmy et al., 2019; Qiu et al., 2017; Tóth et al., 2016; Tóth et al., 2017; Zhao et al., 2020). Although an official report confirmed that CM is not sensitive to moisture and heat, the entrapment of drug in CD can alter its physicochemical properties (EMA, 2016; Loftsson et al., 2002).

γ CD is the common natural of CDs consist of eight glucopyranose units with a spatial structure in the toroid shape. The internal part is hydrophobic, whereas the external part of the γ CD molecule is hydrophilic due to the arrangement of hydroxyl groups around outer rim (Loftsson et al., 2019; Saokham and Loftsson, 2017). In animals and humans, γ CD is degraded by α -amylase that is found in, for example, saliva, bile fluid and tears (Lumholdt et al., 2012; Munro et al., 2004). From a toxicity view in the use of CDs, γ CD is generally

recognized as safe by the U.S. FDA and shows the most favorable toxicological profiles (Saokham and Loftsson, 2017). The suitability of different CDs for pharmaceutical applications varies in relation to the size of the guest molecule which the CD ring should accommodate. With its larger ring size, γ CD is more suitable for larger molecules i.e. KIs than α - or β CD (Meier et al., 2001). Like other CDs, γ CD can enhance solubility of drugs through formation of water-soluble complex. Drug/CD complexes, especially those of the natural CDs are known to self-assemble to form nanosized aggregates in aqueous medium. In aqueous γ CD solutions the size of the aggregates increases with increasing γ CD concentration until they precipitate to form micro- or nanoparticle platform (Jansook et al., 2018; Loftsson and Duchêne, 2007). Heating is used to prepare drug/CD complexes both on laboratory scale and in industry. However, this method is applicable only for heat stable guests (Loftsson et al., 2005). In general, CDs are used to protect compounds against light, heat, and oxygen (Loftsson and Brewster, 1996). γ CD at higher concentration has tendency to form larger aggregates that probably induces an adversary effect instead. Thus, preparation of CD nanoparticle suspension by heating may require the use of thermal stabilizer.

The stabilizer is added in aqueous suspension for enhancing its stability against high temperature environment. Another main chemical reaction that affects the stability of a drug is oxidation. The oxidation involves the addition of oxygen or the removal of electrons from a drug molecule. Such reaction can be initiated by heat, light, or certain trace metals (Hovorka and Schöneich, 2001; Waterman et al., 2002). A rational choice of stabilizers involves an empirical basis since its protective effect is variable depending on the drug behavior in concentrated CD aggregates. For example, the stabilizer is expected to yield a thermally stable system by inhibiting oxidation, changing conformation of drug/CD complexes, or even disrupting CD aggregates. Additives employed to prevent oxidation include inert gas for exclusion of oxygen, antioxidants, and chelating agents. KIs have more aromatic carbon and nitrogen atoms on their complex

heterocyclic structure than non-kinase compounds (Lackey, 2008). Thus a change in conformation of CM/CD complex requires the binding in a flat lipophilic pocket and to make the essential hydrogen bonds. The idea was extended to combinations of such binary complex with an inert molecule such as amino acids, nitrogenous compounds (i.e. caffeine, riboflavin) that are capable of hydrogen bonding. Selection of amino acids was based on the binding site of KIs at the biological receptors, for example, lysine (LYS) and arginine (ARG) (Suebsuwong et al., 2018). Caffeine is a purine analogue which has been used as complexing agent to stabilize drugs by stacking formation due to aromatic ring (Yoshioka and Stella, 2007). Similar stabilization by caffeine was reported for base-catalyzed degradation and photolysis of riboflavin (Ahmad et al., 2009; Guttman, 1962). Riboflavin is generally stable to heat sterilization and oxidation. Its stability increases as acidity increases with optimal stability to thermal degradation being at pH 2-5 (Al-Ani, 2006; Combs and McClung, 2017; Pinto and Zemleni, 2016). In aqueous condition, riboflavin can form complex with small molecules such as quinine sulfate via hydrogen bond and van der Waals force, and with salicylic acid in other mechanisms i.e. charge transfer or stacking interaction (Bhattar et al., 2010; Patil et al., 2011). Chaotropic agents (e.g., urea) can modify the structural order of water molecules (Szente et al., 1998). Sá Couto and colleagues found that urea disrupted γ CD aggregates into smaller units through hindering formation of H-bonds which is applicable to pharmaceutical formulation (Sá Couto et al., 2018). The efficacy of additives is compared, belonging to different chemical groups against thermal degradation as shown in Table 1. It should be optimized for specific and desired functions in further formulation. The present study was aimed to enhance thermal stability of cediranib maleate/gamma cyclodextrin (γ CD) complex by stabilizer in aqueous suspension.

2. Materials and Methods

2.1. Materials

Cediranib maleate (CM) was purchased from Shanghai, Huirui, Chemical, Technology, Co., Ltd (Shanghai, China). γ -cyclodextrin (γ CD) was purchased from Wacker (München Germany). Nitrogen gas was purchased from AGA (Reykjavik, Iceland). Disodium EDTA, magnesium ascorbate, Sodium thiosulfate, L-lysine, L-arginine, caffeine, riboflavin, urea, viscosity of 2% aqueous solution at 25°C is approximately 50 cP, 0.1N hydrochloric acid, sodium hydroxide, and sodium chloride were purchased from Sigma-Aldrich (St. Louis, MO, USA). Milli-Q water (Millipore, Billerica, MA) was used in the study.

2.2. pH-solubility profiles

The solubility of cediranib maleate was studied at pH 1-11 in triplicate. Excess amount of drug was placed in aqueous medium. The desired pH (Thermo Orion 3 Star™ bench top pH meter, Thermo Fisher Scientific, USA) was adjusted by dropwise titration of the aqueous medium with concentrated sodium hydroxide or hydrochloric acid solution. Those samples were constantly agitated at ambient temperature (22-23°C) for 7 days, and readjusted pH periodically until equilibrium. The supernatant of each sample was harvested by centrifugation at 12,000 rpm for 15 min (Heraeus Pico 17 Centrifuge, Thermo Fisher Scientific, Germany). The centrifuged samples were diluted with 50% MeOH prior to analysis of dissolved drug amount by HPLC.

2.3. Thermal stability studies

Thermal stability of drug was investigated in presence of pure γ CD at 0%, 5%, and 15% (w/v). Excess amount of CM was dissolved in pure water, and constantly agitated at room temperature for 24 h. The centrifuged supernatant was divided into 2 sets. One set was ready for drug analysis while another set further exposed the autoclave heat as described previously. The drug concentration of each set was then determined by HPLC. Thermal stability of CM was presented in % drug amount that compared heated and non-heated samples.

The stabilizer at concentration of 0.1 % (w/v) was included in CM/15% γ CD complex systems as a ternary component. The media were unbuffered and the pH was in range of 5 ± 0.5 . The method for determination of screening thermal stability and 3-cycle thermal stability was described above. The selected stabilizer was re-heated up to 3 cycles. The drug concentration of heated and non-heated sets was analyzed by HPLC.

2.4. Degradation products

The degradation products of non-heated CM, 3-cycle heated CM, and CM at pH1 solutions were characterized by UPLC/MS (Waters ACQUITY QDa detector 2.0, Massachusetts, USA). The ESI source conditions were also optimized to obtain high sensitivity and a good signal. Different conditions as drying gas flow, nebulizing gas flow, capillary voltage and spray voltage were optimized to maximize the sensitivity at a very low concentration to identify and characterize the degradation products. The chromatographic separation was performed on an Acquity UPLC BEH C18 column, (130° A, 1.7 μ m, 3 mm x 50 mm). The mobile phase used was a mixture of 0.1% (v/v) formic acid and acetonitrile in a ratio of (70:30 v/v). The mobile phase was freshly prepared and filtered by vacuum filtration through 0.45 μ m filter and degassed by ultrasound sonicator prior to use. The analysis was performed under isocratic condition at a flow rate 0.3 mL min⁻¹ and at 30°C using UV detector at 234 nm.

2.5. Phase-solubility studies

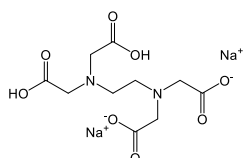
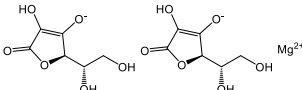
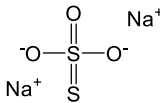
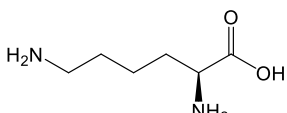
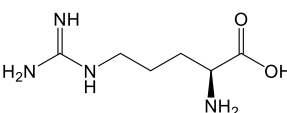
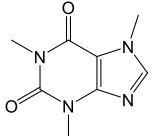
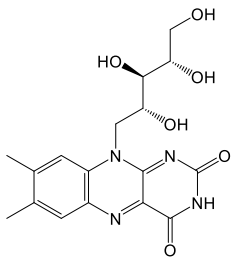
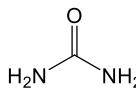
The complexes were prepared by a heating method in triplicate. Excess amount of cediranib maleate was added in unbuffered aqueous γ CD solutions of different concentrations, and the pH was between 4.5 and 5.5. The calculated pKa of cediranib is 10.1 (ACS, 2019), thus the drug can be fully ionized at such pH range. These mixtures were heated in an autoclave at 121°C for 20 min, then equilibrated at room temperature (22-23°C) under constant agitation for 7 days. Their centrifuged supernatant was collected for drug analysis.

The stabilizer that protected the drug from thermal degradation was selected to determine phase-solubility profiles in ternary complexes with γ CD following a method mentioned in binary complexes.

The determination of phase-solubility was performed according to Higuchi and Connors method (Higuchi and Connors, 1965). The apparent solubility ($K_{1:1}$) of the CM/ γ CD 1:1 (molar ratio) complex and the complexation efficiency (CE) were derived from the slope of initial linear phase-solubility diagrams (a diagram of the reciprocal of the apparent partition coefficient vs. the total CD concentration) using the following equations:

$$K_{1:1} = \frac{\text{slope}}{S_0(1-\text{slope})} \quad (1)$$

Table 1. The structure and physicochemical properties of the stabilizer (NCBI, 2019; Rowe et al., 2009).

| Stabilizer | Chemical structure | Molecular weight | Melting point (°C) | Log P _{o/w} | pK _a | S _o (mg/mL) in water at RT |
|----------------------|---|------------------|--------------------|----------------------|----------------------|---------------------------------------|
| Oxidation inhibitor | | | | | | |
| Nitrogen gas | $\text{N}\equiv\text{N}$ | 28.014 | -210 | 0.67 | - | 18.1 mg/mL at 21°C |
| EDTA.2Na |  | 336.21 | 252 | - | 2.0, 2.7, 6.2, 10.31 | 110 |
| Mg ascorbate |  | 374.54 | 415-416 | -2.65 | - | >0.95 ^a |
| Sodium thiosulfate |  | 158.11 | 48.5 | -4.35 | 11.35 | 209 at 20°C |
| Amino acid | | | | | | |
| L-lysine |  | 146.19 | 224.5 | -3.05 | 3.12 | 1,000 |
| L-arginine |  | 174.2 | 244 | -4.2 | 2.18, 9.09, 13.2 | 182 |
| Nitrogenous compound | | | | | | |
| Caffeine |  | 194.19 | 238 | -0.07 | 14 | 21.6 |
| Riboflavin |  | 376.4 | 280 | 1.46 | 10.2 | 0.1 |
| Chaotropic agent | | | | | | |
| Urea |  | 60.056 | 132.7 | -2.11 | 0.21 at 21°C | 545 |

$$CE = S_0 \cdot K_{1:1} = \frac{\text{slope}}{(1-\text{slope})} = \frac{[CM/\gamma CD \text{ complex}]}{[\gamma CD]} \quad (2)$$

where S_0 is the intrinsic solubility of drug, $[CM/\gamma CD \text{ complex}]$ is the concentration of dissolved complex and $[\gamma CD]$ is the concentration of dissolved γCD in the aqueous complexation media.

2.6. NMR studies

1H -NMR spectra of complexes were recorded in combined NMR solvents at 400 MHz and 298 K using Bruker AVANCE 400 instrument (Bruker Biospin GmbH, Karlsruhe, Germany). The sample preparation was separated into 2 sets that are non-heated technique and heated techniques. For non-heated set, solid samples of γCD , CM, CM/ γCD binary complex, and CM/ γCD /riboflavin ternary complex were dissolved separately in a mixture of deuterated dimethyl sulfoxide (DMSO- d_6) and deuterium dioxide (D_2O), volume ratio 9:1. All samples of heated set were dissolved in pure water, autoclaved at 121°C for 20 min, lyophilized those solutions into solid form, and finally dissolved them with NMR solvents as described previously. The magnitude of chemical shifts was recorded in ppm (δ). The resonance at 2.5000 ppm, due to residual solvent (DMSO- d_6), was used as internal reference. The change of 1H -NMR chemical shift due to complexation was calculated according to Eq. 4:

$$\Delta\delta = \delta_{\text{complex}} - \delta_{\text{free}} \quad (4)$$

2D-NMR experiment or Nuclear Overhauser Effect Spectroscopy (NOESY) of CM/ γCD /riboflavin was acquired using the following conditions: pulse delay time, 1.929 s; mixing time, 300 ms; 16 scans; 1024 x 1024 data points. The data were process with TopSpin 4.0.7 software.

2.7. In vitro permeation studies

The effect of γCD with and without riboflavin on CM permeation was conducted using unjacketed Franz diffusion cells (SES GmbH-Analyze system, Germany). The donor chamber and the receptor chamber were separated with a single layer of semi-permeable cellophane membrane (MWCO 12–14 000 Da, diffusion area of 1.77 cm²). The membrane was soaked overnight in the receptor phase that consisted of aqueous solution containing phosphate buffer saline solution pH 7.4 and 2.5% (w/v) γCD . γCD was added to the receptor phase to ensure sufficient drug solubility. The receptor phase (12 ml) was sonicated under vacuum to remove dissolved gas. The sample (1 ml) was added to the donor chamber after filtration through 0.45 mm membrane filter. The study was carried out at ambient temperature (22–23°C) under continuous stirring of the receptor phase (12 ml) by magnetic stirring bar rotating at 300 rpm. A 150 ml sample of receptor medium was withdrawn at 30, 60, 120, 180, 240, 300, and 360 min and replaced immediately with an equal volume of fresh receptor phase. The drug concentration was determined by HPLC.

The calculation of steady state flux (J) of CM/ γCD was obtained from the slope (dq/dt) of linear regression relationship between the amount of drug in the receptor chamber (q) and time (t) profiles, and the apparent permeability coefficient (P_{app}) was calculated from the flux (J) according to Eq. (3):

$$J = \frac{dq}{A \times dt} = P_{app} \times C_d \quad (3)$$

where A is the diffusion area (1.77 cm²) and C_d is initial concentration of CM in the donor phase. Each experiment was performed in triplicate and the results reported as the mean values \pm standard deviation (SD).

2.8. Quantitative determination method

Quantitative determination of CM was performed in a reversed-phase high performance liquid chromatography (HPLC) system (Dionex, Softron GmbH Ultimate 3000 series, Germany). The equipment composed of a P680 pump, operated at 1.0 ml/min, with a DG-1210 degasser, an ASI-100 autosampler, VWD-3400 UV-VIS detector, operated at 234 nm, and a column heater, operated at 30°C, containing a C18 column (100A 150 x 4.6 mm, 5 μ m) from Kinetex Core-shell technology and a guard column (Phenomenex, UK). The mobile phase consisted of acetonitrile, and 0.05% (v/v) phosphoric acid (volume ratio 35:65). The injection volume was 20 μ L.

2.9. Transmission electron microscope (TEM)

The morphology of CM/ γCD aggregates in aqueous solutions and suspension were evaluated using Model JEM-1400 transmission electron microscope (JEOL, Tokyo, Japan). The negative straining technique was used. Firstly, a small amount of clear liquid (i.e. the aggregate solution) was dropped on a 200 mesh coated grid and dried at 37 to 40°C for one hour. Then a drop of centrifuged 4%w/w uranyl acetate was added to the loaded grid. After 6 min of straining, the sample was dried overnight at room temperature. Finally, the strained specimen was placed in holder and inserted into the microscope.

3. Results and discussions

3.1. pH-solubility studies

The aqueous solubility of cediranib maleate was pH-dependent. As the drug is weak basic, it was more soluble in acidic media (Fig. 1). However, the solubility tended to be decreased at pH 3. A change in color of sample was observed from colorless to pink, and it became darker in strongly acidic condition due to degradation.

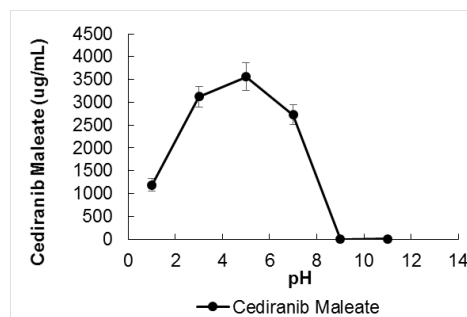


Fig. 1 pH profile of CM in pure water (n=3).

3.2. Thermal stability study

Thermal stability data in Fig. 2 showed that cediranib maleate was slightly sensitive to heat (about 5% drug loss during autoclaving), but stable in presence of 5% (w/v) γCD . The remaining drug amount was significantly lower in 15% (w/v) aqueous γCD solution. Drug/CD complexes can self-assemble to form aggregates. In aqueous CD solutions the size of the aggregates increases with increasing CD concentration until they precipitate. Such solid has the potential of being developed into novel drug delivery systems (Loftsson et al., 2004; Messner et al., 2010). In other words, CD platforms are formed in concentrated CD solution. However, the results indicated that cediranib maleate underwent thermal degradation at high γCD concentration. Thus it is necessary to prevent the drug degradation in that condition.

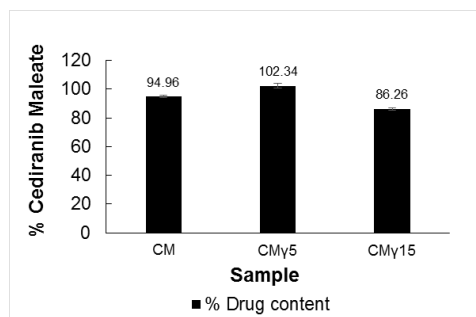


Fig. 2 Thermal stability of CM in aqueous γ CD solutions at concentration of 0%, 5%, and 15% (w/v) (n=3).

Addition of stabilizer in binary complex improved the remaining drug amount (Fig. 3). According to European Pharmacopeia (Ph. Eur.), the standard specification for content from assay test limits in a range of 95 to 105% of the declared content in units of mass/volume (e.g. mg/ml). The official criterion is applied to this study. The stabilizer has a good potency against thermal degradation in cediranib maleate when the drug content is at least 95% of concentration basis. Riboflavin acted as the most effective stabilizer preventing drug loss (100.50%) during autoclaving, followed by EDTA (96.26%), and L-arginine (95.55%). Urea had the lowest ability (87.27%) to protect drug from heat by disrupting CD aggregates (Sá Couto et al., 2018). The larger units of aggregation might not be the main cause of thermal degradation. Thus, two possible roles of effective stabilizers are inhibiting oxidative stress probably caused by metal ion, and changing conformation of drug/CD complexes.

Trace metal ions may remain from CD synthesis. The amount of this impurity can be increased when increasing the γ CD concentration. EDTA is a very powerful chelating agent for divalent metals, thus it can literally reduce radical reactions and oxidation process (Flora and Pachauri, 2010). In pharmaceutical formulations, EDTA is applied to prevent oxidative degradation of drug by chelating metal ion impurities (E Mohr, 2006). Jansook and colleagues reported that EDTA might protect dovitinib from thermal degradation via metal chelation. In present study, inhibiting reactions (usually oxidations) by EDTA is presumed to be the mechanism that improves thermal stability of cediranib maleate. Furthermore, L-arginine and riboflavin can also act as chelating agent. For examples, L-arginine inhibited the oxidation of lipids and proteins in emulsion sausage by chelating ferrous ions, and scavenging free radicals (Xu et al., 2018). Riboflavin has the ability to chelate or complex various metal ions such as Fe(II), Mn(II), Co(II), Ni(II), Cu(II) and Zn(II) (Harkins and Freiser, 1959; Khan and Mohan, 1973).

The change in complex conformation may affect the thermal behavior of drug. The driving forces for formation of the drug/CD complex include enthalpy-rich water molecules from the cavity, hydrogen bonding, van der Waals interaction, electrostatic interactions, and charge-transfer interaction (Liu and Guo, 2002; Loftsson et al., 2005). L-arginine has been found to improve the drug stability where cyclodextrin inclusion complex are formed. The direct interaction between L-arginine and omeprazole attributes to hydrogen bonds in drug molecule, and a significant desolvation of the omeprazole molecule. This amino acid plays an active role in the multicomponent complex formation by having a tendency to be located near the inner surface of host cavity (Figueiras et al., 2010). The simulation study discovered that feature of the aqueous arginine solutions is the self-association of arginine molecules. The stronger arginine-arginine hydrogen bonds take place of the weak hydrogen bonds between arginine and water to form cluster. The carboxylate group of

such arginine clusters is found to interact with the aromatic and charged sides of protein via cation- π interactions and hydrogen bonding, respectively (Shukla and Trout, 2010). For the present study, it might be anticipated that L-arginine thermally stabilized the drug/CD complex by intermolecular interactions from its single molecule and self-cluster.

In aqueous environment, riboflavin can interact with small molecules. For examples, several indoles were formed a weak complex with riboflavin in acidic solution due to charge transfer forces (Mitsuda et al., 1970). Hydrogen bonds and van der Waals interactions played major role in stabilizing complex between quinine sulfate and riboflavin (Patil et al., 2011). In case of acidic drug like salicylic acid, charge transfer or stacking interaction may take place in complexation (Bhattar et al., 2010). The interaction between riboflavin and CDs i.e. β CD, γ CD, and HPCDs, is found in inclusion complex mainly (Loukas et al., 1995; Terekhova et al., 2011). The ribityl side chain of riboflavin prevents deep inclusions, especially in HPCDs, and can expose to destruction in the bulk solvent (Terekhova et al., 2011). However, ternary drug/CD/riboflavin complex have not been addressed. CM is an indole ether quinazoline derivative, thus its structure has some similarities to those drug molecules which riboflavin potentially forms complex. Consequently, riboflavin might interrupt the formation of CM/ γ CD complex somehow. In these screening data, riboflavin was the best candidate, thus the investigation of its binary and ternary complex is further studied.

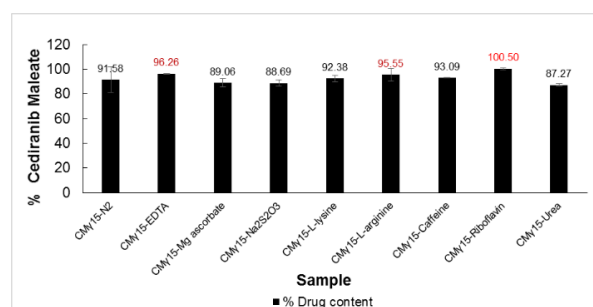


Fig. 3 Thermal stabilizer of CM in 15% (w/v) γ CD aqueous solution in presence of stabilizer (n=3).

Fig. 4 presents the remaining drug amount after moist-heat exposure for 1-3 cycles. In plain CM solution, the drug slightly degraded. The presence of γ CD affected the drug amount in different way. For 5% (w/v) γ CD, CM was stable at first cycle, then tended to degrade in next cycles. For 15% (w/v) γ CD, the drug was lost about 15% each step. All systems became more stable at least one cycle when added riboflavin. In brief, it was proven that riboflavin had the potential to thermally stabilize CM in aqueous γ CD solution.

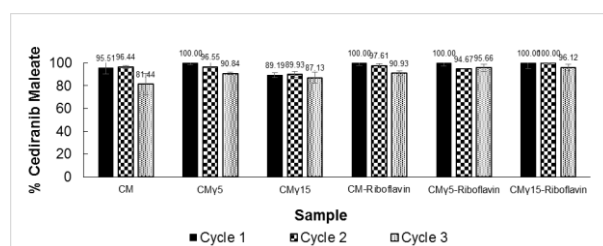


Fig. 4 Thermal stability of CM after 3 cycle of autoclaving in aqueous γ CD solutions and stabilizer (n=3).

3.3 Degradation products

After treating CM with autoclaving and strong acid, the appearance changed from colorless to purple color. Heated CM for 3 cycles and CM at pH1 showed an identical degradation peak with the same λ_{max} and R_t (data not

shown). Autoclaving and strong acidic condition can induce drug degradation in similar way. Strong acid is more powerful to degrade the drug due to higher intensity of degradation peak and darker color.

LC-MS showed the UV spectrum of CM and its degradation products similarly to LC-UV (Fig.5). Both instruments indicated that the drug was degraded under autoclaving and strong acidic condition in similar pathway. The m/z of drug peak included 451 and its one half that was 226 - the other half is the electron which was removed in the ionization process. The m/z of degradation peak could be 166 and 304.08 or 309 (Table 2). The possible degradation products under strong acid or autoclaving process were proposed in Fig. 6.

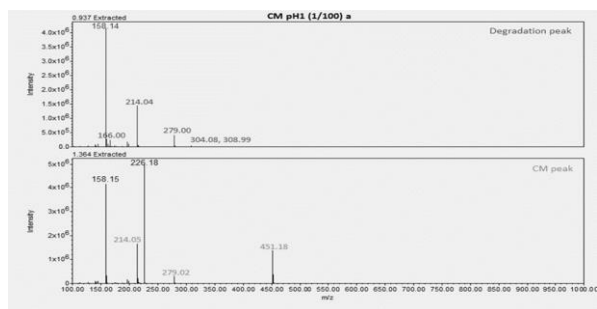


Fig. 5 LC/PDA/MS Peak spectrum of CM at pH 1

Table 2 Peak characteristics of CM determined by LC/MS

| Sample | Drug peak | | | Degradation peak | | |
|-------------|----------------------|-------------|----------|----------------------|-------------|--------------------|
| | λ_{max} (nm) | R_t (min) | m/z | λ_{max} (nm) | R_t (min) | m/z |
| CM | 236 | 1.3 | 226, 451 | - | - | - |
| CM 3 cycles | 236 | 1.3 | N/A | 265 | 0.95 | N/A |
| CM pH1 | 236 | 1.3 | 226, 451 | 265 | 0.95 | 166, 304.08 or 309 |

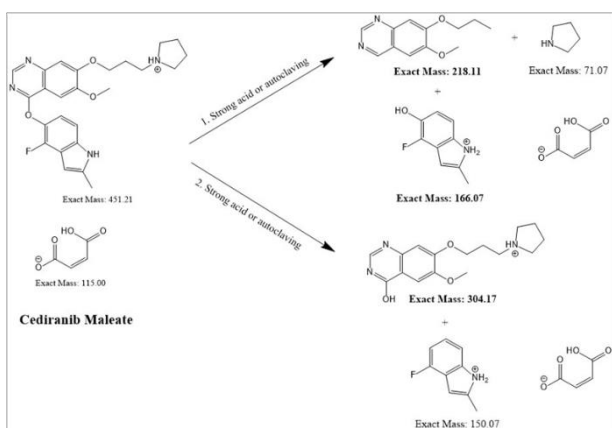


Fig. 6 Possible degradation products of CM.

3.3 Phase solubility studies

The phase-solubility profiles (Fig. 7) showed formation of binary CM/ γ CD complex and ternary CM/ γ CD/riboflavin complexes were B_s type. The solubility tended to be limited when increasing γ CD concentration from 10% (w/v). Riboflavin slightly decreased the amount of dissolved CM. However, the drug amount was higher in presence of riboflavin at 15% (w/v) γ CD solution due to thermal stability effect. The calculated phase solubility (PS) parameters in Table 3 indicated that riboflavin did not affect the interaction between CM and γ CD, and complex stability significantly.

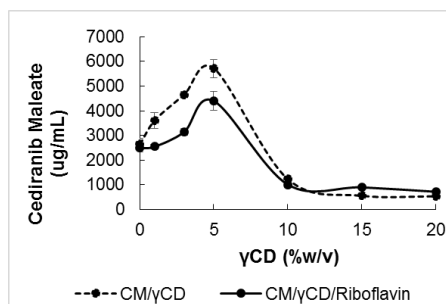


Fig. 7 Phase solubility profile of CM containing riboflavin in aqueous γ CD solution (n=3).

Table 3 Amount of dissolved γ CD from CM/ γ CD/Riboflavin complexes in pure water.

| System | pH | S_0 (ug/mL) | Phase solubility parameters | | |
|----------------------------|---------------|---------------|-----------------------------|------------------------|------|
| | | | PS-type | $K_{1:1}$ (M^{-1}) | CE |
| CM/ γ CD | 4.9 ± 0.5 | 2,639 | B_s | 33.70 | 0.16 |
| CM/ γ CD/Riboflavin | 4.8 ± 0.4 | 2,486 | B_s | 22.03 | 0.10 |

3.4 1H -NMR studies

The 1H -NMR spectra of pure substances including γ CD, CM, and riboflavin prepared at room temperature along with their labelled chemical structure are presented in Fig. 8. Only CM spectrum was slightly changed due to autoclaving treatment, its proton signals i.e. H-1', H-9', and H-11' disappeared.

Table 4 showed the $\Delta\delta$ shifts of γ CD for the binary and ternary complexes prepared in different condition. In ambient preparation, the proton resonances are at γ CD cavity (H-3 and H-5) and external rim (H-1, H-2, H-4, and H-6) (Schneider et al., 1998). Those signals displaces downfield shift ($\Delta\delta > 0$) due to de-shielding effect caused by changes in local polarity, or the van der Waals interaction between host and guest molecules (Djedaini et al., 1990). For complexes exposed the moist heat, the assigned protons locate in both internal and external cavity of γ CD as well as in the ambient condition. However, the chemical shifts behave in binary complexes differently. In case of riboflavin/ γ CD complexes, majority of proton signals shift to upfield ($\Delta\delta < 0$) due to shielding effect of the guest molecule (i.e. flavin moiety of riboflavin) (Ribeiro et al., 2005). In case of CM/ γ CD complex, the upfield ($\Delta\delta < 0$) presents at H-1 only, and H-6 has no proton replacement. In other words, a conformation of γ CD was changed when applied moist heat to such systems containing riboflavin or CM. The introduction of riboflavin in that binary complex returns those proton signals to downfield shift ($\Delta\delta > 0$), or it allows γ CD behaved similarly to the ambient condition. This is clearly visible that there might be some molecular interactions among CM, riboflavin and γ CD which can protect the drug from thermal degradation.

The expansion of the NOESY spectra of ternary system exposed the heat is presented in Fig. 9, and the observed molecular NOE cross-peaks were marked by the dotted line. Firstly, the riboflavin- γ CD interactions were observed between H-6'', H-7'', H-10'' of riboflavin (RF) and the H-1, H-2 protons located on surface of γ CD. Secondly, some cross-peaks H-12', H-14' protons of CM interacted with the external rim H-1, H-2, H-4, H-6 protons of γ CD. Lastly, the interaction between guest molecules appeared at H-1', H-14' protons of CM, and H-4'', H-7'', H-10'' protons of riboflavin (RF). These results indicate that the pyrrolidinyl-propoxy group of CM and ribityl chain of riboflavin were located near the outer cavity of γ CD. These functional groups share some intermolecular interactions. However, the partial inclusion into the CD cavity could be assumed according to 1H -NMR, since the expansion

formation. Riboflavin did not change the morphology of drug/ γ CD complexes.

4. Conclusion

Riboflavin is the most effective thermal stabilizer for CM in 15% (w/v) γ CD solution. In the binary and ternary complexes, it could decrease thermal degradation of cediranib maleate at least 1 autoclaving cycle. NMR studies indicated that this stabilizer interacted with the drug from inside and outside of host cavity. Furthermore, riboflavin did not alter the pattern of phase-solubility, permeation, and aggregate morphology.

5. Acknowledgement

This study was granted by Icelandic center of Research, (RANNÍS), and gratefully supported by the University of Iceland. The authors acknowledge Maonian Xu, a postdoc at University of Iceland for his technical assist during determination of degradation products by LC/MS.

References

- ACS, 2019. SciFinder (scifinder.cas.org). American Chemical Society.
- Ahmad, I., Ahmed, S., Sheraz, M.A., Aminuddin, M., Vaid, F.H., 2009. Effect of caffeine complexation on the photolysis of riboflavin in aqueous solution: a kinetic study. *Chemical & pharmaceutical bulletin* 57, 1363-1370.
- Al-Ani, M.R., 2006. A Review of: "Vitamins in Foods/Analysis, Bioavailability, and Stability". *International Journal of Food Properties* 9, 927-928.
- Bhatter, S.L., Kolekar, G.B., Patil, S.R., 2010. Spectroscopic studies on the molecular interaction between salicylic acid and riboflavin (B2) in micellar solution. *Journal of Luminescence* 130, 355-359.
- Bychkova, S.A., Katrovtsseva, A.V., Kozlovskii, E.V., 2008. Complex formation of maleic acid with the Zn²⁺, Ni²⁺, Co²⁺, Cu²⁺ in aqueous solution. *Russian Journal of Coordination Chemistry* 34, 93-96.
- Combs, G.F., McClung, J.P., 2017. Chapter 12 - Riboflavin, in: Combs, G.F., McClung, J.P. (Eds.), *The Vitamins* (Fifth Edition). Academic Press, pp. 315-329.
- Djedaïni, F., Lin, S.Z., Perly, B., Wouessidjewe, D., 1990. High-Field Nuclear Magnetic Resonance Techniques for the Investigation of a β -Cyclodextrin:Indomethacin Inclusion Complex. *Journal of Pharmaceutical Sciences* 79, 643-646.
- E Mohr, M., 2006. Remington: The Science and Practice of Pharmacy, 21st Edition.
- EFSA, 2009. Scientific Opinion of the Panel on Food Additives and Nutrient Sources added to Food on a request from the Commission on magnesium ascorbate, zinc ascorbate and calcium ascorbate added for nutritional purposes in food supplements. *EFSA Journal* 994, 1-22.
- EMA, E.M.A., 2016. EMA/CHMP/616303/2016, Assessment Report: Cediranib maleate.
- Fahmy, S.A., Brübler, J., Alawak, M., El-Sayed, M.M.H., Bakowsky, U., Shoeib, T., 2019. Chemotherapy Based on Supramolecular Chemistry: A Promising Strategy in Cancer Therapy. *Pharmaceutics* 11, 292.
- Figueiras, A., Sarraguca, J.M., Pais, A.A., Carvalho, R.A., Veiga, J.F., 2010. The role of L-arginine in inclusion complexes of omeprazole with cyclodextrins. *AAPS PharmSciTech* 11, 233-240.
- Flora, S.J.S., Pachauri, V., 2010. Chelation in metal intoxication. *Int J Environ Res Public Health* 7, 2745-2788.
- Foye, W.O., Lange, W.E., 1954. Metal Chelates of Riboflavin. *Journal of the American Chemical Society* 76, 2199-2201.
- Guttman, D.E., 1962. Complex formation influence on reaction rate. I. Effect of caffeine on riboflavin base-catalyzed degradation rate. *J Pharm Sci* 51, 1162-1166.
- Harkins, T.R., Freiser, H., 1959. The Chelating Tendency of Riboflavin. *The Journal of Physical Chemistry* 63, 309-311.
- Higuchi, T., Connors, K.A., 1965. Phase-solubility techniques, in: (Ed.), C.N.R. (Ed.), *Advances in Analytical Chemistry and Instrumentation*. Wiley-Interscience, New York, pp. 117-212.
- Hovorka, S.W., Schöneich, C., 2001. Oxidative degradation of pharmaceuticals: Theory, mechanisms and inhibition. *Journal of Pharmaceutical Sciences* 90, 253-269.
- Khan, M.M.T., Mohan, M.S., 1973. The metal chelates of riboflavin and riboflavin monophosphate. *Journal of Inorganic and Nuclear Chemistry* 35, 1749-1755.
- Lackey, K., 2008. Gene Family Targeted Molecular Design. Wiley.
- Liu, J.F., Barry, W.T., Birrer, M., Lee, J.-M., Buckanovich, R.J., Fleming, G.F., Rimel, B., Buss, M.K., Nattam, S., Hurteau, J., Luo, W., Quy, P., Whalen, C., Obermayer, L., Lee, H., Winer, E.P., Kohn, E.C., Ivy, S.P., Matulonis, U.A., 2014. Combination cediranib and olaparib versus olaparib alone for women with recurrent platinum-sensitive ovarian cancer: a randomised phase 2 study. *Lancet Oncol* 15, 1207-1214.
- Liu, L., Guo, Q.-X., 2002. The Driving Forces in the Inclusion Complexation of Cyclodextrins. *Journal of inclusion phenomena and macrocyclic chemistry* 42, 1-14.
- Loftsson, T., Duchêne, D., 2007. Cyclodextrins and their pharmaceutical applications. *International Journal of Pharmaceutics* 329, 1-11.
- Loftsson, T., Jarho, P., Masson, M., Jarvinen, T., 2005. Cyclodextrins in drug delivery. *Expert opinion on drug delivery* 2, 335-351.
- Loftsson, T., Másson, M., Brewster, M.E., 2004. Self-Association of Cyclodextrins and Cyclodextrin Complexes. *Journal of Pharmaceutical Sciences* 93, 1091-1099.
- Loftsson, T., Saokham, P., Sá Couto, A.R., 2019. Self-association of cyclodextrins and cyclodextrin complexes in aqueous solutions. *International Journal of Pharmaceutics* 560, 228-234.
- Loftsson, T., Stefansson, E., 2017. Cyclodextrins and topical drug delivery to the anterior and posterior segments of the eye. *Int J Pharm* 531, 413-423.
- Loukas, Y.L., Jayasekera, P., Gregoriadis, G., 1995. Novel liposome-based multicomponent systems for the protection of photolabile agents. *International Journal of Pharmaceutics* 117, 85-94.

- Lumholdt, L.R., Holm, R., Jorgensen, E.B., Larsen, K.L., 2012. In vitro investigations of alpha-amylase mediated hydrolysis of cyclodextrins in the presence of ibuprofen, flurbiprofen, or benzo[a]pyrene. *Carbohydrate research* 362, 56-61.
- Matsuda, H., Arima, H., 1999. Cyclodextrins in transdermal and rectal delivery. *Advanced drug delivery reviews* 36, 81-99.
- Meier, M., Bordignon-Luiz, M., Farmer, P., Szpoganicz, B., 2001. The Influence of β - and γ -Cyclodextrin Cavity Size on the Association Constant with Decanoate and Octanoate Anions. *Journal of Inclusion Phenomena* 40, 291-295.
- Merkus, F.W.H.M., Verhoef, J.C., Marttin, E., Romeijn, S.G., van der Kuy, H., Hermens, W., Schipper, N., 1999. Cyclodextrin in nasal drug delivery. *Advanced drug delivery reviews* 36, 41-57.
- Messner, M., Kurkov, S.V., Jansook, P., Loftsson, T., 2010. Self-assembled cyclodextrin aggregates and nanoparticles. *International Journal of Pharmaceutics* 387, 199-208.
- Mitsuda, H., Tsuge, H., Kawai, F., Tanaka, K.E.N., 1970. Riboflavin-Indoles Interaction in Acid Solution. *THE JOURNAL OF VITAMINOLOGY* 16, 215-218.
- Munro, I.C., Newberne, P.M., Young, V.R., Bar, A., 2004. Safety assessment of gamma-cyclodextrin. *Regulatory toxicology and pharmacology : RTP* 39 Suppl 1, S3-13.
- NCBI, 2019. PubChem(Pubchem.ncbi.nlm.nih.gov). National Center for Biotechnology Information.
- Orbegoso, C., Marquina, G., George, A., Banerjee, S., 2017. The role of Cediranib in ovarian cancer. *Expert Opinion on Pharmacotherapy* 18, 1637-1648.
- Patil, D.T., Bhattar, S.L., Kolekar, G.B., Patil, S.R., 2011. Spectrofluorimetric Studies of the Interaction Between Quinine Sulfate and Riboflavin. *Journal of Solution Chemistry* 40, 211-223.
- Pinto, J.T., Zemleni, J., 2016. Riboflavin. *Advances in Nutrition* 7, 973-975.
- Qiu, N., Li, X., Liu, J., 2017. Application of cyclodextrins in cancer treatment. *Journal of Inclusion Phenomena and Macrocyclic Chemistry* 89, 229-246.
- Ribeiro, L., Carvalho, R.A., Ferreira, D.C., Veiga, F.J., 2005. Multicomponent complex formation between vinpocetine, cyclodextrins, tartaric acid and water-soluble polymers monitored by NMR and solubility studies. *European journal of pharmaceutical sciences : official journal of the European Federation for Pharmaceutical Sciences* 24, 1-13.
- Rowe, R.C., Sheskey, P.J., Quinn, M.E., Association, A.P., 2009. *Handbook of pharmaceutical excipients*, 6th ed. ed. London ; Chicago : Washington, DC : Pharmaceutical Press ; American Pharmacists Association.
- Sá Couto, A.R., Ryzhakov, A., Loftsson, T., 2018. Disruption of α - and γ -cyclodextrin aggregates promoted by chaotropic agent (urea). *Journal of Drug Delivery Science and Technology* 48, 209-214.
- Saokham, P., Loftsson, T., 2017. γ -Cyclodextrin. *International Journal of Pharmaceutics* 516, 278-292.
- Schneider, H.J., Hacket, F., Rudiger, V., Ikeda, H., 1998. NMR Studies of Cyclodextrins and Cyclodextrin Complexes. *Chem Rev* 98, 1755-1786.
- Semalty, A., 2014. Cyclodextrin and phospholipid complexation in solubility and dissolution enhancement: a critical and meta-analysis. *Expert opinion on drug delivery* 11, 1255-1272.
- Shukla, D., Trout, B.L., 2010. Interaction of arginine with proteins and the mechanism by which it inhibits aggregation. *The journal of physical chemistry. B* 114, 13426-13438.
- Suebsuwong, C., Pinkas, D.M., Ray, S.S., Bufton, J.C., Dai, B., Bullock, A.N., Degterev, A., Cuny, G.D., 2018. Activation loop targeting strategy for design of receptor-interacting protein kinase 2 (RIPK2) inhibitors. *Bioorg Med Chem Lett* 28, 577-583.
- Szente, L., Szejtli, J., Kis, G.L., 1998. Spontaneous Opalescence of Aqueous γ -Cyclodextrin Solutions: Complex Formation or Self-Aggregation? *Journal of Pharmaceutical Sciences* 87, 778-781.
- Terekhova, I.V., Koźbiał, M., Kumeev, R.S., Alper, G.A., 2011. Inclusion Complex Formation Between Modified Cyclodextrins and Riboflavin and Alloxazine in Aqueous Solution. *Journal of Solution Chemistry* 40, 1435.
- Tóth, G., Jánoska, Á., Szabó, Z.-I., Völgyi, G., Orgován, G., Szente, L., Noszál, B., 2016. Physicochemical characterisation and cyclodextrin complexation of erlotinib. *Supramolecular Chemistry* 28, 656-664.
- Tóth, G., Jánoska, Á., Völgyi, G., Szabó, Z.I., Orgován, G., Mirzahosseini, A., 2017. Physicochemical characterization and cyclodextrin complexation of the anticancer drug lapatinib. *Journal of Chemistry*.
- Waterman, K.C., Adami, R.C., Alsante, K.M., Hong, J., Landis, M.S., Lombardo, F., Roberts, C.J., 2002. Stabilization of Pharmaceuticals to Oxidative Degradation. *Pharmaceutical development and technology* 7, 1-32.
- Xu, P., Zheng, Y., Zhu, X., Li, S., Zhou, C., 2018. L-lysine and L-arginine inhibit the oxidation of lipids and proteins of emulsion sausage by chelating iron ion and scavenging radical. *Asian-Australas J Anim Sci* 31, 905-913.
- Yoshioka, S., Stella, V.J., 2007. *Stability of Drugs and Dosage Forms*. Springer US.
- Zhao, L., Tang, B., Tang, P., Sun, Q., Suo, Z., Zhang, M., Gan, N., Yang, H., Li, H., 2020. Chitosan/Sulfobutylether- β -Cyclodextrin Nanoparticles for Ibrutinib Delivery: A Potential Nanoformulation of Novel Kinase Inhibitor. *Journal of Pharmaceutical Sciences* 109, 1136-1144.

Paper V

Development of Thermostable Formulation of Cediranib Maleate based Cyclodextrin for Ocular Drug Delivery

Pitsiree Praphanwittaya¹, Phennapha Saokham², Phatsawee Jansook³, Thorsteinn Loftsson^{1,*}

¹Faculty of Pharmaceutical Sciences, University of Iceland, Hofsvallagata 53, IS-107 Reykjavik, Iceland

²Department of Manufacturing Pharmacy, Faculty of Pharmacy, Rangsit University, Pathum Thani 12000, Thailand

³Faculty of Pharmaceutical Sciences, Chulalongkorn University, 254 Payathai Road, Pathumwan, Bangkok, 10330, Thailand

*Corresponding author. Tel.: +354 525 4464; Fax: +354 525 4071; E-mail: thorstlo@hi.is

Abstract

Cediranib maleate (CM) is a small molecular kinase inhibitor (KI) with low aqueous solubility. The complexation of drug/cyclodextrin (CD) can solubilize that poorly water soluble drug. Heating technique is commonly used to prepare such complexes both on laboratory scale and in industry. CDs are capable of protecting the drug molecule from environmental conditions such as oxygen, light, and heat. However, the adversary effect may be induced due to formation of larger aggregates in concentrated CD solution. This present study was aimed to develop thermally stable aqueous suspension of CM containing concentrated cyclodextrin (γ CD), and investigate *in vivo* drug delivery in rabbit's eyes. Heating technique by autoclave at 121°C for 20 min was used to prepare complexes. In concentrated γ CD solution, the solubility of CM was limited, and the amount of γ CD was decreased due to precipitation. The drug was loaded (drug load up to 3%) in cyclodextrin-based nanoparticles at pH 5. Riboflavin lowered thermal degradation of the drug. To obtain high drug load, co-solubilizers/stabilizers such as some polymers were also included. Stable aqueous drug/ γ CD complex formulations were prepared in such moist-heat condition. The zeta potential, particle size, viscosity and pH of formulations were within in acceptable criteria. After 3-month storage period, samples shown a good stability at 25°C. Formulation could deliver CM to the target site.

Keywords

Cediranib maleate, γ -cyclodextrin, complexation, thermal stability, stabilizer

1. Introduction

Cediranib maleate (CM) is an active tyrosine kinase inhibitor (KI) blocking angiogenesis (Westin et al., 2018). The maleate is a commercial salt form with promising metastable polymorph (Black et al., 2020). Cediranib has demonstrated anti-tumor activity in many cancers, including ovarian, breast, colorectal, renal, lung, sarcoma and glioblastoma (Medinger et al., 2009). Moreover, it has been reported that cediranib could inhibit laser-induced choroidal neovascularization in mice by oral administration at 1 or 5 mg/kg daily. From the result, this KI may have therapeutic potential for patients with neovascular age-related macular degeneration (AMD) (Kang et al., 2013). AMD is ocular disease that causes damage to the retinal macula located in posterior segment of eye (Ehrlich et al., 2008). The treatment of posterior eye disease requires e.g. oral, intravitreal, or topical administration to the eye (Shah et al., 2010). The non-invasive drug delivery like applicable topical eye drops is an attractive alternative due to painless effect and ease of use (Mathias and Hussain, 2010). The eye drops containing cediranib (up to 40 mg/mL) which achieved an effective concentration of drug in the back of eye was prepared in non-aqueous suspension (Telser, 2015). However, the most common adverse event related to the application of lipid-based ophthalmic products with an increased viscosity was blurred vision, thus limiting the sufficient overnight treatment (Dogru and Tsubota, 2011; Pery and Donnenfeld, 2003). Cediranib consists of indole ethers and quinazoline ring that cause very low solubility (EMA, 2016). Although the maleate salt is more soluble in water about 2 mg/mL, pH 4.5 at 22-23°C (Praphanwittaya et al., 2020x), the amount of dissolved drug still cannot meet that large requirement of daily dose. Cyclodextrin (CD) complexation is one of the most efficient method to improve aqueous solubility of drug and its bioavailability (Loftsson and Duchêne, 2007). Non-invasive formulations containing CD have been applied via various drug delivery routes such as topical and transmucosal administration (Muankaew and

Loftsson, 2018). CDs can be used to enhance aqueous solubility of KIs such as erlotinib, gefitinib, ibrutinib, lapatinib (Fahmy et al., 2019; Qiu et al., 2017; Tóth et al., 2016; Tóth et al., 2017; Zhao et al., 2020). The official report confirmed that CM is not sensitive to moisture and heat (EMA, 2016). Practically, pure CM undergoes the thermal degradation under moist-heat process but the drug can be fully protected in presence of small amount of γ CD i.e. at concentration of 5% (w/v) (Praphanwittaya et al., 2020x).

Cyclodextrins (CDs) are cyclic torus-shaped oligosaccharide with a lipophilic central cavity and hydrophilic exterior rim (Brewster and Loftsson, 2007; Loftsson and Duchêne, 2007). The natural CDs including α -cyclodextrin (α CD), β -cyclodextrin (β CD) and γ -cyclodextrin (γ CD) are approved by FDA they are generally recognized as safe (GRAS) on list of food additives (Loftsson and Brewster, 2012; Loftsson et al., 2005). In addition, only γ CD was susceptible to be hydrolyzed by α -amylase in tear fluid, saliva, and gastrointestinal tract (Lumholdt et al., 2012), that shows more safety than other types. γ CD that have relatively large hydrophobic cavity is suitable for accommodating a wide range of drug molecules i.e. KI (Meier et al., 2001). The use of γ CD as well as other CDs is increasing drug solubility in the pharmaceutical industry due to their fascinating ability to form water-soluble complexes (Loftsson and Brewster, 2010). The spontaneous self-assembly of drug/ γ CD complex into aggregates can lead to innovative drug delivery systems such as nanoparticles (Loftsson, 2014). In industry and laboratory scale, the complex is simply prepared by heating method. Many studies have been performed to use CDs for protecting guest molecules against heat, oxygen, evaporation, and light (Jin, 2013; Loftsson and Brewster, 1996). γ CD at higher concentration has tendency to form larger aggregates that probably induces an adversary effect instead. Thus, preparation of CD nanoparticle suspension by heating may require the use of thermal stabilizer. It was confirmed that CM

thermally degraded in aqueous 15% (w/v) γ CD (Praphanwittaya et al., 2020x).

Thermal stability of drug containing pharmaceutical preparation is important and closely monitored in order to maintain the pharmaceutical potency of the formulation. Manufacturing and storing the drug under controlled conditions challenge that thermal stability (Niazi, 2016). The consequences of exposure to heat and thermal oxidation may result in not only the loss of potency but also degradation products of formulation which could be harmful to the human body (Küpper et al., 2006). In general, drug degradation may be affected by changes in pH, buffer, medium components (e.g. co-solvent, other excipients), air exposure, and use of stabilizer. In case if the dosage form compositions are not appropriate then modification of a formulation can be considered to improve the stability and shelf-life of the product (Lieberman and Murti Vemuri, 2015). Our previous study found that riboflavin is very actively thermal stabilizer for CM in concentrated γ CD solution. However, only riboflavin may exhibit inadequate improvement of drug degradation in saturated system like suspension with high drug loading. Based on that research, the stable formulation containing CM/ γ CD aggregates at high temperature still remains a challenge. Other compounds such as EDTA, L-arginine, have the potential to suppress thermal degradation (Praphanwittaya et al., 2020x). Yet it requires excessively large amounts of these stabilizers, which is beyond the FDA criteria for eye products. In theory, the co-solvent could dissolve the excess guest molecule which are not incorporated into the CDs cavity. In addition, it helps facilitating the complex formation by dissolving the guest before entering the cavity (Viernstein et al., 2003). Thus addition of co-solvent may resolve the thermal degradation. Moreover, polymeric compounds are also particularly promising in this regard, as many parameters such as functionality, shape, and etc. can be friendly adjusted to meet the formulation requirements. In addition, polymer is often the excipient of choice to enhance physical stability of dispersed systems (Jones, 2004). Few researches reported the application of polymers induced the favorable thermal stability for pharmaceutical platform. For examples, poly-anionic polymers could stabilize microcapsule containing protein for at least about 60 minutes in retort processing at 121°C and 15 PSI or hot fill pasteurization at 104°C (Lee, 2009). The thermal stability of retinol (vitamin A) encapsulated nanoparticles is influenced by the types of polyester used for the nanoparticles (Cho, 2012). Poloxamers significantly enhanced the thermal stability of *in situ* hydrogels with high loading levels of modified nanocrystals (Lin and Dufresne, 2013) or insulin (Li et al., 2017).

The efficiency of co-solvent (e.g. polyols), polymeric stabilizers, and pH were initially compared against thermal degradation. All ingredients should be optimized for specific and desired functions in the formulation. This present study was aimed to develop the thermally stable suspension containing CM/ γ CD complex, and investigate *in vivo* drug delivery in rabbit's eyes.

2. Materials and Methods

2.1. Materials

Cediranib maleate (CM) was purchased from Shanghai, Huirui, Chemical, Technology, Co., Ltd (Shanghai, China). γ -cyclodextrin (γ CD) was purchased from Wacker (München Germany). Nitrogen gas was purchased from AGA (Reykjavik, Iceland). Disodium EDTA, L-arginine, riboflavin, urea, propylene glycol (PG), poly(ethylene glycol 400) (PEG400), glycerol, poloxamer 407, poly(vinyl alcohol) molecular weight 30-70 kDa (PVA), hydroxypropyl methylcellulose (HPMC), viscosity of 2% aqueous solution at 25°C is approximately 50 cP, tyloxapol, poloxamer 407, 0.1N hydrochloric acid, sodium hydroxide, and sodium chloride were purchased from Sigma-

Aldrich (St. Louis, MO, USA). Milli-Q water (Millipore, Billerica, MA) was used in the study.

2.2. Phase-solubility studies

Heating technique was used to prepare CM/ γ CD complexes in triplicate. Excess amount of drug was saturated in 0-20 % (w/v) γ CD solution. The systems were unbuffered, and the pH was between 4.5 and 5.5. The calculated pKa of cediranib is 10.1 (ACS, 2019), thus the drug can be fully ionized at such pH range. These suspensions were autoclaved at 121°C for 20 min in sealed glass vials, then allowed to cool at room temperature (22-23°C). Small amount of solid drug was added to each vial. The resealed sample was then equilibrated at room temperature under constant agitation for 7 days. The supernatant of each sample was harvested by centrifugation at 12,000 rpm for 15 min (Heraeus Pico 17 Centrifuge, Thermo Fisher Scientific, Germany). The centrifuged samples were diluted with 50% MeOH prior to analysis of the dissolved drug amount by HPLC.

The phase-solubility was determined according to the method reported by Higuchi and Connors (Higuchi and Connors, 1965). The apparent solubility ($K_{1:1}$) of the CM/ γ CD 1:1 (molar ratio) complex and the complexation efficiency (CE) were derived from the slope of initial linear phase-solubility diagrams (a diagram of the reciprocal of the apparent partition coefficient vs. the total CD concentration) using the following equations:

$$K_{1:1} = \frac{\text{slope}}{S_0(1-\text{slope})} \quad (1)$$

$$CE = S_0 \cdot K_{1:1} = \frac{\text{slope}}{(1-\text{slope})} = \frac{[\text{CM}/\gamma\text{CD complex}]}{[\gamma\text{CD}]} \quad (2)$$

where S_0 is the intrinsic solubility of drug, [CM/ γ CD complex] is the concentration of dissolved complex and [γ CD] is the concentration of dissolved γ CD in the aqueous complexation media.

2.3. Ternary stabilizer complexes preparation

Ternary CM/ γ CD/stabilizer complexes were prepared in triplicate by adding 0.1% (w/v) stabilizer to the complex system. The concentration of γ CD dissolved in the ternary complex medium was determined from the phase solubility profile prepared according to Section 2.2. The complexes were formed by previously described heating technique (see Section 2.2).

2.4. Thermal stability studies

The stabilizer at concentration of 0.1 % (w/v) was included in 15% (w/v) γ CD solution as a ternary component. The complexation media were unbuffered, and pH was in range of 5 ± 0.5 . Those samples were constantly agitated at ambient temperature overnight. One set was ready for drug analysis while another set further exposed the autoclave heat as described previously. The drug concentration of each set was then determined by HPLC. Thermal stability of CM was presented in % drug amount that compared heated and non-heated samples.

Thermal stability of CM in aqueous solution containing 15% (w/v) γ CD was determined at different pH. Excess amount of drug was added in media, and adjusted the desired pH (Thermo Orion 3 Star™ bench top pH meter, Thermo Fisher Scientific, USA) by dropwise titration of the aqueous medium with concentrated sodium hydroxide or hydrochloric acid solution. The samples were incubated as mentioned above. The drug content of heated and non-heated sets was analyzed by HPLC.

2.5. Quantitative determination method

The concentration of CM was analyzed in a reversed-phase high performance liquid chromatography (HPLC) system (Dionex, Softron GmbH Ultimate 3000 series, Germany). The analytical instrument composed of a P680 pump with a DG-1210 degasser, an ASI-100 autosampler, VWD-3400 UV-VIS detector, and a column heater, containing a C18 column (100A 150 × 4.6 mm, 5 μm) from Kinetex Core-shell technology and a guard column (Phenomenex, UK). The HPLC system was operated under 30°C, isocratic condition, flow rate was 1.0 mL/min, detection wavelength was 234 nm, and injection volume was 20 μL. The mobile phase consisted of acetonitrile and 0.05% (v/v) phosphoric acid (volume ratio 35:65).

Quantitative analysis of γCD was determined in a reverse-phase high-performance liquid chromatography system (Dionex, Softron GmbH Ultimate 3000 series, Germany) consisting of a LPG-3400SD pump with a built-in degasser, a WPS-3000 autosampler, a TCC-3100 column compartment, and a Coronary® ultra RS CAD detector. The HPLC conditions were applied from CD USP monograph 35 and previous investigators (Saokham and Loftsson, 2015). The mobile phase consisted of acetonitrile and water (volume ratio 7:93). The temperatures of the column and sampler compartments were set at 30°C. The flow rate was 1.0 mL/min. The injection volume was 10 μL.

2.6. Formulation process

Aqueous cediranib maleate/γCD suspensions were formulated by including selected stabilizer, other excipients, then adjusted to pH 5 with sodium hydroxide or hydrochloric acid prior to heating under autoclave. The autoclaved solution at 60°C was sonicated in ice bath for 30 min. The suspension was further incubated at room temperature under constant agitation for 3 days. The pH of formulation was monitor during this process.

2.7 Solid-drug fraction

The tested formulation was centrifuged as previously described in phase-solubility study (see Section 2.2.). The supernatant was determined by HPLC. The drug content in solid phase was calculated as:

$$\% \text{ solid drug fraction} = \left(\frac{\text{Total drug-dissolved drug}}{\text{Total drug content}} \right) \times 100 \quad (3)$$

2.8. Physicochemical characterizations

2.8.1. pH and Osmolality

The pH values of suspension were determined by Thermo Orion Star TM Series pH meter (Thermo Scientific, USA) at ambient temperature (22-23°C) and the osmolality with a Knauer K- 7000 vapor pressure osmometer (Germany) operated at 25°C.

2.8.2. Dynamic Light Scattering (DLS)

The particle size of suspension was determined by dynamic light scattering (DLS) using Nanotrak Wave particle size analyzer (Microtrac Inc., York, PA). The diluted sample (20 folds) was illuminated by a laser beam at wavelength of 780 nm and its intensity fluctuation in scattered lights from Brownian motion of particles was detected at known scattering angle θ of 180° at 25±0.2°C. The size population of the aggregates was interpreted according equation:

$$M_i = \frac{A_i/R_i^6}{\sum A_i/R_i^6} \times 100 \quad (4)$$

where M_i is the mass distribution percentage, A_i is the intensity area, R_i is the hydrodynamic radius of the size population i ,

and a is the shape parameter that equals 3, assuming spherical shaped particles (Bhattacharjee, 2016; Stetefeld et al., 2016).

The measurement of zeta potential was performed by Zetasizer Nano series (Nano-Z, Malvern Instruments, UK). The disposable folded capillary cell for loading diluted sample (20 folds) is DTS1070. The data of each sample were calculated by mean zeta potential from 3 measurements, duration 20 runs/measurement, and delay 60s between measurements.

2.8.3. Viscosity

A cone and plate viscometer (Brookfield model DV-II+, Brookfield Engineering Laboratories, Inc., Massachusetts, USA) was used for determining the apparent viscosity of CM suspension at 25°C and 37°C. The calibration check of instrument was verified through the use of mineral oil standard with cone spindle no. CPE-40 prior to run the sample. The appropriate sample volume required for the spindle is 0.5 mL.

2.9. Stability studies

The standard conditions for stability study was performed following ICH guideline. The freshly prepared suspensions were incubated at 5±3°C (refrigerator), and at 25±2°C, 60±5%RH (incubator) and 40±2°C, 75±5%RH (incubator). Each sample was taken for three months (i.e., at 0, 1, 2 and 3 months) to capture the photo, measure pH and particle size, and analyze the drug content by HPLC.

2.10. Morphology studies

2.10.1. Light microscope

The morphology were determined using the optical light microscope (Model BHT, Olympus, Japan). One drop of each formulation was placed on a microscope slide and observed under 400-fold magnification. The results were interpreted according to the monograph for Eye Preparations in the European Pharmacopeia 8.0 (01/2008:1163).

2.10.2. Transmission electron microscope (TEM)

The morphology of CM/γCD aggregates in aqueous solutions and suspension were evaluated using Model JEM-1400 transmission electron microscope (JEOL, Tokyo, Japan). The negative straining technique was used. Firstly, a small amount of clear liquid (i.e. the aggregate solution) was dropped on a 200 mesh coated grid and dried at 37 to 40°C for one hour. Then a drop of centrifuged 4%w/w uranyl acetate was added to the loaded grid. After 6 min of straining, the sample was dried overnight at room temperature. Finally, the strained specimen was placed in holder and inserted into the microscope.

2.11. In vivo permeation

Confidential information

3. Results and discussions

3.1. Phase solubility studies

The phase-solubility profile showed formation of binary CM/γCD complexes has limited solubility in water or classified as B_s type profiles (Fig. 1). γCD started precipitating at concentration of 10% (w/v) due to larger aggregates (Fig.1). The optimal γCD concentration was determined to be 15% (w/v) γCD.

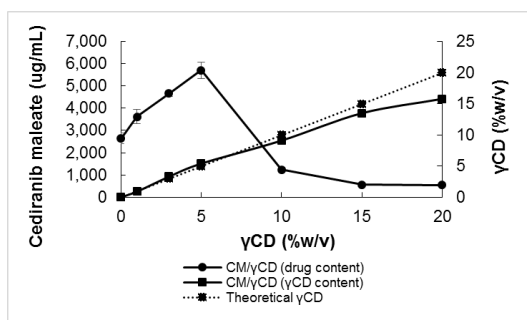


Fig. 1. Phase solubility profile of CM in aqueous γ CD solution, and amount of dissolved γ CD from such a system.

3.2. Thermal stability study

Thermal stability data in Fig. 2 showed that the presence of stabilizer such as co-solvents (e.g. PG, PEG400, and glycerin), and polymers (e.g. PVA, HPMC, tyloxapol, and poloxamer 407) in CM/ γ CD complex could protect the drug from thermal degradation.

The co-solvent can change the polarity of the complexation media (Loftsson et al., 2005). Here drug stability through thermal effect was dependent on the polarity of co-solvent. The dielectric constant (δ) of a compound is an index of its polarity. For examples, glycerin (46 δ), PG (32.1 δ), and PEG400 (12.4 δ) at 20°C. Increasing polarity showed a serial decrease in drug loss. Glycerin and PG are relatively higher polar than PEG400. The drug was thermally stabilized in presence of glycerin followed by PG, and PEG400. CM is in ionized form, higher polar co-solvent could also dissolve the excess guest molecules before entering the cavity (Vierstein et al., 2003).

In case of polymers, the drug survived from heat due to different types of polymeric stabilizer similarly. Hydrophilic polymers are known to stabilize various types of aqueous particulated or dispersed systems (Fendler, 1996; Malmsten, 2002). Cellulose derivatives and other polymers may act as steric stabilizer (Parfitt and Barnes, 1992). They also have been shown to have a stabilizing effect on CD aggregate (Loftsson et al., 1994; Ryzhakov et al., 2016). The interaction between polymers and CDs and drug/CD complexes begins to occur on the external surface of the CD molecule via van der Waal and hydrogen bonding (Loftsson and Duchêne, 2007). In aqueous solutions, it is believed that polymers reduce CD mobility by changing the hydration properties of CD molecules (Loftsson et al., 2005; Veiga et al., 2006). The steric inclusion-dissociation behaviors between host and guest molecules response to temperature change (Amiri and Amiri, 2017). Thus, the elevated temperature due to autoclaving process may change the rotation of polymer i.e. PVA, HPMC, tyloxapol, or poloxamer 407 to γ CD and CM/ γ CD complexes that caused a steric barrier against thermal degradation of CM.

The stabilizers with at least 95% drug content according to European Pharmacopeia (Ph. Eur.) specification such as PG, glycerol, PVA, HPMC, and poloxamer 407, were also selected to further formulate the aqueous suspensions. Tyloxapol was also a good choice but this polymer can generate bubbles as well as the drug itself. Therefore it was excluded from the study to prevent eye irritation.

The pH of binary complex apparently affected the thermal stability of CM (Fig. 3). The drug had lower thermal degradation at acidic environment. The pH 5 was the optimal point to be used in further formulation study.

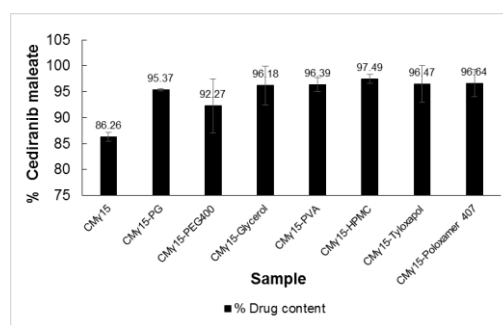


Fig. 2. Thermal stability of CM/ γ CD complex in presence of stabilizer (n=3).

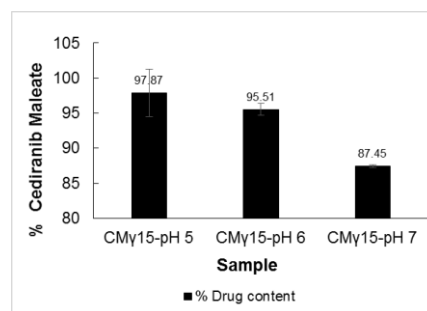


Fig. 3. Thermal stability of CM/ γ CD complex in different pH (n=3).

3.3. CM suspension formulations

All CM suspension were formulated at pH 5 due to the least degradation of CM. Cediranib maleate was highly loaded in cyclodextrin-based formulation up to 3% (w/v). Previously, Praphanwittaya and colleagues reported that riboflavin could lower thermal degradation of the drug in a plain suspension. Regarding very high drug load, riboflavin and supportive stabilizers such as L-arginine, polymers at concentration of 0.1% (w/v) were introduced step by step in order to protect the drug from thermal degradation. Nitrogen (N_2) is widely used to purge oxygen from the packaging before sealing that will also help preserve and protect the product during storage from oxidation. Although N_2 performed slightly less thermal protection on CM than those stabilizers as reported in that study, it was still included in formulations in order to prolong the shelf-life. Hydrophilic polymers are known to enhance the solubility of drug i.e. kinase inhibitors by synergist effect with γ CD (Loftsson and Masson, 2004; Praphanwittaya et al., 2020). In previous research, cediranib (free base) was solubilized by PVP whereas HPMC and poloxamer 407 tended to decrease the drug solubility (Praphanwittaya et al., 2020). Thus, the concentration of PVP was elevated to 0.2% (w/v) in such formulations for maintaining the solid-liquid fraction. Drug content was improved up to 90-100% when added those different thermal stabilizers (Table 1). The combination of stabilizers, especially polymers might enhance the steric network which hindered thermal degradation of drug in complexation media. In overall, the solid fraction meets the criteria about 70-75% of total drug. CM-F6 is the optimal formulation with acceptable values of 102% drug content, 23% liquid fraction, and 74% solid fraction. This formula was selected to further study.

Table 1 CM suspension formula containing 15% (w/v) γ CD.

| No. | Ingredient | Purpose | Concentration (% w/v) | | | | | | |
|-------------------|-------------------|-----------------------|-----------------------|--------|--------|--------|--------|--------|--|
| | | | CM-F1 | CM-F2 | CM-F3 | CM-F4 | CM-F5 | CM-F6 | |
| 1 | Cediranib Maleate | API | 3 | 3 | 3 | 3 | 3 | 3 | |
| 2 | gCD | Solubilizer | 15 | 15 | 15 | 15 | 15 | 15 | |
| - | PG | Supportive stabilizer | - | - | - | - | - | 0.1 | |
| 4 | Glycerol | Supportive stabilizer | - | - | - | - | 0.1 | 0.1 | |
| 5 | PVA (30-70k) | Supportive stabilizer | - | - | 0.2 | 0.2 | 0.2 | 0.2 | |
| 6 | HPMC (50 cP) | Supportive stabilizer | - | - | 0.1 | 0.1 | 0.1 | 0.1 | |
| 7 | Poloxamer 407 | Supportive stabilizer | - | - | 0.1 | 0.1 | 0.1 | 0.1 | |
| 8 | EDTA | Chelating agent | 0.1 | 0.1 | 0.1 | 0.1 | 0.1 | 0.1 | |
| 9 | Riboflavin | Main stabilizer | - | 0.1 | 0.1 | 0.1 | 0.1 | 0.1 | |
| 10 | L-arginine | Supportive stabilizer | - | - | - | 0.1 | 0.1 | 0.1 | |
| 11 | NaCl | Isotonicity agent | 0.5 | 0.5 | 0.5 | 0.5 | 0.5 | 0.5 | |
| 12 | HCl/NaOH | pH adjustment | pH 5 | pH 5 | pH 5 | pH 5 | pH 5 | pH 5 | |
| 14 | Purified water | Vehicle | qs 100 | qs 100 | qs 100 | qs 100 | qs 100 | qs 100 | |
| 15 | N ₂ | Oxidation inhibitor | purge | purge | purge | purge | purge | purge | |
| % Drug content | | | 82.99 | 90.02 | 92.31 | 93.92 | 97.67 | 102.68 | |
| % Liquid fraction | | | 30.88 | 27.30 | 28.91 | 25.41 | 25.32 | 23.46 | |
| % Solid fraction | | | 69.12 | 72.70 | 71.09 | 74.59 | 74.68 | 76.54 | |

3.4. Physicochemical Properties of formulation

The appearance of CM-F6 had yellow color due to riboflavin. The suspension was thick and homogeneous. It separated into two parts at room temperature overnight. Table 2 shows that drug assay, pH, osmolality, and viscosity are within the acceptable range. The drug content of CM-F6 was equal to the theoretical value. The particle size is mainly in nanometer range. However, zeta potential is very low that might affect the long-term stability of colloidal system.

Table 2 Physicochemical data of CM-F6 suspension.

| No. | Physicochemical properties | Part | n = 3 mean | SD | Criteria |
|-----|------------------------------------|----------------------------|---------------------------|--------|---------------------------|
| 1 | Assay at initial | Suspension | 30.69 mg/mL 102.27% LA | 0.10 | 27-33 mg/mL 90-110% LA |
| | | Supernatant | 24.14% F | 0.07 | 10-30% Fraction (F) |
| | | Solid | 75.86% F | 0.07 | 70-90% Fraction (F) |
| | Assay 4 months (ambient condition) | Suspension | 30.07 mg/mL 100.24% LA | 0.05 | 27-33 mg/mL 90-110% LA |
| | | Supernatant | 24.19% F | 0.05 | 10-30% Fraction (F) |
| | | Solid | 75.81% F | 0.05 | 70-90% Fraction (F) |
| 2 | pH ^a | Suspension | 5.02 | 0.03 | min 4.0-5.0 |
| 3 | Osmolality ^b | Suspension | 0.257 | 0.002 | 200-280 |
| | | Supernatant | 0.262 | 0.002 | mOsm/kg |
| 4 | Viscosity at 25°C ^c | Suspension | 13.463 | 0.345 | 2-20 cP |
| | | Suspension | 5.757 | 0.256 | at 25°C |
| 5 | Particle size by DLS (nm) | Suspension | 356 | 85.80% | - |
| | | (Dilution 1/20) | 1.06 | 12.20% | - |
| | | | 1689 | 2.00% | - |
| 6 | Zeta potential | Suspension (Dilution 1/20) | 1.20 | 0.11 | - |

^a refers to Ph. Eur. 07/2016:20203 used as reference.

^b refers to Ph. Eur. 01/2010:20235 used as reference.

^c refers to Ph. Eur. 01/2008:20210 used as reference.

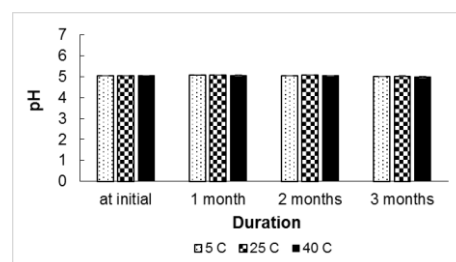
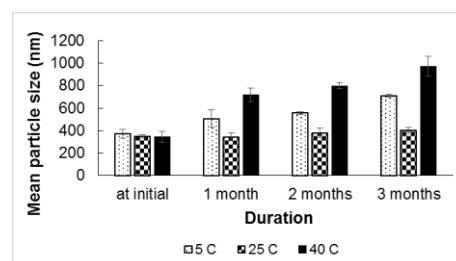
3.5. Stability studies

Table 3 show that % drug content of CM-F6 at 5 and 25°C is stable throughout 3 months, and the drug starts degradation after storage for 1 months at 40°C. Furthermore, suspension is still stable when stored at ambient condition for 4 months (Table 2)

Table 3 Drug assay of CM-F6 in 3 months (n=2).

| Formulation | Cediranib maleate assay | | | |
|----------------------|-------------------------|----------------|--------|------|
| | Drug amount (mg/mL) | % Drug content | mean | SD |
| CM-F6 at 5°C | | | | |
| 0 month | 30.56 | 1.54 | 101.87 | 5.12 |
| 1 month | 30.46 | 1.59 | 101.54 | 5.30 |
| 2 months | 31.24 | 0.24 | 104.12 | 0.81 |
| 3 months | 30.74 | 1.46 | 102.47 | 4.86 |
| CM-F6 at 25°C | | | | |
| 0 month | 31.18 | 0.57 | 103.91 | 1.86 |
| 1 month | 30.30 | 0.06 | 100.98 | 0.16 |
| 2 months | 30.25 | 0.19 | 100.81 | 0.59 |
| 3 months | 30.05 | 0.05 | 100.15 | 0.20 |
| CM-F6 at 40°C | | | | |
| 0 month | 30.84 | 0.40 | 102.81 | 1.35 |
| 1 month | 29.26 | 0.11 | 97.52 | 0.35 |
| 2 months | 27.02 | 0.16 | 90.06 | 0.53 |
| 3 months | 26.28 | 0.37 | 87.59 | 1.22 |

At 5°C, CM-F6 suspension has good appearance such as thick texture, stable bright yellow color, constantly re-separation rate after gentle shaking. However, this formulation cannot tolerate the high temperature, particularly at 40°C. The color becomes very darker. The separation of suspension also occurs up to 40% of product height. Although storing CM-F6 at 25°C still does not change %drug content (data not shown), its color is slightly darker by time. Storage temperature does not affect to pH of CM-F6 in 3 months (Fig. 4). The aggregates size and distribution of CM-F6 are larger at 5°C and 40°C only (Fig. 5). The aggregates of such suspension remains stable at 25°C.

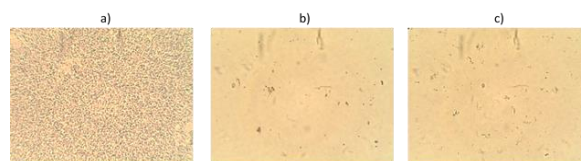
**Fig. 4.** pH of CM-F6 in 3 months (n=2).**Fig. 5.** Mean particle size (nm) of CM-F6 in 3 months (n=2).

3.6. Morphology studies

3.6.1 Light microscope

Examination of the CM-F6 by light microscope in Fig. 6 shows that 15% (w/v) γ CD-based formulation produced irregular spherical particles indicating a formation of amorphous complex. Both suspension (Fig. 6a) and diluted suspension (Fig. 6b) display similar size of aggregates with diameter less than 1 μ m. For supernatant (Fig. 6c), those particles formed a cluster-like aggregates which are slightly larger.

The official specification (Ph. Eur. 01/2008:1163) for eye drop suspension requires that each 10 μ g of solid active substance, not more than 20 particles have a maximum dimension greater than 25 μ m, and not more than 2 of these particles have a maximum dimension greater than 50 μ m. None of the particles has a maximum dimension greater than 90 μ m. Thus, all types of CM-F6 samples obtain particles within acceptable range according to Ph. Eur. 01/2008:1163.

**Fig. 6.** Light microscope images of a) suspension, b) diluted suspension (dilution of 1/20), and c) supernatant at 400X magnitude.

3.6.2. TEM

In order to get more information about complex formation, TEM measurements were also employed to investigate the morphological features of CM-F6 containing 15% (w/v) γ CD as shown in Fig. 7. TEM micrograms demonstrate that CM-F6 samples at initial stage obtain spherical particles with an average size of hundreds nanometers. For diluted suspension, not only spherical nanoaggregates but also irregular nanocrystals can be seen. The size of those crystals vary up to 1-2 μ m while spherical aggregates are between 100 and 300 nm in diameter which is similar to nanoparticles existed in typical suspension. It indicated that diluting sample with pure water did not change the particle size. Supernatant shows a greater diameter of spherical aggregates from 300 to 500 nm.

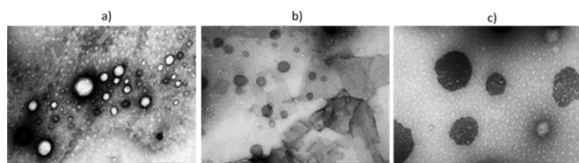


Fig. 7. TEM image at magnitude 25,000x of CM-F6 a) suspension, b) diluted suspension, c) supernatant.

After 3-month storage period, nanoparticles behaved in different way (Fig. 8). Temperature is a critical factor affecting the morphologies of suspension. Samples has good stability at 25°C. Aggregates become larger in less and higher temperature. The suspension forms crystalline at 5°C whereas it tends to produce irregular debris due to thermal degradation from incubation at 40°C. All results are nearly the same as derived from DLS observation.

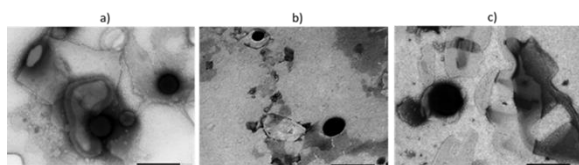


Fig. 8. TEM images at magnitude 25,000x of 3-month CM-F6 at a) 5°C, b) 25°C, and c) 40°C.

3.7. *In vivo* permeation

The data is confidential.

4. Conclusion

Suspension formulations containing riboflavin and polymers did retard or prevent the drug loss during heating process. Temperature at 25°C is an appropriate storage condition. Drug content, pH, particle size and shape of such suspension are not different from the initial point. The optimal formulation can deliver drug to the target site.

5. Acknowledgement

This study was granted by Icelandic center of Research, (RANNÍS), and gratefully supported by the University of Iceland. The authors acknowledge Jóhann Arnfinnsson, an expert at University of Iceland for his technical assist in viewing of morphology by TEM.

Reference

- ACS, 2019. SciFinder (scifinder.cas.org). American Chemical Society.
- Amiri, S., Amiri, S., 2017. Cyclodextrins: Properties and Industrial Applications. Wiley.
- Bhattacharjee, S., 2016. DLS and zeta potential - What they are and what they are not? *Journal of controlled release : official journal of the Controlled Release Society* 235, 337-351.
- Black, S.N., Wheatcroft, H.P., Roberts, R., Jones, M.F., McFarlane, I., Pettersen, A., 2020. Cediranib Maleate—From Crystal Structure Toward Materials Control. *Journal of Pharmaceutical Sciences* 109, 1509-1518.
- Brewster, M.E., Loftsson, T., 2007. Cyclodextrins as pharmaceutical solubilizers. *Advanced drug delivery reviews* 59, 645-666.
- Cho, E.-C., 2012. Effect of Polymer Characteristics on the Thermal Stability of Retinol Encapsulated in Aliphatic Polyester Nanoparticles. *Bulletin of the Korean Chemical Society* 33.
- Dogru, M., Tsubota, K., 2011. Pharmacotherapy of dry eye. *Expert Opin Pharmacother* 12, 325-334.
- Ehrlich, R., Harris, A., Kheradiya, N.S., Winston, D.M., Ciulla, T.A., Wirostko, B., 2008. Age-related macular degeneration and the aging eye. *Clin Interv Aging* 3, 473-482.
- EMA, E.M.A., 2016. EMA/CHMP/616303/2016, Assessment Report: Cediranib maleate.
- Fahmy, S.A., Brüßler, J., Alawak, M., El-Sayed, M.M.H., Bakowsky, U., Shoeib, T., 2019. Chemotherapy Based on Supramolecular Chemistry: A Promising Strategy in Cancer Therapy. *Pharmaceutics* 11, 292.
- Fendler, J.H., 1996. Self-assembled nanostructured materials. *Chemistry of Materials* 8, 1616-1624.
- Higuchi, T., Connors, K.A., 1965. Phase Solubility Techniques. *Advanced Analytical Chemistry of Instrumentation* 4, 117-212.
- Jin, Z.Y., 2013. Cyclodextrin Chemistry: Preparation and Application. World Scientific and Chemical Industry Press.
- Jones, D., 2004. Pharmaceutical Applications of Polymers for Drug Delivery. Rapra Technology Limited.
- Kang, S., Park, K.C., Yang, K.J., Choi, H.S., Kim, S.H., Roh, Y.J., 2013. Effect of cediranib, an inhibitor of vascular endothelial growth factor receptor tyrosine kinase, in a mouse model of choroidal neovascularization. *Clinical & experimental ophthalmology* 41, 63-72.
- Küpper, T.E.A.H., Schraut, B., Rieke, B., Hemmerling, A.V., Schöffl, V., Steffgen, J., 2006. Drugs and Drug Administration in Extreme Environments. *Journal of Travel Medicine* 13, 35-47.
- Lee, P.K., 2009. Heat stable microcapsules and methods for making and using the same, US.
- Li, J., Chu, M.K., Lu, B., Mirzaie, S., Chen, K., Gordijo, C.R., Plettenburg, O., Giacca, A., Wu, X.Y., 2017. Enhancing thermal stability of a highly concentrated insulin formulation

- with Pluronic F-127 for long-term use in microfabricated implantable devices. *Drug delivery and translational research* 7, 529-543.
- Lieberman, H., Murti Vemuri, N., 2015. Chapter 32 - Chemical and Physicochemical Approaches to Solve Formulation Problems, in: Wermuth, C.G., Aldous, D., Raboisson, P., Rognan, D. (Eds.), *The Practice of Medicinal Chemistry* (Fourth Edition). Academic Press, San Diego, pp. 767-791.
- Lin, N., Dufresne, A., 2013. Supramolecular hydrogels from in situ host-guest inclusion between chemically modified cellulose nanocrystals and cyclodextrin. *Biomacromolecules* 14, 871-880.
- Loftsson, T., 2014. Self-assembled cyclodextrin nanoparticles and drug delivery. *Journal of Inclusion Phenomena and Macrocyclic Chemistry* 80, 1-7.
- Loftsson, T., Brewster, M.E., 1996. Pharmaceutical Applications of Cyclodextrins. 1. Drug Solubilization and Stabilization. *Journal of Pharmaceutical Sciences* 85, 1017-1025.
- Loftsson, T., Brewster, M.E., 2010. Pharmaceutical applications of cyclodextrins: basic science and product development. *Journal of Pharmacy and Pharmacology* 62, 1607-1621.
- Loftsson, T., Brewster, M.E., 2012. Cyclodextrins as functional excipients: methods to enhance complexation efficiency. *J Pharm Sci* 101, 3019-3032.
- Loftsson, T., Duchêne, D., 2007. Cyclodextrins and their pharmaceutical applications. *International Journal of Pharmaceutics* 329, 1-11.
- Loftsson, T., Frikdriksdóttir, H., Sigurkardóttir, A.M., Ueda, H., 1994. The effect of water-soluble polymers on drug-cyclodextrin complexation. *International Journal of Pharmaceutics* 110, 169-177.
- Loftsson, T., Jarho, P., Masson, M., Jarvinen, T., 2005. Cyclodextrins in drug delivery. *Expert opinion on drug delivery* 2, 335-351.
- Loftsson, T., Masson, M., 2004. The effects of water-soluble polymers on cyclodextrins and cyclodextrin solubilization of drugs. *Journal of Drug Delivery Science and Technology* 14, 35-43.
- Lumholdt, L.R., Holm, R., Jorgensen, E.B., Larsen, K.L., 2012. In vitro investigations of alpha-amylase mediated hydrolysis of cyclodextrins in the presence of ibuprofen, flurbiprofen, or benzo[a]pyrene. *Carbohydrate research* 362, 56-61.
- Malmsten, M., 2002. Surfactants and polymers in drug delivery.
- Mathias, N.R., Hussain, M.A., 2010. Non-invasive systemic drug delivery: developability considerations for alternate routes of administration. *J Pharm Sci* 99, 1-20.
- Medinger, M., Esser, N., Zirrgiebel, U., Ryan, A., Jurgensmeier, J.M., Dreves, J., 2009. Antitumor and antiangiogenic activity of cediranib in a preclinical model of renal cell carcinoma. *Anticancer research* 29, 5065-5076.
- Meier, M., Bordignon-Luiz, M., Farmer, P., Szpoganicz, B., 2001. The Influence of β - and γ -Cyclodextrin Cavity Size on the Association Constant with Decanoate and Octanoate Anions. *Journal of Inclusion Phenomena* 40, 291-295.
- Muankaew, C., Loftsson, T., 2018. Cyclodextrin-Based Formulations: A Non-Invasive Platform for Targeted Drug Delivery. *Basic & clinical pharmacology & toxicology* 122, 46-55.
- Niazi, S.K., 2016. *Handbook of Pharmaceutical Manufacturing Formulations: Volume Three, Liquid Products*. CRC Press.
- Parfitt, G.D., Barnes, H.A., 1992. Chapter 6 - The dispersion of fine particles in liquid media, in: Harnby, N., Edwards, M.F., Nienow, A.W. (Eds.), *Mixing in the Process Industries*. Butterworth-Heinemann, Oxford, pp. 99-117.
- Perry, H.D., Donnenfeld, E.D., 2003. Medications for dry eye syndrome: a drug-therapy review. *Managed care* (Langhorne, Pa.) 12, 26-32.
- Praphanwittaya, P., Saokham, P., Jansook, P., Loftsson, T., 2020. Aqueous solubility of kinase inhibitors: I the effect of hydrophilic polymers on their γ -cyclodextrin solubilization. *Journal of Drug Delivery Science and Technology* 55, 101462.
- Qiu, N., Li, X., Liu, J., 2017. Application of cyclodextrins in cancer treatment. *Journal of Inclusion Phenomena and Macrocyclic Chemistry* 89, 229-246.
- Ryzhakov, A., Do Thi, T., Stappaerts, J., Bertoletti, L., Kimpe, K., Sa Couto, A.R., Saokham, P., Van den Mooter, G., Augustijns, P., Somsen, G.W., Kurkov, S., Inghelbrecht, S., Arien, A., Jimidar, M.I., Schrijnemakers, K., Loftsson, T., 2016. Self-Assembly of Cyclodextrins and Their Complexes in Aqueous Solutions. *J Pharm Sci* 105, 2556-2569.
- Saokham, P., Loftsson, T., 2015. A New Approach for Quantitative Determination of γ -Cyclodextrin in Aqueous Solutions: Application in Aggregate Determinations and Solubility in Hydrocortisone/ γ -Cyclodextrin Inclusion Complex. *Journal of Pharmaceutical Sciences* 104, 3925-3933.
- Shah, S.S., Denham, L.V., Elison, J.R., Bhattacharjee, P.S., Clement, C., Huq, T., Hill, J.M., 2010. Drug delivery to the posterior segment of the eye for pharmacologic therapy. *Expert Rev Ophthalmol* 5, 75-93.
- Stetefeld, J., McKenna, S.A., Patel, T.R., 2016. Dynamic light scattering: a practical guide and applications in biomedical sciences. *Biophys Rev* 8, 409-427.
- Telser, M.B.G.V.D.J.F.C.H.-D.J.K.J.K.U.M.A.O.A.R.B.R.J., 2015. Topical ophthalmological pharmaceutical composition containing cediranib, in: LLC, B.H. (Ed.), JUSTIA patent, A61K 47/06 (20060101); A61K 9/00 (20060101); A61K 31/517 (20060101); ed, US.
- Tóth, G., Jánoska, Á., Szabó, Z.-I., Völgyi, G., Orgován, G., Szente, L., Noszál, B., 2016. Physicochemical characterisation and cyclodextrin complexation of erlotinib. *Supramolecular Chemistry* 28, 656-664.
- Tóth, G., Jánoska, Á., Völgyi, G., Szabó, Z.I., Orgován, G., Mirzahosseini, A., 2017. Physicochemical characterization and cyclodextrin complexation of the anticancer drug lapatinib. *Journal of Chemistry*.
- Veiga, F., Pecorelli, C., Ribeiro, L., 2006. As ciclodextrinas em tecnologia farmacêutica. *MinervaCoimbra*
- Viernstein, H., Weiss-Greiler, P., Wolschann, P., 2003. Solubility enhancement of low soluble biologically active compounds—temperature and cosolvent dependent inclusion

complexation. *International Journal of Pharmaceutics* 256, 85-94.

Westin, S.N., Sood, A.K., Coleman, R.L., 2018. 18 - Targeted Therapy and Molecular Genetics, in: DiSaia, P.J., Creasman, W.T., Mannel, R.S., McMeekin, D.S., Mutch, D.G. (Eds.), *Clinical Gynecologic Oncology* (Ninth Edition). Elsevier, pp. 470-492.e410.

Zhao, L., Tang, B., Tang, P., Sun, Q., Suo, Z., Zhang, M., Gan, N., Yang, H., Li, H., 2020. Chitosan/Sulfobutylether- β -Cyclodextrin Nanoparticles for Ibrutinib Delivery: A Potential Nanoformulation of Novel Kinase Inhibitor. *Journal of Pharmaceutical Sciences* 109, 1136-1144.

